

REPUBLIQUE DE CÔTE D'IVOIRE
Union-Discipline-Travail

Ministère de l'Enseignement Supérieur
et de la Recherche Scientifique



Graduate Research Program
CLIMATE CHANGE AND BIODIVERSITY

Order no.: 08

Academic year: 2015 – 2016

THESIS

**Submitted for the obtention of the degree of DOCTOR of
PHILOSOPHY at the Université Félix HOUPHOUËT-BOIGNY**

Speciality: Climate Change and Biodiversity

Isimemen OSEMWEGIE nee Aburime

**The Impacts of Seasonality on Coastal Water
Systems in Southeast Côte d'Ivoire**

Public defense on December 20, 2016

Dissertation committee

Mr. MAHAMANE Ali	Professor	University of Diffa, Niger	President
Mr. BIEMI Jean	Professor	University FHB, Côte d'Ivoire	Supervisor
Ms. REICHERT Barbara	Professor	University of Bonn, Germany	Co-supervisor
Mr. AFFIAN Kouadio	Professor	University FHB, Côte d'Ivoire	Referee
Mr. SAVANE Issiaka	Professor	University NA, Côte d'Ivoire	Referee
Mr. KONÉ Tidiani	Professor	University JLoG, Côte d'Ivoire	Examiner



Année Universitaire : 2015-2016

THÈSE

Présentée pour l'obtention du Titre de Docteur de
L'Université Félix HOUPHOUËT-BOIGNY

Spécialité: Changement climatique et Biodiversité

OSEMWEGIE Isimemen née Aburime

*Impacts de la saisonnalité sur les systèmes
hydrologiques côtiers au Sud-Est de la Côte d'Ivoire*

Soutenu publiquement le, 20 Décembre 2016

Commission du jury

M. MAHAMANE Ali	Professeur Titulaire	UDA, Niger	Président
M. BIEMI Jean	Professeur Titulaire	UFHB, Côte d'Ivoire	Directeur
Mme. REICHERT Barbara	Professeur Titulaire	UB, Germany	Co-directeur
M. AFFIAN Kouadio	Professeur Titulaire	UFHB, Côte d'Ivoire	Rapporteur
M. SAVANE Issiaka	Professeur Titulaire	UNA, Côte d'Ivoire	Rapporteur
M. KONÉ Tidiani	Professeur Titulaire	UJLoG, Côte d'Ivoire	Examineur

DEDICATION

with love to Osanobua Ndazi, my wonderful parents, Engr.& Mrs. B.A. Aburime and my beloved husband, Harry

Acknowledgements

I acknowledge the full scholarship and financial support from the German Federal Ministry of Higher Education and Research (BMBF) and the West African Science Service Centre on Climate Change & Adapted Land Use (WASCAL, www.wascal.org) that accorded me opportunities to collaborate with international institutions and numerous scientific partners. A heartfelt thanks to my supervisors, Prof. Jean BIEMI of the UFR Science de la Terre et des Ressources Minieres (STRM), University Felix Houphouët-Boigny, Côte d'Ivoire and Prof. Barbara REICHERT of the Steinmann-Institute, University of Bonn, Germany for their close supervision, high standards, and guidance throughout the duration of this project.

Special thanks to members of the dissertation committee: Prof. Ali MAHAMANE, Rector of the University of Diffa, Niger, Prof. Affian KOUADIO, Vice-president of the University of Felix Houphouët-Boigny, Côte d'Ivoire, Prof. Issiaka SAVANE, University of Nangui-Abrogua, Côte d'Ivoire and Prof. Tidiani KONÉ of the Université Jean Lorougnon Guédé, Côte d'Ivoire, for their constructive criticisms and contributions to improve the quality and readability of the text.

Special thank goes to Prof. Kone DAOUDA, the director of WASCAL Graduate Studies Programme, 'climate change and biodiversity' for his encouragement, direction and leadership, Prof. Souleymane KONATE, the co-director and Dr. N'guessan KOUAME, ex-director for their moral support. I am also grateful to faculty staff and members of the department for their material supports. In addition, I would like to acknowledge Dr. Mamadou, OUATTARA, ex-director of the WASCAL capacity-building program, Accra, Ghana for the orientation, support, and coordination of my work abroad. Not forgetting here to mention Ms. Minnittallah Boutros for her immense help with the procurement of travel documents.

I wish to express my sincere gratitude to all members of the hydrogeology group, especially Ms. Sonja BEUEL, Mr. Maximillian GEIST and Ms. Isa GÖRLICH. Not forgetting here to mention Dr. Sven-Oliver FRANZ, Mrs. Camilla KURTH, Mrs. Bettina SCHULTE-VAN-BERKUM, Mr. Sven BERKAU and Ms. Beate HACKER of the Steinmann-Institute, Rheinische Friedrich-Wilhelms University of Bonn, Germany for their hospitality, scientific contributions and help with my work during the period of stay at the Institute. I feel greatly indebted to Mrs. Carola KUBUS of the Steinmann-Institute library, University of Bonn for her warmth and unwavering help with research materials.

Special thanks to my scientific collaborators; PD. Dr. Christine STUMPP, head of the hydrogeology group, Institute of Groundwater ecology, IGÖ, Helmholtz Zentrum, München, Germany for believing in me and taking out time to supervise the stable isotope studies.

Also thanks to Dr. Evgenia RYANBEKO, Ms. Petra SEIBEL, Mr. Michael STÖCKL, Ms. Katrin HÖRMANN, Mr. Harald LOWAG and Ms. Ramona BREJCHA of the same institute for their unyielding support and time taken out to guide me through the technical aspects of my work throughout the duration of my stay at the institute. I would also like here to mention now Dr. Liu YOUZHONG for his help with the preparation of R scripts and codes.

I wish to thank Prof. Kouassi DONGO and Prof. Marie-Solange OGA of the UFR-STRM, University of Felix Houphouët-Boigny, Côte d'Ivoire for their timely interventions by way of comments, suggestions, and criticisms of the work. Special thanks to Prof. Allassane OUATTARA and Dr. Juliette Niamien-EBROTTIÉ of the Laboratoire d'Environnement et de Biologie Aquatique (LEBA), University of Nangui Abrogua, Côte d'Ivoire. They helped establish the link with biodiversity in my work. I am also grateful to Dr. Matthieu Y. F. KONE of the Centre of Oceanographic Research, CRO, Côte d'Ivoire for help with field mapping and manuscript preparation/editing. I am also grateful to Mr. Jean-Marie KONE of the same institute for chlorophyll-a dosage.

My sincere gratitude goes to Prof. Mireille DOSSO, director of the Institute Pasteur, Côte d'Ivoire, Dr. Kouame KOUADIO, Dr. Coulibaly KALPY, Ms. Amon E. SEY, Mr. BAMBA and Mr Timoté GUEU, interns of the above-named institute for their guidance and help with microbiological analyses.

Not forgetting here to mention Dr. Matthieu Wadja EGNANKOU of SOS forest and Dr. Dibi Hyppolite of CNF, University of Felix Houphouët-Boigny for timely help with vegetation mapping, remote sensing and geographic information systems analyses of satellite images. Special thanks also to Dr. Frank THONFELD, Ms. Fridah KIRIMI, Mr. Tobias HENNING, Mr. Kilian STAAR and Ms. Esther AMLER of the department of Geography, University of Bonn, Germany for their help with creation of study maps and lectures on the use of mapping software.

Sincere gratitude to Mr. Coulibaly BELENAHOU for his support and technical assistance with information technology. I would also like to appreciate all village chiefs and elders I encountered during the course of my work for their hospitality and time taken to guide me through their communities.

Many thanks to my colleagues, Dr. Aniko POLO-AKPISSO, Dr. Mariama CAMARA, Dr. Sanogo KAPOURY, Dr. Issaka ISSAHAROU, Dr. Adam CEESAY, Dr. Linda LEABO and Dr. Achille HOUNKPEVI for their inputs, assistance and moral support. Finally, I am especially grateful to friends, family, and my kids, Heidi and David for their encouragement and moral support.

Abstract

To have a compendium of responses from coastal water systems along the east Ivorian coast under different seasons, samples of rainwater (n= 30), groundwater (wells and boreholes, n= 81 and surface water (Ébrié lagoon and Atlantic coastline, n= 69) were collected for geochemical, isotopic and biological analyses during the dry (January/February) and rainy (September/October) seasons of 2014.

From geomorphological viewpoint, the slope of the study area is between 0 and 70 % relative to the sea. Present land use cover includes farmlands (50 %), water bodies (32 %), settlements (13 %) and forests (5 %). Within 25 years (1989/90 - 2014/15), urbanization has claimed 31.83 % of forestlands and 37.42 % of farmlands. As regards hydrology, moderate hydrological drought spells were revealed for 1987, 1998/99, and 2013/14 based on Standardised Precipitation Evapotranspiration Indices (SPEI) of multi-decadal (1971 – 2014) meteorological data. The aquifer materials comprise up to 98 % silicate. The implications of this is groundwater acidification (pH: 3.9 – 7.4) on dissolution.

From hydrogeological perspective, changing hydrological regimes exerts strong influence on coastal water chemistry and contaminant export. Based on geochemical and stable isotope analyses, marine influence dominates during the dry season, while continental (fluvial and precipitation) processes dominate during the rainy season. Piper diagrams showed that majority (dry season: 87 %; rainy season: 80 %) of groundwater samples belong to the Na-Cl facies, depicting saltwater intrusion. Maximum chloride concentration was 1,088 mg/L and 785.2 mg/L for the groundwater during dry and rainy seasons, respectively. Conversely, nitrate concentrations in groundwater ranged from 0.3 – 139.5 mg/L and 0.0 – 165.9 mg/L for the dry and rainy seasons, respectively and for the surface waters, between 0.01 – 3.6 mg/L and 0.01 - 332.3 mg/L for the dry and rainy seasons, respectively.

From the viewpoint of biology, seasonal influx of nutrients into the coastal surface waters also influences phytoplankton distribution. Maximum phytoplankton biomass was 11.3×10^6 and 15.4×10^6 cells/mL for the dry and rainy seasons respectively with floristic growth response ranging between 16.4 and 80.8 %. Highest temporal variations in biomass were recorded in areas of the Ébrié lagoon with high marine influence. Diatoms were the dominant taxa, while cyanobacteria are the most abundant. The overall low phytoplankton diversity (Shannon index, H' less than 1) and localized monospecies dominance are vital signs of disturbances.

Finally, survey results show that the riverine communities are sensitive to coastal water degradation. These waters constitute the primary source of domestic water for 53 % and a secondary source for 97 % of the population. Additionally, about 30 % of the population depend directly on aquatic resources from these coastal waters for livelihood.

Keywords: coastal waters, phytoplankton, saltwater intrusion, seasonality, Côte d'Ivoire.

RÉSUMÉ

Pour avoir un compendium des réponses des systèmes hydrologiques côtiers le long de la côte est ivoirienne sous différentes saisons, des échantillons d'eaux de pluie ($n=30$), d'eau souterraine (puits et forages, $n= 81$) et d'eau de surface (lagune Ebrié et littoral Atlantique, $n= 69$) ont été prélevés pour des analyses géochimiques, isotopiques et biologiques pendant les saisons sèche (janvier/février) et hivernale (septembre/octobre) de l'année 2014

Du point de vue géomorphologique, la pente de la zone d'étude se situe approximativement entre zéro (0) et 70 degrés vers la mer. Les unités d'occupation du sol sont les terres agricoles (50 %), les plans d'eau (32 %), les établissements (13 %) et les forêts (5 %). En 25 ans (1989/90 – 2014/15), l'urbanisation a englouti 31,83 % des forêts et 37.42 % des terres agricoles. S'agissant de l'hydrologie, les indices standardisés de précipitation et d'évapotranspiration (ISPE) déterminés sur la base des données météorologiques multi-décennales (1971 - 2014) ont révélé des sécheresses modérées au cours des années 1987, 1998/99 et 2013/14.

Au plan hydrogéologique, les terrains aquifères sont composés de plus de 98 % de silice, ce qui favorise une acidification importante des eaux souterraines (pH de 3,9 à 7,4) en rapport avec la capacité de dissolution rapide de la silice. Dans cette région, les changements de régimes hydrologiques exercent une forte influence sur la chimie de l'eau côtière et le transport des contaminants. Sur la base des analyses géochimiques et des isotopes stables (oxygène-18 et deutérium), l'influence marine est dominante pendant la saison sèche contrairement aux processus continentaux (fluviaux et pluviométriques) qui ne deviennent très actifs que pendant la saison des pluies. Le diagramme de Piper a montré que la majorité des échantillons d'eau souterraine (87 % et 80 % respectivement pour la saison sèche et hivernale) appartiennent au faciès chloruré sodique (Na-Cl), traduisant ainsi l'intrusion saline. La concentration maximale en chlorure de l'eau souterraine est de 1088 mgL^{-1} et de $785,2 \text{ mgL}^{-1}$ respectivement pendant la saison sèche et des pluies. Quant aux nitrates, leurs concentrations varient entre 0,3 - $139,5 \text{ mgL}^{-1}$ et 0 – $165,9 \text{ mgL}^{-1}$ dans les eaux souterraines; et entre 0,01 – $3,6 \text{ mgL}^{-1}$ et 0,01 – $332,3 \text{ mgL}^{-1}$ dans les eaux de surface, respectivement pendant les saisons sèche et pluvieuse.

Du point de vue de la biologie, le flux saisonnier des nutriments dans les eaux de surface du littoral influence aussi la distribution du phytoplancton. La biomasse maximale de phytoplancton était de $11,3.10^6$ et de $15,4.10^6$ cellules par millilitre respectivement pour la saison sèche et la saison des pluies avec une croissance floristique variant entre 16,4 et 80,8 %. Les variations temporelles, les plus élevées en biomasse, ont été relevées dans les alentours de la lagune Ebrié soumise à une forte influence marine. Les diatomées étaient le taxon dominant en espèces, alors que les cyanobactéries étaient les plus abondantes en quantité. La diversité relativement faible du phytoplancton (indice de Shannon inférieur à 1) et la dominance mono-spécifique localisée sont des signes de perturbations du milieu aquatique sur le littoral ivoirien.

Enfin, les résultats des enquêtes ont montré que les communautés riveraines sont exposées à la dégradation des eaux côtières. En effet, ces eaux constituent la source principale d'approvisionnement en eau potable des ménages pour 53 % et une source secondaire pour 97 % de la population. En plus, environ 30 % de la population dépend directement de ces ressources en eau du littoral pour leur subsistance.

Mots clés: eaux côtières, phytoplancton, intrusion de l'eau marine, saisonnier, Côte d'Ivoire.

Table of contents

Acknowledgements.....	iv
Abstract.....	vi
Table of contents.....	viii
List of figures.....	xi
List of photos.....	xiv
List of tables.....	xv
List of abbreviations and acronyms	xvi

INTRODUCTION.....	18
Thesis rationale	21
Aim and objectives.....	23
Thesis outline	24

PART I: LITERATURE REVIEW.....26

CHAPTER 1: Physiographical environment27

1.1. The geology of Côte d'Ivoire	27
1.1.1. The basement rocks.....	27
1.1.2. The Tertiary-Quaternary sedimentary basin	28
1.1.2.1 The stratigraphic succession of the basin	30
1.1.2.2. The structural development of the sedimentary basin	32
1.1.3. The regional geology of the Ébrié lagoon sub-catchment (the study area).....	33
1.2. Hydrological and hydrogeological settings of the Ebrié lagoon subcatchment	33
1.3. The climate of the littoral zone.....	38
1.3.1. The maritime climate (ocean upwelling)	38
1.3.2. Climate change perspectives	41

PART II: MATERIALS AND METHODS.....43

CHAPTER 2: Physical habitat assessment44

2.1. Land use dynamics	44
2.2. Mangrove forest characterization	46
2.2.1. Above-ground root biomass and carbon stock estimation	49
2.2.2. Natural regeneration capacity	49
2.3. Lithological analyses	49
2.4. Water quality assessment (abiotic environmental factors)	53
2.4.1. Precipitation	53

2.4.1.1. Drought indices.....	53
2.4.2. Surface water and groundwater.....	54
2.4.2.1. Hydrologic information and estimation of groundwater recharge.....	54
2.4.2.2. Hydrochemistry	56
2.4.2.3. Stable isotope analyses (natural tracers).....	57
2.4.2.4. Hydrological modelling - End-member mixing model (EMMA)	62
2.5. Biocenosis analyses – phytoplankton dynamics.....	62
2.5.1. Phytoplankton sampling, identification, and enumeration.....	63
2.5.2. Data analysis – SOM map.....	65
2.5.3. Community indices	66
2.5.4. . Faecal coliform bacteria – supplementary water quality indicator	67
2.6. Socio-economic survey.....	68
PART III: RESULTS AND DISCUSSIONS	69
CHAPTER 3: Physical habitat assessment	70
3.1. Coastal topography	70
3.2. Dynamics of land use	70
3.3. <i>Rhizophora</i> forest characterization.....	73
3.3.1. Carbon storage potentials.....	73
3.3.2. Regenerative capacity	75
3.4. Lithological analyses	75
CHAPTER 4: Water quality assessment.....	81
4.1. Precipitation.....	81
4.1.1. Drought indices.....	81
4.1.2. Hydrochemistry of precipitation	88
4.2. Groundwater aquifers	89
4.2.1 Physico-chemical parameters.....	94
4.2.2. Hydrochemical characterisation.....	95
4.2.3. Microbial safety of groundwater wells	102
4.3. Surface water systems	102
4.4. Correlation between environmental abiotic components	108
4.5. Seasonal hydrologic interactions between coastal waters	109
4.6. Hydrological modelling	111
CHAPTER 5: Biocenosis analyses	117
5.1. Seasonal phytoplankton distribution patterns.....	117
5.1.1. Biotic indices.....	121
5.1.2. SOM patterning of phytoplankton assemblages	121

5.1.3. Abiotic controls on phytoplankton distribution patterns.....	123
CHAPTER 6: Socio-economic considerations	128
6.1. Indigenous perception of climate change	128
6.2. Social vulnerability.....	131
6.3. Resource value.....	131
CONCLUSION.....	137
REFERENCES.....	142
Webography.....	163
APPENDICES.....	164
PUBLICATIONS.....	164

List of figures

Figure 1:	Geology map of Côte d'Ivoire (Kouamelan, 1996).	29
Figure 2:	The subdivisions of the sedimentary basin of Côte d'Ivoire (Petroci & Beicip, 1990).	31
Figure 3:	The structural geology of the Ivorian sedimentary basin after Tastet and Guiral (1994).	31
Figure 4:	A north-south cross-section through the sedimentary basin in the Abidjan area after Tastet (1971).	31
Figure 5:	The geology map of the study area after Delor <i>et al.</i> (1992); Simeon <i>et al.</i> (1992). .	34
Figure 6:	Map of the river basins of Côte d'Ivoire (top). Hatched areas represent the Agnéby-Mé coastal river basin (bottom). The Ébrié lagoon sub-catchment (study area) is highlighted in red.	36
Figure 7:	Hydrogeological log of the aquifers of the Ivorian sedimentary basin. Modified from Aghui and Biemi (1984).	37
Figure 8:	Monthly variations of sea surface temperatures, SST (pink line) (data source: maree.shom.fr), and mean tidal sea level, MSL (blue line) (data source: http://seatemperature.info) of the Atlantic Ocean off the Abidjan coast for 2014.	40
Figure 9:	Temperature (T) and salinity (S) fluctuations of the Atlantic Ocean in front of Abidjan (average: 1966 - 1990). (Source: Morlière, 1970).	40
Figure 10:	Monthly mean CO ₂ levels at Mauna Loa Observatory, Hawaii. Current denotes average global atmospheric CO ₂ level as at April 2015 (404.35 ppm). (Source: National Oceanic and Atmospheric Administration, 2016).	42
Figure 11:	Global sea levels have been rising since 1800. The rate of rise has been constant for the past 150 years. Grey shadings represent the standard error. (Source: Jevrejeva <i>et al.</i> , 2008).	42
Figure 12:	Agricultural land expansion at the expense of primary forest areas: The year, 1955 (top) and 1988 (bottom). (Source: Institute of Research for Development, 1996). ...	45
Figure 13:	Temporal trends in mangrove forest area in Côte d'Ivoire.	48
Figure 14:	Mangrove forest sampling points along the Ébrié lagoon.	48
Figure 15:	Sequence of occurrence and impacts of common drought types (Source: National Drought Mitigation Centre, 2007, Nebraska-Lincoln, U.S.).	55
Figure 16:	Map of the study area with water sampling points. Top: surface water sampling points. Prefixes R-, L- and S- represent river, lagoon, and Atlantic coast, respectively. Bottom: groundwater sampling points. Prefixes, P- and F- represent wells and boreholes, respectively. Circled areas were sampled only during the rainy period. Green areas represent forested areas.	58
Figure 17:	Summary of field and laboratory analytical methods.	60
Figure 18:	Map showing phytoplankton sampling stations along the Ébrié lagoon (L) and the adjacent inshore (S). Blue lines are subdivisions according to Durand and Guiral (1994).	64
Figure 19:	Digital elevation model (DEM) of the study area. The unit of slope is in percentage.	71

Figure 20:	Temporal patterns (1989/90 and 2014/15) of land use/cover categories as observed from remotely sensed images.	72
Figure 21:	Lognormal plots of mangrove prop root density in 1 x 1 m plots at Eloka-To (A), Agban (B), Audoin-Bégréto (C) and Mois (D).	74
Figure 22:	Box plots of seedlings density on 1 x 1 m plots from Eloka-To (A), Agban (B), Audoin-Bégréto (C) and Mois (D) forest stands. Values are means \pm range.	76
Figure 23:	Ternary plot of Al_2O_3 – $CaO+Na_2O$ – K_2O (A-CN-K) of rock samples.....	80
Figure 24:	Graph showing average monthly rainfall amount (data source: SODEXAM). LDS is long dry season; LRS is long rainy season; SDS is short dry season and SRS, short rainy season for the Abidjan (central parts of the study area), Bingerville (eastern parts), and Jacqueville (western parts) meteorological stations.	82
Figure 25:	The mean position of ITD, CAB and ITCZ. Top: 3rd decade of January 2014 (black), 2nd decade of January, 2014 (blue). Bottom: 3rd decade of October 2014 (black), 2nd decade of October, 2014 (blue). The red and green triangles represent their maximum and minimum displacements respectively. (Source: ACMAD, 2014a, b).	83
Figure 26:	Yearly trend in precipitation across the study area. Abidjan (top) Jacqueville (middle), and Bingerville (bottom). Thick lines represent moving average, while dashed lines are second order polynomial fitted curves.	85
Figure 27:	Temporal evolution of SPEI at different time scales for the Abidjan meteorological station. Time scale of 3-, 6- and 24-months depicts meteorological, agricultural, and hydrological/socio-economic droughts, respectively.	86
Figure 28:	Temporal evolution of SPEI at different time scales for the Bingerville meteorological station. Time scale of 3-, 6- and 24-months depicts meteorological, agricultural, and hydrological/socio-economic droughts, respectively.	87
Figure 29:	$\delta^{18}O$ - δ^2H plot of precipitation waters of Abidjan.....	90
Figure 30:	Potentiometric surface maps showing flow direction from static, non-pumping water levels (m below land surface) of the unconfined aquifers for the dry (top) and rainy season (bottom).	92
Figure 31:	Groundwater recharge history as shown by monthly fluctuations in water table level recorded from piezometers (GWL) (data source: L'Office National d'Eau Portable, 2014) superimposed on umbrothermic diagram. Abidjan (top), Dabou (middle), and Bingerville (bottom). The borehole responded to peak rain event after a time lag of one-month for Abidjan and Dabou, and simultaneously for Bingerville.	93
Figure 32:	Chloride concentration (mg/L) versus perpendicular distance to the coastlines (km) for the dry and rainy seasons.....	97
Figure 33:	Chloride concentration (mg/L) versus total well depth (m) for the dry and rainy seasons.....	97
Figure 34:	Trilinear diagram (Piper, 1944) of major ions of the groundwater and inshore systems for the dry (top) and rainy (below) seasons.....	98
Figure 35:	Plot of TDS versus $Na/(Na + Ca)$ molar ratios (Gibbs, 1992) for the dry (top) and rainy (bottom) seasons.....	99
Figure 36:	Expanded Durov diagram (Durov, 1948) with pH and TDS data of major ion analyses of the different coastal water systems for the dry (top) and rainy (bottom) season, respectively. Thick blue diagonal line is a theoretical mixing line.	101

Figure 37:	Nitrate concentration (mg/L) in drinking water wells for the dry (top) and rainy (bottom) seasons.....	103
Figure 38:	Faecal coliform density (CFU/100 mL) in all studied wells during the rainy season.	103
Figure 39:	Voronoi tessellation to highlight contamination hotspot of nitrate (mg/L) on the Ebrié lagoon during the rainy period of 2014. The green shade areas have nitrate values below the WHO acceptable levels.....	107
Figure 40:	Spatiotemporal shifts in mean isotopic composition of coastal waters. Text in red are dry season values, while text in blue are wet season values.	112
Figure 41:	$\delta^2\text{H}$ versus $\delta^{18}\text{O}$ plot of coastal waters during the dry (top) and rainy (bottom) seasons, respectively.....	113
Figure 42:	Ternary plot/mixing triangle of coastal water systems during the dry season (top) and rainy season (bottom).	115
Figure 43:	Seasonal composition shifts in phytoplankton as observed in the lagoon (top) and the Atlantic coastline (bottom).	122
Figure 44:	Clusters between virtual map units by hierarchical cluster analysis (A) and a SOM map (B) formed by 12 hexagons representing neurons. Shading intensity indicates the different clusters. The first letters of the names represents study sites: L; Ébrié lagoon and S; the inshore environment respectively, while suffixes –DS and –WS represents the dry and rainy seasons, respectively.	125
Figure 45:	Species abundance (A) and environmental factors (B). Each component plane is scaled independently over the SOM. Darker shades represents higher values and vice versa. (DO: dissolved oxygen, PO: phosphate, SiO: silicate, Temp: temperature and TDS: total dissolved solids). List of taxa and acronyms are shown in Table XXIII.	125
Figure 46:	Age distribution (top) and main occupation (bottom) of the respondents.	130
Figure 47:	Respondents perception of key climate parameters.	132
Figure 48:	Main sources of domestic water supply.	133
Figure 49:	Existing alternative domestic water sources.	133
Figure 50:	Responses to if water is treated prior to use (left) and treatment methods (right). ..	133
Figure 51:	Ways of disposal of domestic wastewater.....	134
Figure 52:	Radar chart on the perception of locals on coastal water degradation and most likely period of occurrence.	134
Figure 53:	Amounts respondents are willing to pay to safeguard coastal water resources.	136

List of photos

Photo 1:	Impressions of the area under investigation: abandoned recreational facility at Azuretti along the coast (left), destroyed fence of a restaurant at Vridi (right).	22
Photo 2:	Field measurements on <i>Rhizophora</i> roots. 1m ² PVC pipes (top image) and vernier caliper (bottom image).	50
Photo 3:	Summary of analytical steps for whole rock mineralogy.	52
Photo 4:	Measuring water level in a dug well in Songon-Té using water level meter (left) and a typical borehole in Nguessandan (right).	58
Photo 5:	Some field measuring instruments. Handheld WAGTECH turbidity meter (left) and HANNA HI-9878 multiparameter hand held meter (right).	59
Photo 6:	Materials for a two-step water filtration during field survey. Whatman filter paper (left) and syringe 0.45 µm PVDF membrane filter (right).	59
Photo 7:	HACH UV-VIS spectrophotometer (Analytik, Jena Specord 50).	59
Photo 8:	Ion chromatograph (DIONEX ICS-1100) (top) and automated water sample holders (bottom).	60
Photo 9:	The laser isotope analyser (LS2120- <i>i</i> , Picarro Inc., US).	61
Photo 10:	Materials for biocenosis analyses. Plankton net (left). Zeiss microscope (right).	64
Photo 11:	Lithology of surface outcrops at coarse scale across the study area. Persons and object are scales.	78
Photo 12:	The sandy beach of Azuretti covered by mats of brown macroalgae <i>sargassum</i> (October, 2014) <that on decay give off putrid smell.	107
Photo 13-29:	Phytoplankton belonging to the phylum Bacillariophyta.	118
Photo 30-37:	Phytoplankton belonging to the phylum Cyanophyta.	119
Photo 38-41:	Phytoplankton belonging to the phylum Euglenophyta.	119
Photo 42-48:	Phytoplankton belonging to the phylum Chlorophyta.	120
Photo 49:	Phytoplankton belonging to the phylum Chrysophyta.	120
Photo 50:	Some ecosystem goods and services delivered by the coastal water systems.	129
Photo 51:	Fishing boats lined up in Eloka-To community (Bngerville, Côte d'Ivoire).	136

List of tables

Table I:	Lithologic ratios used for siliciclastic rock classification (Sprague <i>et al.</i> , 2009)	52
Table II:	SPEI classification scheme (World Meteorological Organization, 2012).	55
Table III:	Detection limit of analytes (mg/L) according to DIN 32645.	61
Table IV:	Trophic categories of surface waters based on chlorophyll-a concentration (Schmitt, 1998).....	64
Table V:	Accuracy of land use categories for 1989/90 (above) and 2014/15 (below). The class specific accuracy is highlighted in yellow.	71
Table VI:	Land use cover categories (%) of the study area for the year 1989/90 and 2014/15.	72
Table VII:	Matrix of transition for the different land use categories between 1989/90 and 2014/15.	72
Table VIII:	Mean and range (in parenthesis) of estimates of vegetation parameters for Eloka-To (A), Agban (B), Audoin-Bégréto (C) and Mois (D) forest stands.	74
Table IX:	Moisture content (%) and loss on ignition (%) of outcrops surrounding the Ebrié lagoon subcatchment.	76
Table X:	Summary of physicochemical parameters of rainwater (n = 30).	90
Table XI:	Water table level from ground surface in wells for the dry and rainy season and their total depth.....	91
Table XII:	Categories of groundwater after Kelly (2005).	99
Table XIII:	The range of environmental variables measured of the surface water systems for the dry (top) and rainy (bottom) seasons.....	104
Table XIV:	Water quality rating for the different stations of the Ébrié lagoon during the investigation period.	110
Table XV:	Correlation (Pearson) matrix of coastal surface water systems for the dry (top) and rainy (bottom) seasons, respectively	110
Table XVI:	Correlation matrix (Pearson) of selected solute concentrations in coastal inland waters for the dry (top) and rainy (bottom) seasons, respectively.....	114
Table XVII:	Factor loadings after Varimax rotation for the dry (left) and rainy (right) seasons, respectively.....	114
Table XVIII:	Spatiotemporal variations in phytoplankton cell abundance along the Ébrié lagoon	122
Table XIX:	Spatiotemporal variations in phytoplankton cell abundance along the Atlantic coastline.....	122
Table XX:	Correlation (Pearson, n) between abiotic environmental factors and the dominant genus, <i>Phormidium foveolarum</i>	124
Table XXI:	Key indicator species for the different bioclimate zones (clusters).	124
Table XXII:	List of taxa in order of decreasing abundance as distributed by SOM in each cluster	124
Table XXIII:	List of taxa and their acronyms	126

List of abbreviations and acronyms

ACMAD	African Centre of Meteorological Applications for Development.
CAB	Congo Air Boundary
CBD	Convention on Biodiversity
CFU	Colony forming unit
CO ₂	Carbon dioxide
CRED	Centre for Research on the Epidemiology of Disasters
DEM	Digital Elevation Map
EMMA	End member Mixing Analyses
ENSO	El Niño Southern Oscillation
ENVI	Environment for Visualizing Images
ESRI	Environmental Systems Research Institute
FAO	Food and Agriculture Organization (United Nations)
GHGs	Greenhouse gases
GMWL	Global Meteoric Water Line
GW	Global Water Intelligence magazine
IAEA	International Atomic Energy Agency
INS	Institut National de la Statistique; National Statistics Institute
IPCC	Intergovernmental Panel on Climate Change
IRMS	Isotope Ratio Mass Spectrometry
ITCZ	Inter-Tropical Convergence Zone
ITD	Inter-Tropical Discontinuity
LAI	Leaf Area Index
LDC	Least Developed Countries
LDS	Long Dry Season
LRS	Long Rainy Season
LMWL	Local Meteoric Water Line
MDG	Millennium Development Goals
MSL	Mean Sea Level
NOAA	U.S. National Oceanic and Atmospheric Administration
NTU	Nephelometric Turbidity Units
OFDA/CRED	Office of U.S. Foreign Disaster Assistance/the Centre for Research on the Epidemiology of Disasters
ONEP	Office National d'Eau Portable
ORSTOM	Office de Recherche Scientifique et Technique d'Outre-Mer

RAMSAR	Convention on Wetlands (Ramsar, Iran, 1971)
RGPH	Recensement Général de la Population et de l'Habitat ; General Census of Population and Housing
SDG	Sustainable Development Goals
SDS	Short Dry Season
SHOM	Service Hydrographique et Oceanographique de la Marine
SLAP	Standard Light Antarctic Precipitation
SODECI	Société des Eaux du Côte d'Ivoire; water company
SODEXAM	Société d'exploitation et de développement aéroportuaire, aéronautique et Météorologique
SOM	Self-organizing feature maps
SPEI	Standard Precipitation Evapotranspiration Index
SRS	Short Rainy Season
SST	Sea Surface Temperature
SWAC/OECD	Sahel and West African Club
UFR-STRM	Unité de Formation et Recherche en Sciences de la Terre et des Ressources Minières
UNDP	United Nations Development Programme
UNEP	United Nations Environment Programme
UNFCCC	United Nations Framework Convention on Climate Change
UNICEF	United Nations Children's Fund
USAID	United States Agency for International Development
USGS	United States Geological Survey
V-SMOW	Vienna-Standard Mean Ocean Water
WHO	World Health Organization
WMO	World Meteorological Organization
WWAP	World Water Assessment Programme
WWDR	World Water Development Report

INTRODUCTION

Water covers approximately 71 % (361.13 million km²) of the Earth's surface (**Martinez *et al.*, 2007**) estimated at 510 million km² (**Weast, 1981**). Only about 29 % (148.94 million km²) is dry land. The substance water is one of the fundamental life-support services provided naturally by ecological systems. It is the elixir of life (**Fetter, 1994**), lifeblood of the environment, essential to the survival of every life form on earth – humans, animals, plants, and other organisms (**Stuckelberger, 2008**). Good quality water maintains good health status of terrestrial and aquatic systems and provides vital ecosystem services to man. It therefore follows that changes in its quality and/or quantity have important consequences on ecosystems and inherent biodiversity. Furthermore, water has intricate relationship with other key elements of climate such as air temperature, relative humidity, wind speed, and solar irradiation that drives changes in global climate systems. According to a World Water Assessment Report (**World Water Assessment Programme, 2009**), water is the primary medium through which climate exhibits its impacts on the earth's ecosystem and people. Some manifestations are as too much water (floodings and erosions), too little water (drought), and eustatic sea level rise, a direct consequence of melting glaciers. According to IPCC climate change working group II (**Parry *et al.*, 2007**), many of the worst climate change effects are related to water. Statistics from the Belgian Centre for Research on the Epidemiology of Disasters (CRED) in Belgium showed that during the ten-year period (2004 to 2013), about 91.4 % of natural disasters were either of climatological (droughts, glacial lake outburst, wildfire), meteorological (storm, heat waves, fog) and/or hydrological origin (flood, landslide, sea wave action) (**Guha-Sapir *et al.*, 2015**). Majority, of natural disaster-related mortality were recorded in low- and middle-income countries (**Twigg, 2004; Guha-Sapir *et al.*, 2015**). This is due partly to geographical emplacement, tropical/subtropical climate, economic dependence on climate sensitive sectors and the limited human, institutional, and financial capacity to anticipate and respond to the negative impacts of climate change (**United Nations Framework Convention on Climate Change, 2007; Abeygunawardena *et al.*, 2009**). In Côte d'Ivoire, between 1996 and 2005, 237 deaths were reported as a result of floods, landslides and landslips (**Allah-Kouadio *et al.*, 2016**). Therefore, adequate knowledge of, sustainable use and proper management of water resources is of crucial importance to foster sustainable economic development, prevent disasters (**World Water Assessment Programme, 2009**), and overcome the predicted continued negative impacts of climate change on natural water balance and availability (**IPCC, 2014**). It is clear that future development across the African continent depends highly on water availability (**Desanker & Magadza, 2001**).

Globally, water resources exhibit uneven spatial and temporal distribution patterns (**Chang, 2006**). For instance, in Côte d'Ivoire, large variations exist between different agro-climatological regions.

Rainfall events are more intense in the southern parts (mean annual average up to 2,500 mm) with an equatorial humid climate compared to the northern parts of the country (annual average less than 800 mm) with a savannah climate. The strong ties between water availability and socio-economic activities (tourism, ports, industries, fisheries) results in disproportionate human loads along the coastal zones (**Nicholls *et al.*, 2007**).

Coastal ecosystems occupy 8 % of the Earth's surface (**Ray & Hayden, 1992**) and more than 60 % of global population lives within 40 km from the coasts (**Lindeboom, 2002**). In Côte d'Ivoire, the coastal zone, with an approximate length of 600 km (**Koffi, 1992**), constitutes 1 % (32, 960 km²) of national landmass of 322, 463 km² (**Adopo *et al.*, 2014**). Five (San-Pedro, Gbôklé, Grands-Ponts, Abidjan, and Sud-Comoé) of the thirty-one administrative regions of the country borders on the coast, which is home to over 48 % of the total population of 22,671,331 inhabitants (**INS, 2014**). In addition to supporting disproportionate human load, 60 % of national industries are within few kilometres from the Ivorian coastal areas, into which they dump directly raw and untreated effluents (**CBD Fourth National report, 2009**). Furthermore, the two main seaports (in San Pedro and Abidjan) harbours on the coast. These socio-economic activities exert enormous pressures on, and pose serious challenges to coastal aquatic ecosystems (**Carpenter *et al.*, 1992**; **Meyer *et al.*, 1999**; **Rabalais *et al.*, 2009**). The major challenges facing Africa's coastal countries are coastal erosion, resource over-use, pollution and the potential impacts of climate change (**Bauer, 2002**). Sea level rise is regarded as the most important aspect of climate change along the coasts (**Tsyban *et al.*, 1990**). A recent report on the vulnerability of 139 coastal cities to sea level rise designates the Ivorian coastal zone as highly vulnerable (**Hallegate *et al.*, 2013**). A one-meter rise in sea level in the 2100 decade will lead to the inundation of 1,800 km² of Ivorian lowlands (**IPCC, 1997**), affecting coastal infrastructures, ecotourism activities and economically important areas such as national seaports and the international airport (**Jallow *et al.*, 1999**) with relative economic annual average loss of US\$ 38 million dollars (**Hallegate *et al.*, 2013**). Sea-level rise produces a range of impacts (**Tsyban *et al.*, 1990**; **Huppert *et al.*, 2009**):

- Inundation and displacement of wetlands and lowlands;
- Coastal erosion and degradation of shorelines;
- Hypoxia;
- Coastal flooding during storm surges;
- Altered hydrological regimes and
- Saltwater intrusion into estuaries and freshwater aquifers.

Saltwater intrusion into freshwater aquifers is the most characteristic type of water quality degradation in the coastal environment (**Vengosh *et al.*, 1999**). Saltwater intrusion has been reported for the Benin and Niger delta coastal sedimentary basins of Nigeria (**Oteri & Atolagbe, 2003**), Keta Basin of Ghana (**Yidana *et al.*, 2010**), sedimentary basin of Togo (**Akouvi *et al.*, 2008**), quaternary aquifer of the Dar es Salaam region of Tanzania (**Mtoni *et al.*, 2012**), and for the karstified coastal aquifers of Central Lebanon (**El-Moujabber *et al.*, 2006**). In Côte d'Ivoire, although the impacts of sea level rise on coastal infrastructures are well documented (**Koffi, 1992; Kouakou *et al.*, 2012; Touré *et al.*, 2012; Wognin *et al.*, 2013**) and as shown in Photo 1. Two-third of the coastal extent of 566 km has been destabilized by coastal erosion (**Anoh & Pottier, 2008**). However, the impacts of these seasonal fluctuations of the tidal sea levels on the quality of adjoining coastal aquifers remain largely unknown (**UNEP, 2010**). Geochemical data on the Ivorian coastal water systems are either decades-old (**Durand & Guiral, 1994; Scheren *et al.*, 2004**) or limited in scope (**Seu-Anoi *et al.*, 2013**). Hence, this study was undertaken to narrow scientific gap by assessing the impacts of seasonality on coastal water systems along the east Ivorian coast.

Thesis rationale

Côte d'Ivoire does not suffer from physical water scarcity. According to **FAO (2015)**, for the year 2014, total renewable water resources per capita ($\text{m}^3/\text{inhabitant}/\text{year}$) for Côte d'Ivoire was 3,385, more than what is available to individuals in neighbouring Ghana (2,050), Benin (2,426), Togo (2,012), Nigeria (1,571) and even Germany (1,909). The country is rather facing economic water scarcity due to improper management and lack of investments in water infrastructures. According to **UNICEF Humanitarian Action report (2007)**, 40 % of rural water boreholes are defective. Water supply to rural communities along the coastal plains is via long-distance pipeline networks majority of boreholes along the coastal plains have been abandoned because of saltwater intrusion. Despite the more than 100-fold increase in annual groundwater abstraction rates from $95 \text{ Mm}^3/\text{year}$ in 2000 to $145 \text{ Mm}^3/\text{year}$ in 2010 (**Jourda, 2002**), Société de distribution d'eau de Côte d'Ivoire (SODECI), is still faced with a daily supply deficit of $225,000 \text{ m}^3/\text{day}$ (**Global Water Intelligence, 2014**). Rural communities are the most affected as only 50 % have access to portable drinking water (**Fonds Monétaire International, 2009**). This therefore makes for a high dependence on private wells and surface water systems to combat water stress. Although, the total renewable water per capita in Côte d'Ivoire exceeds the benchmark value of $1,700 \text{ m}^3/\text{inhab}/\text{year}$, indicative of water stress (**Falkenmark, 1989**), the total renewable water per capita registers a progressive decline. From the FAO AQUASTAT database, total renewable water per capita ($\text{m}^3/\text{inhab}/\text{year}$) was 5,024 in 1997, 4,074 in 2007, and now 3,385.



Photo 1: Impressions of the area under investigation: abandoned recreational facility at Azuretti along the coast (left), destroyed fence of a restaurant at Vridi (right).

One of the consequences of a decrease in total renewable water is the lowering of piezometric levels of coastal aquifers (**Oga *et al.*, 1998; Saley *et al.*, 2009**), predicted to worsen by the 21st century (**Allah-Kouadio *et al.*, 2016**). As regards the coastal surface water systems, crude oil spill of about 5,075 m³ along the littoral (**Struder, 2006**) with inadequate remediation and the death of thousands of tons of wild and farm fishes in the western parts of the Ébrié lagoon (**N'kaka, 2013**) are physical evidences of coastal water degradation that will be exacerbated by climate change. However, the ability of the coastal rural communities to respond in a rational way and remain resilient in the face of natural hazards is largely dependent on the understanding of their potential exposures and vulnerabilities. As a first attempt to quantify seawater component in coastal aquifers, this work will furnish baseline data necessary to highlight vulnerable areas and monitor future changes in coastal water quality. Results would also serve to inform feasible local community adaptive response strategies.

Thesis statement: Coastal waters are climate-sensitive systems; as such, changes in climatic conditions will affect their quality and inadvertently the inherent biodiversity.

Aim and objectives

The main aim of this study is a sound understanding of the status and seasonal trends of existing stressors (human and natural) on coastal water systems along the east Ivorian coast, and the impacts of these changes on phytoplankton as a measure of the inherent biodiversity. Focus was on underground (wells and boreholes) and surface water (rivers, Ébrié lagoon, and Atlantic coastlines) systems within 15 km inland from the Atlantic Ocean. The following are some questions to be answered:

- Is coastal water quality influenced by seasonality?
- Are there spatiotemporal variations in coastal water quality?
- Is there hydrologic interaction between coastal water systems? Is this subject to seasonality?
- What are the main abiotic environmental variables controlling coastal water chemistry?
- How do the seasonal changes in coastal water quality affect inherent aquatic biodiversity?

To achieve its aims, this study adopted the change assessment framework for the rapid ecological assessment of biodiversity in inland water, coastal and marine areas (**CBD/Ramsar, 2006**), an integrated approach that cuts across the fields of geology, geochemistry, biology, and sociology.

Thesis outline

This document consists essentially of five main parts: a general introduction, the main section of the work (parts I, II and III) and a concluding part. Under the section of general introduction, the topic was duly presented together with the rationale for the study, aims, objectives, and conceptual framework were also described under this section. Part I presents the outcome of desktop study. It exposes the physiographical environment, climate, geology, hydrology and hydrogeology of the Ivorian coastal area. Part II, the first research chapters provided details on materials and analytical methods inclusive of sampling size, duration, plot sizes, field and laboratory analyses and statistical tools and software employed for data exploration and interpretation. Part III discusses the results in detail under four main headings. Each heading corresponds to a chapter:

1. Physical habitat assessment
 - Coastal topography based on digital elevation model.
 - Land use dynamics within a 25-year period (1989/90 – 2014/15) based on satellite imagery from Landsat using remote sensing and GIS techniques.
 - Coarse-scale lithological analyses of surface rock exposures to ascertain natural contributions to water quality.
2. Water quality (abiotic environmental variables)
 - Characterize coastal inland waters based on chemistry, isotopic signatures, and microbiological attributes (faecal coliform bacteria).
 - Estimate groundwater recharge using climatic parameters (temperature, precipitation, and evapotranspiration) and mathematical operations,
 - Determine fractional composition of different water sources (seawater intrusion assessment) using quasi-conservative elemental proxies and isotopic signature (oxygen-18) in an Endmember Mixing Analyses (EMMA) modelling approach (mass balance models and multivariate analyses).
3. Biocenosis analyses (phytoplankton)
 - Establish a link between water quality and biodiversity (phytoplankton) from randomly selected points on coastal surface water systems using diversity indices (species richness, abundance, density).
 - Determine main environmental abiotic factors controlling phytoplankton dynamics using Kohonen self-organizing feature maps, a novel artificial neural network (ANN) technique.

4. Socio-economic survey - *a pilot study*

- Address socio-economic concerns of the riverine communities regarding changes in coastal water quality and underpin their vulnerability to coastal resources degradation.

The text culminates in concluding remarks and recommendations for further monitoring of resources and local adaptation and mitigation strategies.

PART I:
LITERATURE REVIEW

CHAPTER 1: Physiographical environment

As a sub-Saharan country in West Africa, Côte d'Ivoire is geographically located between latitudes 4° 30' and 10° 30' N and longitudes 2° 30' and 8° 30' W. It is bordered by Liberia and Guinea in the west, by Mali and Burkina-Faso in the north, by Ghana in the east and in the south by the Atlantic Ocean. Geomorphologically, the Ivorian coast is divided into two parts (**Koffi, 1992; Nicole, 1994**): the first part, the west coast extends from Liberia (western border) to Fresco in the central parts. It is the most stable part of the coast, underlain mainly by metamorphic rocks and sands (**Koffi, 1992**). The second part, the east coast with an approximate length of 360 km extends from Fresco to Axim (Ghana border). This area is characterized by coastal lakes (Labion, Dadié and M'bakre) and interlinked lagoons (Grand-Lahou, Ébrié and Aby) that together occupy an area of 1,200 km² (**Durand & Skubich, 1982**), separated from the Atlantic Ocean by a narrow coastal strip between 1 and 8 km wide (**Dufour, 1982**). The east coast has a permanent link to the Atlantic Ocean via the artificial Vridi canal, 2.7 km in length, width of 370 m and a dredged depth of 13.5 m, dug up in 1950 to foster international trade (**Chantraine & Dufour, 1983**). The eastern coast is underlain mostly by sands and therefore highly prone to coastal erosions. Landward retreat of coastline has been estimated between 1 and 3 m/yr (**Abe *et al.*, 2014**).

1.1. The geology of Côte d'Ivoire

Côte d'Ivoire evolved as a fault-fault-ridge (FFR) junction during the separation of the African plate from the Australia/Antarctica during Early Cretaceous (~ 145 million years ago) (**Sclater *et al.*, 1976**). The separation of the African and South America plate lasted over a period of 100 Ma, from early Jurassic to middle Cretaceous (**Schwartz, 2005**). The geology constitutes 97.5 % basement rock and the rest sedimentary basin (**Martin & Tastet, 1972**). The basement rocks of Precambrian-age belong to the West African Craton (**Rougerie, 1960; Martin & Tastet, 1972**), whereas the sedimentary rocks formed at the culmination of late Jurassic to Early Cretaceous tectonism (**Brownfield & Charpentier, 2006**).

1.1.1. The basement rocks

The basement rocks belong to the West African Craton (**Tagini, 1971**), consolidated towards the end of the middle Precambrian (**Bonhomme, 1962**). It comprises three distinct age provinces (**Tagini, 1971**):

1. The Liberian age (~ 2300 – 3000 Ma) or Kénéma-Man province (**Schlüter, 2008**) is restricted to the Man area and the southwestern part of the country comprised of migmatites, granites, granitic gneiss, and charnockites (**Tagini, 1971; Hurley *et al.*, 1971**).

2. The Birimian age (~ 1500 - 2300 Ma) province or Baoulé-Mossi domain (**Schlüter, 2008**) that covers a greater part of national territory includes rocks of the NE-SW trending rock sequences of the Birimian greenstone belt of Paleoproterozoic age (~ 2166 ± 66 Ma). It is composed of metamorphic rocks (schist, mica schist, and quartzite), massive migmatites, and plutonic rocks (granites and granodiorites).
3. Localized Carboniferous to Precambrian age (~280 – 1700 Ma) basic rocks (dolerites) of little importance.

The basement area (Figure 1) is divided into two principal geological domains separated by the major north-south trending Sassandra fault (mylonitic zone) (**Bessoles, 1977; Schlüter, 2008**). The western flank of the Sassandra fault is dominated by rocks of Archaean age (Kénéma-Man domain) and the central and eastern flank is dominated by rocks of Paleoproterozoic age (Baoulé-Mossi domain) (**Kouamelan, 1996; Schlüter, 2008**). The crystalline rocks of Archaean age are the oldest in the country.

1.1.2. The Tertiary-Quaternary sedimentary basin

The sedimentary basin of Côte d'Ivoire is a mega pull-apart basin (**Blarez, 1986**). It is bordered in the south by the northern shores of the Gulf of Guinea. The basin has a crescentiform shape as its development follows the concave contours of the basement rocks (**Salard-Cheboldaeff, 1990**). The basin has a length of 360 km and a maximum width of 35 km at the eastern border (**Wright *et al.*, 1985**). It is a transboundary basin and extends laterally from Fresco in the central parts to Axim (Ghana) in the east, where it forms the Tano Basin (**Salard-Cheboldaeff, 1990**). The basin is composed of onshore and offshore parts (Figure 2) (**Durand & Skubich, 1982**). The onshore part occupies an area of 9,500 km², out of which coastal lakes (Labion, Dadié & M'bakré) and lagoons (Grand-Lahou, Ébrié, and Aby from west to east) occupy 1,200 km² (**Durand & Skubich, 1982**). The offshore part is the largest part of the basin with a surface area of 22,000 km² and width of 750 km. It extends seaward from the coastline to a depth of 10,000 m, where it is exploited for its hydrocarbon potentials (**Blarez, 1986**). The evolution of the Ivorian sedimentary basin began during the Early Cretaceous (possibly during the Neocomian) (**Nairn & Stehli, 1973**). It is traversed by a major east-west trending fault, an extension of the St. Paul transform fault zone referred to as '*faille des lagunes*' (Figure 3), (**Spengler & Delteil, 1964**). This fault separates it into two distinct blocks: the northern flank of the fault is made up of Mio-Pliocene (5 – 8 Ma) age sediments with altitude between 50 and 100 m (**Martin & Tastet, 1972**). This crustal piece is referred to as high plateau (hauts plateaux) (**Martin & Tastet, 1972**). The southern flank of the fault with Pleistocene age sediments has a depth of up to 5,000 m to the basement along the coast (**Wright *et al.*, 1985**).

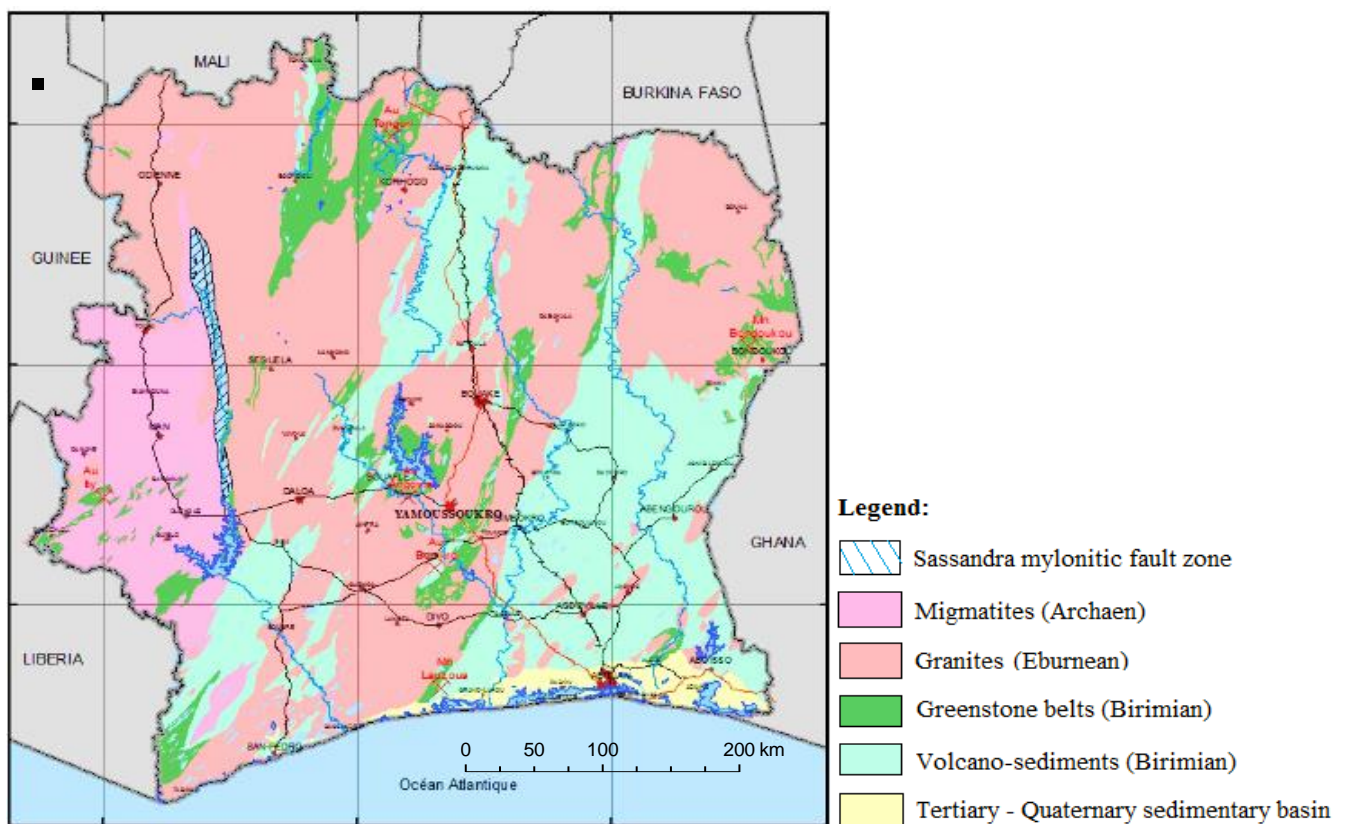


Figure 1: Geology map of Côte d'Ivoire (Kouamelan, 1996).

This block referred to as ‘bas plateaux’ (low plateau), comprised mostly of marine sands with intercalations of clays or carbonates (**Martin & Tastet, 1972**). Figure 4 shows the longitudinal section of the sedimentary formations.

1.1.2.1 The stratigraphic succession of the basin

There are no records of Paleozoic sequences (**Wright *et al.*, 1985**). The **Mesozoic** continental sequences are the oldest sedimentary layer. They overlie discordantly deeply eroded Precambrian shield (**Simon & Amakou, 1984**). These Aptian (~118 Ma) marine sediments were deposited during marine transgression (**Spengler & Delteil, 1964**). They are composed of sands, sandstones, conglomerates, brightly-coloured clays and shales with inclusions of black clay described as the ‘*série versicolore*’. The sedimentary formation of Albian times (~105 Ma), lies concordantly over the basal *série versicolore*. The rock succession with an approximate thickness of 2,600 m is rich in organic materials with traces of oil and gas from borings (**Spengler & Delteil, 1966**). Its lowermost parts are composed mainly of finely bedded black clayey shale with occasional sandy intercalations, while coarse-grain deposits, indicative of paralic (coastal plain) sedimentation, characterize its uppermost parts (**Spengler & Delteil, 1964**). The Cenomanian (~95 Ma) layer recognised only in drill cuttings lies concordantly on the Albian and passes without break into the Turonian (~90 Ma). This formation is composed mainly of clastic materials with constant thickness (**Spengler & Delteil, 1964**). The sea was once again transgressive during the Turonian-Maestrichtian (~90 – 70 Ma). This period marked the break-up of the old continent into two regions. The layers are composed of sandy facies with clayey facies further to the west. As observed from studies of its microfauna, this formation prograde into the Coniacian-Maestrichtian (~88 – 70 Ma) layer (**Apostolescu, 1961; Spengler & Delteil, 1964**). After a regression during the Late Cretaceous, the sea was again transgressive during the Palaeocene (~60 Ma) and Eocene (~53 Ma) times. The Paleocene formation reaches a thickness of 500 m in the western part of the basin (Grand Lahou). This however diminishes in its eastern parts (**Nairn & Stehli, 1973**). It comprise mainly of glauconitic clays at its western end and limestone, glauconite-bearing sandstones, and sandy clays at its eastern end. The basin maintained its form during the Eocene. Eocene sediments lie concordantly on the Palaeocene layers, with thickness up to 490 m in the western part (**Nairn & Stehli, 1973**). It is composed of more or less sandy clays with intercalations of thin limestone bands at the lower parts (**Nairn & Stehli, 1973**). Following the retreat of the sea at the end of the Middle Eocene, Oligocene (~30 Ma) sequence is completely absent due to sea regression. This unconformity is commonly referred to as the mid-Oligocene circum-African unconformity (**Wozazek, 2001**).

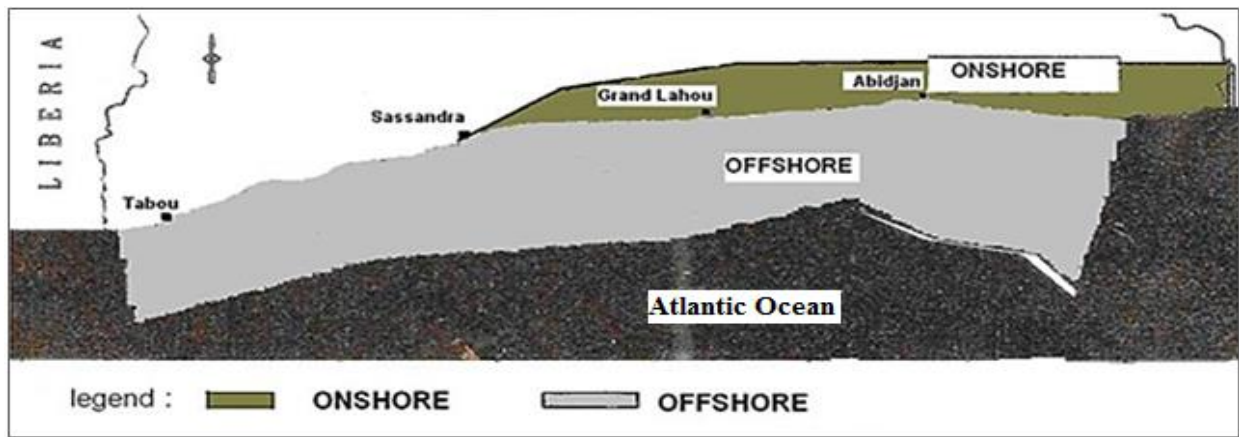


Figure 2: The subdivisions of the sedimentary basin of Côte d'Ivoire (Petroci & Beicip, 1990).

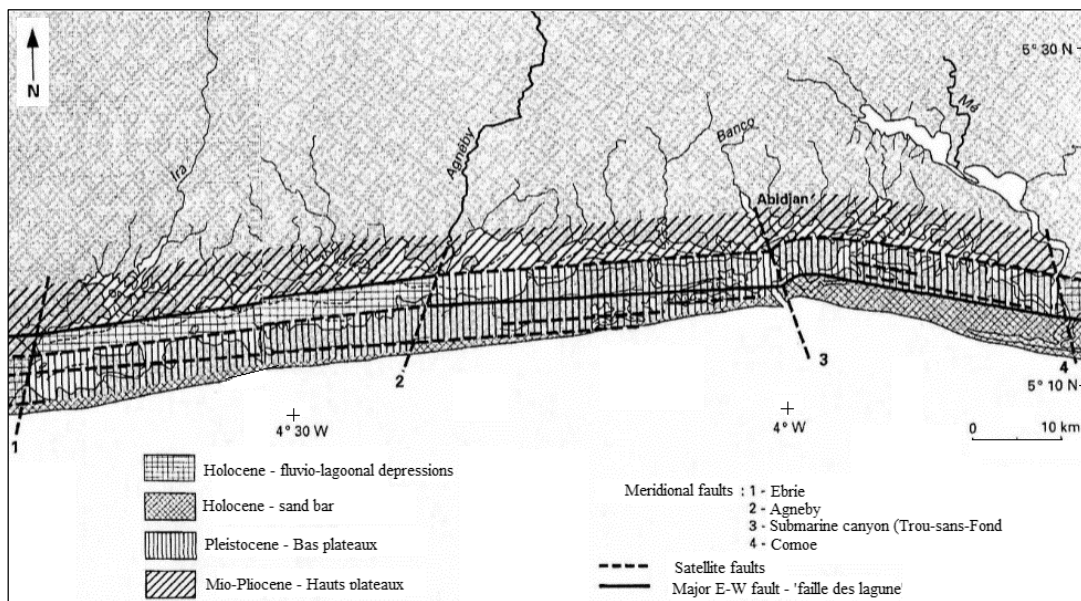


Figure 3: The structural geology of the Ivorian sedimentary basin after Tastet and Guiral (1994).

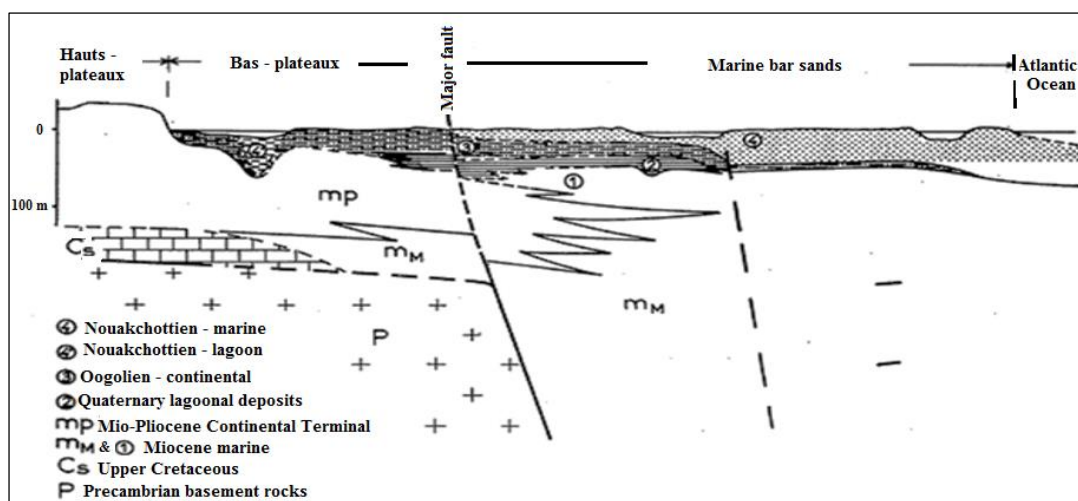


Figure 4: A north-south cross-section through the sedimentary basin in the Abidjan area after Tastet (1971).

During this period, more than 390 m of Tertiary rocks were eroded by the regressing sea (**Brownfield & Charpentier, 2006**). During the Miocene (~ 20 Ma), the sea was once again transgressive, but only flooded the continental margins. This triggered the formation of a small marginal basin whose landward extent is limited by a large fault. The east-west extent of the basin is nearly 35 km with a thickness of approximately 600 m (observed in drillings near Abidjan). It comprises of grey-black and greenish-grey clays with occasional sandy intercalations. It lies discordantly on the Cenomanian, marking the end of the marine phase in Côte d'Ivoire. Continental sediments, sands, reddish clays, and coarse-iron stained sandstones with a total thickness of 50 – 100 meters represent the Pliocene formation (**Digbehi *et al.*, 2001**). Above this Pliocene sequence, in the coastal region lies the Quaternary (with a thickness of 50 m), represented by coastal sands and dark lagoon muds. It is the topmost layer of the sedimentary formation.

1.1.2.2. The structural development of the sedimentary basin

The basin has undergone complex geologic history (**Blarez & Mascle, 1988; Chierici, 1996**). It is similar in structure (wrench-shaped) and stratigraphy to the coastal sedimentary basins of Ghana (Tano and saltpond), Togo (Keta), Benin (Benin), and Nigeria (Dahomey embayment) (**Clifford, 1986**). The geologic history of the basin can be divided into pre-transform (late Proterozoic to Late Jurassic), syn-transform (Late Jurassic to Early Cretaceous), and post-transform (Late Cretaceous to Holocene) stages of basin development (**Brownfield & Charpentier, 2006**). The basin has a southward deepening due to a major ENE-WSW trending fault with vertical and lateral displacements resulting in steep coasts and tear faulting respectively (**Spengler & Delteil, 1964; Affian *et al.*, 1987**). The middle Mesozoic (Late Jurassic ~ 164 Ma) marked the depression of the upper Guinean arch (to a thickness of about 2,000 m) and the formation of the sedimentary basin in the present coastal region of the country (**Nairn & Stehli, 1973**). The Albian (~ 113 Ma) times marked the formation of the continental marginal flexure in Côte d'Ivoire (**Nairn & Stehli, 1973**). During the Cenomanian (~ 100 Ma), there was the relaxation of a strong sinking tendency. Deposits formed during this period have strong clastic character in some parts. During this period, the basin tilted in such a way that the western part was uplifted and already formed deposits were eroded in some parts. Conversely, the eastern part of the basin underwent expansion and now includes part of Ghana (**Nairn & Stehli, 1973**). The Turonian (~ 93.9 Ma) was a main period of sea transgression while seaward regression occurred during the Maestrichtian (~ 72.1 Ma). During the Turonian, the east - west directed continental marginal fault became active accentuated by tectonic processes: south of which developed a thick predominantly clay sedimentation, while in the north, a relatively thinner sequence of detrital sediments developed. The sea remained in the coastal basins until Maestrichtian (**Nairn & Stehli,**

1973). The Paleogene (Palaeocene to Oligocene) period marked a clear-cut structural difference in basin development: regions close to the Atlantic and regions lying to the north within the continents (**Nairn & Stehli, 1973**). During the Neogene (Miocene – Pliocene) to Quaternary period, the sea transgressed over the country for a short time (not extending far into the continental area). This trigger the formation of east-west directed coastal basins with northern margins a little north of the present coastlines, owing their origin to the ENE – WSW flexure-like bending of southern margin of the upper Guinean arch (**Nairn & Stehli, 1973**). The width of the flexure zone is between 50 and 100 km, characterized by a strong sinking of its southern flanks and strong uplift of its northern limb that results from a permanent oscillation of the blocks, in relative position against one another (**Nairn & Stehli, 1973**). In the south, extremely thicker sedimentary sequence accumulated, in some areas passed into a fault or series of faults arranged *en echelon*. This resulted in a depression of the southern limb accompanied by synsedimentary faults and an increase in thickness of sedimentary layers towards the Atlantic Ocean (**Nairn & Stehli, 1973**).

1.1.3. The regional geology of the Ébrié lagoon sub-catchment (the study area)

The study area belongs to the sedimentary basin area. It is geographically located between longitudes 5° and 5° 30' N and latitudes 3° 40' and 5° W, covering an area of approximately 1,200 km² (Figure 5). The present coastal morphology is a result of young parallel faults running in an ENE-WSW direction; with vertical displacement (resulting in steep coast) and lateral displacements (tear faulting) (**Nairn & Stehli, 1973**). This is reflected by the eastward deflection of the mouth of river courses (**Spengler & Delteil, 1964**). The regions north of the fault were uplifted and displaced towards the west while, the south of the fault sank and was displaced towards the east (**Nairn & Stehli, 1973**). The major lagoon fault separates the area into two parts consisting of lithology of different ages; rocks of Tertiary (Mio-Pliocene) age underlie the north of the lagoon, whereas Quaternary age rocks underlie areas south of the Ébrié Lagoon (**Martin & Tastet, 1972**).

1.2. Hydrological and hydrogeological settings of the Ebrié lagoon subcatchment

Côte d'Ivoire has four main river basins (Figure 6) with covering an area of 265,000 km². These are from west to east: Cavally (basin area: 28,800 km²), Sassandra (75,000 km²), Bandama (97,000 km²) and Comoé (78,000 km²) with average flow rate of 600 m³/s, 575 m³/s, 400 m³/s and 300 m³/s, respectively (**Avenard et al., 1971**). Regional river flow direction is in a north-south direction towards the Atlantic Ocean via the Ébrié lagoon, constrained by the gently sloping nature of the coastal plains, or directly into the Ocean as in the case of the Bandama River. Other smaller basins are:

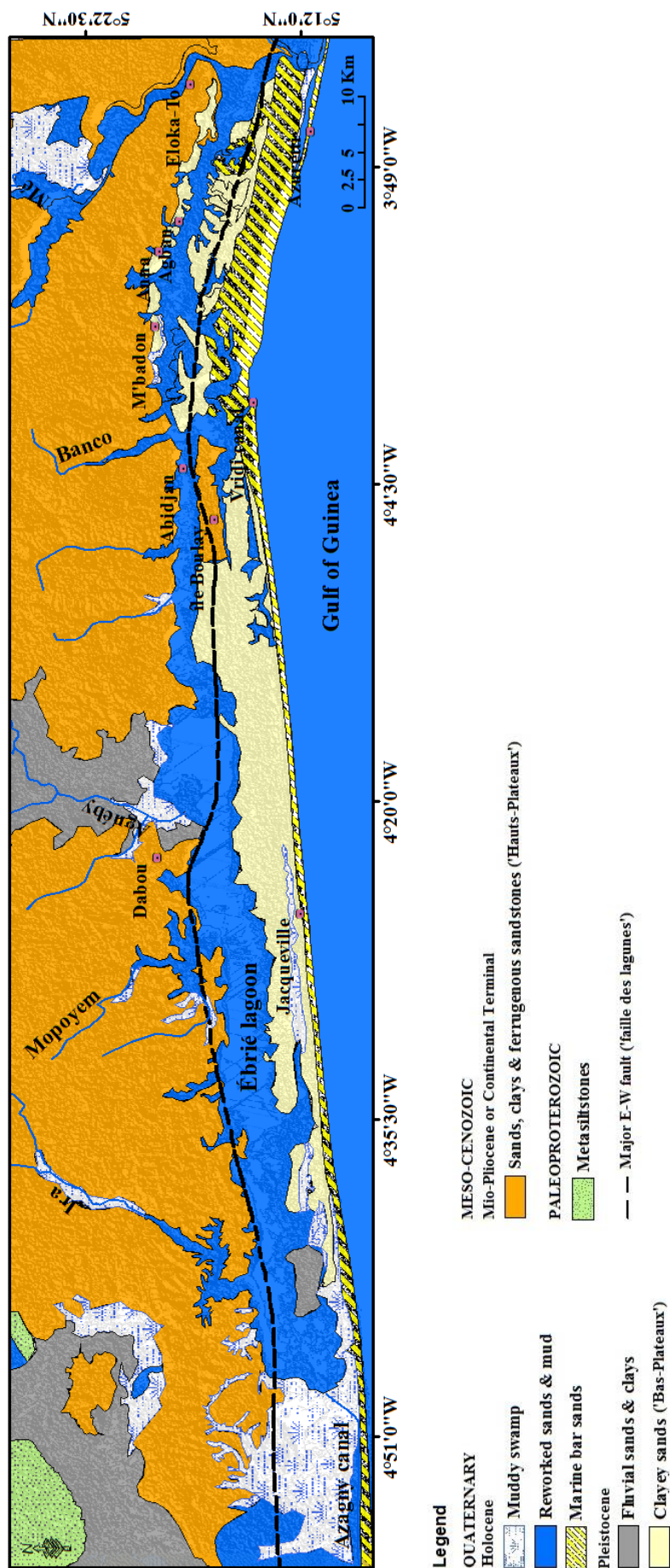


Figure 5: The geology map of the study area after Delor *et al.* (1992); Simeon *et al.* (1992).

1. tributaries of the river Niger; Baoulé, Bagoé and Gbanhala,
2. coastal rivers with surface area of 23,000 km². These are Tabou, San Pedro, Niouniourou, Boubo, Agnéby, Mé and the Bia rivers, from west to east.

The coastal rivers are part of networks of rivers and streams known as 'rivières côtières'. Together the Agnéby and Mé Rivers make up the Agnéby-Mé river basin, of which the Ebrié lagoon is a sub-catchment (Figure 6). The headwater of the Agnéby River is at an altitude of 250 m in Agoua. It has a basin area of 8,900 km² and its main tributaries are M'pébo, Kavi and Séguié Rivers (**Avenard *et al.*, 1971**). The Mé River, on the other hand covers an area of 4,300 km² and its main affluent is the Mafou River (**Avenard *et al.*, 1971**). The main aquifer systems within the sedimentary basin are (**Jourda, 2002**):

- The Maastrichtian age semi-artesian layer,
- The Mio-Pliocene age (5 – 8 Ma) Continental Terminal (CT) layer and
- The Quaternary (less than 1.8 million years old) layer (QM).

In this study, only the Continental Terminal (CT) and Quaternary (QM) are the main interest of this study. The CT aquifer represented by n3 and n4 in Figure 7, is Mio-Pliocene age (**Charpy & Nahon, 1978**). It is a confined unit referred to as the aquifer of Abidjan (**Aghui & Biemi, 1984**). It is the principal aquifer and main drinking water source for the Abidjan population (**Guérin-Villeaubreil, 1962; Jourda, 2002**). It has a lateral extent of 100 km (**Jourda, 1987**) and is comprised mainly of detrital clayey-sands, sands and few clay lens (**Berton, 1961; Roose & Chéroux, 1966**). The aquifer has a transmissivity of between 0.14 and 20 m²/s (**Jourda, 2002**). Its permeability is 10⁻³ m/s, but may reduce to values between 10⁻⁵ and 10⁻⁶ m/s due to lithofacies variations (**Loroux, 1978; Aghui & Biemi, 1984; Jourda, 2002**). The cuirass and/or cuirasse ferrugineuse (Figure 7), the top layer of the CT is likely an extension of the Upper Miocene/Lower Pliocene planation surface (**Wozazek, 2001**). It is observed west of Abidjan along Dabou-Toupah-Grand Lahou axes (**Roose & Chéroux, 1966**). The Quaternary aquifer (QM) represented by H3 and H4 in Figure 7 comprise of two subunits: coarse-grained sands of marine origin (Nouakchottien aquifer) and fine to coarse-grained fluvial sands (Oögolien aquifer). It is highly vulnerable to contamination because of its shallow depth (**Jourda, 2002**). Its permeability ranges between 10⁻³ and 10⁻⁴ m/s (**Jourda, 1987; Jourda, 2002**).

The Ébrié lagoon

The Ébrié lagoon is the main hydrologic structure within the Ébrié lagoon sub-catchment. It is an elongate brackish water reservoir parallel to the Atlantic coast. It is separated from the Atlantic Ocean by a narrow coastal strip of width between 0.1 and 8 km (**Roose & Chéroux, 1966**).

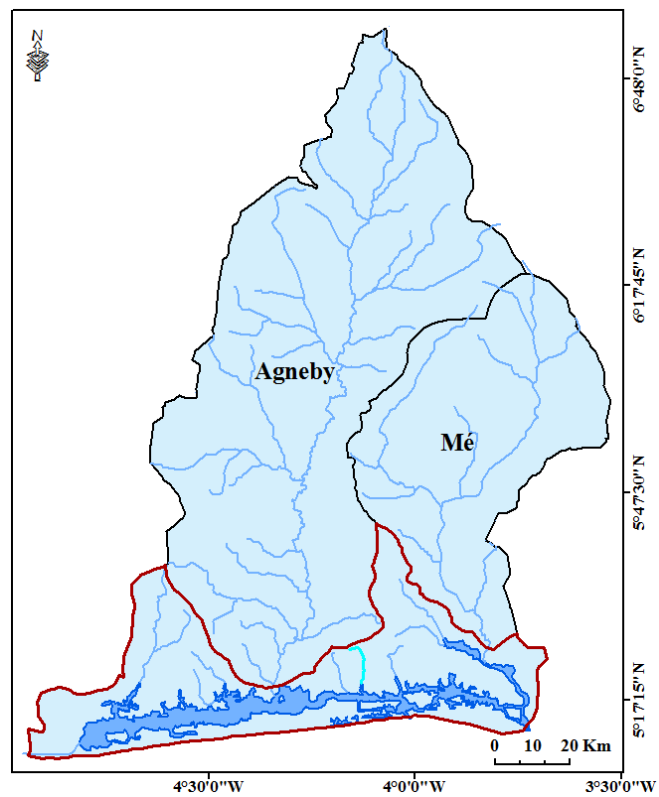
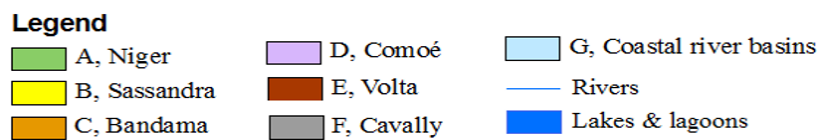
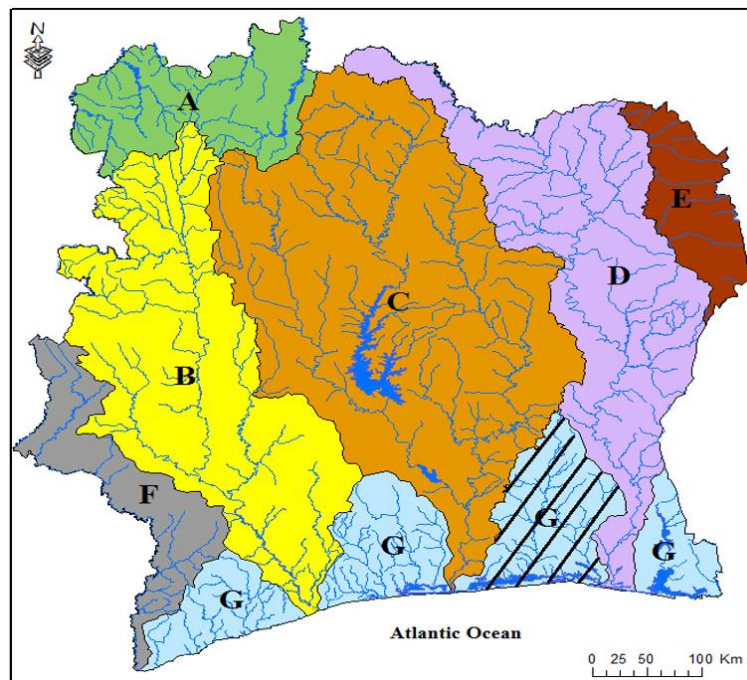


Figure 6: Map of the river basins of Côte d'Ivoire (top). Hatched areas represent the Agnėby-Mė coastal river basin (bottom). The Ebriė lagoon sub-catchment (study area) is highlighted in red.

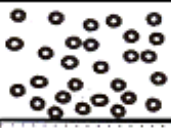

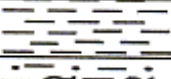

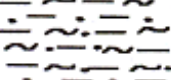


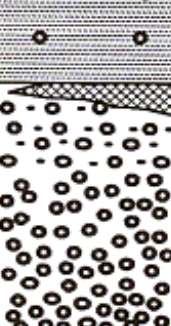


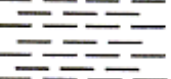

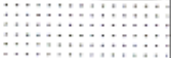
EPOCH	LITHOLOGY		HYDRO-LITHOLOGY	HYDRO-GEOLOGIC LOG	DESCRIPTION	Maximum thickness (m)
QUATERNARY	Coarse sands (marine)	H4		aquifer	Nouakchottien	50
	Fine to coarse sands	H3		aquifer	Oögolien	30
	Peaty clays	H2			Impermeable	16
	Silty marls	H1			sometimes discontinuous	40
TERTIARY	Cuirass	n4		aquifer	Continental Terminal (CT) clay lens	70
	Clayey sands					90
	Coarse sands (fluviatiles)	n3		aquifer		
	Black clay	n2		aquifer	Impermeable	10
	Gravelly sands	n1			Base of Tertiary	20
PALEO-CENE	Ferruginous clayey sandstone			aquifer	Impermeable	20
MAEST-RICHTIAN	Calcareous sandstone				Upper Cretaceous	50
	Sands					

Figure 7: Hydrogeological log of the aquifers of the Ivorian sedimentary basin. Modified from Aghui and Biemi (1984).

It is the largest estuarine system in West Africa with volume of $2.7 \times 10^9 \text{ m}^3$ (**Guiral, 1992**). It has a surface area of 566 km^2 , a length of 130 km, an average width of 7 km, and an average depth of 4.8 m (**Varlet, 1978**), although its dimensions have long been reduced by silting and land reclamation. In its eastern borders, the lagoon is connected to Aby lagoon via the Assinie canal, 48 km, dredged between 1955 and 1957 (**Pàges *et al.*, 1979**). It is bounded in the west by the Azagny national park (Ramsar site since 1996). In these parts, it is connected to Grand-Lahou lagoon via the Azagny canal, 17 km long dug up in 1939 to facilitate the exploitation of manganese (**Pàges *et al.*, 1979**). Permanent exchanges with the Atlantic Ocean are via the artificial Vridi canal in its central parts. This accounts for its 38 billion m^3 per annum seawater input into the lagoon. Conversely, the ocean receives approximately 50 billion m^3 per annum of mixt water sources via the lagoon (**Varlet, 1978**). Direct precipitation accounts for a smaller fraction ($1,100 \text{ Mm}^3$ per annum) (**Varlet, 1978**). It is drained from west to east by four rivers: the Ira, Agnéby, Mé, and Comoé, together they account for over 90 % ($9,850 \text{ Mm}^3$ per annum) of its freshwater input. The Ébrié lagoon lies at the focal of two distinct geological provinces. The Continental Terminal lies at its northern areas, while the southern coastal plains are underlain by Quaternary marine bar sands. Two biosphere reserves borders on the Ébrié lagoon. These are:

- Banco (3,200 hectares) in its central part and
- Azagny national park (9,400 hectares) at its western fringe.

The soils in the coastal areas are mostly sandy and sandy clays in the northern areas of the lagoon, and mainly hydromorphic and podzols in its southern parts (**Roose & Chérour, 1966**).

1.3. The climate of the littoral zone

Côte d'Ivoire has four distinct agro-climatic zones, defined by variations in the frequency and rainfall amount (**Goula *et al.*, 2007**). This ranges from semi-arid conditions in the extreme north to humid, equatorial climate in the south (**Goula *et al.*, 2007**). The coastal area exhibits the equatorial climate, characterized by bimodal rainfall patterns intercepted by two dry seasons. Total annual precipitation for 2014 was 2,142 mm (**National meteorological station, SODEXAM**). Surface air temperature is constant and ranged between 24°C and 28°C . Air temperature reaches its maximum of 32°C in April and its minimum of 24°C in August. Relative humidity is constant for the year with an annual average of 83 %.

1.3.1. The maritime climate (ocean upwelling)

The Ivorian coastal zone exhibits hydro-climatological regimes slightly different from its inland areas. During this period, sea surface temperature is higher than surface air temperature.

Morlière (1970) identified three principal marine seasons. These are:

- Short cold season (December - January): Sea surface temperature is between 27 °C and 29 °C and salinity is on the average of 34.9 ‰ (Figure 9) during this period. The marine frontals are cold. Cold nutrient rich waters are superimposed on the warm waters of the southern Atlantic and dissolved oxygen levels generally fall (**Mensah & Koranteng, 1988**).
- Long hot season (February - May): a period just before the onset of the upwelling, when temperatures are rising and peaks at 28 °C in the month of May (**Pàges *et al.*, 1979**). Salinity levels are high (35 ‰) during this period. This warm signal is damped by the onset of the long cold season (July – October).
- Long cold season (July – October): this is the major ocean upwelling. Nutrient-rich cold water with higher salinity is transported to the ocean surface during this period (**Bjerknes, 1969**). The cold water welling up to the surface cools the air in the region. This promotes the development of sea fog. This period coincides with the dry season inland, off the coast.
- Short hot season (November – December): The annual maritime seasonal cycle culminates in a small hot season. Fluvial processes still dominate the coastal environment during this period marked by a relative increase in temperature and salinity on the Atlantic coast.

Supporting details from the works of **Colin (1988)**, **Binet and Marchal (1993)**, **Aman, 2007**, **Aman and Fofana (1998)**, **Aman *et al.* (2007)** and **Djagoua *et al.* (2011)** confirms the Ivorian coastlines as a strong upwelling front. This seasonal phenomenon occurs off the coast between Cape Palmas (Liberia) and Cape Three Points (Ghana), driving the productivity of the system (**Djagoua *et al.*, 2006**). The area is part of the Central West African Upwelling (CWAU) zone (**Hardman-Mountford & McGlade, 2003**). Ocean upwelling is consistent with global solar energy imbalance and eustatic sea level rise. It has close links to the seasonal variations of sea surface temperature (SST) in the Gulf of Guinea (**Aman & Fofana, 1998**). Two upwelling periods have been identified, a major upwelling between June and October and a minor upwelling lasting only three weeks between January and February (**Koranteng, 1998**). Upwelling is more intense at the west coast (Sassandra – Abidjan), with a WSW-ENE trending coastline as compared to the east coast (Abidjan – Ghana) with a WNW-ESE coastline orientation (**Morlière, 1970; Allersma & Tilmans, 1993**). Sea surface temperature, SST drops to 23 °C during the major upwelling season and to 24.5 °C during the minor upwelling season (**Longhurst, 1962**). It however, varies between 27 and 29 °C outside the upwelling seasons (**Allersma & Tilmans, 1993**).

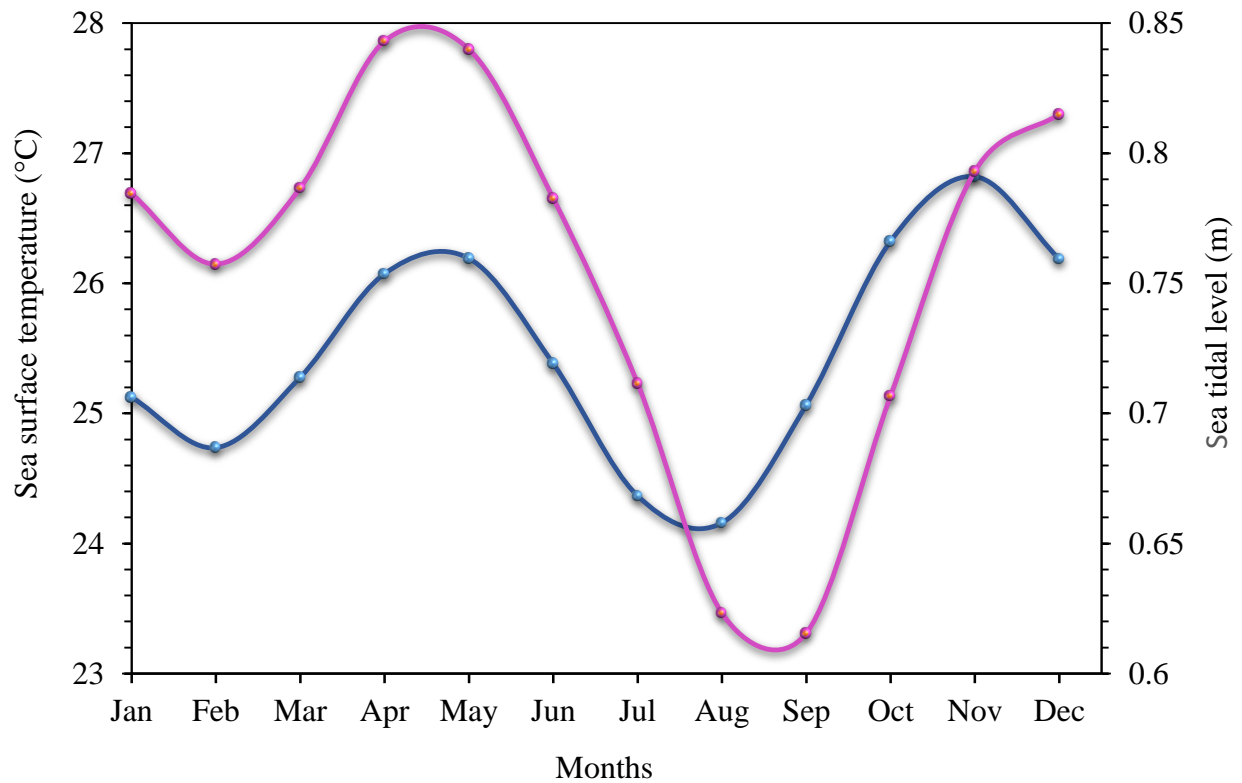


Figure 8: Monthly variations of sea surface temperatures, SST (pink line) (data source: maree.shom.fr), and mean tidal sea level, MSL (blue line) (data source: <http://seatemperature.info>) of the Atlantic Ocean off the Abidjan coast for 2014.

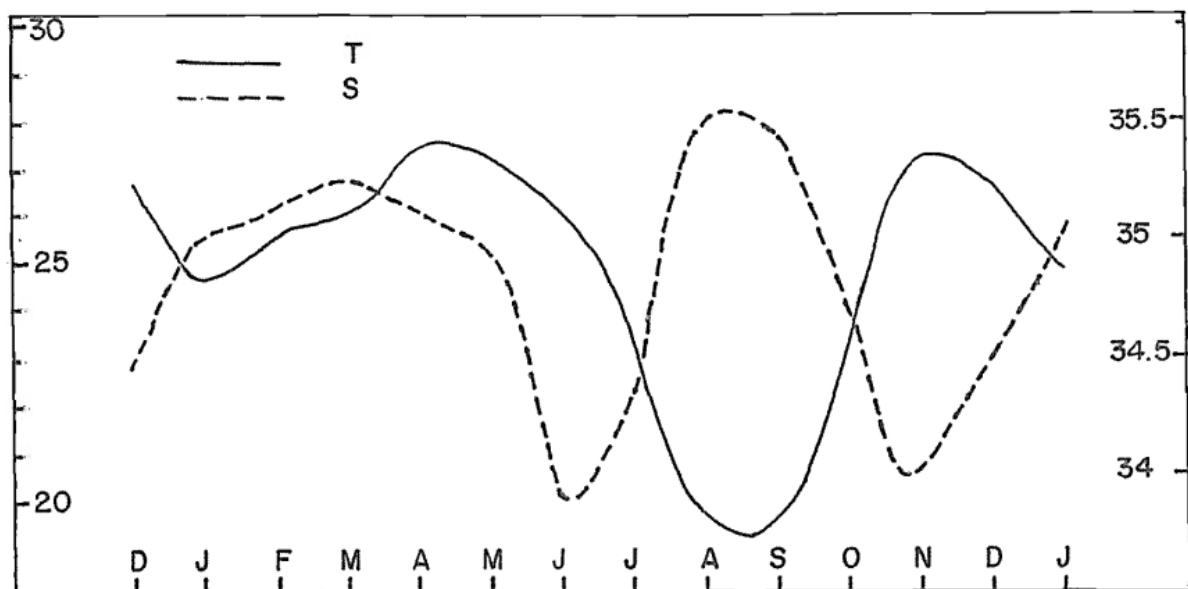


Figure 9: Temperature (T) and salinity (S) fluctuations of the Atlantic Ocean in front of Abidjan (average: 1966 - 1990). (Source: Morlière, 1970).

Mean monthly variations in sea surface temperature (SST) and tidal sea levels (m) for 2014 are given in Figure 8. Maximum SST of 27.9 °C was recorded in April, while minimum SST of 23.3 °C was recorded in the month of September. The tides of the Atlantic Ocean off the Abidjan coast are semi-diurnal (**Simon, 2007**), characterized daily by two maximum (high) tides and two low tides. Tidal height was on the average of 0.2 m during low tides, and 1.1 m during high tides in 2014 (**maree.shom.fr**).

1.3.2. Climate change perspectives

Climate changes because of imbalance between the Earth's incoming and outgoing radiation energy (**Oude Essink, 1996**). The Earth now absorbs 0.85 ± 0.15 watts/m² more energy from the sun than it is emitting into space (**Hansen et al., 2005**). This imbalance attributable to increase of greenhouse gases viz. carbon dioxide results in warming of the Earth (**Church et al., 2013**). Scientific evidence for warming of the Earth's climate system is unequivocal (**IPCC, 2014**). Atmospheric concentrations of carbon dioxide fluctuated between 180 ppm and 280 ppm (Figure 10) in the past 800,000 years (**National Oceanic and Atmospheric Administration, 2016**). In May 2013, carbon levels reached the 400 ppm mark and as at December 2015, atmospheric level was 401.85 ppm (**National Oceanic and Atmospheric Administration, 2016**), 13 % higher than the upper limit safety value of 350 ppm. Furthermore, from 1964 to 1964, the rate of CO₂ increase was 0.73 ppm/year. Presently, it increases at an alarming rate of 2.11 ppm/year, 100 times more than pre-industrialized times, and this with a tendency for continuity (**National Oceanic and Atmospheric Administration, 2016**). A fact however, is that since its inception, the Earth's climate has always changed in response to changes in Earth's orbits, variation in the tilt of its axis and continent drift (**Wyman, 1991**). The main threat to humanity today is not climate change; it is rather the potential rate of change (**Wyman, 1991**). A consequence of this increase is global warming. Increases in sea level are consistent with warming (**IPCC, 2007**). On the average, global sea level rose by 1.7 mm/year from 1961 to 2003, but since satellite measurements began in 1992; the global rate has been 3.1 mm/year for 1993 to 2003 (**IPCC, 2007**). Higher sea levels can change salinity and water circulation patterns of coastal estuaries and bays, with wide and varied consequences for the inherent biota such as phenological changes, spatial shifts, low productivity, mortality, and extinction. The main impact of sea level rise along the African coast inclusive of the Abidjan coast is/would be landward retreat of coastlines (beach erosion) with consequent flooding and forced migration of coastal populations (**Ibe & Awosika, 1991; Brown et al., 2011**)

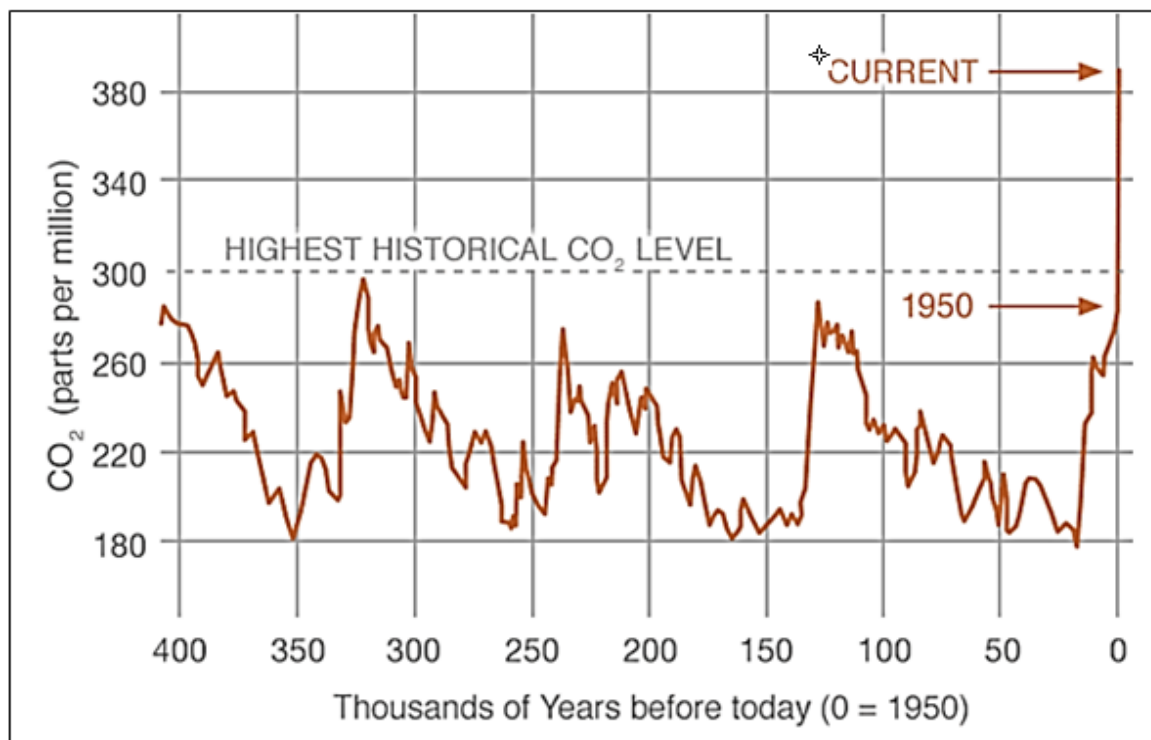


Figure 10: Monthly mean CO₂ levels at Mauna Loa Observatory, Hawaii. Current denotes average global atmospheric CO₂ level as at April 2015 (404.35 ppm). (Source: National Oceanic and Atmospheric Administration, 2016).

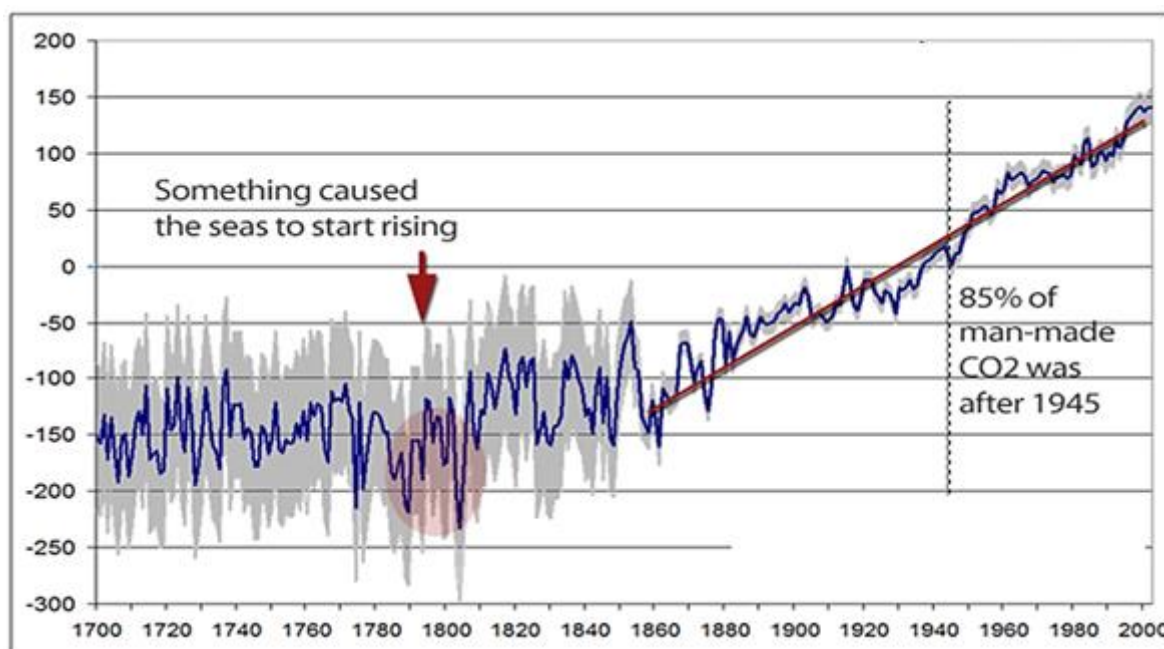


Figure 11: Global sea levels have been rising since 1800. The rate of rise has been constant for the past 150 years. Grey shadings represent the standard error. (Source: Jevrejeva *et al.*, 2008).

PART II:
MATERIALS AND METHODS

CHAPTER 2: Physical habitat assessment

Reconnaissance survey was conducted prior to field sampling activities at the end of the short rainy season in November 2013. The main goal of this was to get familiar with the study area, select study sites, confirm objectives, determine feasibility and suitability of sampling methodology, and to inform local chiefs of the intended study. First main field sampling activities commenced in January, 2014. Spatiotemporal variations in coastal water quality were investigated, performed by two snapshot sampling campaigns during the dry (January/February) and rainy (September/October) seasons of 2014. The sampling cuts across 6 communes and 44 rural communities: Grand-Lahou, Jacqueville, Dabou, Abidjan, Bingerville and Grand-Bassam. The main ethnic groups of the riverine communities are Ébrié, Adioukrou, Ahizi, and Avicam. Agriculture is the mainstay of the riverine population. The principal cash crops within the study area are coconut, pineapple, and the African palm. There are also animal rearing and fishing activities along the Ébrié lagoon and the sandy beaches of the Atlantic coastlines. Physical habitat assessment encompasses determination of coastal topography, land use dynamics, and regional geology of surface rock outcrops. Coastal topography was extracted from the digital elevation map, DEM (www.diva-gis.org/gdata) using the ArcGIS software (ArcGIS 10.2, ESRI Inc.) as part of a desktop study.

2.1. Land use dynamics

Spatial and temporal changes in land use cover and the drivers of change were assessed for the southeastern coast. Land use patterns have direct influence on surface run-offs and water retention capacity of soils (**BIO intelligence Service, 2014**) and consequently on agricultural and hydrological drought. In addition, land use patterns (forest lands) play important role in aquatic ecosystems functions, as surface water bodies are highly dependent upon organic matter inputs, especially leaf fall for their energy supply (**Allan *et al.*, 2005**). Therefore, shifts in land cover patterns might be intricate pathways by which aquatic ecosystems and biodiversity can be negatively affected. In Côte d'Ivoire, heavy reliance on rain-fed agriculture and old traditional farming practices (slash and burn cultivation) coupled with urban expansion have led to habitat fragmentation and loss of fertile forestlands (Figure 12). Deforestation and/or forest degradation have direct negative influence on local microclimate as it leads to a decrease in evapotranspiration from plants and lands, modifying microclimates (**Russi *et al.*, 2012; Sanderson *et al.*, 2012**). Spatial characterization of land use cover was from multi-temporal satellite (WRS series) images using ENVI 4.8 software (ITT Corporation) and Geographical Information Systems, GIS (ArcGIS version 10.2, ESRI Inc.). The study window (longitudes 3° 15" and 3° 40" W and latitudes 6° 15" and 6° 40" N) has an area of 236,843 hectares. Satellite images were mosaics of:

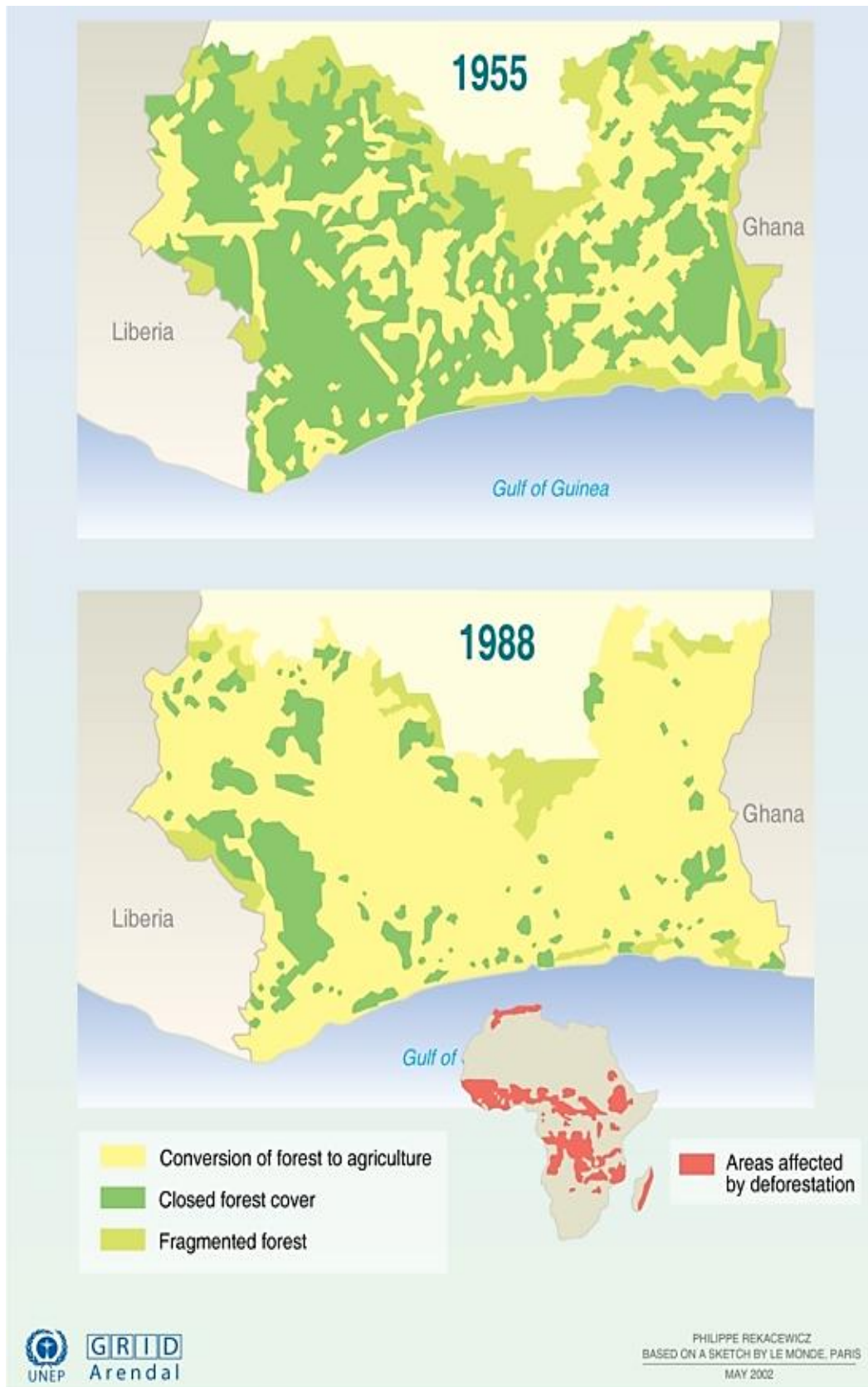


Figure 12: Agricultural land expansion at the expense of primary forest areas: The year, 1955 (top) and 1988 (bottom). (Source: Institute of Research for Development, 1996).

- Landsat 5 Thematic Mapper (TM) images (January 1989 (path/row 195/56) and January 1990 (196/56)) and
- Landsat 8 Operational Land Imager (OLI) images (November 2014 (path/row 195/56) and January 2015 (196/56)) on a 30 x 30 m spatial resolution.

This implied that land areas less than 30 hectares were not represented. Image pre-processing steps include layer stacking, cloud masking (cloud covers 7 % of study area), atmospheric correction, and sub-setting. Image processing techniques made use of a combination of spectral signal analyses (principal component analysis (PCA), normalized difference vegetation index (NDVI) calculated as:

$$\text{Near Infrared (Band 4)} - \text{Red (Band 3)} / \text{Near Infrared (Band 4)} + \text{Red (Band 3)} \quad \text{Eq. 1}$$

The differences in wetness index, the third channel in the TM Tasseled Cap Transformation (**Crist & Cicone, 1984**) was used to more accurately separate forest classes (mangroves and terrestrial rain forest trees). The Tasseled cap coefficient used to create the tasseled cap bands was statistically derived from images as wetness index (WI):

$$\text{WI} = 0.1509\text{ETM1} + 0.1973\text{ETM2} + 0.3279\text{ETM3} + 0.3406\text{ETM4} - 0.7112\text{ETM5} - 0.4572 \quad \text{Eq. 2}$$

In each time steps, land use/cover categories (mangroves, other forest types, settlements/bare soils, water bodies and agricultural lands) were classified based on maximum likelihood algorithm. Ground data was collected randomly from eighty locations within the study area. Subsequently, a matrix of transition was generated by the intersection of the two maps following the procedures and classification of **Lagabrielle et al. (2005; 2007)**. Supplementary ground vegetation mapping was carried out in four selected mangrove forest stands (Eloka-To, Agban 2, Songon-Té (Mois encampment), and Audoin-Beugréto).

2.2. Mangrove forest characterization

The presence of mangrove forests along the up tidal areas of the Ébrié lagoon was confirmed during ecological site visits. Their conservation is however, contingent on information on their vegetation structure hence, this attempt to characterize the eastern group of mangroves, growing in the upland tidal areas of the Ébrié lagoon. Mangroves are trees and shrubs limited to tropical and subtropical coastlines between 25° N and 38° S (**Tomlinson, 1986; Spalding et al., 2010**), adapted to harsh (high salinity and anoxic) conditions of growth (**Tomlinson, 1986; Alongi, 2002**). They are key ecosystems within wetlands that provide ecosystem services ranging from regulating, provisioning, cultural, and aesthetic to humanity (**Millenium Ecosystem Assessment, 2005**). As soft coastal defence structures, they make immense contributions to the resilience and adaptation of coastal systems and riverine

communities to climate change (**Adger *et al.*, 2007**). For instance, in Vietnam, 12,000 hectares of planted mangrove forestlands provided protection against a typhoon that devastated neighbouring areas (**Reid & Huq, 2005**). In spite of the heightened awareness of their value, economic and ecologic importance, indiscriminate exploitation, and degradation continue unabated. Globally, increasing human pressures have resulted in loss of over 50 % of mangrove forests (**Saenger and Bellan, 1995**), at a rate of 0.7 % per annum, more than three to five times compared to terrestrial rainforests (**FAO, 2006**). In Côte d'Ivoire, these forests have undergone severe decline (Figure 13), continuing at a disappearance rate of 0.1 % per annum (**FAO, 2007**). Field measurements were carried out in four selected mangrove forest stands (Figure 14). These are mangrove forest stand in:

- **Eloka-To** (longitude 3° 44' 08" W and latitude 5° 18' 04" N), hereinafter referred to as site A,
- **Agban** (longitude 3° 18' 38" W and latitude 5° 18' 04" N), located 27 kilometres southwest of Eloka-To, hereinafter refer to as site B;
- **Audoin-Bégréto** (longitude 4° 08' 01" W and latitude 5° 17' 16" N), hereinafter refer to as site C and
- **Mois** (longitude 4° 14' 42" W and latitude 5° 17' 22" N), hereinafter refer to as site D.

Forest survey followed the procedures of **Kathiresan**. Counts and measurements were random within ten, 1 x 1 m plots marked by PVC pipes (Photo 2), perpendicular to the shorelines. Maximum canopy height (m) was estimated using a clinometer. Canopy cover was by ocular estimation.

Leaf area index, LAI (leaf area/ground area, m².m⁻²) was estimated from measurements of light absorption by the forest canopy (**Komiyama *et al.*, 2005**):

$$LAI = \frac{\log_e(I/I_0)}{-k} \times \cos \theta \quad \text{Eq. 3}$$

Where I/I₀ is ratio of photon flux density beneath the canopy and at ground level under direct sunlight. K, a light extinction coefficient was set as 0.5. For each sampled site, log_e (I/I₀) was calculated for pairs of simultaneous readings and averaged. Corrections were made for the angle of the sun from the vertical (Cos θ).

LAI was in turn used to estimate net canopy photosynthesis (PN) using the formula of **English *et al.* (1994)**:

$$\text{Net carbon fixed, } P_N (\text{Mg C ha}^{-1} \text{ year}^{-1}), P_N = A \times d \times LAI \quad \text{Eq. 4}$$

Where d is the day length (average of 12.4 hours) and A is the average rate of photosynthesis per unit leaf area (0.216 g C m⁻² leaf area hr⁻¹).

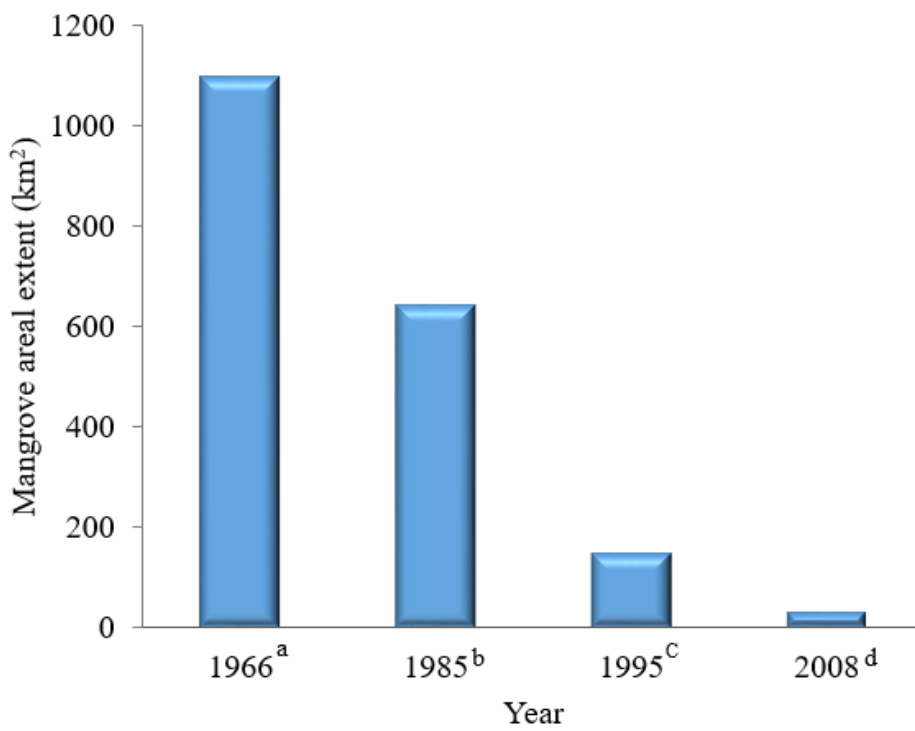


Figure 13: Temporal trends in mangrove forest area in Côte d'Ivoire. ^aFAO and UNEP (1981); ^bSpalding *et al.* (1997); ^cSaenger and Bellan (1995) and ^dGiri *et al.* (2011).

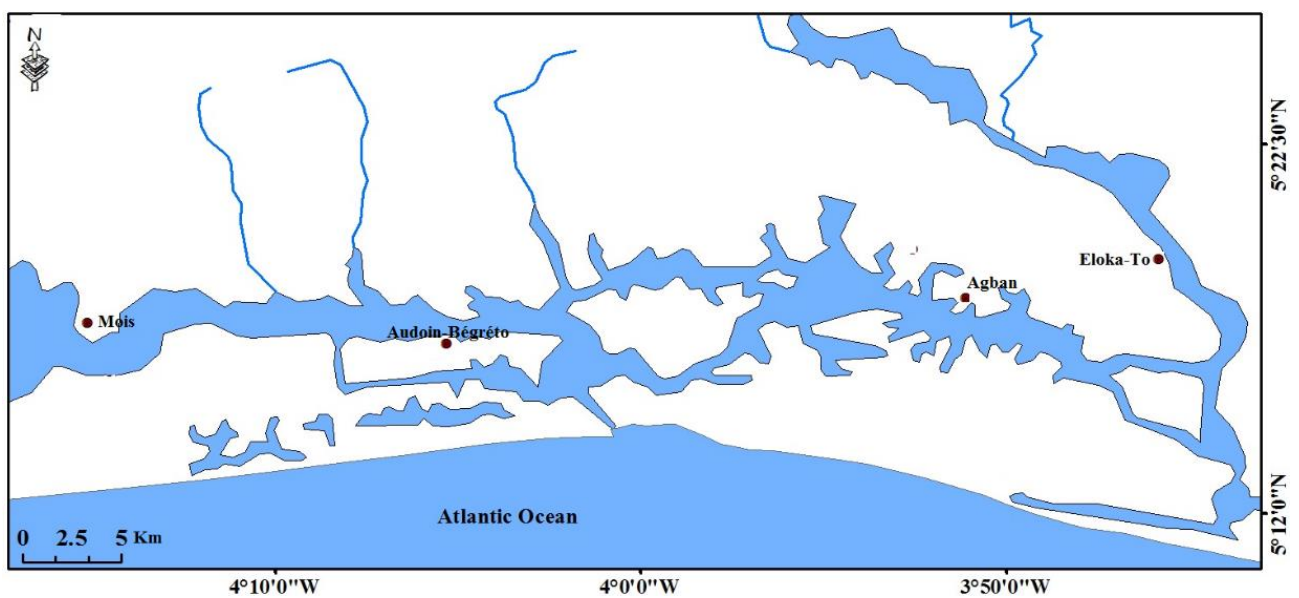


Figure 14: Mangrove forest sampling points along the Ébrié lagoon.

2.2.1. Above-ground root biomass and carbon stock estimation

Rhizophora prop root diameter at 30 cm above ground was measured with a vernier caliper. Root density was determined from fresh/dry weight ratio (oven drying at 70 °C for 72 hours) of disk samples. Carbon content of the roots were determined by combusting 600 µg vacuum-dried wood chips from 3 centimeter thick sample disks in a EURO EA elemental Analyser at 1700 °C. The resulting carbon dioxide, CO₂ was cryogenically separated using a manual extraction line and isotope ratios were determined on Isotope Ratio Mass Spectrometer, IRMS (Finnigan MAT 253; Thermo Electron). $\delta^{13}\text{C}$ ($^{13}\text{C}/^{12}\text{C}$ ratio) values were expressed as per mil relative to Vienna-Pee Dee Belemnite. Triplicate analyses indicate precision of ± 0.17 ‰. Above-ground root biomass (kg/root) was estimated from species-specific allometric equation of (Komiyama *et al.*, 2005) as:

$$\text{Above-ground root biomass} = 0.196\rho^{0.899}(D_{0.30})^{2.22} \quad \text{Eq. 5}$$

Where ρ is root density (t.m^{-3}) and $D_{0.3}$ is diameter at 30 cm for the *Rhizophoraceae* family. Results were multiplied by carbon content to determine carbon stocks.

2.2.2. Natural regeneration capacity

Rhizophora regenerative capacity was determined from seedlings (established propagules less than 1.3 m height) density, counted within ten, 1 x 1 m plots.

2.3. Lithological analyses

The geologic history of sedimentary basins plays a critical role in its hydrologic development (Kreitler, 1989). Fluid flow pathways and eventual storage in aquifers always occurs within the porous media of rocks. Rock materials may therefore influence the quality and/or quantity of percolating water depending on its residence time. Therefore, to determine the natural elemental contributions from geology to a catchment, it is imperative to have knowledge of its elemental composition. Twenty-one rock samples were randomly collected from outcrops from surrounding geology. The following formations were represented:

- Continental Terminal (CTeast) (samples: G8, G11, G15, G16, G18, G19, G20, G21) were collected from outcrops at the eastern area of the Ébrié lagoon catchment.
- Continental Terminal, (CTwest) (G1, G2, G3, G4, G5, G6, G7, G19) were collected from the central and western areas of the catchment.
- Nouakchottien (Quaternary age marine sands (QM) represented by samples: G9, G10 was collected along the coastal plains



Photo 2: Field measurements on *Rhizophora* roots. 1m² PVC pipes (top image) and vernier caliper (bottom image).

Samples were stored in zip-lock plastic bags until analyses. Rock colour was identified based on geological rock colour chart (**Munsell color, 2011**) and *In situ* test was made for the presence of carbonate using drops of hydrochloric acid. In the laboratory, moisture content (w) was determined for each sample:

$$w (\%) = \left(\frac{m - m_d}{m_d} \right) \times 100 \quad \text{Eq. 6}$$

Where: w is moisture content (%), m is mass of soil (g) and m_d is mass of dried soil (g).

The organic matter content (C_{org}) of the rock materials was also determined by loss on ignition (LOI):

$$LOI = \frac{m_{pre-ignition} - m_{post-ignition}}{m_{pre-ignition}} \quad \text{Eq. 7}$$

A basic assumption for the use of LOI as a surrogate for organic carbon (**Konen *et al.*, 2002**) is that mass loss is solely attributable to organic carbon. Crushed rock samples were oven-dried at 105 °C overnight. Five grams of samples were weighed onto porcelain crucible, and ignited in a muffle furnace (1000 °C) for two hours. Subsequently, samples were placed in a desiccator to cool for 1 hour. Finally, comparisons were made between pre- and post-ignition sample weight.

Whole rock mineralogy

Semi-quantitative determination of mineralogical (SiO_2 , TiO_2 , Al_2O_3 , FeO , MnO , MgO , CaO , Na_2O , K_2O , and P_2O_5) composition of rock was on powdered samples by x-ray diffractometry, XRD (Bruker Axs D8 Advance) with nickel-filtered $CuK\alpha$ radiation, following standard procedures at the Steinmann-Institute, University of Bonn, Germany. Analytical steps are shown in Photo 3. The diffraction line of quartz was used as an internal standard for the accurate and precise measurement of d-values, because Quartz has high stability (**Croneis & Krumbein, 1936**). Base correction, peak identification, and analyses of diffractograms was with MacDiff 4.2.5 software (**Petschick, 2000**). Peak positions and intensities were compared to published values. The resulting values were corrected according to Cook indices (**Cook *et al.*, 1975**). Lithology was classified according to **Sprague *et al.* (2009)** on the basis of weight ratios of SiO_2/Al_2O_3 and Fe_2O_3 (Table I).

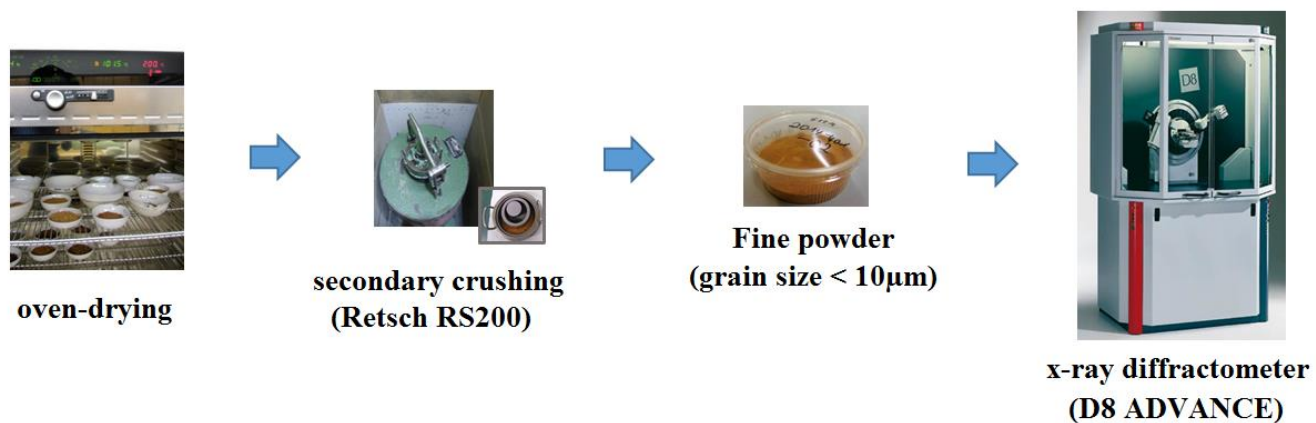


Photo 3: Summary of analytical steps for whole rock mineralogy.

Table I: Lithologic ratios used for siliciclastic rock classification (Sprague *et al.*, 2009)

Silty claystone / claystone	$\text{SiO}_2/\text{Al}_2\text{O}_3 < 4$
Siltstone	$\text{SiO}_2/\text{Al}_2\text{O}_3 = 4 - 6$
Argillaceous sandstone	$\text{SiO}_2/\text{Al}_2\text{O}_3 = 6 - 10$
Sandstone	$\text{SiO}_2/\text{Al}_2\text{O}_3 > 10$
Dolomitic sandstone	$\text{SiO}_2/\text{Al}_2\text{O}_3 > 10$ and $\text{MgO} > 5 \%$
Fe-rich lithology	$\text{Fe}_2\text{O}_3 > 10 \%$

2.4. Water quality assessment (abiotic environmental factors)

The quality of different coastal water systems (precipitation, groundwater wells, boreholes, rivers, Ebrié lagoon and the Atlantic Ocean) was studied over the dry (January/February) and rainy (September/October) seasons.

2.4.1. Precipitation

Precipitation samples (sample size, $n = 30$) were collected between September, 2013 and October, 2014 from a temporary weather station (latitude $5^{\circ} 24' 36''$ N and longitude $3^{\circ} 59' 21''$ W). Samples were collected into 50 mL airtight polyethylene bottles for geochemical and isotopic analyses. Transient physicochemical parameters (temperature, pH, specific conductance, dissolved oxygen, and alkalinity) of precipitation were measured *in situ*.

2.4.1.1. Drought indices

To analyse drought indices, multi-decadal (1970 - 2014) meteorological data was acquired from the national meteorological station, SODEXAM. Arithmetic mean of yearly precipitation amount and surface air temperature were computed as:

$$\text{Mean} = \sum_{i=1}^n x_i / n \quad \text{Eq. 8}$$

On the variety of rainfall patterns, dry and wet months are distinguished based on the Bagnouls-Gausson bioclimatic diagram (umbrothermic diagram) which states that:

$P > 3T \rightarrow$ wet

$3T > P > 2T \rightarrow$ moderately wet

$P < 2T \rightarrow$ dry

Where: P is the total precipitation for the month, i (mm) and T is the mean air temperature for the month, i ($^{\circ}\text{C}$).

On the umbrothermic diagram, precipitation values below the temperature curve signifies dry conditions, when the precipitation curve plots above the temperature curve there is a wet period, and when the precipitation curve exceeds the 100 mm mark indicates excess water. Kendall's non-parametric test (**Kendall, 1975**) was employed to determine the probability of the existence of a trend on time series data at a 5 % significance level.

Drought (Figure 15) is an aftermath of precipitation deficit (meteorological drought). Long-term meteorological drought engenders other types of drought (**Wilhite & Glantz, 1985**). A multi-scalar drought index, Standardised Precipitation Evapotranspiration index (SPEI) was computed on meteorological data using the SPEI package version 1.6 (**Vicente-Serrano et al., 2010**) on the

statistical package R (**R core team, 2012**). SPEI takes into account precipitation and potential evapotranspiration (PET) to determine drought at different time scales. Time scale functionally separates different drought levels. Drought at 3-, 6-, 18-, and 24-month time scales represent the effect on meteorology/agriculture/soil moisture (3 and 6 months), groundwater hydrology (12 months), and socio-economic impacts (24 months), respectively. Positive SPEI implies greater than median precipitation, while values of -1 marks the onset of drought event. Different drought categories are given in Table II. Potential evapotranspiration (PET) was calculated from Thornthwaite's equation (**Thornthwaite, 1948**) using the statistical package R (**R core team, 2012**).

2.4.2. Surface water and groundwater

Water sampling was bi-annual following standard procedures, in January/February (dry season) and in September/October (rainy season) of 2014. The sampling seasons coincide with the minor and major ocean upwelling seasons, respectively. As a rule of the thumb, samples were collected in such a way that sampling points were at least 10 km apart from each other (**Manikandan et al., 2012**), to ensure data independence and ease geo-referencing.

One hundred and fifty water samples were collected from surface (sample size, $n = 69$) and groundwater ($n = 81$) systems for geochemical and isotopic analyses. Surface water systems collection points were the mouth of coastal rivers (Ira, Agnéby, Mopoyem, Layo, Banco), the Ébrié lagoon and the Atlantic coast using polyethylene bailers. Site navigation was with the aid of non-motorized boats to minimize site disturbances. For regional structuring, sampling points of the lagoon were combined into zones, predefined by **Durand and Guiral (1994)** (Figure 16): I, II, III and IV corresponding to the eastern, urban/estuarine, peri-urban and western end of the Ébrié lagoon respectively. Shallow phreatic and deeper aquifer layers were assessed from hand dug wells and boreholes, respectively (Figure 16). Water samples were partitioned into three broad categories based on the geology of its confining layers. These are wells within:

- Quaternary marine sands (QM), (samples: p2, p3, p4, p15, p23, p25, p28, p29, p31, p32, p33, p34, p35);
- CTeast (p1, p5, p6, p7, p8, p9, p10, p11, p12, p22, p36, p37) and
- CTwest (p13, p14, p16, p17, p18, p19, p20, p21, p26).

2.4.2.1. Hydrologic information and estimation of groundwater recharge

Water level measurements are the most direct evidence of impacts of land use change on groundwater recharge (**Finch, 2001; Scanlon et al., 2005**) as groundwater responds slowly to changes in rainfall, impacts of meteorological droughts are often buffered (**Calow et al., 1997**).

Table II: SPEI classification scheme (World Meteorological Organization, 2012).

SPEI value	Classification
2.0 and more	Extremely wet
1.5 to 1.99	Very wet
1.0 to 1.49	Moderately wet
-0.99 to 0.99	Near normal
-1.0 to -1.49	Moderately dry
-1.5 to -1.99	Severely dry
-2.0 and less	Extremely dry

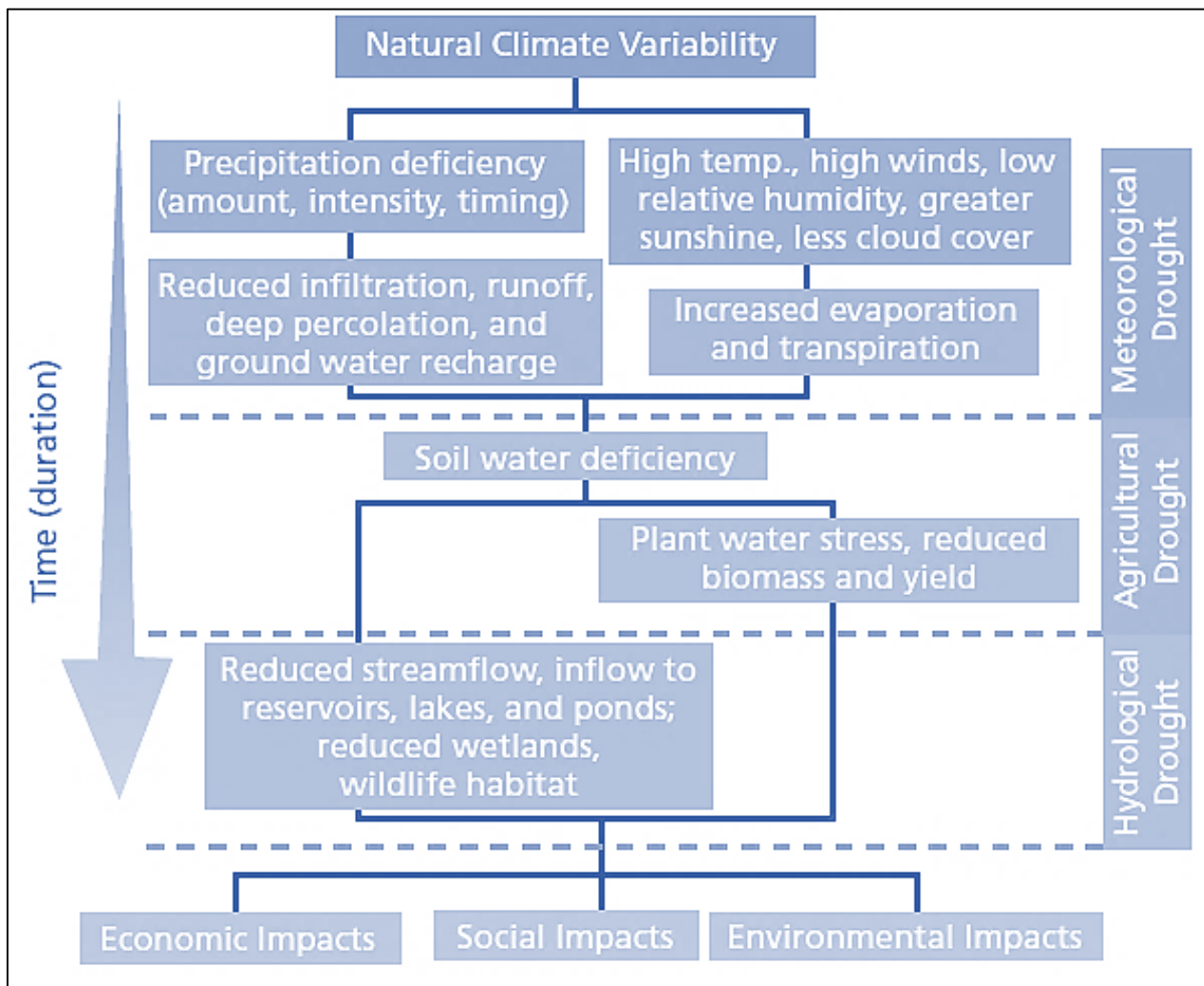


Figure 15: Sequence of occurrence and impacts of common drought types (Source: National Drought Mitigation Centre, 2007, Nebraska-Lincoln, U.S.).

Information on total well depth and static water level was determined at each wellhead prior to sample collection. Static water level was measured with a sonic contact meter (KLL type, SEBA GmbH & Co. KG) (Photo 4, left image). Groundwater recharge rates for the shallow phreatic aquifer were calculated using the simple chloride mass balance formula by **Allison *et al.* (1990)**:

$$R = \frac{P \cdot Cl_{pi}}{Cl_{gw}} \quad \text{Eq. 9}$$

Where: R is the monthly recharge (mm/month), P is monthly precipitation (mm), Cl_{pi} is chloride concentration in precipitation (mg/L) and Cl_{gw} is chloride concentration in groundwater (mg/L).

Furthermore, water level data from piezometers across the coastal area was obtained from l'Office National d'Eau Portable (ONEP) to have a good understanding of seasonal fluctuations in regional water table levels.

2.4.2.2. Hydrochemistry

Transient physicochemical parameters (pH, dissolved oxygen, specific electrical conductivity (EC) and temperature) were measured *in situ* with multiparameter handheld instruments (HANNA HI-9878) (Photo 5, right image). Turbidity was measured by a Wagtech turbidity meter (Photo 5, left image). Water were classified based on total dissolved solids (TDS) according to **Freeze and Cherry (1979)**, as freshwater (TDS: 0 – 1000); brackish water (TDS: 1000 – 10,000); saline water (TDS: 10,000 – 100,000) and brine water (> 100,000). All water samples were filtered in two successive steps with VWR filter paper (250 mm diameter) and a syringe PVDF filter (Photo 6). Analyses of alkalinity was by titrimetry within 24 hours of sampling. 100 mL of sample was titrated with 0.2 N sodium chloride (NaOH) in the presence of phenolphthalein to an endpoint of 8.3. Samples with pH between 4.3 and 8.3 have bicarbonate alkalinity, while those with pH less than 4 contain free carbon dioxide. Analyses of silicate (SiO_4^+), nitrate (NO_3^-), Ammonium (NH_4^+), and phosphate (PO_4^{3-}) concentrations was by spectrophotometry (DR6000 UV-VIS, Hach, USA) (Photo 7) following standard procedures at the Steinman Institute, University of Bonn, Germany. Changes occurred in laboratory analytical procedures between the sampling campaigns. First set of analyses were performed at the Steinmann-Institute, Bonn, while the second were at the Institute of Groundwater Ecology, Helmholtz Zentrum, München, Germany. At the laboratory of the Steinmann-Institute, cations (Na^+ , K^+ , Mg^{2+} , Ca^{2+}) were analysed on acidified samples using flame atomic absorption spectrometry (AAS) (Perkin Elmer A Analyst 700). Anions (SO_4^{2-} , Cl^- and NO_3^-) were analysed on non-acidified samples using ion chromatograph (Shimadzu, HIC-6A) with appropriate dilutions. However, subsequent major ion measurements were by ion chromatography (DIONEX-ICS 1100) (Photo 8) at the Helmholtz Zentrum, München, Germany. Comparison of results from the different

analytical methods showed differences in values of less than 10 %. Summary of field and laboratory analytical methods are presented in Figure 17. Detection limit of analytes are shown in Table III. The quality of analyses was checked by calculating the error of ion balance:

$$\text{Ion balance error (\%)} = \frac{(\sum \text{cations} - \sum \text{anions})}{(\sum \text{cations} + \sum \text{anions})} \times 100 \quad \text{Eq. 10}$$

Although, a cut-off between 2 % and 5 % is the norm (**Mazor, 1991**), values of ± 10.4 % are acceptable (**Güler et al., 2002**). Biplots were drawn between major ions versus chloride (Appendix I). A straight regression line showed they are behaving as conservative elements and thus not interacting with aquifer materials (**Mazor, 1991**). To further investigate this hydrologic relationship amongst coastal waters, elucidate evolutionary trends and understand the origin of water chemistry, major ions were displayed on geochemical plots (**Piper, 1946**), Gibb's diagram (**Gibbs, 1992**) and Durov plot (**Durov, 1948**) using the AqQa software (Rockware Inc.). Interpretation of the central diamond field of the piper plot was based on the works of **Back (1960)** and **Kelly (2005)**. Furthermore, point sources of nitrate was highlighted on the Ebrie lagoon on a Voronoi tessellation (**Voronoi, 1907**) using QUIMET (**Velasco et al., 2014**), a GIS-based hydrogeochemical analysis tool.

2.4.2.3. Stable isotope analyses (natural tracers)

Different water types have specific isotopic signatures, which they carry along their flow paths. This makes them very effective tools in any regional water studies to trace origin, recharge processes, sources of pollution and hydrologic interactions along its main flow path; hydrologic cycle (**Kendall & Doctor, 2003; McGuire & McDonnell, 2007; Aggarwal et al., 2009**). These signatures however changes due to fractionation processes (**Clark & Fritz, 1997**). Fractionation between different phases of water results from the differences in the physical properties of water molecules containing different isotopic species of oxygen-18 and deuterium. To analyse the stable isotopes, unfiltered water samples were collected into airtight 50 mL polyethylene (PET) bottles. Bottles were kept in an upright position at temperatures slightly lower than *in situ* temperature until analyses. Stable isotope (oxygen-18 and deuterium) analyses were carried out using laser spectrometry (LS2120-*i*, Picarro Inc., US) as shown in Photo 9, at the Helmholtz Zentrum, München, Germany. δ values were normalized relative to Vienna-Standard Mean Ocean Water (V-SMOW) (**Craig, 1961**):

$$\delta (\text{‰ V-SMOW}) = \left(\frac{R_{\text{sample}}}{R_{\text{standard}}} - 1 \right) \times 10^3 \quad \text{Eq. 11}$$

Where: δ ($\delta^{18}\text{O}$ or $\delta^2\text{H}$) is the normalized difference of the isotope ratios R ($^{18}\text{O}/^{16}\text{O}$ or $^2\text{H}/^1\text{H}$) of the sample and the standard.

Triplicate analyses indicate a precision of ± 0.3 ‰ for $\delta^{18}\text{O}$ and ± 1.6 ‰ for $\delta^2\text{H}$.

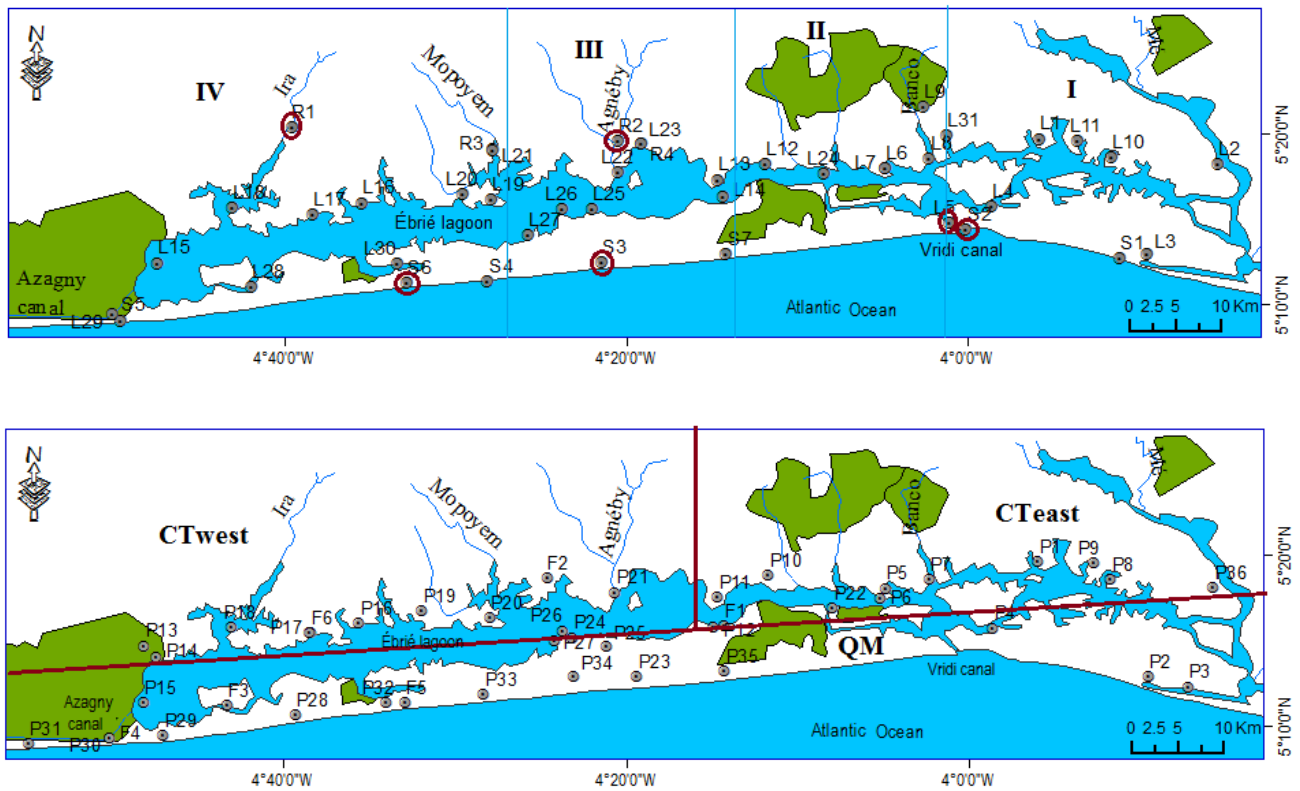


Figure 16: Map of the study area with water sampling points. Top: surface water sampling points. Prefixes R-, L- and S- represent river, lagoon, and Atlantic coast, respectively. Bottom: groundwater sampling points. Prefixes, P- and F- represent wells and boreholes, respectively. Circled areas were sampled only during the rainy period. Green areas represent forested areas.



Photo 4: Measuring water level in a dug well in Songon-Té using water level meter (left) and a typical borehole in Nguessandan (right).



Photo 5: Some field measuring instruments. Handheld WAGTECH turbidity meter (left) and HANNA HI-9878 multiparameter hand held meter (right).



Photo 6: Materials for a two-step water filtration during field survey. Whatman filter paper (left) and syringe 0.45 μ m PVDF membrane filter (right).

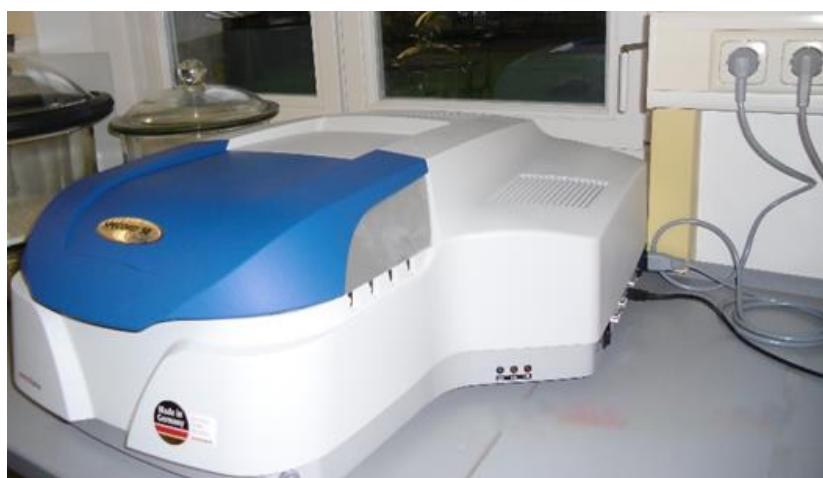


Photo 7: HACH UV-VIS spectrophotometer (Analytik, Jena Specord 50).



Photo 8: Ion chromatograph (DIONEX ICS-1100) (top) and automated water sample holders (bottom).

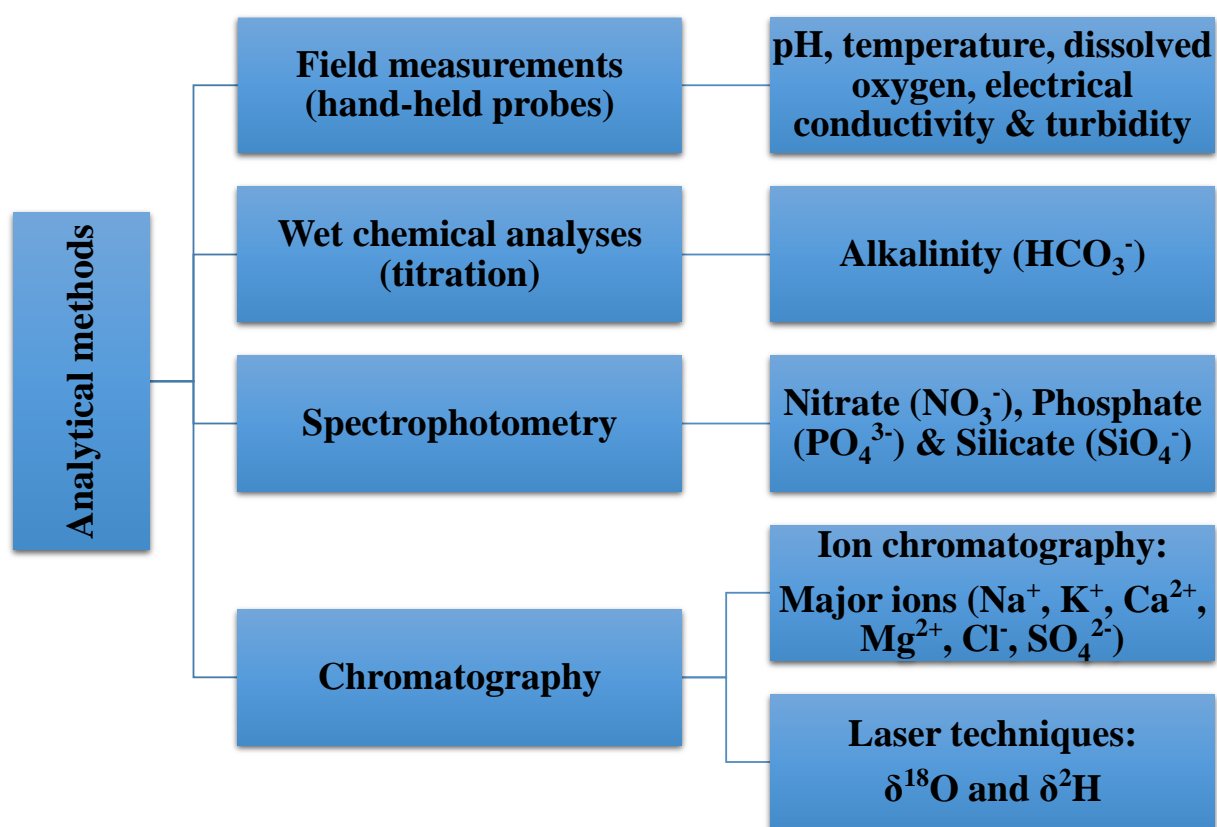


Figure 17: Summary of field and laboratory analytical methods.

Table III: Detection limit of analytes (mg/L) according to DIN 32645.

Analytes	Detection limit (mg/L)
Na^+ , K^+ , Mg^{2+} , Ca^{2+}	0.01
SO_4^{2-}	0.339
Cl^-	0.386
NO_3^-	0.272
NO_2^-	0.073
SiO_2	0.307
PO_4^{3-}	0.043
NH_4^+	0.126
BO_3^{3+}	0.019



Photo 9: The laser isotope analyser (LS2120-i, Picarro Inc., US).

2.4.2.4. Hydrological modelling - End-member mixing model (EMMA)

A three-component model was adopted to determine the seasonal fractional contributions of coastal waters (precipitation, river, lagoon, and Atlantic Ocean) to each other. Fractional contribution of different sources to each water sample was determined algebraically based on end-member mixing analytical model, following the procedures outlined in **Hooper *et al.* (1990)**. A primary assumption of this method is that the tracers in these components mix conservatively, albeit in nature this is often times violated (**Burns *et al.*, 2001**). A second assumption is that isotope fractionation is mass dependent. Precipitation, groundwater, brackish lagoon water, and seawater were considered as potential water sources for the model. The dataset was subjected to principal component analyses (PCA) after standardization in order to estimate the number of end members and inform the choice of tracers. PCA was performed with the XLSTAT software version 10 (Addinsoft, France). Initial dataset consists of the concentration of nine potential chemical variables (Na^+ , K^+ , Mg^{++} , Ca^{++} , Cl^- , SO_4^{--} , NO_3^- , HCO_3^- , SiO_3^+ and isotope delta values ($\delta^{18}\text{O}$ and $\delta^2\text{H}$). Multivariate mixing and mass balance calculation was performed based on the closure relationship defined by:

$$f_x + f_y + f_z = 1 \quad \text{Eq. 12}$$

$$C_1^1 f_x + C_2^1 f_y + C_3^1 f_z = C_t^1 \quad \text{Eq. 13}$$

$$C_1^2 f_x + C_2^2 f_y + C_3^2 f_z = C_t^2 \quad \text{Eq. 14}$$

Where: f is the source water fraction from freshwater (x), lagoon (y) and seawater (z), C is the tracer concentration, subscripts, t, 1, 2, 3 are components of the sample, saltwater, lagoon and freshwater respectively and superscripts 1 and 2 are the tracers: oxygen-18 and Cl^- concentrations, respectively.

Seawater chloride values are based on averages. Freshwater sources (averages of groundwater and precipitation) with similar isotope concentration were combined to avoid ambiguity (**Phillips *et al.*, 2005**). End members were selected and the EMMA model was used to estimate the proportional contribution of different sources to each sample.

2.5. Biocenosis analyses – phytoplankton dynamics

Phytoplankton are microscopic, chlorophyll-a bearing, non-vascular plants that constitutes 99 % of all plant forms in the aquatic ecosystems. They drive the primary productivity of the aquatic ecosystems. As ecosystem engineers, they have the ability to modulate light penetrations to depths, thereby altering surface temperature of water columns (**Jones *et al.*, 1994**). The alteration of water surface temperatures can influence water density, provoking stratification (**Townsend *et al.*, 1992**). Density stratification coupled with wind energy can overturn nutrient supply and trigger the development of oxygen minimum events (**Arthur *et al.*, 1987**). Phytoplankton also makes immense

contributions to atmospheric purification as they replenish global atmospheric oxygen through photosynthetic processes. In addition to their role as planet-savers, they have found usefulness in the fields of medicine, cosmetics, bio-fertilizers, microbiology (agar solutions) and their use as bio-indicators of ecosystem health dates back to the 18th century (**Cohn, 1853**). Their floristic diversity reflects alterations in the quality of host waters (**Nixon *et al.*, 1996**). They provide the most reliable index of eutrophication and changes in water quality. Phytoplankton integrates various human and environmental inputs thereby providing a benchmark for monitoring the synergistic effects of urbanization and climate change (**Kunz & Richardson, 2006**). Their study is therefore an integrative measure of water quality.

2.5.1. Phytoplankton sampling, identification, and enumeration

Phytoplankton harvesting was carried out randomly from twenty sites (Ébrié lagoon, 16; Atlantic Ocean, 4) in the coastal environment. This was carried out in synchrony with that of the environmental variables. Sites were sampled once during the dry and rainy seasons from predefined zones. For the Ébrié lagoon from east to west, sampling points, L1, L2, L3, L10 represent station I, sites, L4, L6, L8, L24 represents station II (urban/estuarine areas of the lagoon), sites L12, L19, L22, L25 represent station III (peri-urban areas of the lagoon), while sites, L15, L17, L18, L29 represent station IV, its western extremity (Figure 18). Four points (S1, S4, S5, S7) were sampled along the Atlantic coastline, representing areas off the coast of Gbamblé, Grand-Jack, Abréby and Nguessadan, respectively. Fifteen litres of depth-integrated water samples were filtered through a plankton net of 20 microns mesh size (Photo 10, left image). Filtrates were collected into 50 mL dark brown polyethylene bottles. Samples were fixed in Lugol's iodine solution in a ratio of 1:100 (**Vollenweider, 1969**). Cell counting was from 1 mL aliquot, mounted onto the Malassez haemocytometer and counted under a ZEISS light microscope (Photo 10, right image) following standard procedures of **Schön (1988)**. Species identification was to species level where possible from works of authors (**Foged, 1966; Compère, 1975; Krammer & Lange-Bertalot, 1991; Cocquyt, 1998; Ouattara *et al.*, 2000; Komárek & Anagnostidis, 2005**).

Chlorophyll-a determination

Chlorophyll-a content of water was determined by spectrophotometry (**Lorenzen, 1967**) only during the rainy season. 250 mL of water samples were concentrated by retention on a glass fibre filter (Whatman GF/F with 25 mm pore diameter). Preparation was by maceration and pre-soaking in 100 % acetone for 24 hours. Thereafter, extracts were centrifuged at 5000 rpm for 60 seconds. Supernatants were filled into 2-cm spectrophotometer cell.

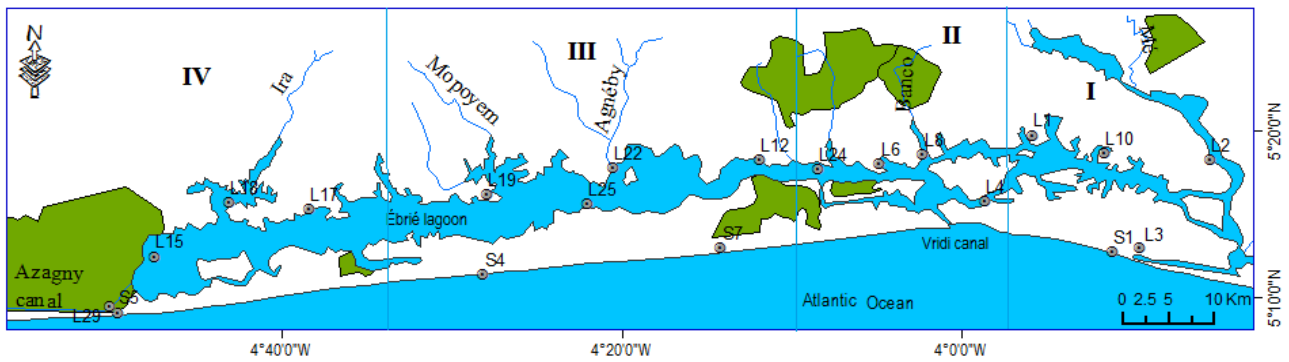


Figure 18: Map showing phytoplankton sampling stations along the Ébrié lagoon (L) and the adjacent inshore (S). Blue lines are subdivisions according to Durand and Guiral (1994).



Photo 10: Materials for biocenosis analyses. Plankton net (left). Zeiss microscope (right).

Table IV: Trophic categories of surface waters based on chlorophyll-a concentration (Schmitt, 1998).

Trophic class	Primary productivity	Chlorophyll a ($\mu\text{g.L}^{-1}$)
I Oligotrophic	Very low	<1 - 4
I – II Mesotrophic	Low to moderate	3 - 8
II Eutrophic	Moderate	7 - 30
II – III Eutrophic to polytrophic	Moderate -high	25 - 50
III Polytrophic	High	50 - 100
III – IV Polytrophic to saprotrophic	Very high	100 - 400
IV Saprotrophic	Extremely high	>400

Differentiation was made between chlorophyll-a and its degradation products based on the relative changes of optical density at 750 µm and in the red spectral region (665 µm), induced by acidification (Moss, 1967; Lorenzen, 1967). The optical density measured at 750 µm is an approximate measure of non-selective ‘background’ absorption by other materials. The values are subtracted from optical density measurements in the red spectral region. Primary productivity and oligotrophic state of surface waters was classified based on the work of Schmitt (1998) as shown in Table IV.

2.5.2. Data analysis – SOM map

Self-organizing feature map (SOM) (Kohonen, 1995), an artificial neural network (ANN) model based on unsupervised batch map learning algorithm was employed in order to relate spatiotemporal variations of abiotic environmental variables to phytoplankton dynamics. SOM algorithm (Lampinen, 1992; Vesanto *et al.*, 1999) was implemented with Matlab 6.5 computing environment by MathWorks, Inc. Taxa contributing less than 1 % (13 taxa) to total cell abundance were excluded from all statistical operations. As a first step, sampling points were clustered into groups based on biological data; a second step relates the resulting clusters to environmental abiotic variables. The SOM consists of two different computational units; input and output layers connected by computational weight vectors. In this study, the dataset (abundance value of 54 taxa in 20 sampling sites studied over 2 seasons) was log-transformed ($\ln(x+1)$), conditioned with nine measured environmental predictors (temperature, dissolved oxygen, pH, turbidity, total dissolved solids, slope, nitrate, phosphate and silicate) and trained with an unsupervised batch map learning rule. Batch map units for each sample were calculated as:

$$m_k(t-1) = \frac{\sum_{i=1}^N h_{c(x_i)k}(t)x_i}{\sum_{i=1}^N h_{c(x_t)k}(t)} \quad \text{Eq. 15}$$

Where: N is the number of sample vectors

Discriminant function is squared Euclidean distance:

$$d(x) = \sum_{i=1}^D (x_i - w_{ji})^2 \quad \text{Eq. 16}$$

The quality of training algorithms was assessed by quantization error (QE) for map resolution and topographic error (TE), a measure of the map’s ability to accurately represent the input layers (topology preservation). Although there exists no reference value for QE and TE (Astel *et al.*, 2013), after machine learning process, the map size with the minimum quantization error value and zero topographic error is selected. Low QE values denote good maps (Kaski & Lagus, 1996), while a zero TE implies perfect topology preservation (Pözlbauer, 2004). Cluster validation was with kruskal-wallis at a significant alpha of 0.05. The output neurons display a 2-dimensional 4 x 3 (12

nodes) map units on hexagonal lattice. The 4 x 3-map size was selected after several iterations. Initial map size was determined by heuristic formula (Matlab SOM Toolbox):

$$\text{Map units} = 5 \cdot n^{0.5431} \quad \text{Eq. 17}$$

Where: n is the number of records in the dataset.

Detailed SOM algorithm for ecological applications can be found in **Park *et al.* (2003)**. Subsequently, divisive clustering tree (dendrogram) of the input variables is formed based on the similarity of the weight vectors of the neurons (map units) (**Miikkulainen, 1990**). Hierarchical cluster with Ward's linkage method subdivided the map into different clusters based on the similarity of the weight vectors of the neurons (map units). Multivariate pairwise statistics were employed to determine the statistical significance of the relationships.

2.5.3. Community indices

Jaccard similarity index, SC_j (**Jaccard, 1912**) was used to check classification consistency and assess similarities between clusters. It is computed as:

$$SC_j(A, B) = \frac{A \cap B}{A \cup B} \quad \text{Eq. 18}$$

Where: A, B is number of species two samples have in common and is number of species represented by both samples.

A maximum value of 1.0 indicates maximum similarity that is all species present in A are also found in B. In terms of biodiversity conservations, areas with low values are treated as top priority as they tend to preserve more biodiversity.

Other studied community indices computed using the Paleontological statistics, PAST Software (**Hammer *et al.*, 2001**) are:

Taxa richness, relative abundance:

$$P_i = N_i / N \quad \text{Eq. 19}$$

Where: N_i is the abundance of the ith species in the sample and N = $\sum_{i=1}^s N_i$, s is the total number of species in the sample.

Shannon index, H' (**Shannon & Weaver, 1949**) to assess the diversities of each community was computed as:

$$H' = - \sum_{i=1}^s p_i \ln p_i \quad \text{Eq. 20}$$

Where: s is the number of species in a sample, 'p_i' is the number of individuals of species, i in a sample and 'n' is the number of individuals in a sample. H' is derived by summing the product for all species in the sample.

Community dominance index, CDI (**Krebs, 1994**) to determine the percentage of abundance contributed to a community by two most abundant species.

It is calculated as:

$$CDI = 100 (n_1 + n_2)/N \quad \text{Eq. 21}$$

Where: n_1 and n_2 are the abundance of the two most common species and N is the total abundance. Index values range between 0 and 100. High values represent less diverse and highly disturbed communities.

Finally, indicator value index, IndVal (**Dufrêne & Legendre, 1997**) was determined for each cluster to identify indicator species using the Indicspecies package version 1.7.1 of **De-Cáceres and Legendre (2009)**. The Indicator value of species, i with respect to cluster, j is the sum of the specificity (A) and fidelity (B), scaled to 100. That is:

$$IndVal_{ij} = 100A_{ij} \times B_{ij} \quad \text{Eq. 22}$$

Where: specificity (A_{ij}) is the ratio of the mean abundance of species, i in cluster j and the sum of means of the same species over all group. A maximum value of one is attained if the species occur only in that cluster. Fidelity (B_{ij}) is the proportion of sites in which species, i is present within cluster, j . Maximum value of one occur when species, i occur in every site in the cluster, j .

The statistical significance was tested using a permutation test.

2.5.4. . Faecal coliform bacteria – supplementary water quality indicator

Faecal (thermo-tolerant) coliform bacteria were analysed as supplementary components of coastal water quality. They have been used as indicator of the bacterial safety of drinking waters (**Leclerc *et al.*, 2001; WHO, 2003**). They are environmental indicators of human or animal faecal contamination of waters. To determine faecal coliform densities, water samples were collected directly into 250 mL sterilised dark brown glass bottles, with 15 mL headspace. The bottles were stored over ice to suppress microbial activity until analyses. Analyses were within 24 hours of sample collection. 10 mL sample were concentrated by filtration onto sterile nitrocellulose membrane filter discs. The membrane filters were placed on top of Violet Red Bile Lactose (VRBL) agar medium in disposable plastic petri dishes and incubated at 44 °C for 24 hours. Resulting visible circular patches/colonies were counted using a colony counter. Colony forming units, CFU/100 mL was determined by the formula:

$$CFU/100 \text{ mL} = \frac{\text{Coliform colonies counted}}{\text{volume of water filtered (mL)}} \times \frac{\text{volume of water filtered (mL)}}{100 \text{ mL}} \quad \text{Eq. 23}$$

Colonies formed were round with diameter ranging between 0.5 – 2 mm. The Colour was red to purple.

2.6. Socio-economic survey

Conservation policy based on only information on the environment is lump-sided. An understanding of the interactions of the four essential ingredients of environmental sustainability: population, economics, environment, and culture, driving every complex global change is important for conservation of natural resources (**Cohen, 1995**). Therefore, policies geared towards the conservation of natural resources must incorporate indigenous knowledge and collaboration to be successful. Indigenous people are at the base of the environmental security system. ‘No matter the resolutions, no genuine and lasting environment improvement can take place without grassroots involvement (**United Nations Environment Programme, 2002**). This survey adopted a stratified random approach. The sample size for the survey was determined using the normal approximation of the binomial distribution (**Dagnelie, 1998**):

$$\text{sample size, } n = \frac{U_{1-\alpha/2}^2 \times p(1-p)}{d^2} \quad \text{Eq. 24}$$

where n is the number of respondents; $U_{1-\alpha/2}$ is the value of the normal random variable for a probability value of $1-\alpha/2$, for $\alpha = 5\%$, $U_{1-\alpha/2}^2 = 3.84$; p was set to an arbitrary value of 50% ; and d is the expected error margin ranging between 1% and 15% . In this study, the margin error was set as 6.8% ($d = 6.8\%$).

The resulting sample size of two hundred and eight respondents was evenly distributed amongst eleven communities. The choice of 18 respondents per community was based on the recommendations of **Julious (2005)**. The survey used detailed questionnaires (Appendix II) with ordinal and nominal questions as its main enumeration tool in order to understand indigenous perception of climate change, underpin social vulnerability and socio-economic concerns arising from coastal water degradation. Questions focused on local perception of key climate change variables (precipitation and temperature), water use, treatment methods, waste disposal methods, and socio-economic concerns.

PART III:
RESULTS AND DISCUSSIONS

CHAPTER 3: Physical habitat assessment

Outlined below is detailed description of the physical environment of the eastern Ivorian coast.

3.1. Coastal topography

The study area has near horizontal topography with slope percent between zero and 70 relative to the sea (Figure 19). Approximately fifty percent of the studied area is topographically low with slope percent values between 0 and 2, making these areas highly vulnerable to a potential sea level rise. Thirty percent of the area have slope percent between 2 and 6, 15 % between 6 and 12; 4 % between 12 and 18 and less than 2 % of the area have slope percent higher than 18. The implications of this low topography are higher impacts of sea level rise and vulnerability to inundation and coastal erosion.

3.2. Dynamics of land use

Land use class specific accuracy for both satellite images ranged between 61.9 % and 97.6 % (Table V). Lowest class specific accuracy (61.9 %) was recorded for the mangrove class, due to difficulties in differentiating between mangroves and other forest vegetation. Average land use classification accuracy was 88.1 and 90.3 % for 1989/90 and 2014/15, respectively. The Kappa coefficient had values above 0.8 for both maps (Table V). Generally, forested areas showed strong reduction in their areal extent (Figure 20). Mangrove forest cover decreased from 7,863 hectares in 1989/90 to 3,867 hectares in 2014/15 representing a net decrease of 3,996 hectares or 49.2 % (Table VI). Matrix of confusion showed that only 18 % of primary forest still exists within the 25-year period (Table VII). Mangroves thrive best with alternating rise and fall of sea level. Their biological response to permanent inundation by saline water due to sea level rise is landward migration (**Alongi, 2008**). However, land use modifications foreclose migratory routes, inhibiting landward propagation. Urbanization accounts for about 70 % of the total loss in forest area. About 31.8 % of forestland has been converted to settlements/bare soils, while a much higher percentage (43.8 %) has been converted to agricultural lands. Abidjan had only 65,000 inhabitants as at the time of the opening of the canal (**Durand & Zabi, 1994**), 2,102,000 inhabitants in 1990 (**United Nations Human Settlements Programme, 2014**). Today, its population is about 4,707,000 inhabitants (**Recensement Général de la Population et de l'Habitat, 2014**). Land under permanent agriculture in the study area was about 50 % during the investigation period. Concerning the water bodies, the position of the shoreline showed a 5 % landward displacement during the investigation period.

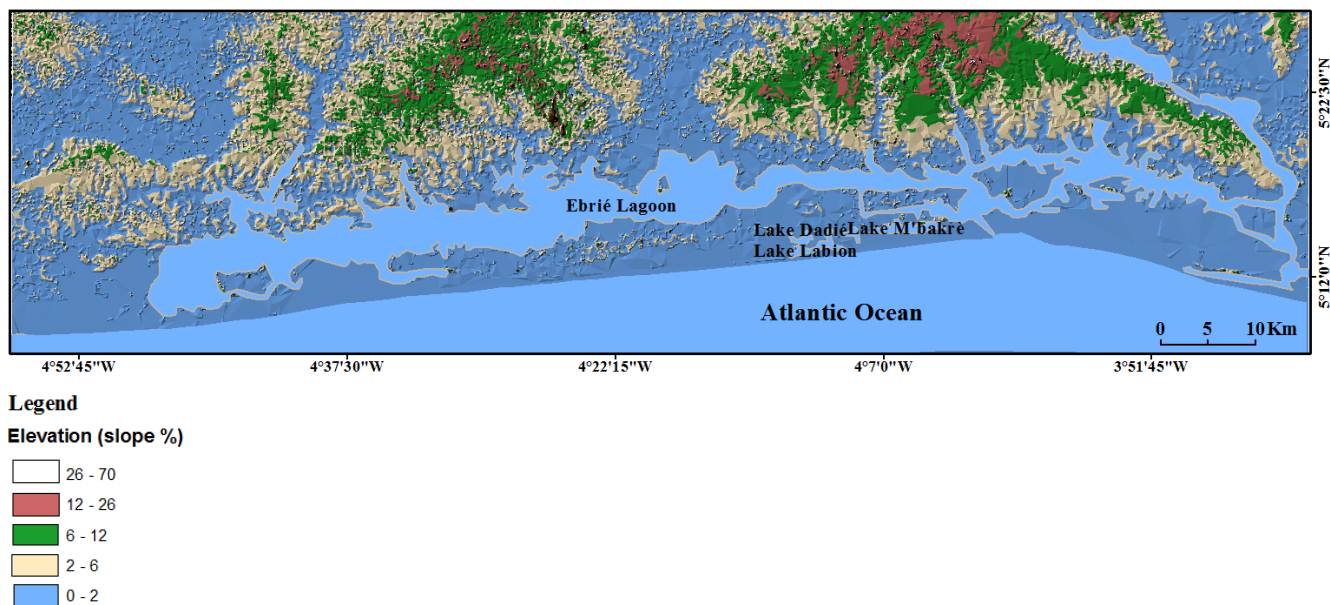


Figure 19: Digital elevation model (DEM) of the study area. The unit of slope is in percentage.

Table V: Accuracy of land use categories for 1989/90 (above) and 2014/15 (below). The class specific accuracy is highlighted in yellow.

		Mangrove	Other forests	Water body	Agricultural lands	Settlement/bare soils	Sum
Categories	Mangrove	61.88	0	5	0.27	0.27	67.42
	Other forests	26.17	95.86	0	8.9	0	130.93
	Water body	0	0	95	0	0	95
	Agricultural lands	11.95	4.14	0	95.4	2.09	113.58
	Settlement/bare soils	0	0	0	1.3	97.64	98.94
	Sum	100	100	100	105.87	100	505.87
Overall accuracy							88.12%
Kappa coefficient							0.87

		Mangrove	Other forests	Water body	Agricultural lands	Settlement/bare soils	Sum
Categories	Mangrove	72.01	0	2	1.27	0	75.28
	Other forests	19	95.86	0	8.2	0	123.06
	Water body	0.94	0	98	0	0	98.94
	Agricultural lands	8.05	4.14	0	90.53	4.7	107.42
	Settlement/bare soils	0	0	0	0	95.3	95.3
	Sum	100	100	100	100	100	500
Overall accuracy							90.30%
Kappa coefficient							0.88

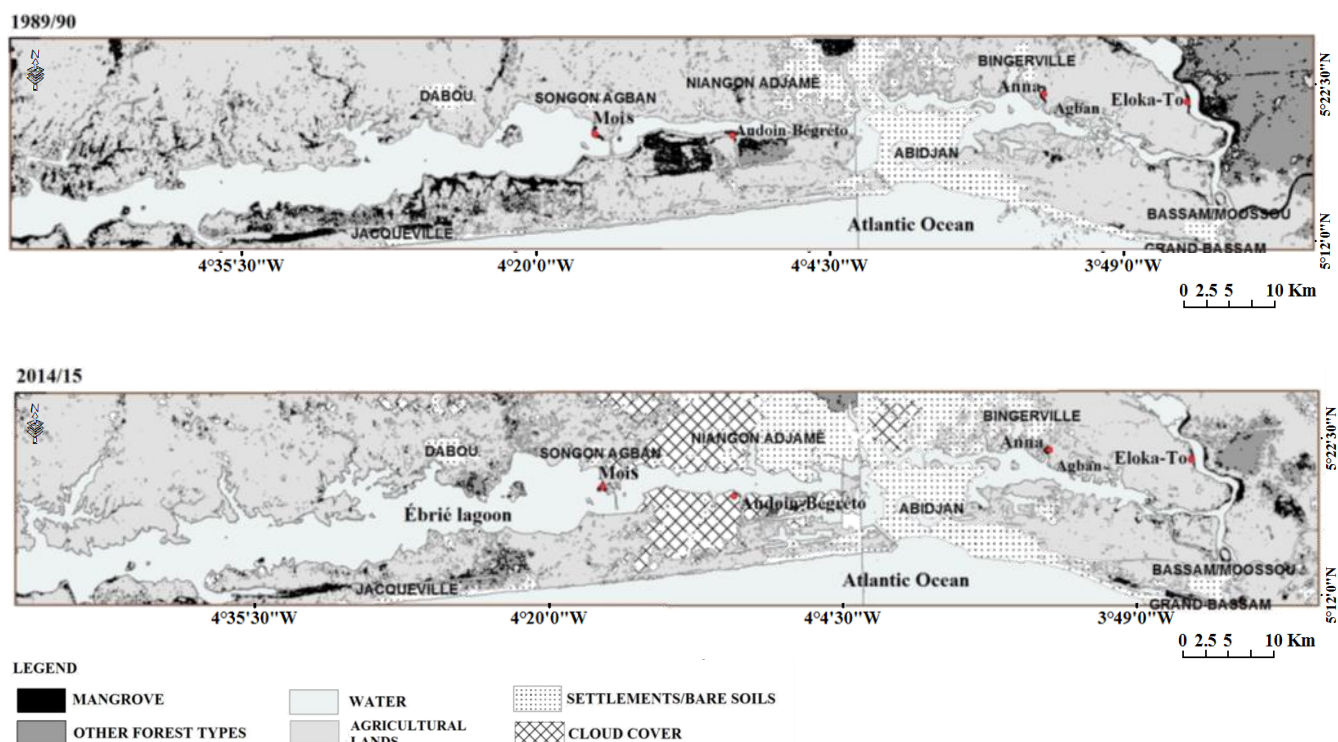


Figure 20: Temporal patterns (1989/90 and 2014/15) of land use/cover categories as observed from remotely sensed images.

Table VI: Land use cover categories (%) of the study area for the year 1989/90 and 2014/15.

Land use categories	1989/90	2014/15	Rate of change (%)
Mangroves	3.21	1.73	-49.15
Other forest types	10.25	3.30	-69.68
Settlements/bare soils	7.66	13.37	+64.42
Water	25.17	31.56	+18.07
Agricultural lands	53.71	50.03	-12.29

Table VII: Matrix of transition for the different land use categories between 1989/90 and 2014/15.

		1989/99				
		Settlements/bare soils	Forest	Mangrove	Agricultural land	Water
2014/15	Settlements/bare soils	77.31	31.83	5.35	37.42	3.50
	Forest	4.25	18.46	2.37	10.32	0.19
	Mangrove	0.73	3.87	87.24	0.96	0.29
	Agricultural land	13.77	43.81	2.32	50.71	0.03
	Water	3.93	1.93	2.70	0.51	96.03

Legend: Low Medium High Stable

3.3. *Rhizophora* forest characterization

Riverine communities are completely oblivious of the fact that forested areas (terrestrial or aquatic) positively influence local microclimates. According to **Servat *et al.* (1998)**, forested areas were less severely affected by the Saharan precipitation deficit compared to the Savannah areas. Presented below is the vegetation structure and carbon sequestration potential of the studied mangrove forest stands. Maximum canopy height ranged between 3.6 and 14.7 m (Table VIII). Canopy cover ranged between 25 – 75 %, 5 – 55 %, 5 - 45 % and 25 – 75 % for sites A (Eloka-To), B (Agban), C (Audoin-Bégreto) and D (Mois, respectively. Canopy exposure as evidenced in some plots of sites B and C leads to direct sunlight penetration, which in turn promotes high transpiration rates with consequences of decline in plant water use efficiency, net photosynthesis, stunted growth, and die-off in extreme cases (**Kathiresan & Bingham, 2001**). Light gaps are however advantageous to seedlings, as they are shade intolerant (**Smith-III, 1992**). *Rhizophora* roots showed aggregate distribution with average root density of 22 individuals/m² for surveyed sites. Lognormal plots (**Gray & Pearson, 1982**) of diametric sizes of roots follows unimodal, negatively skewed distributions (Figure 21), reflect striking disparities in root diameter. This suggests degraded forests. In a lognormal plot, undisturbed communities usually start high on the abscissa and flatten out towards higher classes. Conversely, disturbed communities start lower on the abscissa as observed in the different mangrove stands albeit with varying degrees of disturbances. The LAI observed are similar to those of tropical savannah (mean \pm S.D: 1.88 ± 1.81 , **Asner *et al.*, 2003**). The amount of radiation transmitted from the top of the canopy to the forest ground are averages of 38, 59, 54 and 29 % for sites A, B, C and D respectively. Lower amounts of radiation were transmitted to the forest floors in stands with relatively higher LAI values.

3.3.1. Carbon storage potentials

The lowest carbon influx rates were recorded in site B. Assuming the average annual net primary productivity of 22.28 tC/ha (Table VIII), prop roots within the investigated area are capable of fixing a crude estimate of 0.86 Gt CO₂ annually. Carbon contents of roots constitute an average of 44.9 % of the oven-dry mass (Table VIII). $\delta^{13}\text{C}_{\text{mangrove}}$ were isotopically lighter compared to standards and ranged between -26.09 and -29.08, suggesting a Calvin mechanism (C3) of photosynthesis. These values are comparable to those of the *Rhizophora* mangroves of Malaysia (**Rodelli *et al.*, 1984**), Sri Lanka (**Bouillon *et al.*, 2003**) and Tanzania (**Muzuka & Shunula, 2006**). Carbon pools, on per hectare basis were highest in site A, the freshwater stands, while lowest values were in the degraded forests of site B. Stored carbon values fell within the estimated range of 160 – 200 Mg/ha (**Hutchinson *et al.*, 2014**), except those of sites B and D that were lower.

Table VIII: Mean and range (in parenthesis) of estimates of vegetation parameters for Eloka-To (A), Agban (B), Audoin-Bégréto (C) and Mois (D) forest stands.

	Site A	Site B	Site C	Site D
Individuals, N	261	226	200	230
Maximum canopy height, H (m)	7.5 (4.2 - 12.9)	8.3 (3.6 - 17.9)	5.8 (4.0 - 7.1)	7.5 (4.6 - 14.7)
Root diameter @ 30cm, $D_{0.3}$ (mm)	26.0 (9.1 - 47.3)	15.8 (2.9 - 50.1)	25.1 (12.8 - 41.5)	25.7 (2.7 - 49.3)
Root basal area (m^2)	0.13 (0.05 - 0.24)	0.08 (0.01 - 0.25)	0.14 (0.11 - 0.24)	0.13 (0.02 - 0.25)
Root density (ind. m^{-2})	22	22	26	18
Wood bulk density ($t.m^{-3}$)	1.06	0.86	0.95	0.83
Above-ground root biomass ($t.ha^{-1}$)	382.64	110.67	381.39	246.69
Carbon content (%)	46.2 ± 0.25	46.16 ± 0.24	44.84 ± 0.38	44.6 ± 0.13
Carbon stored ($Mg\ C\ ha^{-1}$)	176.02	50.91	171.62	113.48
Leaf area index, LAI ($m^2 m^{-2}$)	1.9	1.03	1.25	2.52
NPP ($tC\ ha^{-1}\ year^{-1}$)	43.78	8.63	12.15	24.58

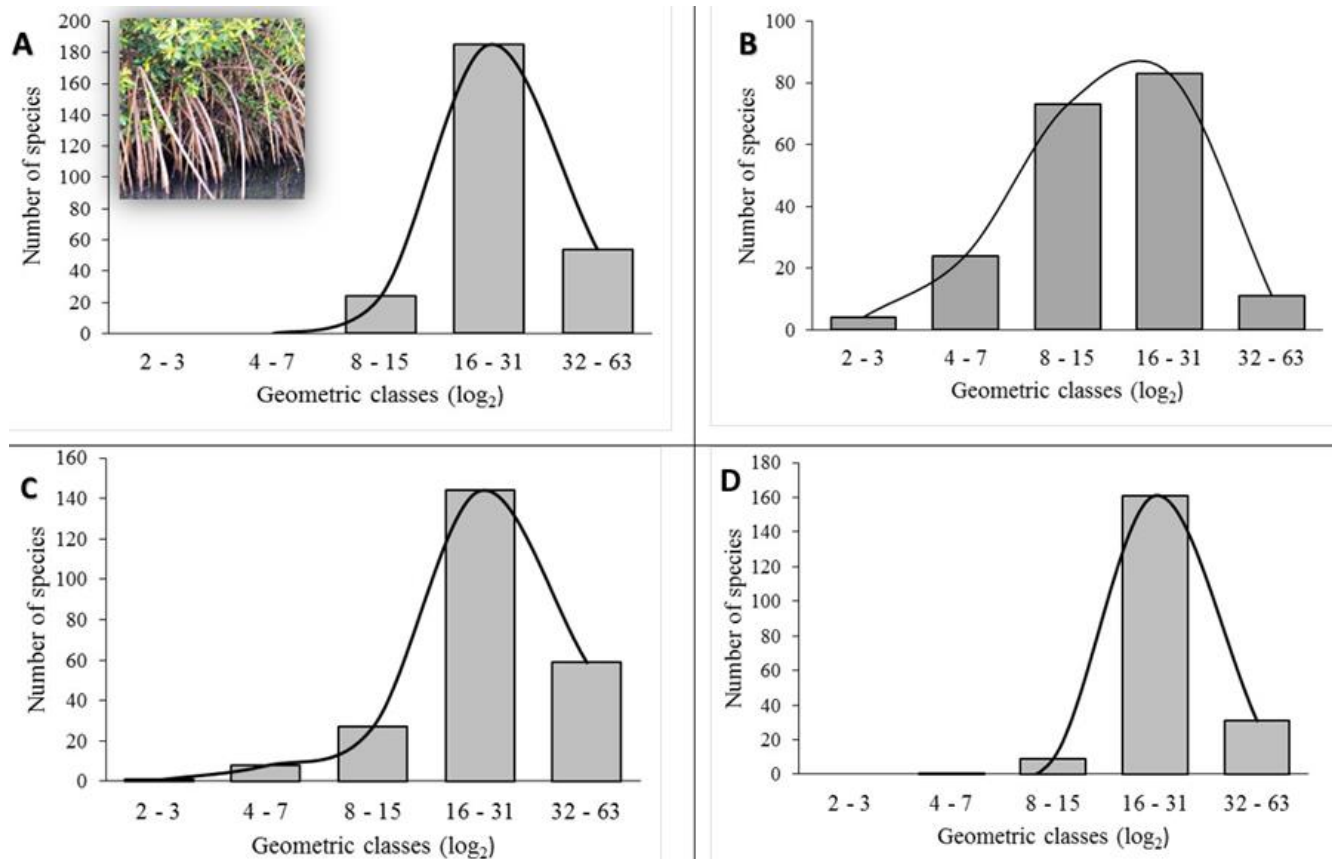


Figure 21: Lognormal plots of mangrove prop root density in 1 x 1 m plots at Eloka-To (A), Agban (B), Audoin-Bégréto (C) and Mois (D).

3.3.2. Regenerative capacity

A common feature of these *Rhizophora* forests is the absence in their under-storey of other vegetation types. Their seedlings constitute the ground-storey. The studied forests showed potential for natural unaided regeneration with an average seedlings density (seedlings/m²) of 10 (Figure 22). Site D demonstrates the highest rate of establishment and survival of propagules with seedlings density up to 73 seedlings/m². This might be probably due to the high sediment flux and firm sandy layers that facilitate their successful establishment. Conversely, site A recorded the lowest seedlings density. Likely causes of low survival rates are the dense canopy cover (absence of light gaps) in these mangrove stands that prevents light penetration/solar radiation to the ground-storey and/or high tides that inundates these seedlings cutting supply to oxygen and sunlight. The conservation and rehabilitation of degraded mangrove forests will not only ensure biodiversity conservation but also inadvertently support climate change mitigation and adaptation strategies. As soft defense structures, mangroves can be more effective in attenuating coastal storm waves and protecting coastlines from erosion and flooding, and its cost of maintenance is minimal compared to hard defense structures such as dams (**Reid & Huq, 2005; Costanza et al., 2008**).

3.4. Lithological analyses

The surface morphology was monotonous, comprising of sandstone beds without distinct bedding. There was no gaseous response (effervescence) on contact with hydrochloric acid (carbonate test). This implies they are carbon-free. Quaternary marine sands (QM) are very light gray (Munsell, N8) to light brown (5 YR 6/4) in colour. They are very coarse, sub-angular to sub-rounded in shape and moderately sorted depicting immaturity and closeness to provenance. The sediments of the eastern part of the Tertiary Continental Terminal (CTeast) are moderate yellow (Munsell, 5YR7/6), moderate reddish orange (10R6/6) to moderate red (5R4/6) in colour. The very fine to coarse grains of the CTeast rocks are sub-rounded to rounded and mostly poorly sorted. The reddish tint suggests the oxidation of immobile Fe-minerals of terrigenous origin. The geology in the central and western parts (Tertiary continental terminal, CTwest) is similar except for the presence of post-depositional, dark coloured iron nodules in its central parts, which suggests synthesized supply of sediments of shallow epicontinental shelf regions followed by chemical and biochemical precipitation (**Dahanayake & Krumbein, 1986**). The CTwest sediments are yellow (10YR6/6) to brownish yellow (10YR7/6) in colour. They are poorly sorted with sub-rounded to rounded grains. In its western fringes, the CTwest comprises surface exposures with mottled structures (spots of different colours), indicative of submergence in water (reducing conditions). The Quaternary marine, QM coarse-grained sands are well drained with very low moisture content (Table IX).

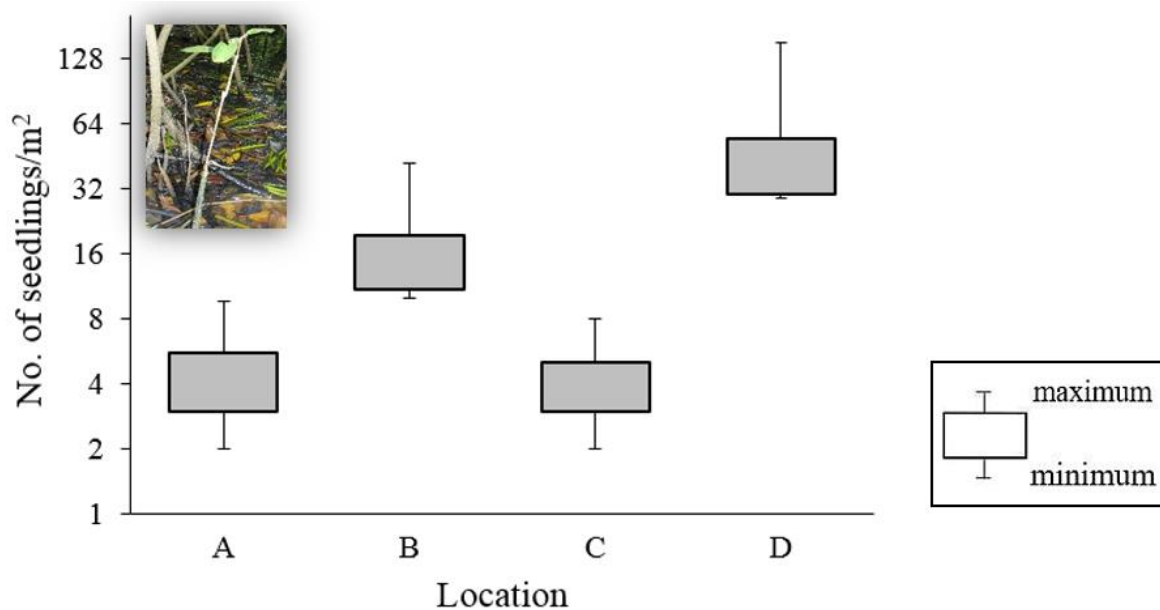


Figure 22: Box plots of seedlings density on 1 x 1 m plots from Eloka-To (A), Agban (B), Audoin-Bégréto (C) and Mois (D) forest stands. Values are means \pm range.

Table IX: Moisture content (%) and loss on ignition (%) of outcrops surrounding the Ebrié lagoon subcatchment.

Sample ID	Formation	MDWF* (%)	LOI ^{*,1} (%)
G1	CTwest	2.2	5.93
G2	CTwest	2.5	13.3
G3	CTwest	2.3	10.55
G4	CTwest	2.8	10.25
G5	CTwest	1.9	11.03
G6	CTwest	2.2	11.54
G7	CTwest	3.5	14.06
G8	CTeast	20.9	4.77
G9	QM	0.0	0.27
G10	QM	0.0	0.15
G11	CTeast	7.4	4.41
G12	CTwest	4.8	4
G13	CTwest	5.0	3.59
G14	CTwest	7.3	3.9
G15	CTeast	5.1	4.77
G16	CTeast	2.7	2.77
G17	CTwest	5.4	3.98
G18	CTeast	10.9	6.12
G19	CTeast	13.2	6.84
G20	CTeast	2.6	3.08
G21	CTeast	7.1	3.82

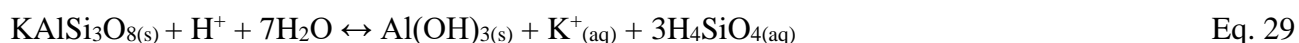
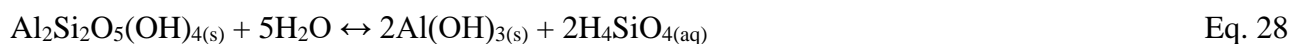
^{*,1} Mean value of two replicas

Highest moisture content (20.9 %) was recorded for the CTeast surface exposures. This implies that they have good water holding capacity and as such are the least prone to agricultural droughts. LOI as a surrogate for organic matter composition (Table IX), showed that the QM have very low organic matter content (0.15 – 0.27 %), followed by CTeast. CTwest sediments are rich in organic matter as it makes up to 14 % of bulk rock composition. CTeast are predominantly silty claystone and siltstones. CTwest are Fe-rich silty claystones. The Quaternary Marine sands, QM of the barrier islands are unconsolidated sandstones (Photo 11). The Quaternary marine sediments are acidic with 94 – 98 % SiO₂ and an Al/Ti ratio between 7 and 29 %. CTwest sediments are ultrabasic with relatively lower percentage of SiO₂ (5 – 25 %) and Al/Ti between 15 and 38 %. CTeast rocks are intermediate to acidic with SiO₂ values between 50 and 86 % and an Al/Ti ratio between 12 and 17 %.

The potential impact of high concentrations of silicon oxide, an acidic oxide in these rocks on dissolution, is groundwater acidification (**Brownlow, 1979**). The hydrolytical weathering of silicon oxide leads can lead to the stepwise formation of weak silicic acid (**Brownlow, 1979**):



Furthermore, the dissolution of other silicate minerals can lead to increase of silicate concentrations in water, e.g. the weathering process of kaolinite, Al₂Si₂O₅(OH)₄ (Eq. 27) and k-feldspar, KAlSi₃O₈ (Eq. 28) result in the formation of gibbsite (Al(OH)₃) and silicon oxide:



From mineralogical perspective, QM are dominated by quartz (97 %) with traces of k-feldspar and plagioclase. CTeast constitute mainly quartz (87 %) with traces of goethite (8 %) and kaolinite (5 %). Generally, CTwest are dominantly goethite (65 %) or haematite (37 %) with kaolinite (14 %), quartz (11 %) and traces of k-feldspar and plagioclase. Goethite is an important constituent of the CTwest rocks with dominance of 100 % in samples G5 and G7. The formation of goethite, the hydrated form of ferric oxide takes place in the presence of organic matter and low iron oxides under oxidizing conditions, Whereas, clays (kaolinite/chlorite) are by-products of extreme chemical weathering (**Harrison, 2007**). Goethite and clays are usually component of old, highly weathered rocks (**Harrison, 2007**). Details of mineralogical composition of rock samples can be found in Appendix I.

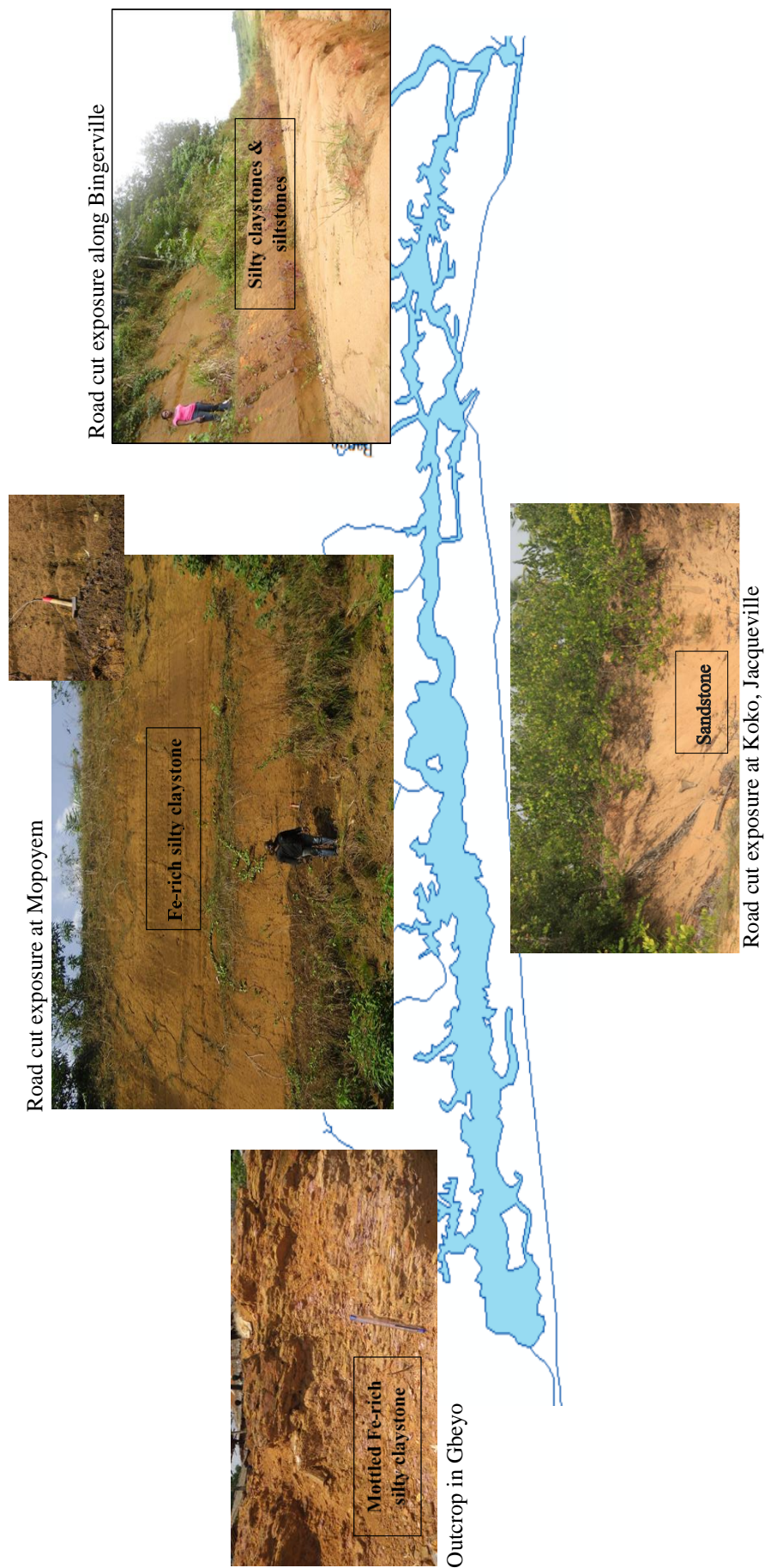


Photo 11: Lithology of surface outcrops at coarse scale across the study area. Persons and object are scales.

The rocks recorded very high alteration index with values between 96 and 100 %, except for the QM with alteration index value of 67 (G9) and 89 % (G10). This depicts the unconsolidated QM sands as the least weathered. The surface exposures plot mainly within the kaolinite/gibbsite/chlorite stability fields of the A-CN-K ternary plot (Figure 23). This implies that hydrolytic weathering have changed the rock compositions towards the apex (**Bahlburg & Dobrzinski, 2011**) with high alteration indices and low Na^+ and Ca^{2+} values. The QM sediments that plot within the illite stability fields were the least altered. The weathering trend strongly suggests granite/rhyolite as precursors. Average Na_2O (%) was 0.06, 0.02 and 0.01 for the QM, CTwest and CT east respectively. Values much lower than that of the upper continental crust of 3.56 (**Wedepohl, 1995**). Average CaO (%) was 0.05, 0.02 and 0.03 for QM, CTwest and CT east, respectively. Values much lower than that of the average upper continental crust of 4.24 % (**Wedepohl, 1995**).

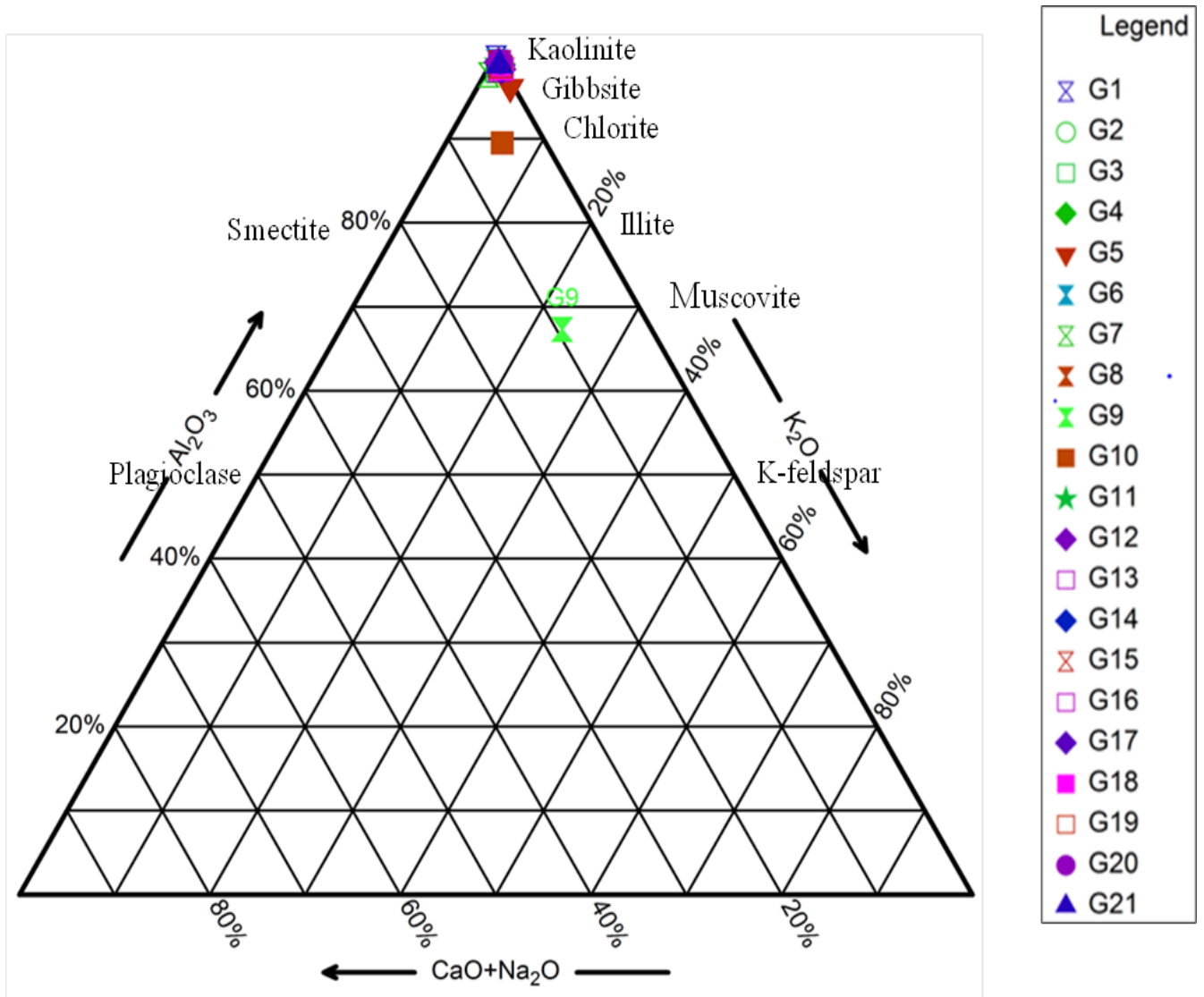


Figure 23: Ternary plot of Al_2O_3 – $\text{CaO}+\text{Na}_2\text{O}$ – K_2O (A-CN-K) of rock samples.

CHAPTER 4: Water quality assessment

Observed spatiotemporal variations in coastal water quality are provided under this section.

4.1. Precipitation

There was a clear longitudinal variation in precipitation amount along the study area based on 5-decade average. Mean annual precipitation was 1,704 mm (mean of 1970-2014) for Abidjan (central part of the sub-catchment), 1,520 mm (mean of 2001 – 2013) for Jacqueville (western part), and 1,727 mm (mean of 1970 – 2012) for Bingerville (eastern part). Bagnouls-Gausson bioclimate (umbrothermic) diagram revealed four inter-annual seasons (Figure 24). These are:

- Long dry season (LDS)
- Long rainy season (LRS)
- Short dry season (SDS)
- Short rainy season (SRS)

Spatial variations were also observed in these inter-annual seasonal cycles. The eastern and central parts of the study had five dry months (months with less than 100 mm of precipitation), while six dry months were observed in the western parts. The tropical monsoon climate is highly influenced by seasonal land-sea temperature differences, reflected by the position of the Inter-Tropical Convergence Zone, ITCZ. The ITCZ is a low-pressure belt of confluence between the northern and southern hemisphere trade winds generally near the equator that migrates in a latitudinal direction (**Binet & Marchal, 1993**). Figure 25 shows the latitudinal position of the ITCZ during the dry (January) and rainy (October) seasons of 2014. February to August, the ITCZ moves steadily upward in a septentrional (northwards) position. During this period, oceanic processes (southwest monsoon rains) dominate, engendering the LDS and LRS, respectively (**Durand & Chantraine, 1982**). Conversely, shifts southwards (meridional) in August to February is with relatively more rapid descent, engendering similar seasons (SRS and SDS), albeit with minimal effects (**Durand & Chantraine, 1982**). During this period, continental processes dominate, dry northeast trade winds (harmattan) sweep across the littoral.

4.1.1. Drought indices

Precipitation deficit have far-reaching impacts on groundwater, stream flow and other ephemeral surface storage systems. Although, the probability of occurrence of extreme weather events is low in the study area, marked seasonal variation is common occurrence.

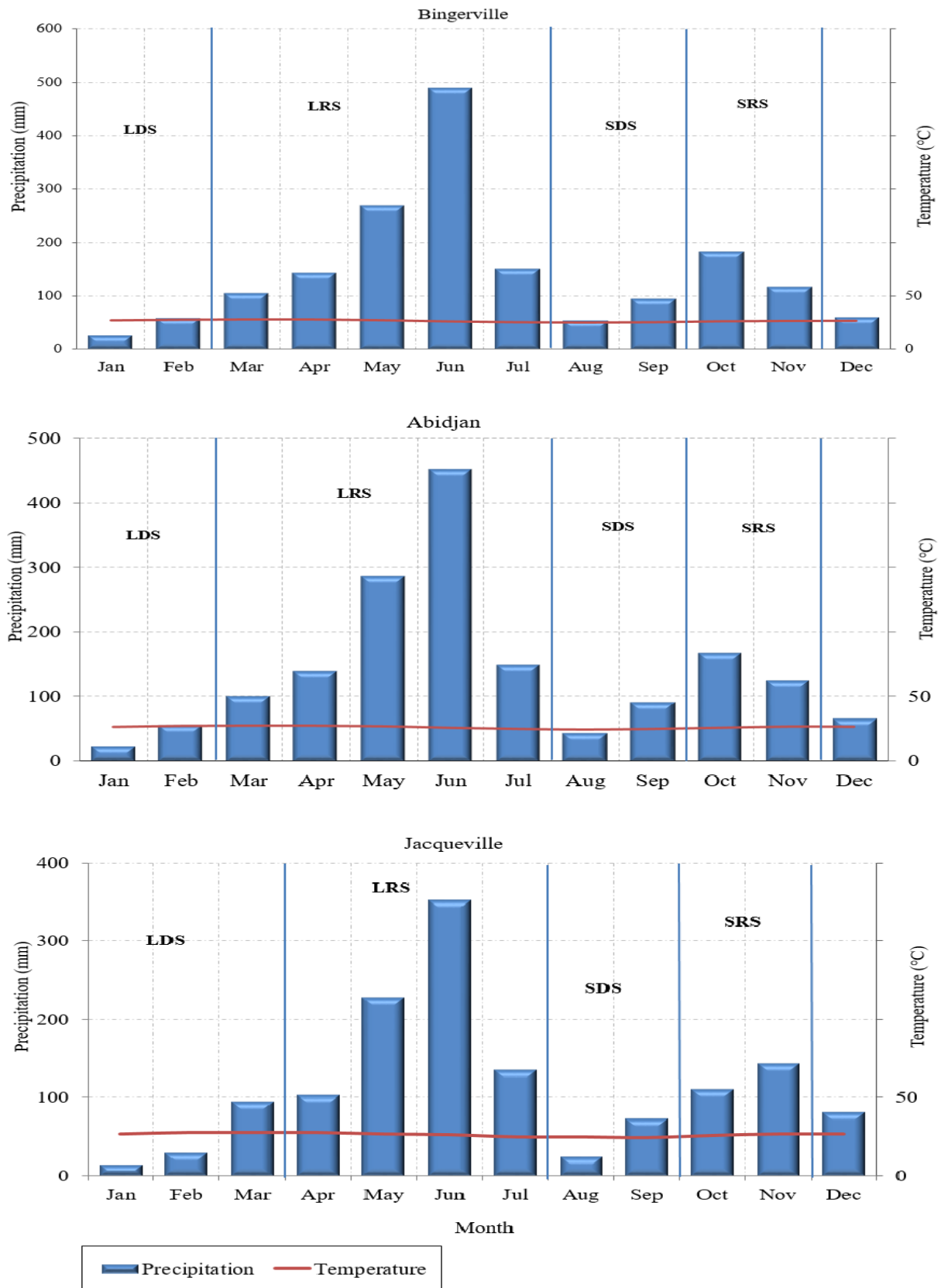


Figure 24: Graph showing average monthly rainfall amount (data source: SODEXAM). LDS is long dry season; LRS is long rainy season; SDS is short dry season and SRS, short rainy season for the Abidjan (central parts of the study area), Bingerville (eastern parts), and Jacqueville (western parts) meteorological stations.

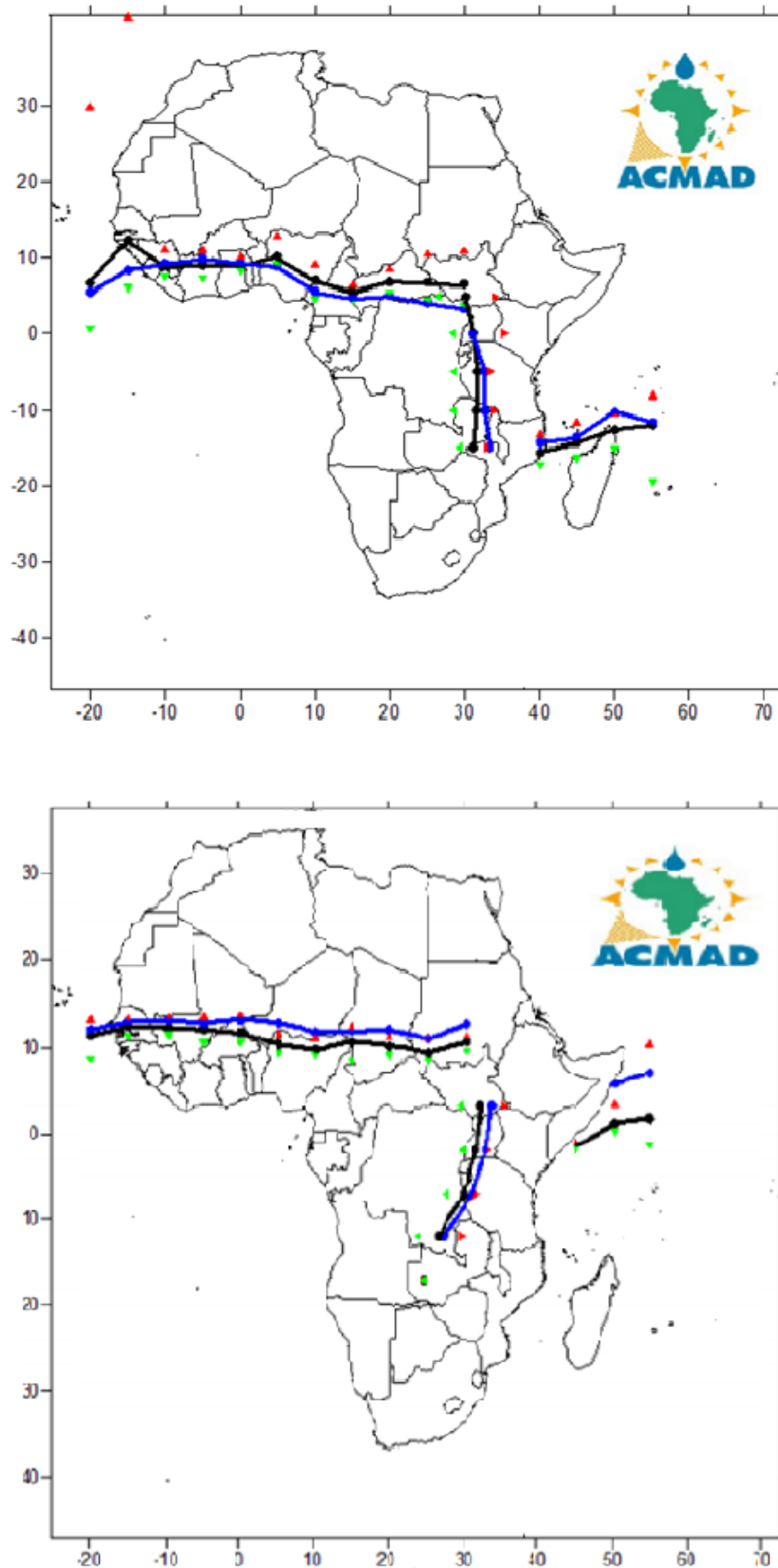


Figure 25: The mean position of ITD, CAB and ITCZ. Top: 3rd decade of January 2014 (black), 2nd decade of January, 2014 (blue). Bottom: 3rd decade of October 2014 (black), 2nd decade of October, 2014 (blue). The red and green triangles represent their maximum and minimum displacements respectively. (Source: ACMAD, 2014a, b).

For the Bingerville area, a 90th percentile (2,420 mm) cut-off designates the years 1976 and 1982 as extremely wet years, while 10th percentile (1,398 mm) cut-off designates the years 1970, 1988, 1989, 1992, 1998 and 2003 as extremely dry years. For the Abidjan area, a 90th percentile (2,175 mm) cut-off designates the years 1974, 1975, 1976 and 1982 as extremely wet years, while a 10th percentile (1,283 mm) cut-off designates the years 1985, 1986, 1995 and 1998 as exceptionally dry years. For the Jacqueville area, a 90th percentile (1,952 mm) cut-off designates the years 1974, 1976, 1996 and 2010 as extremely wet years, while at a 10th percentile (1,109 mm) designates the years 2004, 2011, 2012 and 2013 as extremely dry years. Mann Kendall test revealed this decrease to be statistically significant (p-value less than 0.05). For the Abidjan region, rupture, that is downward trend in precipitation (values below the multi-temporal moving average of 1,704 mm for the observation period between 1970 and 2014), started in the year 1983 after the major ENSO events. The year 1983 was earmarked as a year of intense drought. Precipitation deficit was between 18 and 20 % for this year (**Bigot, 2004**). Climate anomaly was observed over much of the globe during this year due to the intense El Niño-Southern Oscillations (ENSO) event (**Rasmusson & Wallace, 1983**). However, recovery (precipitation amount above moving average) for the Abidjan and Bingerville areas is evident after the 2009/10 ENSO event (Figure 26). On the contrary, for the Jacqueville area, downward trend in precipitation began since the year 1993/94 and continues until present (Figure 26). Since, the flow rate of the rivers draining the Ebrié sub-catchment is mainly controlled by rainfall (**United Nations, 1988**), negative impacts of precipitation deficit is evident on river systems. For instance, the annual average flow rate of the Comoé River, responsible for 75 % of the freshwater input into the sub-catchment (**Guiral, 1992**), reduced from 331 m³/s in 1960-70, to 161 m³/s in 1970–80, 119 m³/s in 1980-90 (**Convention on Biodiversity, 2009**) and 83.8 m³/s in 1993 (**Hauhouot, 2002**). Furthermore, the Agnéby River, one of the largest freshwater reservoirs in the area also recorded a flow deficit of 51 % between 1955 and 2000 (**Jallow *et al.*, 1999; Kouakou *et al.*, 2012**). Evidences of precipitation deficit and reduction in fluvial inputs in the littoral zone are dried up/abandoned groundwater wells and poor agricultural yields (**Brou Yao, 2010**). In addition to high deforestation rates as causative factors influencing local microclimate (**Brou Yao *et al.*, 1998**), substantial evidences exist of a direct relationship between the shape of the shoreline, progression of sea-breeze front and rainfall amount on adjacent inland areas (**Bakun, 1978; Negri *et al.*, 1994; Mazón *et al.*, 2013**). The concavity of the Ivorian coastline diverges oceanic breeze, resulting in scarce precipitation on adjacent inland areas (**Poorter *et al.*, 2004; Mazón *et al.*, 2013**). Coastline orientation is WSW-ENE between Tabou (western border) and Sassandra, E-W from Sassandra to Abidjan and WNW-ESE from Abidjan to its eastern border (**Wozazek, 2001**).

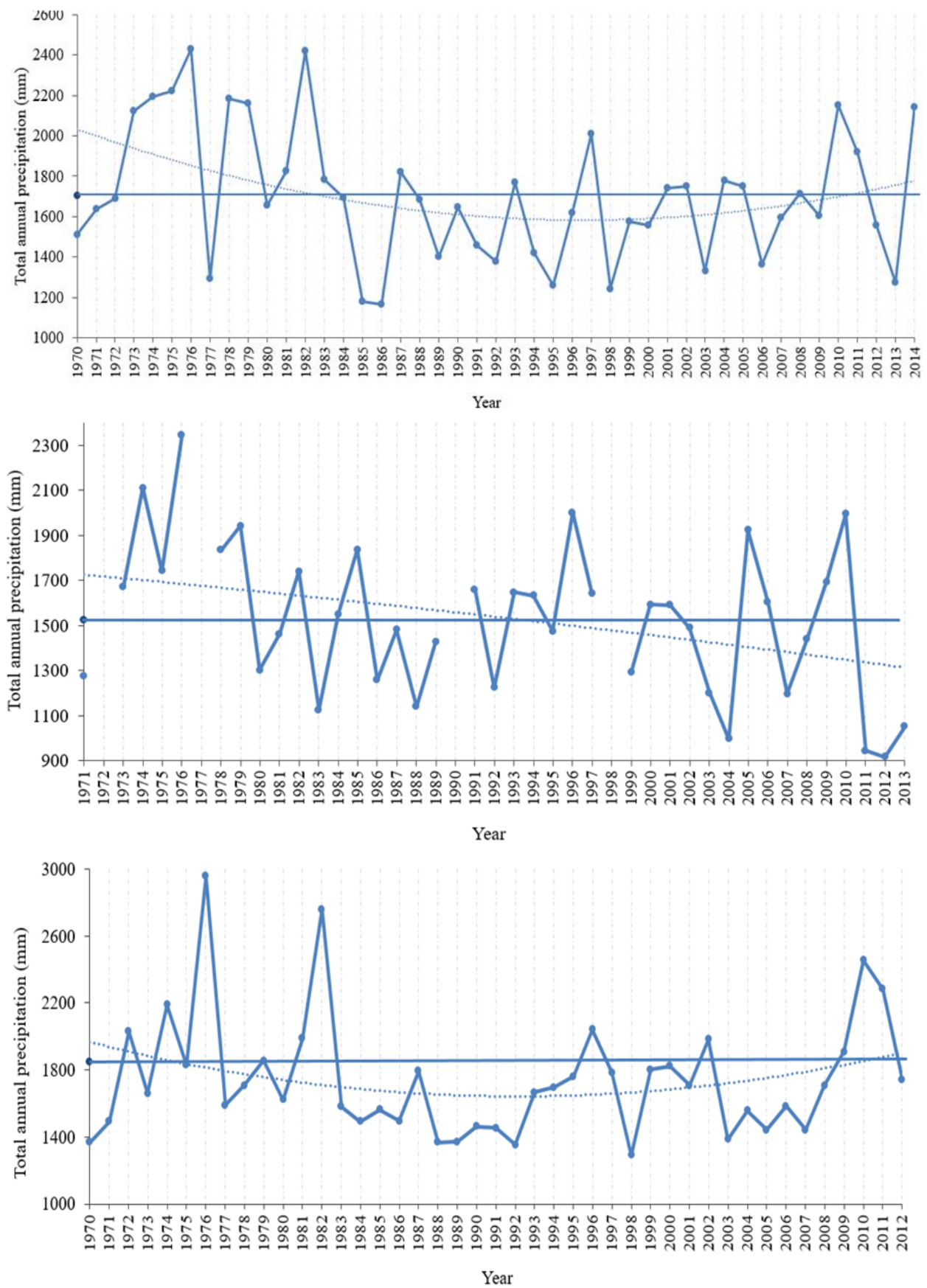


Figure 26: Yearly trend in precipitation across the study area. Abidjan (top) Jacquleville (middle), and Bingerville (bottom). Thick lines represent moving average, while dashed lines are second order polynomial fitted curves.

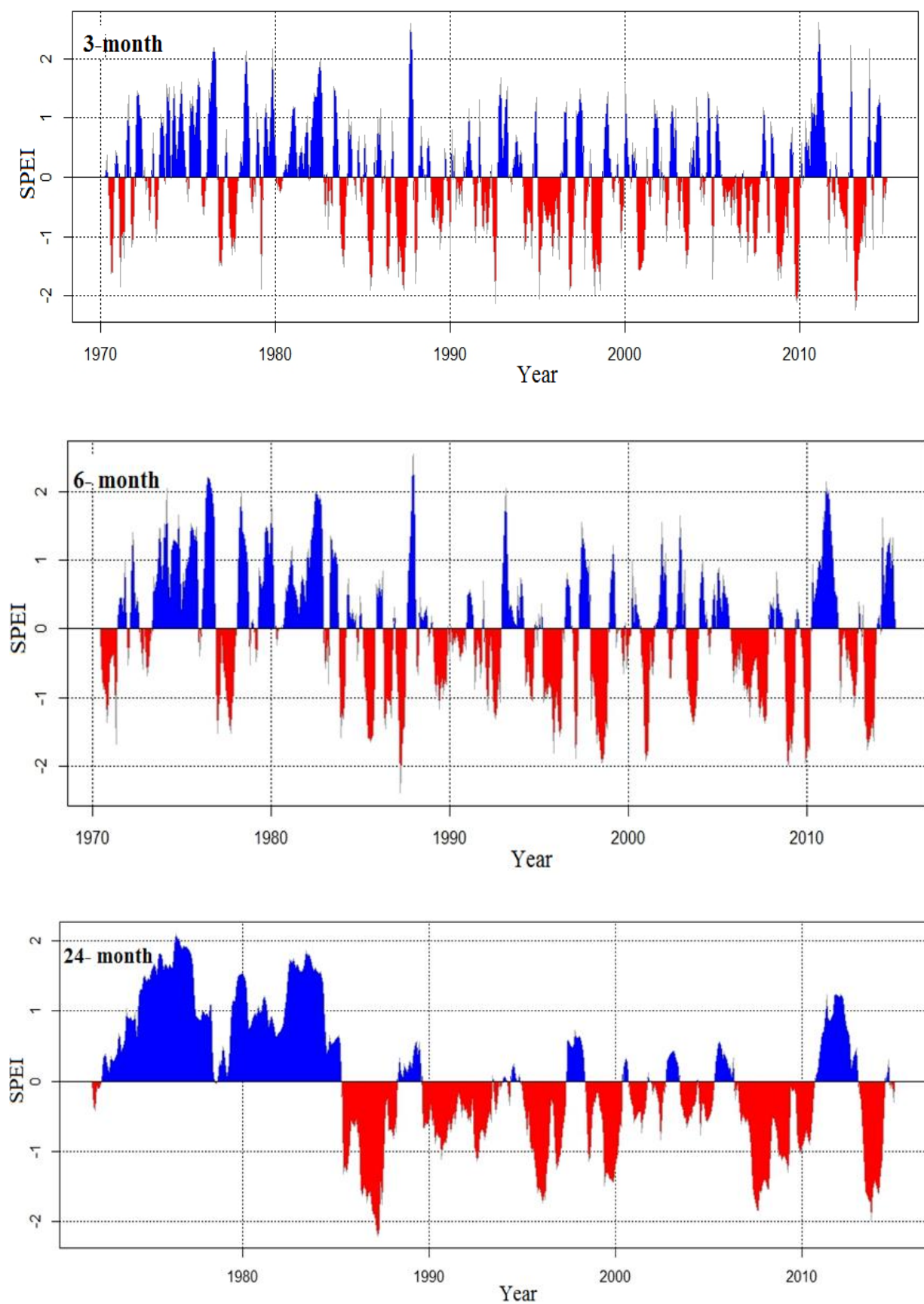


Figure 27: Temporal evolution of SPEI at different time scales for the Abidjan meteorological station. Time scale of 3-, 6- and 24-months depicts meteorological, agricultural, and hydrological/socio-economic droughts, respectively.

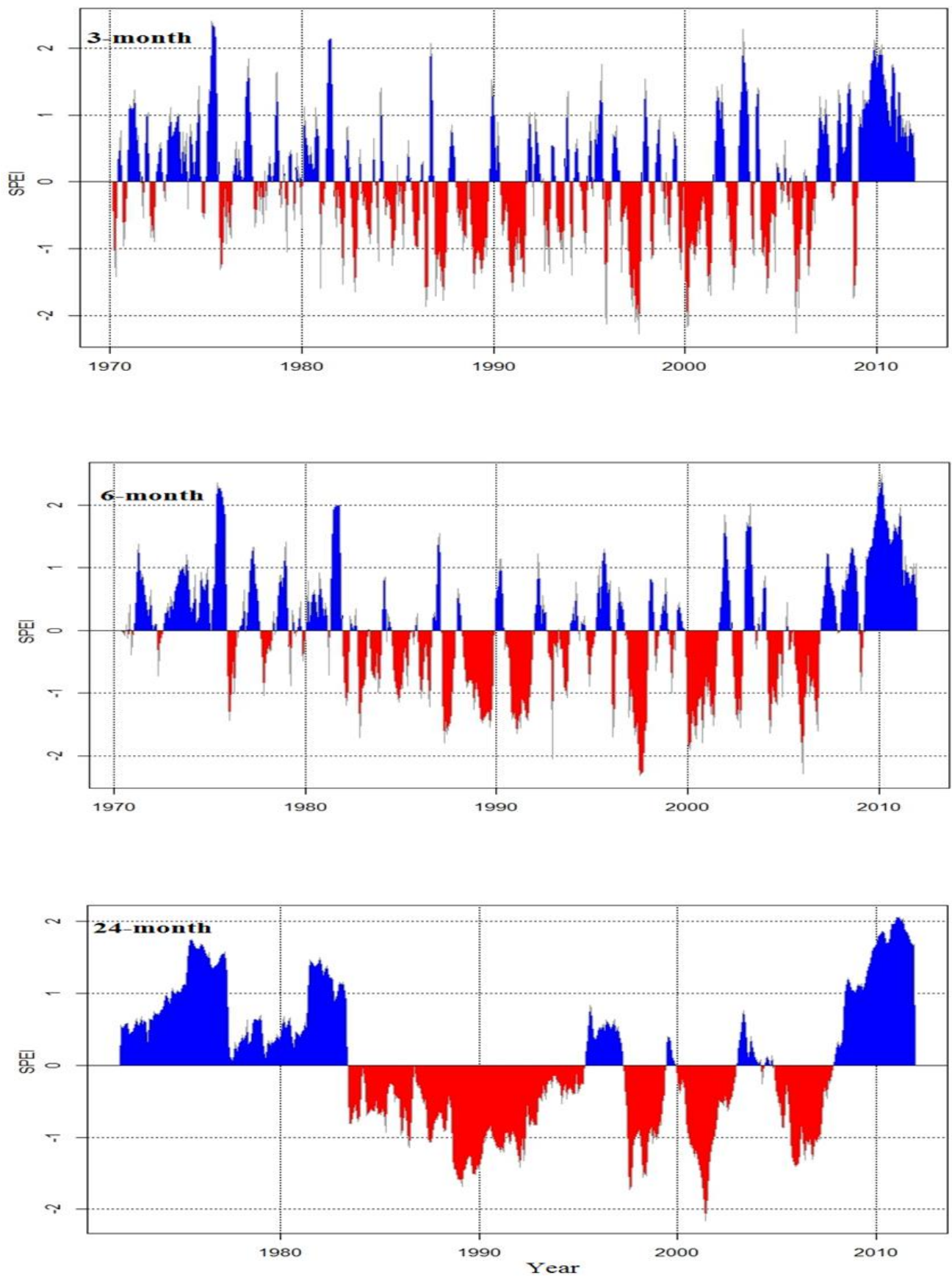


Figure 28: Temporal evolution of SPEI at different time scales for the Bingerville meteorological station. Time scale of 3-, 6- and 24-months depicts meteorological, agricultural, and hydrological/socio-economic droughts, respectively.

This disparity in the distribution of rainfall amount along the Ivorian coastline is reflected further inland by the V-shape delimitation (savannah intrusion) of the Guinea Savannah area commonly referred to as ‘the V-Baoulé’.

Standard Precipitation Evapotranspiration Index (SPEI) was computed for only Abidjan (Figure 27) and Bingerville (Figure 28) meteorological stations. Results were however lacking for Jacqueville station due to incomplete data on temperature. For Abidjan, count of the number of years with SPEI values lower (higher) than -0.1 ($+0.1$) for the SPEI-3 month time scale, showed that the 1980-89 decade had the most persistent meteorological drought with 23 % of the SPEI values below the drought line (-1.00). This is followed by the 1990-99 decade and lastly the 2000-10 decade. The 1970-79 decade was the wettest with over 40 % of SPEI values above the wet line ($+1.00$). Extremely wet years during this period were 1976/77, 1982/83, while severely dry years were 1987, 1998/99 and 2013/14. On the other hand, in Bingerville, the 1990–99 and 2000–10 decades showed the most persistent meteorological drought, both with 18 % of the SPEI values below the drought line (-1.00). The 1980-89 decade was the wettest in this area with 23 % of SPEI values above the wet line ($+1.00$). Presently, the Bingerville area shows no sign of water stress (Figure 28).

4.1.2. Hydrochemistry of precipitation

Analytical precision and accuracy was estimated as better than 15 %. This relatively high ion balance error might be due to the formation of precipitates in some samples or the omission of analyses of some ions with main contributions to water chemistry. For analyses with less than 15 % non-detects, half the value of the method’s detection limit, MDL was substituted for non-detects for statistical and plotting purposes (Mitchell, 2006). The iron and manganese concentrations with non-detects of more than 50 % were excluded from statistical analyses. Furthermore, these parameters were measured once in January (dry season). Physicochemical parameters of rainwater are summarized in Table X. Rainwater were mainly of the Na-HCO_3 hydrochemical facies. The end of the dry season (March) is marked by Ca-SO_4 facies, while the end of the short rainy season was marked by Ca-HCO_3 type. Na-Cl facies were recorded at the end of the long rainy season (June) and a mixture of Ca-Cl and Na-Cl type were recorded during the short dry season (August).

Stable isotopes in Abidjan precipitation

During the dry season, precipitation was more enriched in heavy isotopes of oxygen-18 and deuterium compared to the rainy season. Mean values of $\delta^{18}\text{O}$ and $\delta^2\text{H}$ in precipitation were -0.84 and 1.48 for the dry season, and -2.27 and -7.40 for the rainy season, respectively. The observed changes in

isotopic composition in precipitation reflect the position of the Inter Tropical Convergence Zone (ITCZ). During the dry season (January/February), the ITCZ was closer to the equator in its southward descent (ACMAD, 2014a). The warm, dry harmattan NE trade winds were dominant (Pàges *et al.*, 1979) and as such, rain falls through dry air, leading to secondary evaporation. During evaporation, light isotopes preferentially enter the vapour phase, while heavy isotopes are concentrated in the liquid phase (Dansgaard, 1964). Conversely, during the rainy season (September/October), the ITCZ was furthest north (ACMAD, 2014b) and relatively cold, humid SE trade winds (southwest monsoon) of maritime origin dominates (Morlière & Rebert, 1972), leading to precipitation depleted in heavy isotopes. The relationship between stable isotope composition in precipitation and three major descriptors of climate (surface air temperature, rainfall amount, and relative humidity) was investigated. Results showed that precipitation amount controlled the isotopic composition of precipitation, but temperature did not play an important role. There was rather a correlation with precipitation amount ($r^2 = 0.5$). This is known as the amount effect (Dansgaard, 1964). Based on a $\delta^{18}\text{O}$ - $\delta^2\text{H}$ plot (Figure 29), the local meteoric water line (LMWL) plot on a linear regression of $\delta^2\text{H} = 7.2 * \delta^{18}\text{O} + 8.2$ ($r^2 = 0.95$). This fits perfectly to the revised regression slope of $8.17 \pm 0.07 \text{ ‰}$ and with an intercept of $11.27 \pm 0.65 \text{ ‰}$ (Rozanski *et al.*, 1993).

4.2. Groundwater aquifers

Spatiotemporal trends were observable in groundwater levels. The depth to water table was recorded in all studied wells during the dry (January/February) and rainy (September/October) season. The results are given in Table XI. Water levels representing non-pumping conditions showed seasonal fluctuations. The phreatic groundwater table is usually shallow and ranged between 0.2 and 4.87 m below the soil surface for the dry season. This however, significantly increased to values between 0.05 and 6.4 m during the rainy season. Factors that might influence these variations are rate of groundwater abstraction and aquifer material. As groundwater flow is topography-driven, active recharge areas were identified as high altitude areas from a potentiometric surface map (Figure 30). The general flow direction is north - south, besides few localized exceptions. From the plot of water levels from monitoring wells versus meteorological (temperature and precipitation) data (Figure 31), the movement of the water level clearly illustrates the delay in water transfer after rain events from the surface to the subsurface. Time lag was approximately one month after the peak of seasonal rainfall events for Abidjan and Dabou areas. There was however, a corresponding increase in water table following peak rain events in Bingerville. Regional groundwater recharge by infiltrating precipitation seems possible during April to July and in October –November. The total precipitation for the studied dry season (January/February) of 2014 was 44.5 mm.

Table X: Summary of physicochemical parameters of rainwater (n = 30).

Physicochemical parameters	Mean (\pmS.D.)
Temperature ($^{\circ}$ C)	24.48 ± 0.99
pH	6.3 ± 0.6
Conductivity (μ S/cm)	13 ± 11.7
Dissolved oxygen mg/L)	5.94 ± 1.21
Alkalinity (meq/L)	0.18 ± 0.12
Bicarbonate, HCO_3^- (mgL $^{-1}$)	11.39 ± 3.79
Silicate, SiO_4^{4+} (mg/L)	0.75
Ammonium, NH_4^+ (mg/L)	0.38 ± 0.22
Bromide, Br (mg/L)	0.05 ± 0.04
Nitrate, NO_3^- (mg/L)	3.26
Sodium, Na^+ (mg/L)	4.27 ± 3.49
Potassium, K^+ (mg/L)	0.43
Magnesium, Mg^{2+} (mg/L)	0.31
Calcium, Ca^{2+} (mg/L)	3.32
Chloride, Cl^- (mg/L)	3.63
Sulphate, SO_4^{2-} (mgL $^{-1}$)	4.37

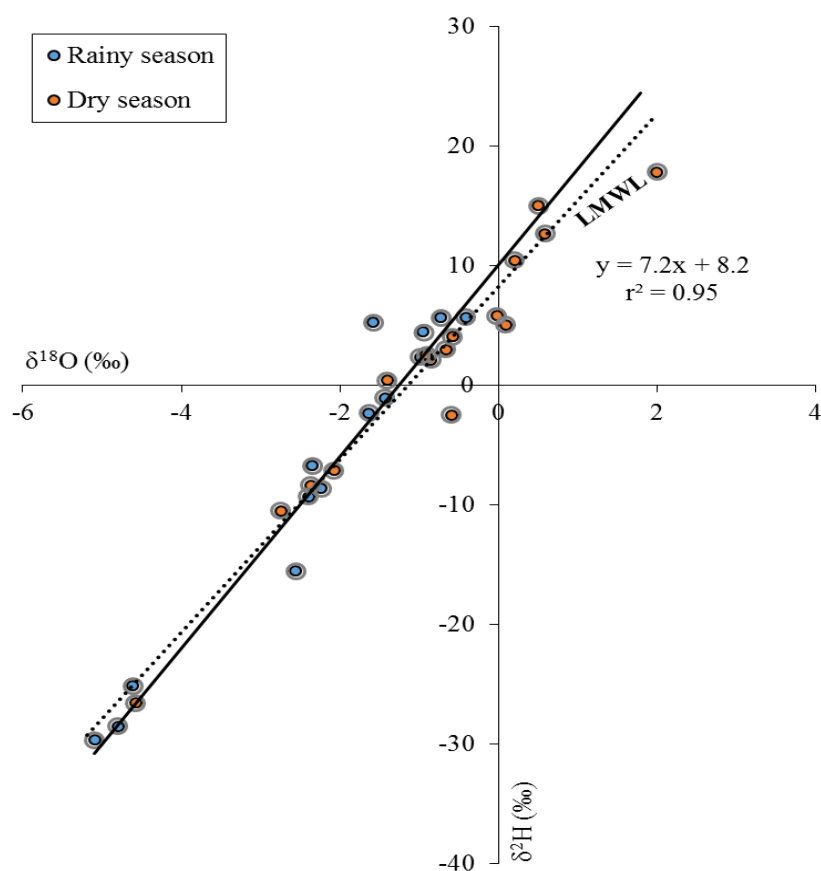


Figure 29: $\delta^{18}\text{O}$ - $\delta^2\text{H}$ plot of precipitation waters of Abidjan.

Table XI: Water table level from ground surface in wells for the dry and rainy season and their total depth

ID	Aquifer	Water level (m)		Total well depth (m)
		Dry	Rainy	
P1	CTeast	-2.76	-2.49	3.35
P2	QM	-3.23	-2.76	3.5
P3	QM	-3.02	-2.52	3.23
P4	QM	-1.8	-1.28	1.85
P5	CTeast	-1.37	-1.58	2
P6	CTeast	-2.68	-2.24	3.13
P7	CTeast	-1.35	-1.01	1.85
P8	CTeast	-4.52	-4.19	4.6
P9	CTeast	-0.66	-0.1	1.04
P10	CTeast	-6.6	-5.08	6.8
P11	CTeast	-2.9	-2.51	3.2
P12	CTeast	-4.2	-3.32	5
P13	CTwest	-11.4	-10.3	14.7
P14	CTwest	-2.12	-1.57	6.44
P15	QM	-1.37	-1.13	1.9
P16	CTwest	-4.5	-4.2	5.66
P17	CTwest	-2.11	-	2.74
P18	CTwest	-2.42	-2.21	3.36
P19	CTwest	-9.2	-9.69	12
P20	CTwest	-2.89	-2.4	3.8
P21	CTwest	-1	-0.4	1.3
P22	QM	-1.87	-1.54	2.72
P23	QM	-0.84	-0.02	1
P25	QM	-4.38	-3.7	6.03
P26	CTwest	-2.2	-1.92	2.3
P28	QM	-4.93	-4.68	5.2
P29	QM	-5.92	-5.8	6
P30	QM	-5.92	-5.3	-
P31	QM	-4.47	-3.7	4.63
P32	QM	-	-3.82	-
P33	QM	-	-6	6.4
P34	QM	-1.36	-0.43	1.6
P35	QM	-5.6	-5.4	5.83
p36	CTeast	spring		

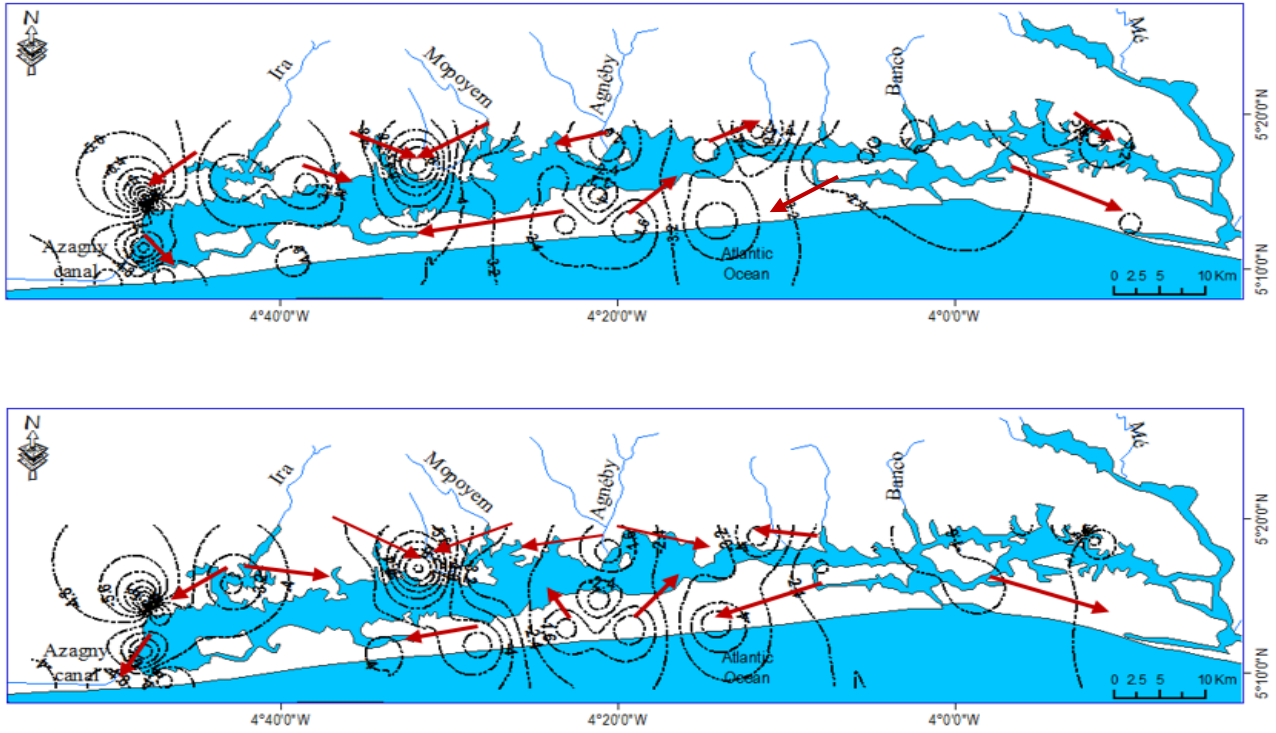


Figure 30: Potentiometric surface maps showing flow direction from static, non-pumping water levels (m below land surface) of the unconfined aquifers for the dry (top) and rainy season (bottom).

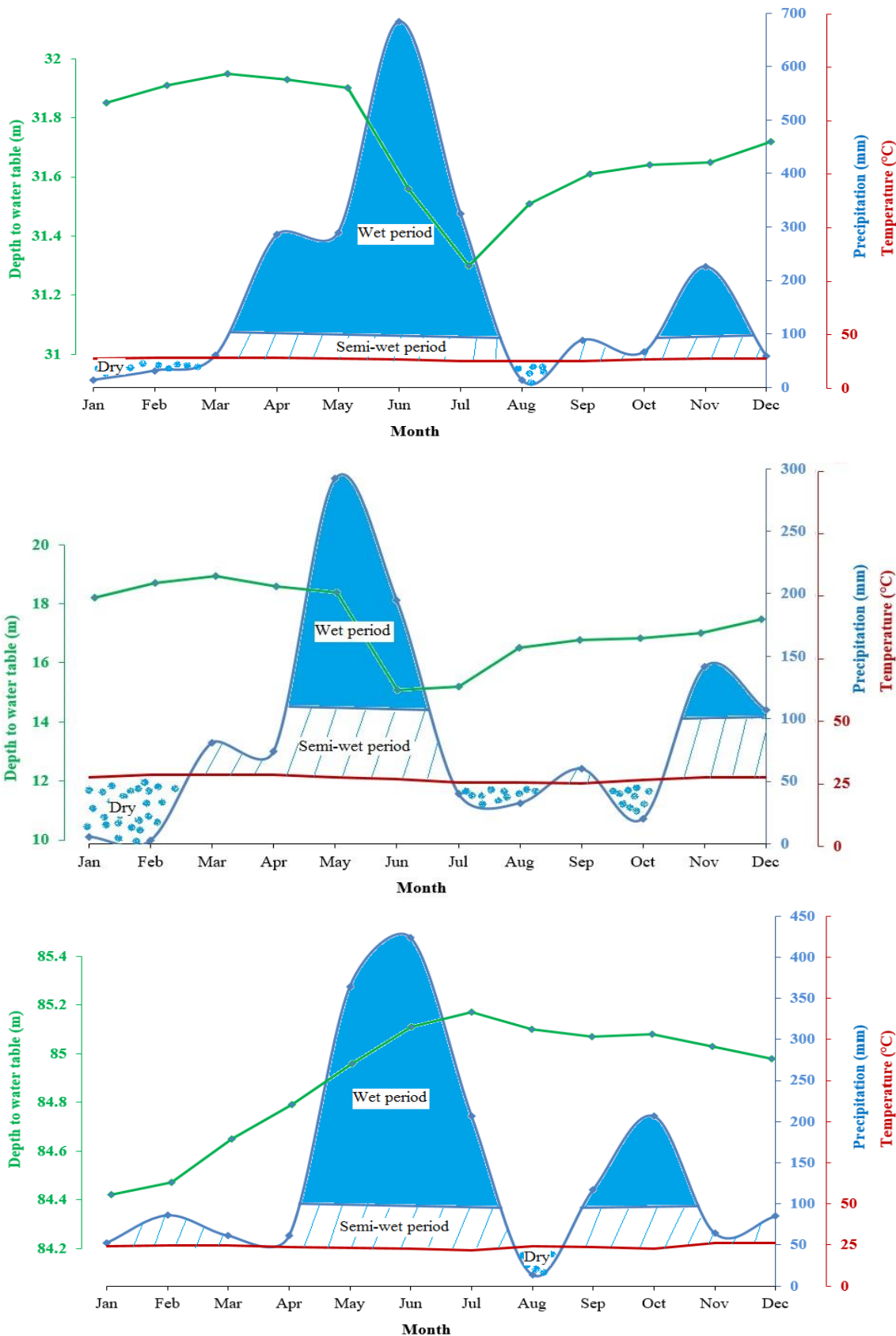


Figure 31: Groundwater recharge history as shown by monthly fluctuations in water table level recorded from piezometers (GWL) (data source: L'Office National d'Eau Portable, 2014) superimposed on umbrothermic diagram. Abidjan (top), Dabou (middle), and Bingerville (bottom). The borehole responded to peak rain event after a time lag of one-month for Abidjan and Dabou, and simultaneously for Bingerville.

This represents only 2.1 % of total annual precipitation amount of 2,141.8 mm, whereas, precipitation for the rainy season (September/October) of 2014 was 154.6 mm; representing 7.22 % of total annual precipitation. Based on a chloride mass-balance calculation; regional mean groundwater recharge was estimated at 0.25 mm/month for the dry season with minimum and maximum values of 0.02 and 16.45 mm/month, respectively. This signifies that between 0.1 % and 37 % of precipitation for this period infiltrated into these aquifers. On the other hand, for the rainy season, mean groundwater recharge was 0.49 mm/month with minimum and maximum of 0.03 and 5.63 mm/month, respectively. This signifies that between 0.02 % and 3.6 % of precipitation for this period infiltrated into these aquifers.

4.2.1 Physico-chemical parameters

pH: The pH mirrors the current condition of the buffer system. Groundwater pH was in the acid range during the investigation period for majority of the water wells. In these coastal wells, groundwater acidification was a more likely occurrence during the rainy season. During the dry season, pH was in the range of 4.3 – 7.1, 4.5 – 6.7 and 4.1 – 6.6 for the QM, CTeast and CTwest aquifers respectively. During this period, wells with pH values lower than the WHO drinking water standard ($6.5 < \text{pH} > 8.5$) were 75 %, 62 % and 69 % for the QM, CTeast and CTwest aquifers respectively. Whereas, during the rainy period, pH ranged between 4.7 – 7.5, 4.6 – 7.2 and 4.4 – 6.6 for the QM, CTeast and CTwest aquifers, respectively. Thirty-nine percent of wells within the QM aquifer recorded pH lower than that of the WHO drinking water standard. 77 % and 89 % of wells within the CTeast and CTwest aquifers, respectively recorded pH lower than the designated WHO standard. Majority (67 %) of the boreholes were acidic during the dry season with values between 3.9 and 7.4. For the rainy season, values did not vary much and range between 3.9 and 7.4. Groundwater acidity provides evidence for silicate mineral hydrolysis and water-rock interaction.

Temperature: Groundwater temperatures were much higher during the dry season with values ranging between 23.5 – 33.2, 27.5 – 30.7, and 27.1 – 30.9 °C for QM, CTeast, and CTwest aquifers, respectively. Whereas, during the rainy season temperatures showed significant decrease with values between 28.2 – 29.8, 26.5 – 29.9 and 26.5 – 29.5 °C for QM, CTeast, and CTwest aquifers, respectively. The CTwest aquifer contained the coolest waters.

Turbidity: Groundwater was relatively more turbid during the dry season. This is because of the relatively lower water table coupled with the fact that the majority of the dug wells are open bottom and well water is in direct contact with aquifer materials. Range of values were 0.45 – 95, 0.31 – 18.5 and 1.5 – 80.9 NTU for the QM, CTeast and CTwest aquifers, respectively. Forty-six percent of wells

within the QM aquifers recorded turbidity values higher than the permissible WHO drinking water standard of 5 NTU. Only 50 % of the wells within the CTeast and CTwest showed values exceeding the WHO standard during dry season.

During the rainy season, highest turbidity (36.9 NTU) was recorded in well p26 within the CTwest with range of values between 0.86 – 36.9 NTU. For the CTeast, turbidity values range between zero and 19.7 NTU, whereas the QM aquifers recorded values between 0.75 and 32.5 NTU. Percentage of wells with turbidity above the permissible WHO standard (5 NTU) was 25 %, 31 % and 33 % for the QM, CTeast and CTwest aquifers, respectively.

Dissolved oxygen: The freshwater wells within the coastal environment are highly anoxic. None of the studied wells attained the WHO drinking water standards for dissolved oxygen during the investigation period. Dissolved oxygen values ranged between 1.8 – 4.5, 1.4 – 5.3 and 1.6 – 5 mg/L for the QM, CTeast and CTwest aquifers, respectively during the dry season. Recorded range of dissolved oxygen values for the rainy season were between 1.1 – 5.6, 0.7 – 4.8 and 1.1 – 5.6 for the QM, CTeast and CTwest aquifers, respectively. The lowest dissolved oxygen value (0.7 mg/L) was recorded in well p9 within the CTeast aquifer during the rainy season. Groundwater hypoxia is indicative of recharge waters with relatively short residence time and as such, oxidation is incomplete producing low dissolved oxygen concentrations (**Verstraeten *et al.*, 2005**).

4.2.2. Hydrochemical characterisation

Overall, 149 samples were analysed for their chemical and isotopic composition. The ion balance error ranged $\pm 10\%$. However, this value was exceeded by about 12 % of the samples during the investigation period. Potential for groundwater salinization was higher during the dry season. Maximum chloride concentration was 1,088 mg/L, 36.8 mg/L, 72.9 mg/L for QM, CTwest and CTeast aquifers, respectively. **Tolman and Poland (1940)** regarded water with chloride concentrations above 100 mg/L as contaminated. Based on their classification, for the dry season, two wells, both within the QM aquifer: p4 (Cl: 105.3 mg/L) and p15 (1,088 mg/L) were considered contaminated. During this period, F5 was the only borehole from the deep aquifers, which was contaminated with a chloride concentration of 380 mg/L.

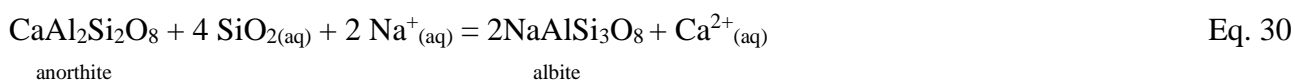
During the rainy season, maximum chloride concentration was 785.24 mg/L, 72.94 mg/L and 36.8 mg/L for the QM, CTeast and CTwest aquifers, respectively. As with the dry season, only wells and one borehole within the QM aquifer recorded chloride concentrations above 100 mg/L: wells p2 (111.24 mg/L), p4 (139.2 mg/L), p15 (785.2 mg/L) and p24 (113.6 mg/L) and borehole, F5 (381.6 mg/L). The QM aquifer is the most susceptible to seawater intrusion.

Although, no health-based guideline value has been proposed for chloride in drinking water, Chloride concentrations in excess of 250 mg/L can give rise to detectable taste (**World Health Organization, 2003**). Drinking of such water can induce fatal dehydration and long-term consumption can lead to kidney damage and even death (**National Oceanic and Atmospheric Administration, 2014**). It is therefore not advisable to drink water from borehole F5 and well p15 with chloride in exceedance of 250 mg/L during the investigation period.

There exists no correlation between chloride concentrations in groundwater wells and their perpendicular distance to the Atlantic coastline (Figure 32). There was however a weak positive correlation ($r^2 = 0.5$) between chloride concentration in water wells with total well depth (Figure 33). The existence of a vertical salinity gradient in these groundwater wells denotes natural salinity sources (**Richter *et al.*, 1991**). Subsequently, plots were made of measured major ions versus chloride (Appendix III). Mixing trends were evident from these composite plots.

The piper plot (Figure 34) showed that majority of the water wells (87 %) belonged to the Na-Cl hydrochemical facies during the dry season. Other hydrochemical facies during this season were mixed cation type- HCO_3 (p7 and p14) and Ca-HCO_3 type (p19 and p22). Both water types probably evolved in disseminated clay zones by ion exchange (**Hiscock, 2009**). Except for borehole F6 (Ca-HCO_3 hydrochemical facies), all boreholes were of the Na-Cl water type during the dry season.

During the rainy season, all boreholes belonged to the Na-Cl facies. Eighty percent of the studied wells belonged to the Na-Cl hydrochemical facies. Wells p7, p8 and p22 were of the Ca-HCO_3 hydrochemical facies. Well p22 maintained the Ca-HCO_3 facies type. The Ca-HCO_3 water type is characteristics of recently recharged waters (**Hiscock, 2009**). Signs of early salinization were evident in well p27 that evolved geochemically as a Ca-Cl water type (**Vengosh *et al.*, 1999**). Wells p3, p31 and p32 evolved as Ca-Mg-Cl water types. Ca^{2+} in these water samples were probably derived from reverse ion exchange and/or plagioclase albitization (**Hiscock, 2009**):



Wells (p7 and p15) and borehole F5 showed carbonate mineral saturation during the rainy season with saturation indices greater than 1. Based on the grading category of **Kelly (2005)**, different groundwater categories are presented in Table XII. $\text{Na}/(\text{Na}+\text{Ca})$ ratio can be used to identify surface and groundwater chemistry (**Gibbs, 1992**). A triad of precipitation, water-rock interactions, and seawater salinization is responsible for the coastal water chemistry from the Gibb's diagram (Figure 35).

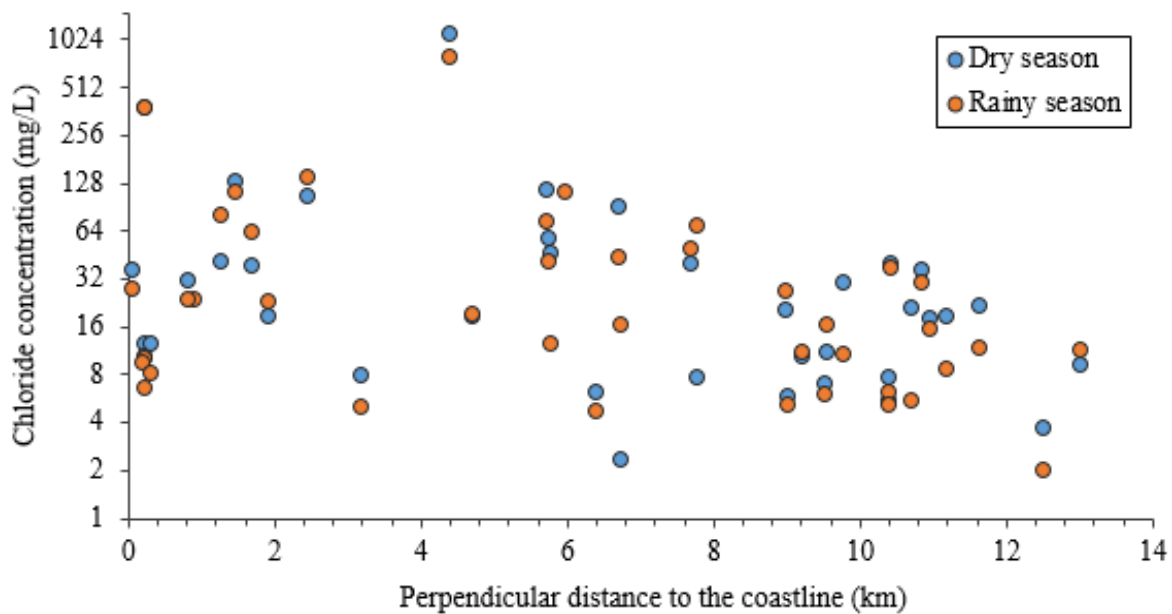


Figure 32: Chloride concentration (mg/L) versus perpendicular distance to the coastlines (km) for the dry and rainy seasons.

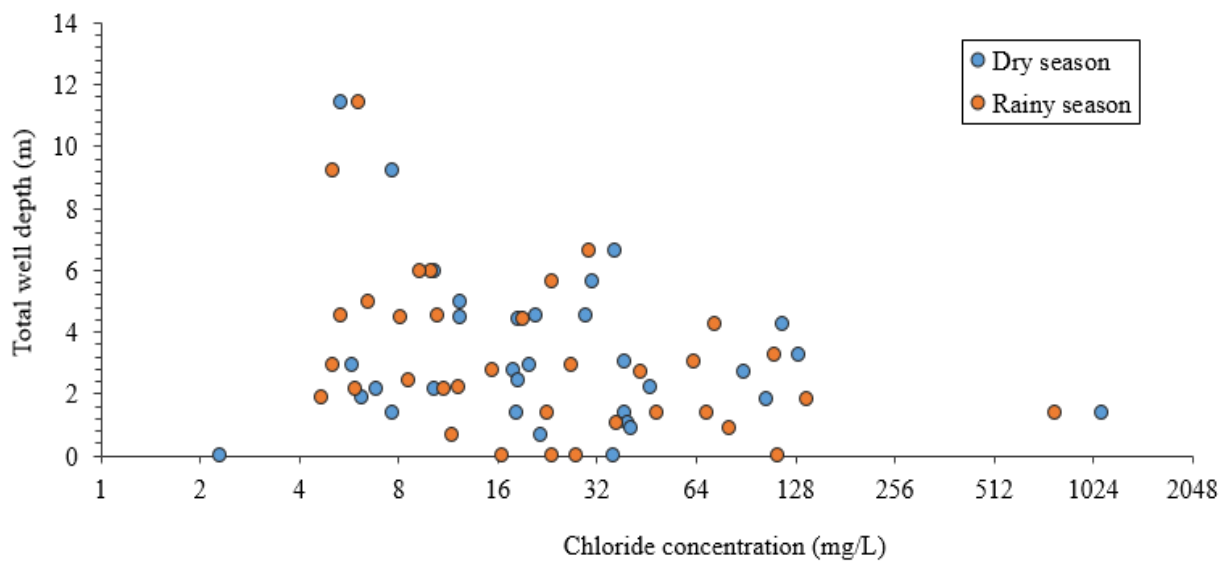


Figure 33: Chloride concentration (mg/L) versus total well depth (m) for the dry and rainy seasons.

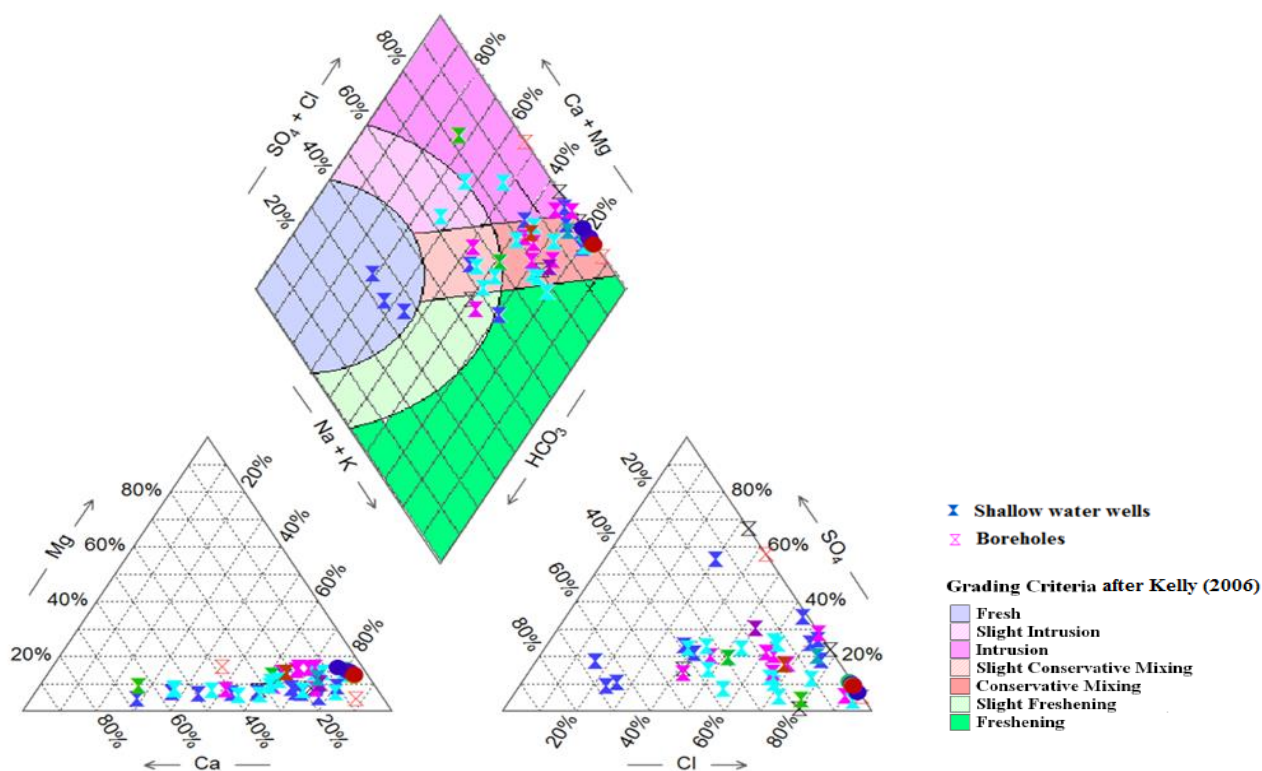
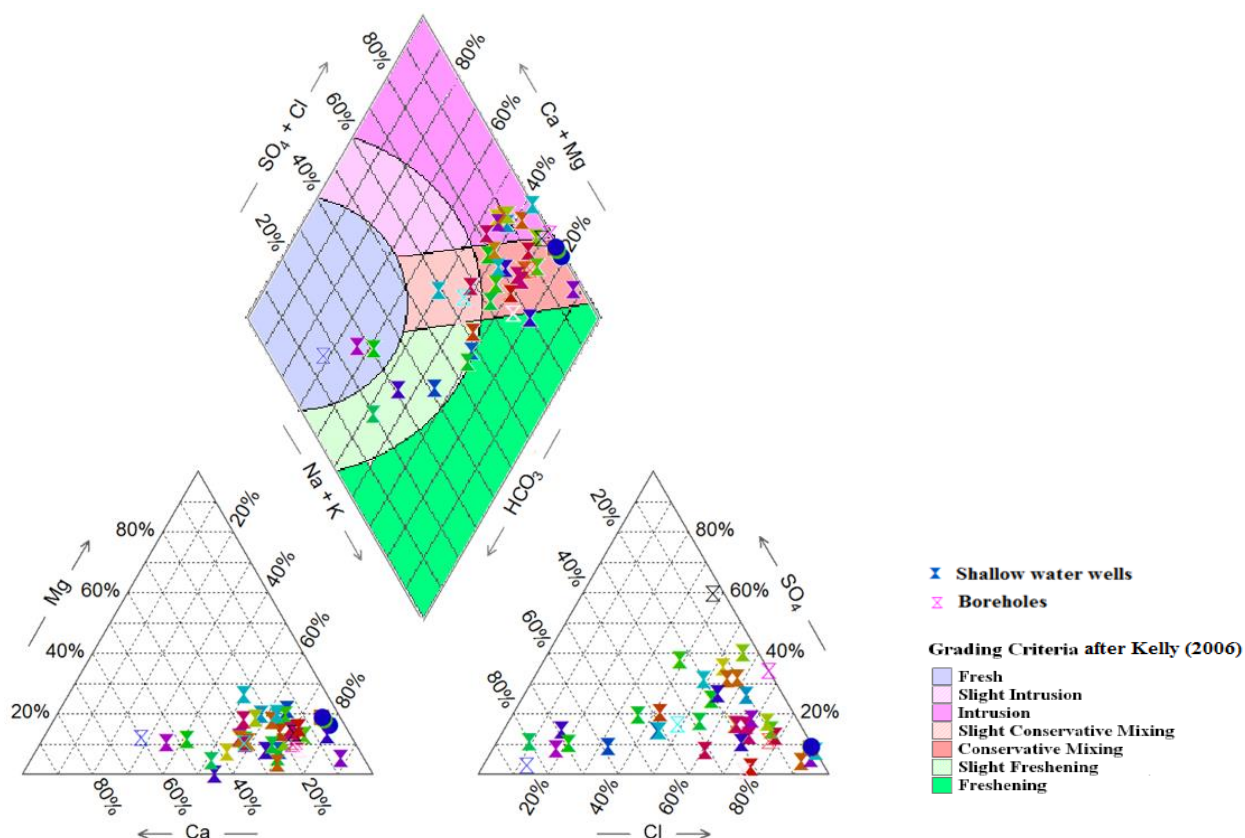


Figure 34: Trilinear diagram (Piper, 1944) of major ions of the groundwater and inshore systems for the dry (top) and rainy (below) seasons.

Table XII: Categories of groundwater after Kelly (2005).

Categories	Dry season	Rainy season
Fresh	wells (p19,p22); borehole (F6)	wells (p7, p8, p22)
Slight intrusion	-	wells (p31, p32)
Intrusion	wells (p1, p16, p21, p26, p29, p31, p33, p36)	wells (p3, p5, p16, p21, p27); boreholes (F4, F6)
Slight conservative mixing	wells (p13, p25); borehole (F3)	wells (p9, p24,p25, p26, p28, p30)
Conservative mixing	wells (p3, p6, p8, p10, p11, p15, p17, p18, p20, p23, p28, p34, p35); boreholes (F1, F2, F4, F5)	wells (p1, p4, p10, p11, p12, p13, p14, p15, p17, p18, p20, p23, p29, p33, p34, p35, p36); borehole (F1, F2, F5)
Slight freshening	wells (p4, p7, p9, p14)	wells (p19); borehole (F3)
Freshening	well (p2)	wells (p2, p6)

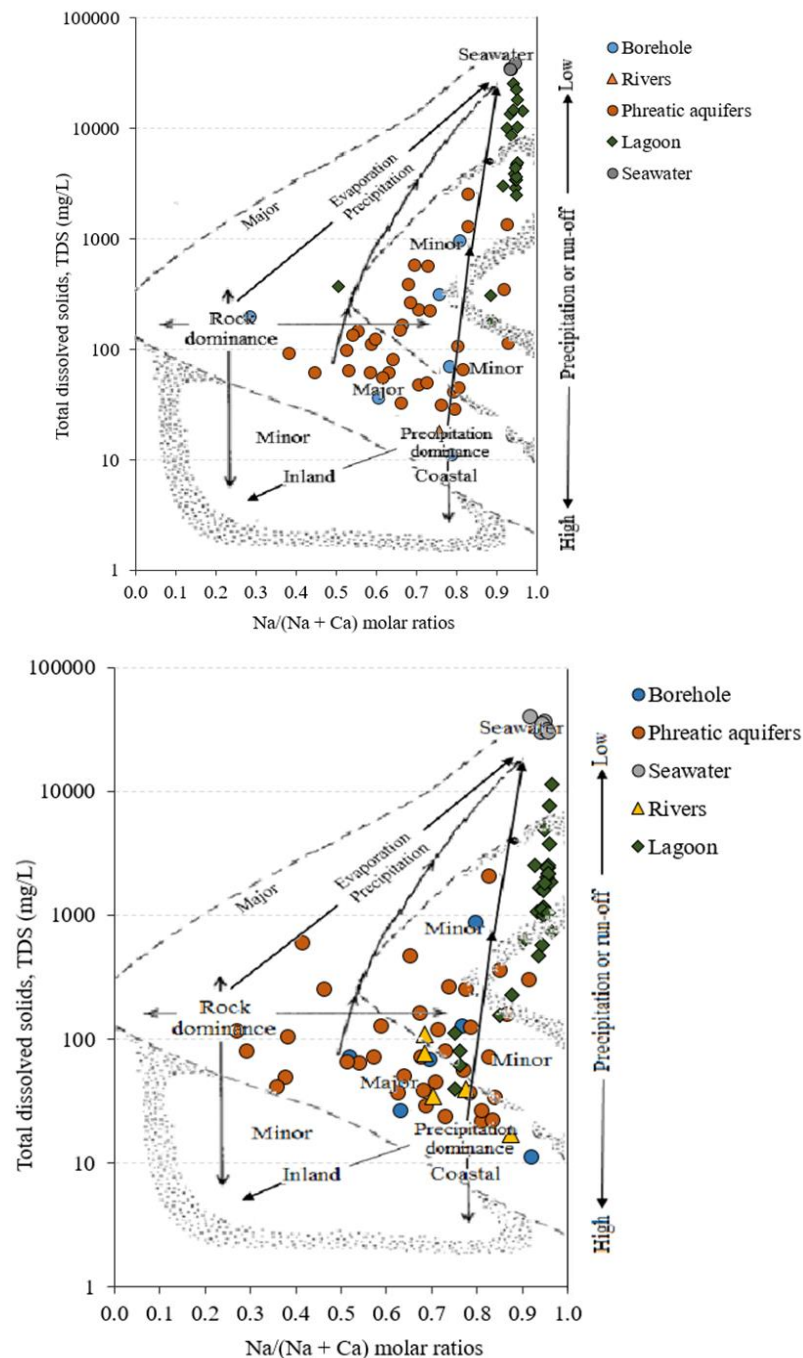


Figure 35: Plot of TDS versus Na/(Na + Ca) molar ratios (Gibbs, 1992) for the dry (top) and rainy (bottom) seasons.

Evaporation and mixing processes exerts the most control on water chemistry during the dry season, while water-rock interactions dominated during the rainy season.

Furthermore, results from the Durov plot (Figure 36) match with those of the Piper and Gibb's plot, but it highlights simple mixing/dissolutions and reverse ion exchanges as the main geochemical processes controlling coastal water chemistry. The mixing relationship is evident from the plot of a high percentage of samples (dry season: 58 %; rainy season: 72 %) along the theoretical mixing line (fields 3-5-7). According to the interpretation of the Durov plot by **Llyod and Heathcote (1985)**, for the dry season, samples (F6), which plotted on field 3 belongs to the Na-HCO₃ facies. Samples on field 4 (p11, p26, p29, p31) denote mixed anion waters – simple dissolution. Samples on field 5 (p13, p25, F3) indicate no dominant ion, on field 6 (p7, p19, p22) indicate probable mixing. Field 7 with majority of the samples (46 %) is indicative of Na-Cl waters, resulting from reverse ion exchange. Lastly, samples that plots on field 8 (p4, p9, p14, p17, p20) were also indicative of reverse ion exchange of Na-Cl waters. Geochemical evolution was evident in the groundwater systems during the rainy season. Samples on field 1 (p27) are recharge waters of the Ca-HCO₃ facies. Only sample, p8 plotted on field 3. Samples on field 4 (p3, p31, F6), Samples, p7 and p22 formerly on field 6 (probable mixing) now plots on field 5 (no dominant ion). During this period, highest percentage of samples (56 %) now plots on field 6 (probable mixing) as opposed to field 7 (reverse ion exchange) during the dry period. Lastly, samples p6 and p30 formerly on field 7 now plots on field 8.

Nitrate contamination of drinking water sources

Nitrate concentrations for the studied groundwater sources are displayed in Figure 37. Nitrate contamination is a serious problem in this coastal environment (**Scheren *et al.*, 2004**). For the wells, nitrate values ranged from 0.3 to 139.5 mg/L during the dry season. Only 21 % of the studied wells had values above the WHO permissible limit of 50 mg/L. These are wells p3, p4 (QM aquifer), p5, p10, p12 (CTeast), p16 and p21 (CTwest). Whereas, during the rainy season, nitrate concentrations ranged from 0.0 to 165.9 mg/L. The WHO threshold value of 50 mg/L was exceeded in about 14 % of the wells. These are wells p3 (QM aquifer), p1, p10, p12 (CTeast), p21 (CTwest). For the boreholes, nitrate concentrations ranged between 0.3 to 130 for the dry, and 0.4 to 92.5 mg/L for the rainy season. WHO drinking water standard was exceeded only in borehole, F1 with values of 130 mg/L for the dry, and 92.5 mg/L for the rainy season. Nitrate contamination of coastal wells is a more likely occurrence during the rainy season. Nitrate concentration greater than 50 mg/L can cause methemoglobinaemia in infants less than six months old and in addition can form carcinogenic nitrosamine in the human intestines (**Environmental Protection Agency, 1976; Heathwaite *et al.*, 1993**).

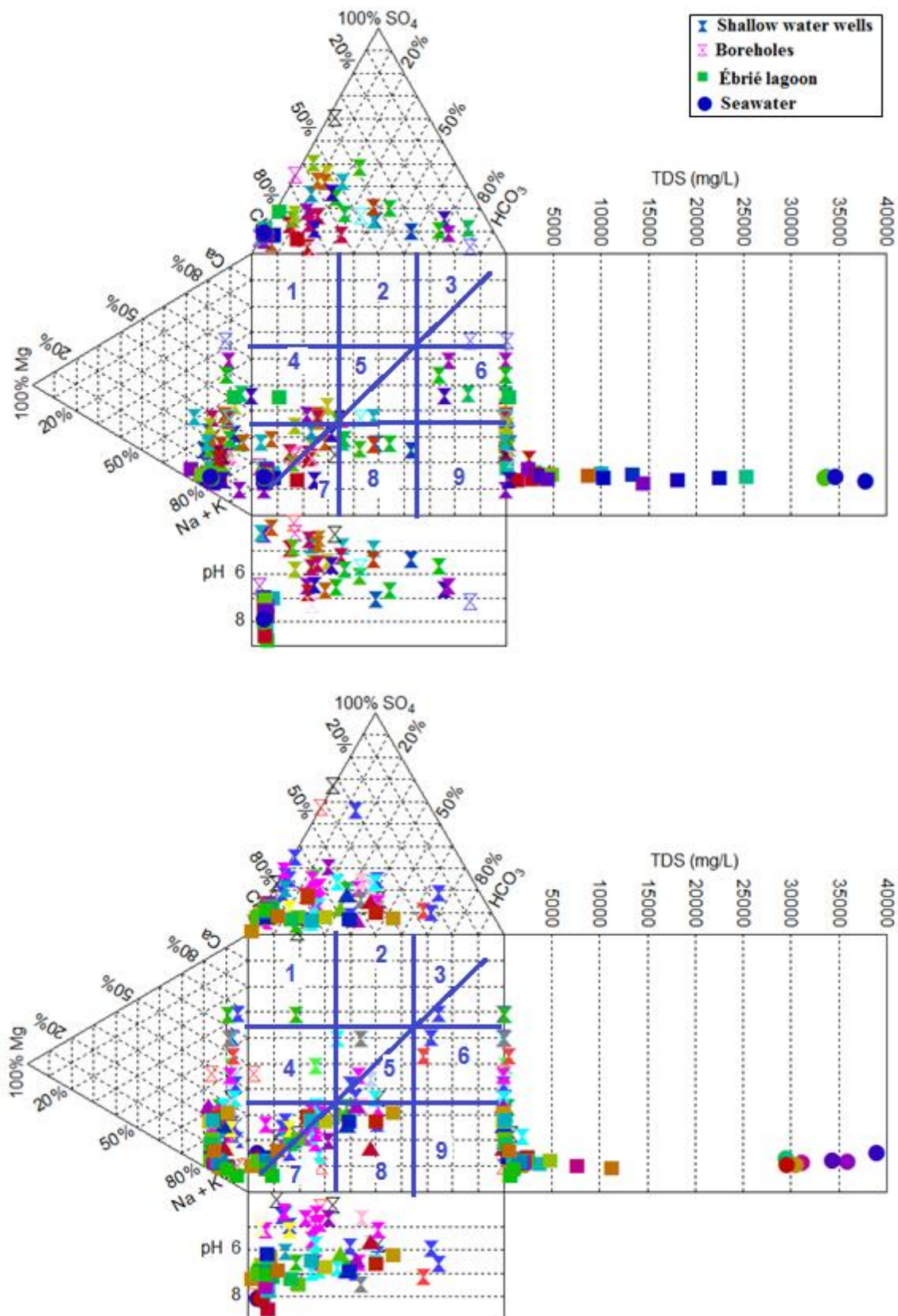


Figure 36: Expanded Durov diagram (Durov, 1948) with pH and TDS data of major ion analyses of the different coastal water systems for the dry (top) and rainy (bottom) season, respectively. Thick blue diagonal line is a theoretical mixing line.

Likely nitrate sources are septic systems with ability to oxidize organic nitrogen from human wastes and produce nitrate, thereby enriching groundwater (**Valiela *et al.*, 1992**).

4.2.3. Microbial safety of groundwater wells

Faecal coliform (thermo-tolerant) bacteria are a subset of total coliform bacteria. Their presence in water indicates human and/or animal faeces. Epidemiological studies have demonstrated a relationship between faecal contamination of waters and adverse health outcomes (**Prüss, 1998**). Although, majority of the faecal bacteria are harmless, the harmful pathogens can lead to illnesses such as gastroenteritis, typhoid, hepatitis A, dysentery, ear infection, and cholera. Results show faecal bacterial contamination in all studied wells (Figure 38). This implies that these wells are microbially unsafe drinking sources. During the rainy season, bacterial load ranged from 610 to 7,580 CFU/mL for CTeast aquifer, 140 to 1,760 CFU/100 mL for CTwest, and 300 to 18,000 CFU/100 mL for the QM aquifer. According to WHO guidelines (**World Health Organization, 1996**), faecal coliform bacteria must not be detectable in any 100 mL sample. Faecal contaminants in these wells portray the poor sanitary conditions, hygienic and sewage disposal systems, prevalent in these coastal rural communities.

4.3. Surface water systems

The main surface water systems are the paralic Ébrié lagoon and the inshore environment of the south Atlantic. The surface water systems are heterogeneous reflected by the spatiotemporal variations in its water quality (Table XIII).

Temperature (°C): temperatures of the Ébrié lagoon decreased significantly from an average of 30.3 ± 0.9 °C during the dry season to 29 ± 1.1 °C during the rainy season. Highest seasonal variations was recorded in stations I and IV. Maximum temperature (31.5°C) was recorded in station I for the investigation period. Along the Atlantic coastline, similar trends were observed. Surface water temperature decreased from mean value of 27.1 ± 0.2 °C during the dry season to 26.5 ± 0.1 °C during the rainy season.

pH: The pH of the lagoon varied between weakly acidic (6.4) to strong alkaline (8.9). Generally, pH decreased from a mean of 7.5 ± 0.5 during the dry season to 7.1 ± 0.5 during the rainy season. The highest spatiotemporal variations were recorded in station IV; areas bordering the Azagny national park, partially shaded by mangroves *Rhizophora racemosa* (**Nicole, 1994**). The alkalinity of the lagoon might be a result of its permanent contact with the sea. Along the Atlantic coastline, there was a slight increase in pH from 8.0 ± 0.1 during the dry season to 8.1 ± 0.1 during the rainy season.

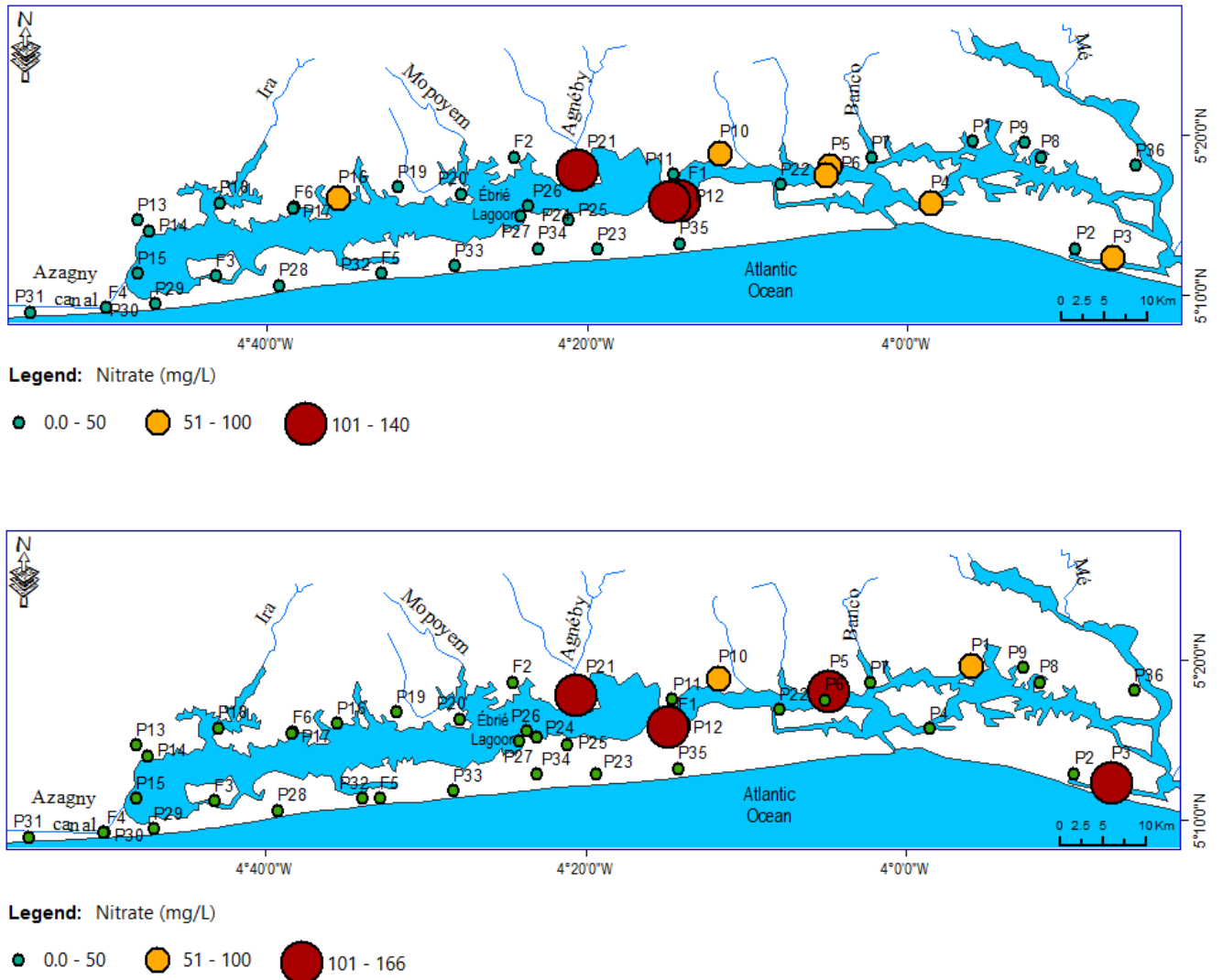


Figure 37: Nitrate concentration (mg/L) in drinking water wells for the dry (top) and rainy (bottom) seasons.

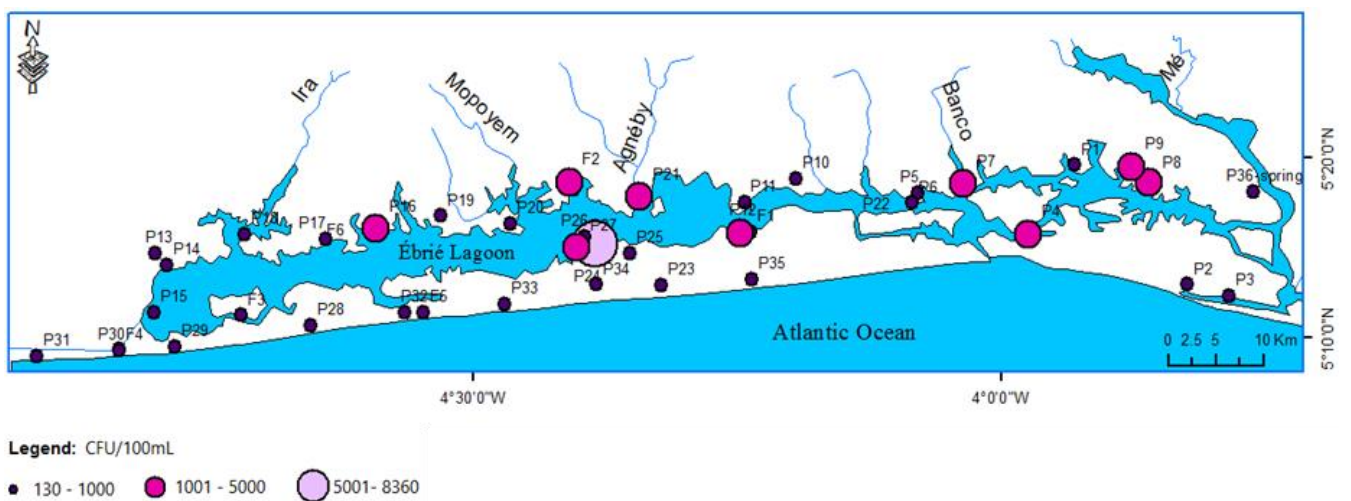


Figure 38: Faecal coliform density (CFU/100 mL) in all studied wells during the rainy season.

Table XIII: The range of environmental variables measured of the surface water systems for the dry (top) and rainy (bottom) seasons.

Environmental variables	Ébrié lagoon				Atlantic
	I	II	III	IV	Mean
pH	7.1 - 8.8	7.4 - 7.9	7.2 - 8	6.5 - 7.9	8
Temperature (°C)	29.6 - 31.5	30 - 30.6	30.2 - 31.3	28.6 - 31.1	27.1
Dissolved oxygen (mg/L)	4.1 - 7.3	7.2 - 8.5	5.4 - 6.6	4.3 - 9.2	6.6
Turbidity (NTU)	4.1 - 24.9	5.6 - 19.8	6.7 - 33.6	4.2 - 15.0	3.6
Silicate, SiO ₃ ²⁻ (mg/L)	6.3 - 13.3	2.8 - 6.8	5.0 - 7.7	6.5 - 11.3	0.01
Nitrate, NO ₃ ⁻ (mg/L)	0.01 - 0.6	0.3 - 1.2	0.2 - 3.6	0.2 - 0.9	0.4
Orthophosphate, PO ₄ ³⁻ (mg/L)	0.1 - 0.3	0.1 - 0.3	0.04 - 0.1	0.1 - 5.8	0.1
Total dissolved solids, TDS (g/L)	0.3 - 14.7	3.6 - 25.4	4.5 - 18.2	2.5 - 4.9	35.7

Environmental variables	Ébrié lagoon				Atlantic
	I	II	III	IV	Mean
pH	6.6 - 6.9	6.8 - 7.8	6.6 - 7.2	6.4 - 8.6	8.1
Temperature (°C)	27.5 - 30.3	27.3 - 29.8	27.9 - 29.9	27.7 - 30.2	26.4
Dissolved oxygen (mg/L)	2.6 - 5.8	5.2 - 9.4	5.0 - 7.2	1.7 - 7.1	6.9
Turbidity (NTU)	6.3 - 76.8	1.6 - 236.0	3.1 - 9.8	6.7 - 22.8	4.5
Silicate, SiO ₃ ²⁻ (mg/L)	0.01 - 12.8	5.9 - 12	7.3 - 9.7	0.01 - 9.6	1.2
Nitrate, NO ₃ ⁻ (mg/L)	0.3 - 332.3	0.3 - 14.6	0.01 - 9.7	0.01 - 4.5	70.7
Orthophosphate, PO ₄ ³⁻ (mg/L)	0.01 - 44.4	0.9 - 8	0.01 - 9.2	0.01 - 13.1	77.6
Total dissolved solids, TDS (g/L)	0.04 - 11.7	1.1 - 3.8	1.0 - 1.6	0.2 - 1.9	31.5

Dissolved oxygen (mg/L): The general trend in dissolved oxygen was a seasonal decrease. Dead zones (DO: 2 - 3 mg/L, **National Oceanic and Atmospheric Administration, 1998**) was observed at stations I (DO: 1.7) and IV (DO: 2.6) respectively were recorded during the rainy season. These are areas harbouring vast acres of mangrove with seasonal infestations of aquatic weeds (**Guiral *et al.*, 1983**). The ecological implication of hypoxia is an increase of carbon dioxide from plant and bacterial respiration that may eventually lead to a lowering of the pH (**Murphy, 2007**). Contrariwise, station II (DO: 12 mg/L) and station IV (DO: 9.2 mg/L) were oxygen supersaturated during the dry period. Oxygen super-saturation indicates active algae photosynthesis and this is a normal occurrence in alkaline and relatively unpolluted waters (**Murphy, 2007**). Along the inshore, mean dissolved oxygen increased from 6.6 ± 0.3 mg/L during the dry season to 6.9 ± 0.7 mg/L during the rainy season.

Turbidity (NTU): Spatiotemporal variations in turbidity values were very high. Turbidity levels of the lagoon increased significantly from a mean of 12.2 NTU during the dry season to 33.5 NTU during the rainy season. High turbidity (236 NTU) recorded during the rainy season in station II is a result of ongoing dredging activities. Along the inshore, mean turbidity values were 3.6 ± 1.2 NTU for the dry season and 5.8 ± 5.0 NTU for the rainy season.

Total dissolved solids, TDS (g/L): Mean TDS value for the lagoon was 10.0 g/L during the dry season. Freshwater inputs during the rainy season diluted the lagoon water to a mean of 2.0 g/L. The highest variations were recorded in station II, being after **Durand and Guiral (1994)** the most hydrodynamically unstable parts of the lagoon. Station I is in a perpetual freshwater state. The higher salinity levels during the dry period are evidence of strong marine influence. Along the inshore, significant seasonal differences in TDS were also recorded. Mean values were 35 and 31.5 g/L for the dry and rainy seasons, respectively. The reduction in salinity during the rainy period attests to continental freshwater inputs. As concerns coastal hydrology, this man-made modification to the coastal system (dredging of the Vridi canal) paved way for salinity fluctuations in the lagoon, which prior to the opening were rarely above 6 mg/L (**Dufour, 1982**) with consequent development of a halocline in the western part of the lagoon (**Binder, 1968**) and hypoxic pockets (**Dufour & Slepoukha, 1975**).

Nutrients (nitrate, phosphate, and silicate) as pollution tracers: Phosphate and nitrate are limiting nutrients in the development of the photosynthetic activity of phytoplankton (**Dufour & Berland, 1999**). Therefore, changes in nutrient concentration and availability can have marked influence on organisms and ecosystem function (**Persson *et al.*, 2000**). The presence of nitrate depicts

relatively older nutrient inputs (**Suthers & Rissik, 2009**). On the Ébrié lagoon, nitrate levels increased from a mean of 9.4 mg/L during the dry season to 371 mg/L during the rainy season. Nitrate contamination hotspots were highlighted by Voronoi (**Voronoi, 1907**) tessellations (Figure 39). The highest value (L3: 332.3 mg/L), recorded east of the lagoon might be a result of from agricultural discharges from adjoining upland commercial farm of vast acres of African palm, *Elaeis guineensis*. Along the inshore, mean values were 6.9 and 722.9 mg/L for the dry and rainy seasons, respectively. On the Ébrié lagoon, mean values of phosphate increased from 4.9 mg/L during the dry season to 61.7 mg/L during the rainy season. Along the inshore, mean values was 0.9 mg/L for the dry season, with a significant increase to 642.5 mg/L during the rainy season. The values of PO₄ exceed the critical value of 0.15 mg/L, considered as the main requirement for the avoidance of eutrophication in surface waters (**Van Dijk et al., 1994**).

Along the sandy beaches, mats of decaying brown *sargassum* seaweed were physical evidence of nutrient over-enrichment during the rainy season (Photo 12). The availability of nitrate and phosphate in combination with changing water circulation patterns fuels macroalgae bloom (**Raffaelli et al., 1998**). High nutrient (nitrate and phosphate) levels in this tropical environment is a decades-old problem (**Dufour et al., 1981; Dufour & Lemasson, 1985**), similar to what is obtainable in Lake Victoria in East Africa (**Zhou et al., 2014**) and some other coastal zones of the world (**Diaz et al., 2011**). **Diaz et al. (2011)** postulate that nutrient enrichment (eutrophication) is a key stressor in coastal ecosystems and the lead cause of hypoxia (low dissolved oxygen) in coastal waters. Hypoxia, a more direct trigger of fish kills is a serious environmental challenge in fisheries managerial strategies. Different authors have put forward theories to support the influx of nutrients into these systems. Proposed sources for the Ébrié lagoon includes urban and agricultural run-offs (**Scheren et al., 2004**), and off the Atlantic coast, vertical upwelling currents that results in the upward movement of the horizontal nitracline from depths into the euphotic zone (**Herbland & Le loeuff, 1993**). Based on observations, periods of high nutrient availability coincide with the major ocean upwelling events off the Atlantic coastlines of Senegal and Mauritania (**Herbland & Le loeuff, 1993**).

Nutrient stoichiometry (N : P molar ratios) gives insight into phytoplankton distribution. Surface water with short residence time usually have N:P ratios less than 26, while waters with longer residence time (more than 6 months) have N:P ratios greater than 30 (**Wetzel, 2001**). Denitrification reduces N : P ratios, while nitrogen fixation increases N : P ratios (**Gruber & Sarmiento, 1997**). N : P ratio greater than 16 infers that P limitation of algae growth is occurring, while less than 14 depicts a N-limiting growth (**Koerselman & Meuleman, 1996**).

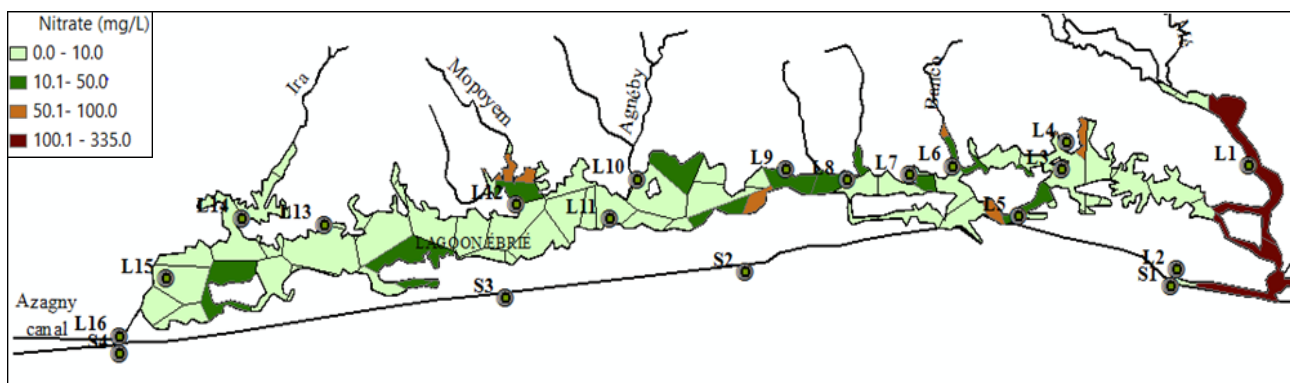


Figure 39: Voronoi tessellation to highlight contamination hotspot of nitrate (mg/L) on the Ebrié lagoon during the rainy period of 2014. The green shade areas have nitrate values below the WHO acceptable levels.



Photo 12: The sandy beach of Azuretti covered by mats of brown macroalgae *sargassum* (October, 2014) <that on decay give off putrid smell.

Based on nitrogen/phosphate (N : P) molar ratios, all stations of the lagoon exhibited N-limiting factor for phytoplankton growth (ratio N/P less than 5), except station III during the dry season, which exhibits P-limiting factor for phytoplankton growth with a N: P ratio of 10.

The shoreline manifested N-limiting factor of growth during the investigation period. On the Ébrié lagoon, threshold values of silicate were observed during the rainy season. While, mean silicate values were 87.7 ± 41.3 mg/L for the dry season, significantly higher values of 98.7 ± 54.9 mg/L were observed during the rainy season. Highest seasonal variations were observed in station I. The inshore was severely depleted in silicate during the dry season. However, a mean value of 15.9 ± 14.9 mg/L was recorded during the rainy season. Silica depletion in water is indicative of very short residence time (**Hem, 1985**). Silicate is the main requirement for diatoms to build their frustules (**DeMaster, 1981**) and as such usually consumed before nitrate and phosphate in Ocean upwelling zones (**Paasche, 1980**).

Surface water quality rating

Water Quality Index (WQI) was developed based on four parameters (pH, dissolved oxygen, nitrate, and phosphate) important for the health of inherent fauna and flora. Curves were used to relate measured concentrations to index scores. Weight of each parameter was the eigenvalues as derived from principal component analysis, PCA. Subsequently, WQI scores for one season are aggregated to single numbers (**Brown et al., 1970**). Resulting water quality classes are presented in Table XIV. The lagoon water is more highly prone to degradation during the rainy season from land-based contamination sources. The creation of a direct link between this environment and the sea via the artificial Vridi canal in 1950 has had adverse effect on coastal hydrologic systems (**Durand & Skubich, 1982**). It resulted in the closure of the Grand Bassam inlet, its natural connection to the sea in 1954 (**Varlet, 1978**). The ecological implication of this is the proliferation of freshwater loving aquatic weeds (*Eichhornia crassipes*, *Pistia stratiotes*, *nelumbo nucifera* and *Salvinia molesta*) in the Ébrié lagoon since 1987 (**Sankare & Etien, 1991**).

4.4. Correlation between environmental abiotic components

The association between the physicochemical parameters of coastal surface waters was based on a correlation (Pearson) matrix (Table XV). Results show strong negative correlation ($r^2 = -0.86$) between silicate and TDS, between temperature and TDS ($r^2 = -0.67$) and between silicate. A positive correlation however existed between Turbidity and nitrate ($r^2 = 0.71$) for the dry season. For the rainy season, there was strong negative correlation ($r^2 = -0.65$) between temperature and TDS. Positive correlation however existed between TDS and phosphate ($r^2 = 0.72$) and TDS and pH ($r^2 =$

0.65). These associations highlight seasonality and contrasting sources. These are abiotic variables with influxes from opposing sources, landward and seaward sides, respectively. Silicates in water is mainly of continental origin from the weathering of silicates and aluminosilicates in bedrock and soils (Neal *et al.*, 2005), while pH and TDS is mainly of marine origin. Seasonal fluctuations in the quality of these shallow coastal waters are largely controlled by changing hydrologic regimes (Dandonneau, 1973; Dufour, 1982). Before the onset of annual rainfall events, during the dry period (December – April), marine processes exert the strongest controls on the system's biogeochemical processes. Whereas, after the rainfall events (June – July) and peak discharge seasons of the draining rivers (September – October), continental (fluvial and precipitation) processes dominates, resulting in the dilution of the coastal waters.

4.5. Seasonal hydrologic interactions between coastal waters

Temporal shifts in stable isotopic composition was observed in all coastal water sources except in the deep-water aquifers (Figure 40). This is indicative of the fact that these deep-water aquifers did not receive recharge during this period, confirming the delayed response in water transfer from surface to the subsurface environment. These deep groundwater systems respond slowly to changes in rainfall (Calow *et al.*, 1997). For the inshore, the waters are isotopically depleted during the dry period relative to the rainy season. This might be due to the preferential loss of light isotopes during evaporation. Contrariwise, on the Ébrié lagoon, there was marked enrichment in heavy isotope during the dry season compared to the rainy season. The mean $\delta^{18}\text{O}$ value of the lagoon during the dry period was similar to that of the seawater, confirming high marine influence on the lagoon. However, during the rainy period, stable isotopes signatures of the lagoon were relatively isotopically lighter, closer to those of the unconfined phreatic aquifers. As observed from the $\delta^{18}\text{O} - \delta^2\text{H}$ plot (Figure 41), during the dry season, the lagoon was a homogenous body of water. Variability in isotopic composition was lower during the dry season relative to the rainy season. Mean stable isotope values were similar to that of the Atlantic Ocean. This suggests high marine influence and surface water evaporation during this period. However, three different water classes were distinguishable from during the rainy season. Group I (L1, L4, L5, L7, L8, L10, L11, L16, L31) are relatively depleted in heavy isotopes ($\delta^{18}\text{O}$, $\delta^2\text{H}$). Group II (L2, L9, L21, L23) encompasses areas of the lagoon with high freshwater influence. These are potential hyporheic zones. Group III (L3, L12, L13, L14, L15, L16, L17, L19, L22, L24, L25, L27, L29, L30) are points intermediate between group I and II.

Table XIV: Water quality rating for the different stations of the Ébrié lagoon during the investigation period.

	Sampling stations			
	IV	III	II	I
Dry season	Moderate	Good	Good	Good
Rainy season	Moderate	Moderate	Moderate	Bad

Table XV: Correlation (Pearson) matrix of coastal surface water systems for the dry (top) and rainy (bottom) seasons, respectively

Variables	pH	DO	NO ₃ ⁻	PO ₄ ³⁻	SiO ₄ ³⁻	Temperature	TDS	Turbidity
pH	1.00							
DO	0.51	1.00						
NO ₃ ⁻	-0.04	-0.23	1.00					
PO ₄ ³⁻	0.59	0.34	0.03	1.00				
SiO ₄ ³⁻	-0.52	-0.57	0.09	0.12	1.00			
Temperature	-0.18	-0.02	0.17	0.23	0.58	1.00		
TDS	0.31	0.26	-0.12	-0.22	-0.86	-0.67	1.00	
Turbidity	-0.27	-0.20	0.71	0.12	0.44	0.51	-0.40	1.00

Values in bold are different from 0 with a significance level $\alpha=0.05$

Variables	pH	DO	NO ₃ ⁻	PO ₄ ³⁻	SiO ₄ ³⁻	Temperature	TDS	Turbidity
pH	1							
DO	0.50	1.00						
NO ₃ ⁻	-0.07	-0.33	1.00					
PO ₄ ³⁻	0.44	0.30	0.18	1.00				
SiO ₄ ³⁻	-0.28	0.10	-0.15	-0.43	1.00			
Temperature	-0.42	-0.07	0.14	-0.46	0.39	1.00		
TDS	0.65	0.33	0.30	0.72	-0.57	-0.65	1.00	
Turbidity	-0.24	-0.09	-0.11	-0.16	0.48	0.01	-0.26	1.00

Values in bold are different from 0 with a significance level $\alpha=0.05$

4.6. Hydrological modelling

The correlation matrices are given in Table XVI. PCA identified three main factors (Table XVII) controlling variations in coastal water chemistry for both seasons. Results were similar for both seasons. For the dry season, component F1 (eigenvalue, λ : 6.7), which accounts for 55 % of variability within the dataset relates to Na^+ - K^+ - Mg^{2+} - Ca^{2+} - Cl^- - SO_4^{2-} ion association derived mainly from water-rock interaction/geogenic source. Component F2 ($\lambda = 1.7$) has high positive loadings on the stable isotopes ($\delta^{18}\text{O}$ and $\delta^2\text{H}$) and a negative loading on nitrate, contrasting climatic and anthropogenic sources, while component F3 ($\lambda = 1.3$) has high loading on bicarbonate and silicate; ions influenced by biological processes and as such not suitable as tracers. Whereas, for the rainy season, component F1 (eigenvalue, λ : 6.18) which accounts for 56 % of variability within the dataset relates to Na^+ - K^+ - Mg^{2+} - Ca^{2+} - Cl^- - SO_4^{2-} ion association derived mainly from water-rock interaction/geogenic source. Component F2 ($\lambda = 1.7$) has high loadings on the stable isotopes ($\delta^{18}\text{O}$ and $\delta^2\text{H}$), confirming their climatic origin, while component F3 (λ of 0.97) has high loading on bicarbonate and silicate; ions influenced by biological processes and as such not suitable as tracers. Two factors were chosen; together, components F1 and F2 explained 76 % of variability within the dataset for the dry season, and 74 % of the variability within the dataset for the rainy season. This implied that a two-tracer, three endmember mixing model was adopted. As a conservative element, chloride was chosen from the primary component, F1 as an intrinsic tracer, while from the second component, F2, oxygen-18 was chosen over deuterium as the latter did not significantly correlate with any other variable in a prior correlation matrix (Table XVI). Results from the EMMA model are displayed as ternary plots (Figure 42). The calculated mixing ratios deduced from isotopic data agreed well with values obtained from chemical data. During the dry season, seawater intruded only into wells p7 (6.1 %) and p15 (1.8 %). All studied wells were however, contaminated in varying degree with the lagoon water. Wells within the QM aquifer display proportions of lagoon water between 3.4 and 68.5 %. Proportions of lagoon water between 1.7 – 28.5 % and 1.5 – 49.4 % was estimated for the CTeast and CTwest aquifers, respectively. During the rainy season, only wells within the QM aquifer (p4: 1.9 %; p15: 0.1 %; p23: 0.2 %; p25: 0.5 %) were susceptible to seawater intrusion. However, all wells were contaminated with lagoon water except wells p4 and p25 (QM aquifer) that recorded no influence. Proportions of lagoon water were between zero and 39.1 % for the QM aquifer, 6.4 and 35.3 % for the CTeast aquifer, and 8.6 and 18.6 % for the CTwest aquifer. For the Ébrié lagoon, during the dry season, the seawater component was between zero and 69.5 %, and freshwater component was between zero and 50.6 %. Those proportions change significantly during the rainy season with seawater proportions between zero and 25.5 %, and freshwater proportions between 31.9 and 99.1 %.

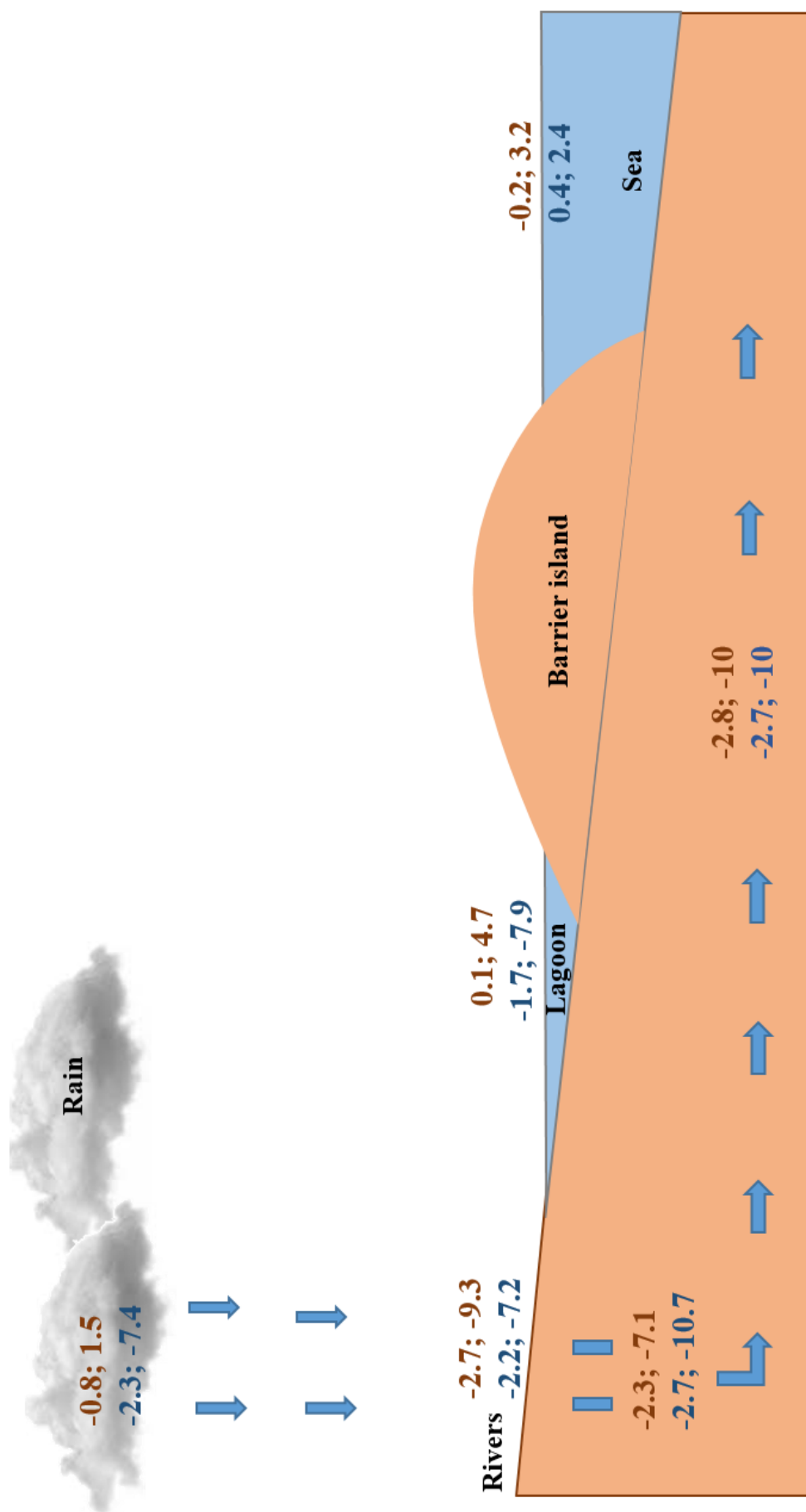


Figure 40: Spatiotemporal shifts in mean isotopic composition of coastal waters. Text in red are dry season values, while text in blue are wet season values.

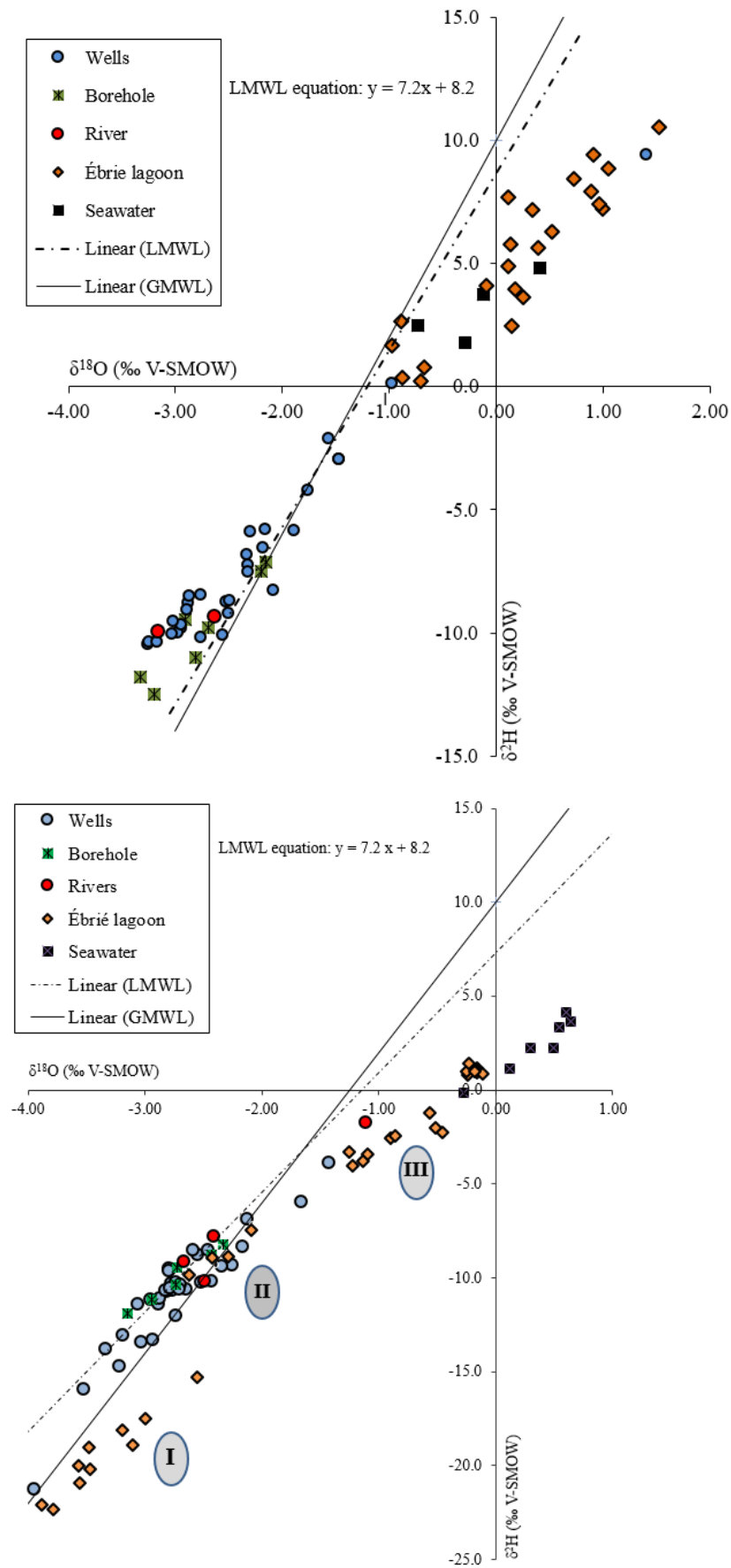


Figure 41: $\delta^2\text{H}$ versus $\delta^{18}\text{O}$ plot of coastal waters during the dry (top) and rainy (bottom) seasons, respectively.

Table XVI: Correlation matrix (Pearson) of selected solute concentrations in coastal inland waters for the dry (top) and rainy (bottom) seasons, respectively

Variables	Na ⁺	K ⁺	Mg ⁺⁺	Ca ⁺⁺	Cl ⁻	SO ₄ ⁼	NO ₃ ⁻	HCO ₃ ⁻	SiO ₃ ⁼	δ ¹⁸ O	δ ² H
Na ⁺	1.0										
K ⁺	1.0	1.0									
Mg ⁺⁺	1.0	1.0	1.0								
Ca ⁺⁺	1.0	1.0	1.0	1.0							
Cl ⁻	1.0	1.0	1.0	1.0	1.0						
SO ₄ ⁼	1.0	1.0	1.0	1.0	1.0	1.0					
NO ₃ ⁻	-0.2	-0.2	-0.2	-0.2	-0.2	-0.2	1.0				
HCO ₃ ⁻	0.3	0.4	0.3	0.3	0.3	0.3	-0.2	1.0			
SiO ₃ ⁼	-0.4	-0.4	-0.4	-0.3	-0.4	-0.4	0.0	0.3	1.0		
δ ¹⁸ O	0.4	0.4	0.4	0.4	0.4	0.4	-0.4	0.1	-0.3	1.0	
δ ² H	0.4	0.4	0.4	0.4	0.4	0.4	-0.3	0.1	-0.3	1.0	1.0

Values in bold are different from 0 with a significance level alpha=0.05

Variables	Na ⁺	K ⁺	Mg ⁺⁺	Ca ⁺⁺	Cl ⁻	SO ₄ ⁼	NO ₃ ⁻	HCO ₃ ⁻	SiO ₃ ⁺	δ ¹⁸ O	δ ² H
Na ⁺	1										
K ⁺	1.0	1.0									
Mg ⁺⁺	1.0	1.0	1.0								
Ca ⁺⁺	1.0	0.9	1.0	1.0							
Cl ⁻	1.0	1.0	1.0	1.0	1.0						
SO ₄ ⁼	1.0	1.0	1.0	0.9	1.0	1.0					
NO ₃ ⁻	0.2	0.3	0.2	0.1	0.2	0.2	1.0				
HCO ₃ ⁻	0.4	0.5	0.4	0.4	0.4	0.4	0.1	1.0			
SiO ₃ ⁺	-0.3	-0.2	-0.3	-0.2	-0.3	-0.3	0.0	0.4	1.0		
δ ¹⁸ O	0.5	0.5	0.5	0.5	0.5	0.5	0.0	0.2	-0.3	1.0	
δ ² H	0.3	0.3	0.3	0.3	0.3	0.3	0.0	0.1	-0.3	0.9	1.0

Values in bold are different from 0 with a significance level alpha=0.05

Table XVII: Factor loadings after Varimax rotation for the dry (left) and rainy (right) seasons, respectively

Variables	F1	F2	F3	Variables	F1	F2	F3
Na ⁺	0.98	0.19	0.00	Na ⁺	0.98	0.18	0.00
K ⁺	0.98	0.16	0.03	K ⁺	0.98	0.16	0.07
Mg ⁺⁺	0.97	0.22	0.00	Mg ⁺⁺	0.98	0.18	0.00
Ca ⁺⁺	0.98	0.16	0.05	Ca ⁺⁺	0.95	0.16	0.05
Cl ⁻	0.98	0.20	0.00	Cl ⁻	0.98	0.18	0.00
SO ₄ ⁼	0.98	0.18	-0.02	SO ₄ ⁼	0.98	0.17	0.01
NO ₃ ⁻	-0.10	-0.58	-0.35	NO ₃ ⁻	0.27	-0.14	0.08
HCO ₃ ⁻	0.33	0.11	0.77	HCO ₃ ⁻	0.40	0.14	0.81
SiO ₃ ⁼	-0.38	-0.16	0.77	SiO ₃ ⁺	-0.24	-0.21	0.87
δ ¹⁸ O	0.25	0.93	-0.11	δ ¹⁸ O	0.33	0.93	-0.02
δ ² H	0.20	0.93	-0.12	δ ² H	0.15	0.97	-0.06

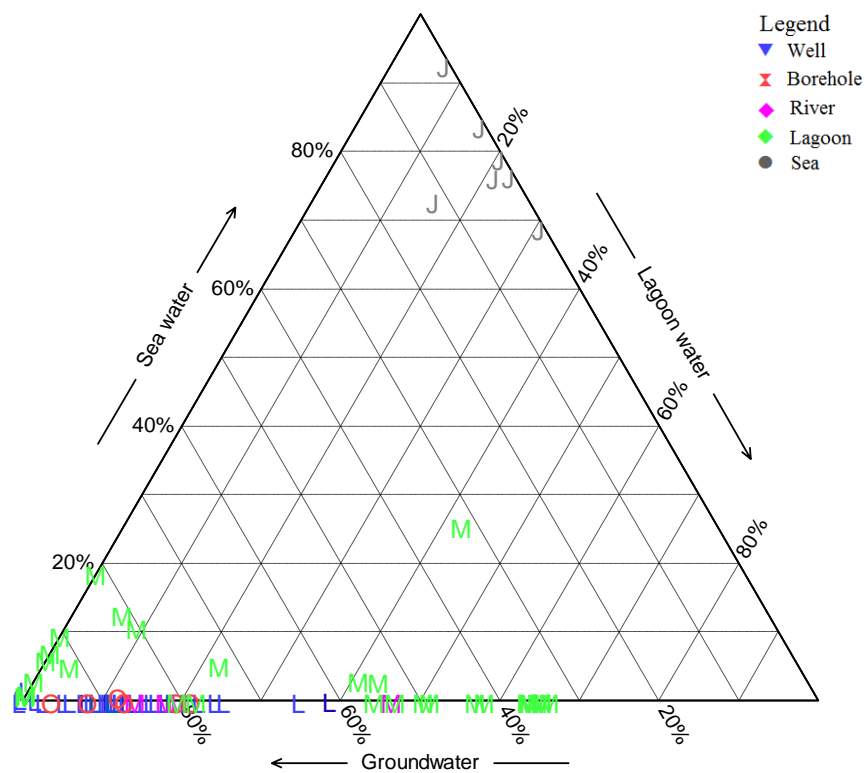
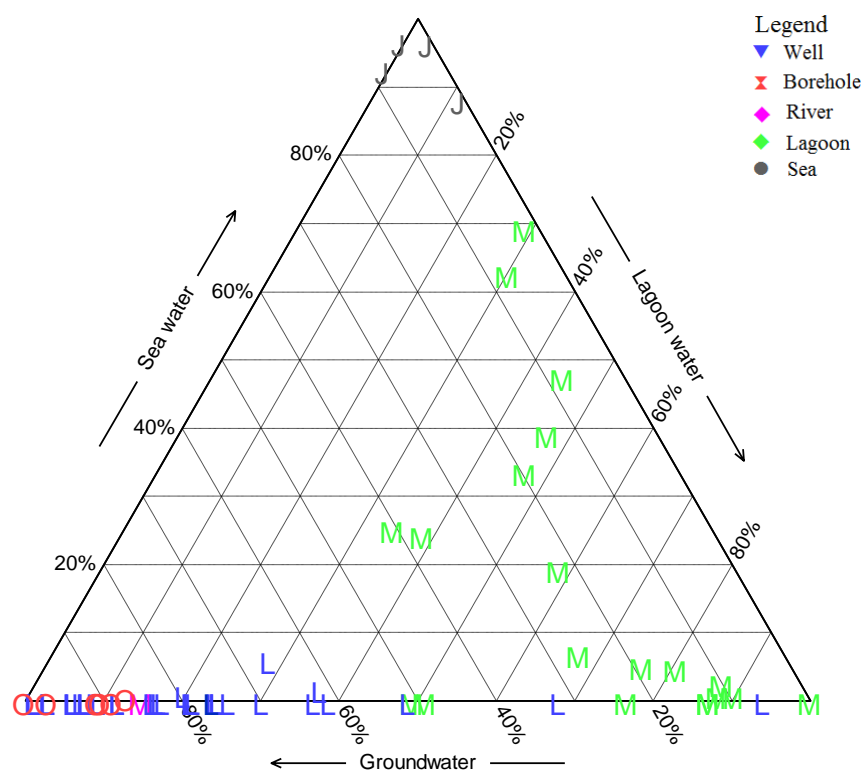


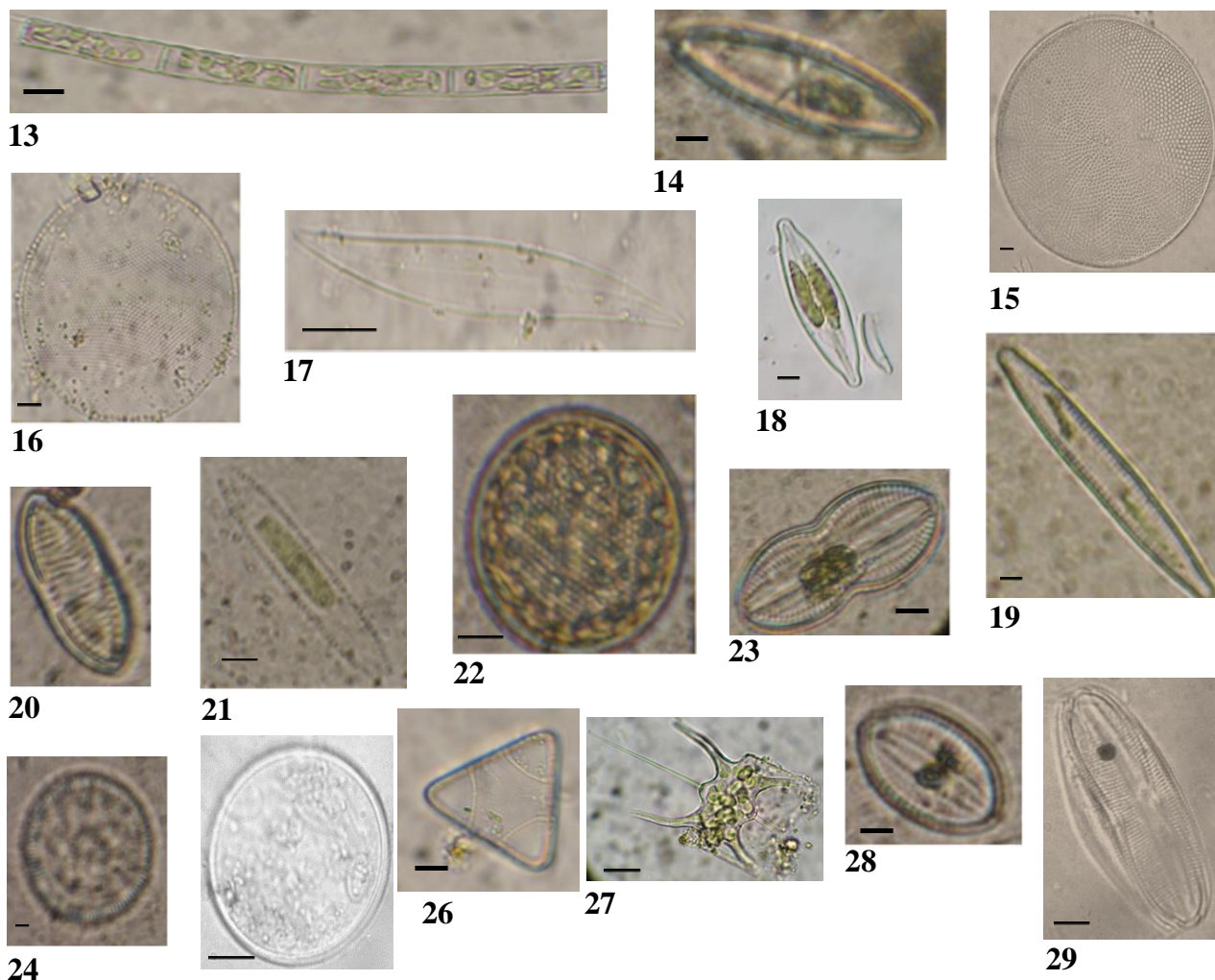
Figure 42: Ternary plot/mixing triangle of coastal water systems during the dry season (top) and rainy season (bottom).

For the Atlantic coastline, areas around Grand-Jack (S3) had the highest lagoon water component (11.8 %) during the dry season, while inshore areas along Abéréby (S2) recorded the highest freshwater component (7.4 %) during this season. However, during the rainy season, freshwater inputs were relatively higher, up to 11.4 % in Gbamblé (S1). Lagoon water contributions to the inshore during this period range between 15.8 and 23.5 %.

CHAPTER 5: Biocenosis analyses

5.1. Seasonal phytoplankton distribution patterns

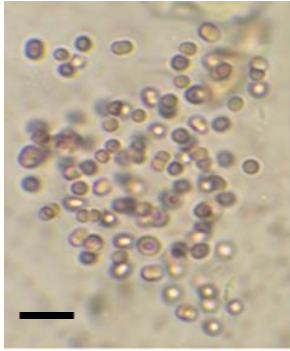
Sixty-seven species were identified and assigned to Bacillariophyceae (49 %), Cyanophyceae (21 %), Chlorophyceae (13 %), Euglenophyceae (10 %), Dinophyceae (4 %) and Chrysophyceae (3 %). Some species are presented in PLATES 1-3 (Photos 13 – 49). The microflora is dominated by freshwater algal species, in concert with the observations of **Seu-Anoi *et al.* (2013)**. The degree of sensitivity of phytoplankton to changes in water quality was assessed by magnitude of growth response to seasonal variability in the Ébrié lagoon (Table XVIII). The estuarine/urbanized areas (station II) and peri-urban areas (station III) of the Ébrié lagoon recorded the highest variation in terms of phytoplankton abundance (cells/mL). These areas are the most sensitive to seasonality. Along the inshore, a negative response was observed in S2 with respect to season. The highest variability was recorded in S3 (Table XIX). Although, diatoms were the most species rich class in the lagoon, Cyanobacteria were dominant with cell densities reaching peak values of 10.5×10^6 cells/mL in station IV of the lagoon during the rainy season (Figure 43). Station III however showed an exception to this trend during the dry season where Chlorophyceae were dominant. The chlorophyceae genus, *Spondylosium* sp. was the most abundant. The most dominant cyanobacteria genus in the lagoon is *phormidium foveolarum* Gomont. Other genera making substantive contributions (more than 1 %) to total phytoplankton biomass in the Ébrié lagoon were *Cocconeis* sp., *Coscinodiscus* sp., *Entomoneis* sp., *Cyclotella meneghiniana* (Kützing), *Eunotia* sp., *Gyrosigma acuminatum* (Kützing), *Gyrosigma* sp., *Melosira* sp., *Nitzschia Oliffii* (Cholnoky), *Orthoseira* sp., *Surirella* sp., *Tryblionella victoriae* (Grunow) (diatom), *Chroococcus minutus* (Kützing), *Cylindrospermopsis* sp., (cyanobacteria), *Monoraphidium* sp., *Pediastrum* sp., *Scenedesmus quadricauda*, (Chlorophyceae) *Phacus* sp., *Trachelomonas* sp., and *Trachelomonas volvocina* (Ehrenberg) (Euglenophyceae). On the adjacent inshore, mean phytoplankton cell densities ($\times 10^6$ cells/mL) increased from 1.1 during the dry season to 1.6 during the rainy season. During the dry season, cyanobacteria were preponderant, contributing more than 78 % to total biomass. The dominant taxon was *Odontella* sp. However, cyanobacteria were conspicuously absent from the inshore during the rainy season, when almost pure stands of the diatom genus, *Aphanocapsa Incerta* dominates, constituting 70 % of total phytoplankton biomass. Other species with more than 1 % contribution to phytoplankton abundance were *Amphora commutata* Grunow, *Coscinodiscus* sp., *Diploneis ovalis* (Hilse) Cleve, *Eunotia* sp., *Gyrosigma* sp., *Melosira* sp., *Nitzschia cf. Nana*, *Orthoseira* sp., *Pleurosigma* sp., (diatoms), *Goniochloris* sp. (Chlorophyceae), *Ceratium* sp., *Peridinium* sp., (Dinophyceae), *Phacus* sp., *Strombomonas* sp., and *Trachelomonas* sp. (Euglenophyceae).



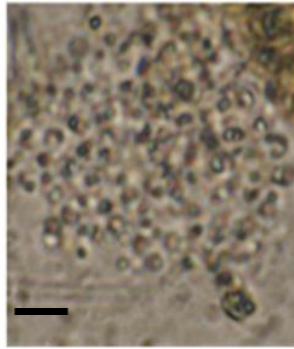
Phylum Bacillariophyceae (diatoms)

Photo 13: *Aulacoseira granulata* (Ehrenberg) Simonsen. **Photo 14:** *Capartogramma crucicula* (Grunow ex Cleve). **Photo 15:** *Coscinodiscus asteromphalus* Ehrenberg. **Photo 16:** *Coscinodiscus radiates* Ehrenberg. **Photo 17:** *Pleurosigma* sp. **Photo 18:** *Frustulia crassinerva* (Brébisson) Lange-Bertalot & Krammer. **Photo 19:** *Nitzschia* sp. **Photo 20:** *Tryblionella levidensis*, (W. Smith) Grunow. **Photo 21:** *Nitzschia* sp. **Photo 22:** *Thalassiosira eccentric* (Ehrenberg) Cleve. **Photo 23:** *Diploneis Stroemii* Hustedt, **Photo 24:** *Cyclotella meneghiniana* Kützing. **Photo 25:** *Coscinodiscus gigas* Ehrenberg. **Photo 26:** *Triceratium alternans* Bailey **Photo 27:** *Odontella longicruris* (Greville) Hoban. **Photo 28:** *Diploneis Ovalis* (Hilse) Cleve. **Photo 29:** *Amphora commutata* Grunow. Dark lines are 10 microns scale.

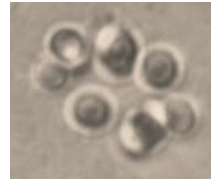
Plate 1: Phytoplankton belonging to the phylum Bacillariophyta (diatoms)



30



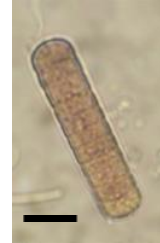
31



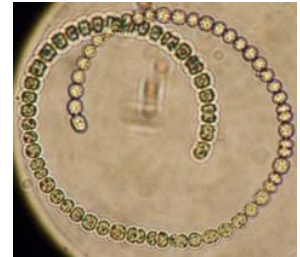
32



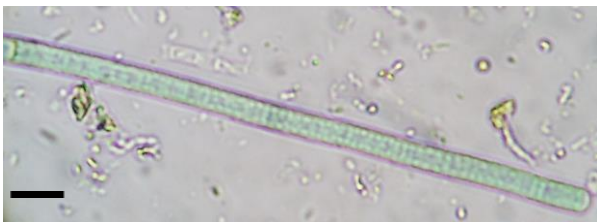
33



34



37



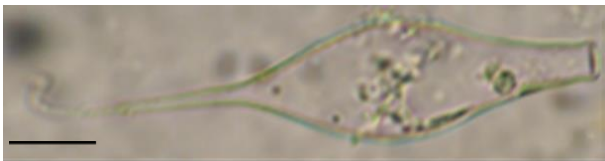
35



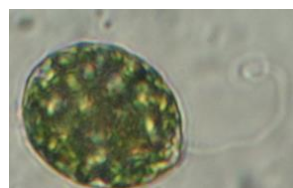
36

Phylum Cyanophyta (Cyanobacteria)

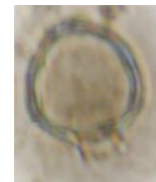
Photo 30: *Aphanocapsa* sp. **Photo 31:** *Aphanocapsa incerta* (Lemmermann) Cronberg & Komárek. **Photo 32:** *Thorakochloris* sp. **Photo 33:** *Merismopedia glauca* (Ehrenberg) Kützing. **Photo 34:** *Plankthotrix* sp. **Photo 35:** *Phormidium foveolarum* Gomont. **Photo 36:** *Pseudanabaena catenata* Lauterborn. **Photo 37:** *Anabaena circinalis* Rabenhorst ex Bornet & Flahault.



38



39



40



41

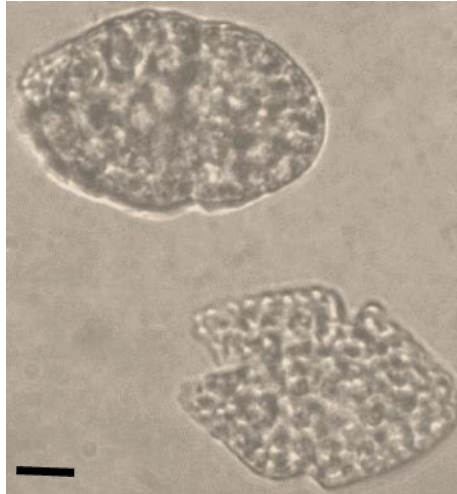
Phylum Euglenophyta (Euglenoids)

Photo 38: *Strombomonas* sp. **Photo 39:** *Lepocinclis ovum* (Ehrenberg) Lemmermann. **Photo 40:** *Trachelomonas* sp. **Photo 41:** *Euglena* sp.

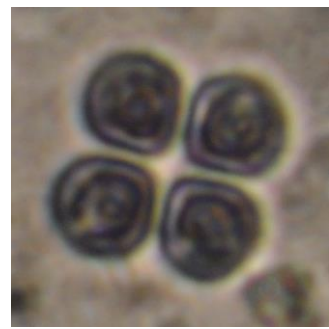
Plate 2: Phytoplankton belonging to the phyla Cyanophyta and Euglenophyta



42



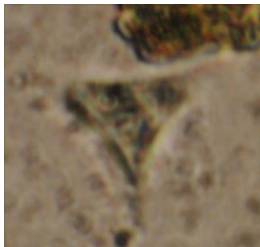
43



44



45



46



47



48a



48b

Phylum Chlorophyta (Green Algae)

Photo 42: *Pediastrum tetras* (Ehrenberg) Ralfs. **Photo 43:** *Peridinium* sp. **Photo 44:** *Tetrastrum triangulare* (Chodat) Komárek. **Photo 45:** *Scenedesmus quadricauda* (Turpin) Brébisson. **Photo 46:** *Tetradron trigonum* Naegeli) Hansgirg. **Photo 47:** *Cosmarium* sp. **Photo 48a,b:** *Scenedesmus* sp.



49

Phylum Chrysophyta (Golden Brown Algae)

Photo 49: *Dinobryon sociale* Ehrenberg.

Plate 3: Phytoplankton belonging to the phyla Chlorophyta and Chrysophyta

The filamentous cyanobacterium *Phormidium foveolarum* Gomont is the most dominant taxon in the Ébrié lagoon with a 75 % frequency of occurrence during the investigation period. It recorded a threshold cell count of 5.2×10^6 cells/mL in station IV during the rainy season. They were however conspicuously absent in areas of the lagoon with p-limiting factors of growth. This genus demonstrated high preference for phosphate-rich, warm, low turbid and oligohaline waters (Table XX). This partly explains its sub-dominant position in areas of the lagoon with high marine influences, where it was outcompeted by the eutraphenic, filamentous form *Anabaena circinalis* Rabenhorst. In highly turbid areas of the lagoon (western fringes) during the rainy season, *Phormidium* was also outcompeted by the genera *Microcystis aeruginosa* Kützinger, *Chroococcus*, *Anabaenopsis*, *Aulacoseira granulata* (Ehrenberg) and *Pediastrum duplex* (Meyen) with competitive advantages in the highly turbid waters. These genera need much turbulence to maintain their heavy cell forms in suspension (Moss, 2010). Physiological tolerances of *Phormidium* was however exceeded during the dry season in station III and during the rainy season in station I as phosphate becomes the limiting nutrient.

5.1.1. Biotic indices

Jaccard's community index confirms the dissimilarity between clusters. Values were 0.25 (between clusters I and IIA), 0.33 (between clusters I and IIB) and 0.37 (between clusters IIA and IIB). Cluster IIA, with the highest CDI (63.42 %) is the least species diverse group. This is followed by cluster I (CDI: 49.83 %) and IIB (CDI: 42.31 %). The two most abundant species in each cluster are *Phormidium foveolarum* Gomont and *Aulacoseira granulata* (cluster I); *Pseudoanabaena* sp. and *Phormidium foveolarum* (cluster IIA) and *Aphanocapsa incerta* and *Oscillatoria* sp. (cluster IIB). Species diversity is generally low in these coastal areas with mean Shannon diversity values of 0.95, 0.88 and 0.74 for clusters I, IIA and IIB respectively. These low values of Shannon diversity are indicative of environments under stress. Only taxa with more than 25 % indicator value (Table XXI) were retained as indicator species (Dufrêne & Legendre, 1997). The freshwater diatom, *Eunotia* sp. best represents cluster 1. Cluster IIA is best represented by the diatom genus associated with eutrophic conditions, *Navicula* sp., while cluster IIB is best represented by the green algae genus *Scenedesmus quadricauda* (Turpin) Brébisson, which can stay buoyant because of its spines.

5.1.2. SOM patterning of phytoplankton assemblages

Self-organizing feature maps (SOM) results in two major clusters (I and II) at a high linkage distance of 1.0. Two sub-clusters, IIA and IIB were observed in cluster II at a linkage distance of 0.62 (Figure 44) after applying hierarchical cluster.

Table XVIII: Spatiotemporal variations in phytoplankton cell abundance along the Ébrié lagoon

	Phytoplankton cell abundance (cells/ml)			
	IV	III	II	I
Dry season	11300000	1200000	1675000	4700000
Rainy season	15400000	6250000	7000000	5625000
Growth response (%)	26.6	80.8	76.1	16.4

Table XIX: Spatiotemporal variations in phytoplankton cell abundance along the Atlantic coastline.

	Phytoplankton cell abundance (cells/ml)			
	S4	S3	S2	S1
Dry season	125000	25000	825000	125000
Rainy season	200000	375000	800000	225000
Growth response (%)	37.5	93.33	-3.13	44.44

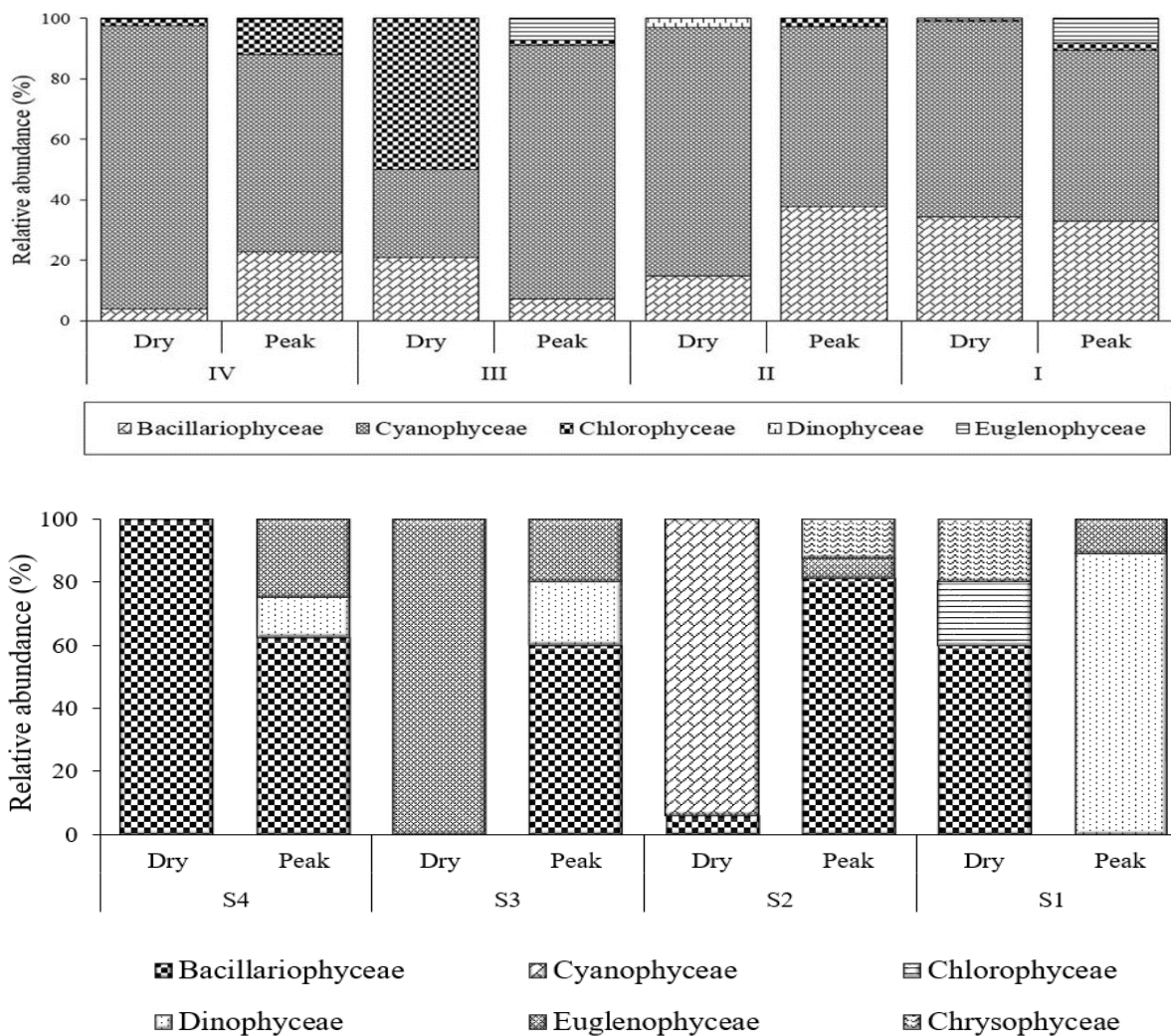


Figure 43: Seasonal composition shifts in phytoplankton as observed in the lagoon (top) and the Atlantic coastline (bottom).

Clusters were highly related to seasonality and salinity gradient (Figure 44). List of taxa as distributed by the SOM map in the different clusters are given in Table XXII. Cluster I (upper part of the map) grouped samples collected from the lagoon during the rainy season. Cluster IIA (lower right area) consists of a high percentage of samples from the central and western end of the lagoon during the dry period and samples from inshore waters during the rainy season. Cluster IIB (lower left area) pooled together samples from the eastern extremity of the lagoon and the Atlantic inshore (Figure 44). Spatial heterogeneity was more pronounced during the dry season relative to the rainy season. Temporal patterns were also apparent in floristic composition (taxonomic diversity) within clusters. During the rainy season, 30 % of the coastal waters fell within the cluster I, while for clusters IIA and IIB was 30 % and 40 % respectively. Conversely, during the rainy season, the biogeographic areas of cluster I expanded (60 %) at the expense of clusters IIA (25 %) and IIB (15 %), respectively.

5.1.3. Abiotic controls on phytoplankton distribution patterns

SOM and multivariate analyses of phytoplankton species abundance projects the different sampling stations according to their common species (Figure 45). pH, dissolved oxygen, silicate and surface water temperature values were widely spread over the trained SOM map (Figure 45). This signifies that they have regular distributions and that their values did not differ much between clusters. For instance, temperature did not vary by more than 3 °C between clusters. On the other hand, phosphate, nitrate, turbidity, total dissolved solids, and slope values showed strong spatiotemporal patterns and were restricted to specific sites on the SOM map. Turbidity and nitrate are strongly and significantly associated with cluster I (upper parts of the map), inland areas of the Ébrié lagoon with high freshwater influx. These parameters have direct relation to precipitation and river discharges (**Morlière, 1970**). The inland areas are also characterized by low TDS, low phosphate, relatively lower pH, temperature and low altitudes (slope percent). These relatively low-lying areas are characterized by high freshwater and nutrient inputs. Phosphate and topographic high areas (slope %) are strongly and significantly associated with areas with high marine influence during the dry season (cluster IIA), whereas total dissolved solids is strongly associated with cluster IIB. Other correlations between measured environmental variables can be deduced from the SOM map. For instance, silicate and total dissolved solids with opposing distribution patterns imply negative correlation. Higher availability of nitrate and phosphate as observed in these environments causes phytoplankton to use more silicate (**Wulff & Rahm, 1988**). Temporal fluctuations in total dissolved solids and silica concentration are the main factors structuring phytoplankton dynamics in these coastal environments. Changing hydrologic regimes in turn influence phytoplankton dynamics.

Table XX: Correlation (Pearson, n) between abiotic environmental factors and the dominant genus, *Phormidium foveolarum*

Variables	pH	DO	NO ₃	PO ₄ ³⁻	SiO ₃	Temperature	TDS	Turbidity	<i>Phormidium sp.</i>
pH	1								
DO	0.5000	1							
NO ₃	-0.3571	-0.0714	1						
PO ₄ ³⁻	-0.2143	-0.1071	0.6786	1					
SiO ₃	-0.6071	-0.1071	0.3214	0.1071	1				
Temperature	0.3571	-0.1429	-0.7857	-0.8929	-0.3929	1			
TDS	0.4643	0.4643	-0.6786	-0.8571	-0.2857	0.7500	1		
Turbidity	0.0000	-0.0714	0.0357	-0.2857	0.2857	0.2143	0.3929	1	
<i>Phormidium sp.</i>	-0.4286	-0.3214	0.6071	0.9286	0.2143	-0.8214	-0.9643	-0.4643	1

Values in bold are different from 0 with a significance level $\alpha=0.05$

Table XXI: Key indicator species for the different bioclimate zones (clusters).

Clusters	Indicator species	Specificity, A	Fidelity, B	IndVal (%)	p-value
I	Eusp	1.00	0.56	56	0.003**
	Eusp + Phfo	1.00	0.33	33	0.022*
	Phfo	0.65	0.50	33	0.048*
IIA	Nasp	0.76	0.89	68	0.001***
	Nasp + Nisp	1.00	0.56	56	0.001***
	Pssp	0.95	0.44	42	0.008**
	Nisp	0.74	0.56	41	0.007**
	Cylra	1.00	0.33	33	0.010**
	Nasp + Pssp	1.00	0.33	33	0.015*
	Acse	1.00	0.33	33	0.010**
IIB	Scqa	0.74	0.39	29	0.033*

Table XXII: List of taxa in order of decreasing abundance as distributed by SOM in each cluster

Clusters	Characteristics taxa
I	<i>Phormidium foveolarum</i> , <i>Aulacoseira granulata</i> , <i>Merismopedia glauca</i> , <i>Anabaena circinalis</i> , <i>Anabaenopsis</i> sp, <i>Microcystis aeruginosa</i> , <i>Pinnularia</i> sp., <i>Microcystis</i> sp., <i>Pediastrum duplex</i> , <i>Chroococcus</i> sp., <i>Pediastrum tetras</i> , <i>Eunotia</i> sp., <i>Lyngbya</i> sp., <i>Euglena</i> sp., <i>Cyclotella meneghiniana</i>
IIA	<i>Pseudanabaena</i> sp., <i>Phormidium foveolarum</i> , <i>Cylindrospermopsis raciborskii</i> , <i>Spondylosum</i> sp., <i>Navicula</i> sp., <i>Nitzschia</i> sp., <i>Chroococcus minutus</i> , <i>Cyclotella</i> sp., <i>Actinopteryx senarius</i> , <i>Scenesdesmus quadricauda</i> ,
IIB	<i>Aphanocapsa Incerta</i> , <i>Oscillatoria</i> sp., <i>Phormidium foveolarum</i> , <i>Anabaena circinalis</i> , <i>Anabaena</i> sp., <i>Aulacoseira granulata</i> <i>Microcystis aeruginosa</i> , <i>Merismopedia glauca</i> , <i>Lyngbya</i> sp., <i>Scenesdesmus quadricauda</i> , <i>Pseudanabaena</i> sp., <i>Gymnodinium</i> sp.

Table XXIII: List of taxa and their acronyms

Taxonomic classes	Code	Taxonomic classes	Code
Bacillariophyceae		Cyanophyceae	
<i>Actinopterychus senarius</i> Ehrenberg	Acse	<i>Anabaena circinalis</i> Rabenhorst	Anci
<i>Amphora commutata</i> Grunow	Amco	<i>Anabaena</i> sp.	Ansp
<i>Amphora</i> sp.	Amsp	<i>Anabaenopsis</i> sp.	Anbsp
<i>Aulacoseira granulata</i> (Ehrenberg) Simonsen	Augr	<i>Aphanocapsa Incerta</i> (Lemmermann) Cronberg	Apin
<i>Cocconeis</i> sp.	Cosp	<i>Chroococcus minutus</i> (Kützing) Nägeli	Chmi
<i>Coscinodiscus asteromphalus</i> Ehrenberg	Coas	<i>Chroococcus</i> sp.	Chsp
<i>Cyclotella meneghiniana</i> Kützing	Cyme	<i>Cylindrospermopsis racoborskii</i> (Woloszynska)	Cylra
<i>Cyclotella</i> sp.	Cysp	<i>Lyngbya</i> sp.	Lysp
<i>Diploneis ovalis</i> (Hilse) Cleve	Diov	<i>Merismopedia glauca</i> (Ehrenberg) Kützing	Megl
<i>Encyonema silesiacum</i> (Bleisch) D.G. Mann	Ensi	<i>Microcystis aeruginosa</i> (Kützing)	Miae
<i>Encyonema</i> sp.	Ensp	<i>Microcystis</i> sp.	Misp
<i>Entomoneis</i> sp.	Entsp	<i>Oscillatoria</i> sp.	Ossp
<i>Eunotia</i> sp.	Eusp	<i>Phormidium foveolarum</i> Gomont	Phfo
<i>Gyrosigma acuminatum</i> Kützing	Gyac	<i>Pseudanabaena</i> sp.	Pssp
<i>Gyrosigma</i> sp.	Gysp	Chlorophyceae	
<i>Hantzschia</i> sp.	Hasp	<i>Closterium</i> sp.	Clsp
<i>Melosira</i> sp.	Mesp	<i>Monoraphidium convolutum</i> Komárková-Legnerová	Moco
<i>Navicula</i> sp.	Nasp	<i>Netrium</i> sp.	Nesp
<i>Nitzschia palea</i> (Kützing) W. Smith	Nisp	<i>Pediastrum duplex</i> Meyen	Pedu
<i>Orthoseira</i> sp.	Orsp	<i>Pediastrum tetras</i> (Ehrenberg) Ralfs	Pete
<i>Pinnularia</i> sp.	Pisp	<i>Scenedesmus quadricauda</i> (Turpin) Brébisson	Scqa
<i>Surirella</i> sp.	Susp	<i>Scenedesmus</i> sp.	Scsp
<i>Ulnaria ulna</i> (Nitzsch) Compère	Ulul	<i>Spondylosum</i> sp.	Sposp
Euglenophyceae		Dinophyceae	
<i>Euglena</i> sp.	Eugsp	<i>Ceratium</i> sp.	Cesp
<i>Phacus</i> sp.	Phsp	<i>Gyrodinium</i> sp.	Gymsp
<i>Strombomonas</i> sp.	Strsp	Chrysophyceae	
<i>Trachelomonas planctonica</i> Svirenko	Trpl	<i>Dinobryon</i> sp.	Dinsp
<i>Trachelomonas</i> sp.	Trsp		
<i>Trachelomonas volvocina</i> Ehrenberg	Trvo		

Algal floristic changes due to environmental fluctuations in this environment are well-documented (Morlière, 1970; Iltis, 1984; Seu-Anoi *et al.*, 2013). The dominance of freshwater species in the lagoon has been linked to strong freshwater influence from its draining rivers (Baran, 2000; Seu-Anoi *et al.*, 2013). Tastet & Guiral (1994) estimated the annual freshwater input into the lagoon between 6 to $12 \times 10^9 \text{ m}^3$ with seawater input of $38 \times 10^9 \text{ m}^3$. Although, diatoms are the most species rich, Cyanobacteria are the most abundant in these coastal waters. They constitute up to 90 % of phytoplankton biomass in some areas especially during the rainy period. Their dominance is favoured by phytoplankton blooms (EEA *et al.*, 2008), a phenomenon triggered by eutrophication. It should however be noted that the dominance of cyanobacteria once established is difficult to reverse (Ekholm, 2008). Low taxonomic diversity of phytoplankton in the study area is comparable to observations made along the nearby Lagos lagoon (Nkwoji *et al.*, 2010). Conversely, phytoplankton abundance exceeds the bloom-forming thresholds of 20,000 cells/mL for recreational purposes (World Health Organization, 2003) in all sites. The dominance and proliferation of the dinoflagellate genus, *Gymnodinium* and bloom-forming cyanobacteria genera such as *Phormidium*, *Anabaena*, *Microcystis*, *cylindrospermopsis* and *plankthotrix* in some areas of this coast represent viable threats to the ecological status of these systems (EEA *et al.*, 2008). Once established, their formation of bloom causes high turbidity, suppressing the growth of other phytoplankton species (Visser, 1990). Although, not established in this study, these potentially toxic genera have been implicated in fish kills events: *Gymnodinium* in Kuwait Bay, Arabian Sea (Heil *et al.*, 2001); *Anabaena circinalis* in Barwon-Darling River in New South Wales, Australia (Bowling & Baker, 1996); *Phormidium* in some lakes in New Zealand (Chorus & Bartram, 1999) and *Microcystis aeruginosa*, notorious for its production of hepatotoxin in Lake Erie in the United States of America (Brittain *et al.*, 2000) and in Krüger national park, South Africa (Oberholster *et al.*, 2009). However, they are not always toxic (Suthers & Rissik, 2009). Prosser *et al.* (2012) showed that fluctuations in environmental variables like pH could act as a stimulant to toxin-production in some potentially toxic species. A likely explanation for the dwindling edible aquatic resource in these coastal waters is the fact that the dominant filamentous forms of cyanobacteria are not the preferred diet for majority of higher order aquatic species (Chorus & Bartram, 1999). Decline in fish productivity in these coastal waters has also been attributed to coastal water degradation (Kouassi & Biney, 1999). Notwithstanding, there is also a strong argument for the key role played by over-fishing, imposed by growing population which cannot be underestimated. Therefore, fish catches should be expected to diminish with continued increase in fishing efforts (Laë, 1997).

CHAPTER 6: Socio-economic considerations

The contribution of coastal aquatic resources to the enhancement of livelihood and poverty alleviation is great. They provide a range of supporting services referred to as ecosystem services (**Millenium Ecosystem Assessment, 2005**) that are highly beneficial to people, society and economy at large. These are services crucial in addressing objectives of food and water security (**Russi et al., 2012**). The Ébrié lagoon is a biodiversity reservoir and a rich source of ecosystem goods and services (Photo 50). As a direct employer, the coastal environment is a source of livelihood to three to four thousand fishermen and about forty thousand others are employed in other fishing related activities such as boat making, net sales (**Dufour et al., 1985**). Other socio-economic activities include surf fishing, recreational activities, sand mining/dredging, motor boat transportation, and mollusc shell (*Corbula trigona*) picking. The lagoon is also a significant source of revenue as about US \$4.36 million was generated from aquaculture on the lagoon in 2008 (**Dufour et al., 1985**). Fisheries production increased from 21 tonnes/year (1984) to 1,290 tonnes (2008). Electricity production from the water system totals 12 TWh per annum (**Dufour et al., 1985**). Shell fishing sell about 1,000 bags /week at 500 Francs CFA (85 cents) per 25-kg bag. However, for these coastal ecosystems to continue the smooth delivery of these monetary and non-monetary services will depend on the ways humans relate with these systems today. Some human activities are detrimental to coastal system health such as commercial exploitation of aquatic mangrove plants and plastic recycling releasing tons of phosphate from detergents into these systems.

6.1. Indigenous perception of climate change

The highest numbers of respondents were from the 31 – 45 age (active groups) categories (Figure 46). Majority of the respondents are traders, followed by farmers mainly involved in subsistence farming and fishermen (Figure 46). There is high awareness amongst riverine populace of the subject of climate change. Ninety percent of respondents opined that the climate is changing (Figure 47). Fifty-seven percent of them attest to precipitation deficit in the last years. This slightly more than half number might be because from the climate indices, the coastal area is only experiencing slight drought and recovery to normal precipitation amount is eminent. Another reason might be that mostly local farmers would feel the impact of precipitation amount. A relatively higher percentage of respondents (66 %) however, affirm to an increase in surface air temperature.



Blue crabs caught from the Ébrié lagoon at Songon-Té



Recreational activities in Nigui-Assoko



Fish (Anchovy) catch from the lagoon (Petit-Bassam inlet)



Sand mining/dredging activities in Bregbo



The Ébrié lagoon as an international trade route (Vridi canal)



Bivalve shells (*Corbula trigona*) harvested from the lagoon at Adiapoto



The Ébrié lagoon as local transportation route (Abobo-doumé)



Fresh firewood from mangrove plant hosted by the Ébrié lagoon



Plastic recycling activities at the Banco bay



Local fish market along the sandy beach in Azuretti



Sea salt from the inshore in Adjue



Island bars of oysters on the Ébrié lagoon

Photo 50: Some ecosystem goods and services delivered by the coastal water systems.

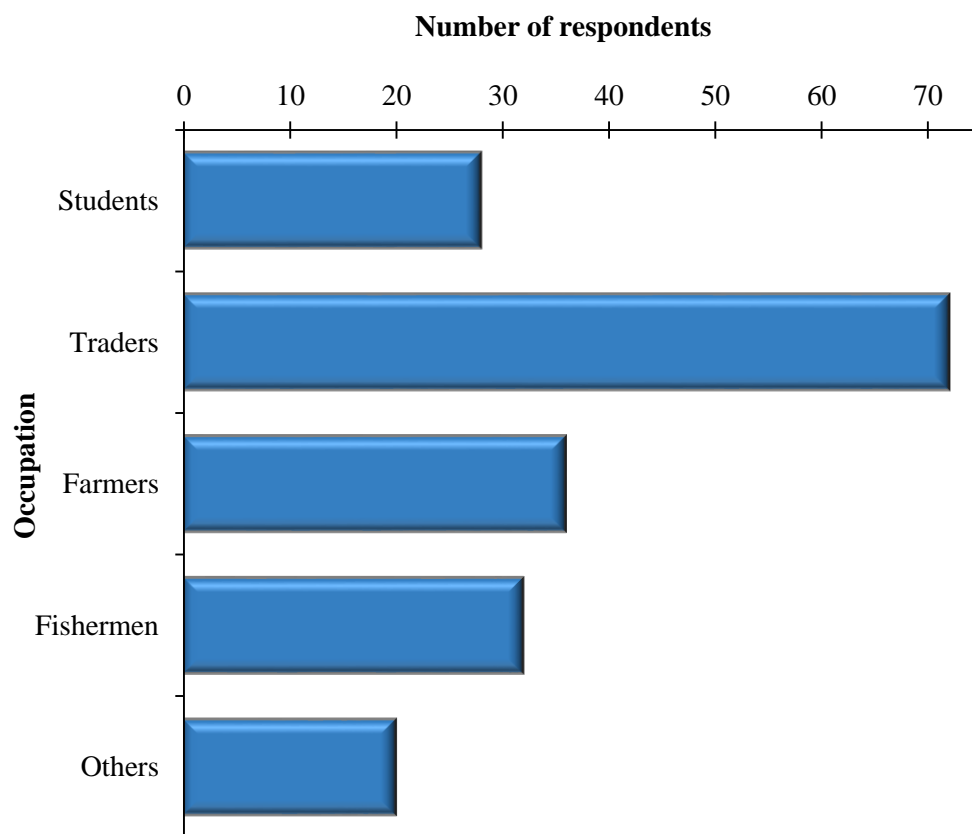
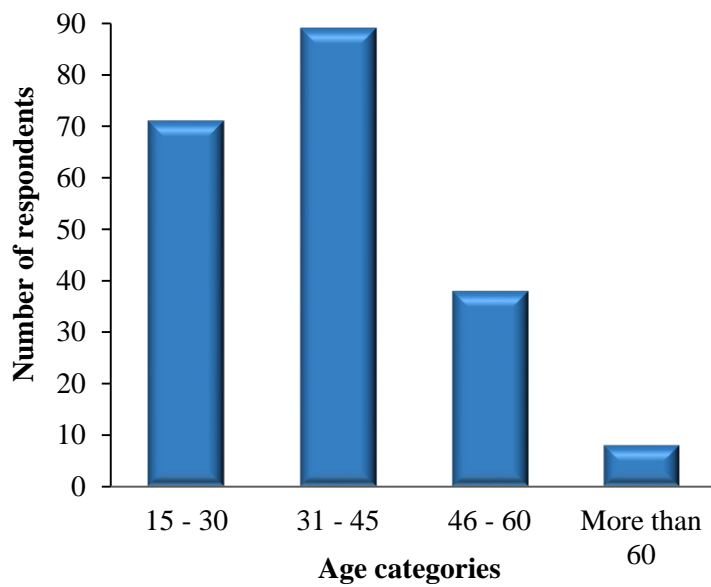


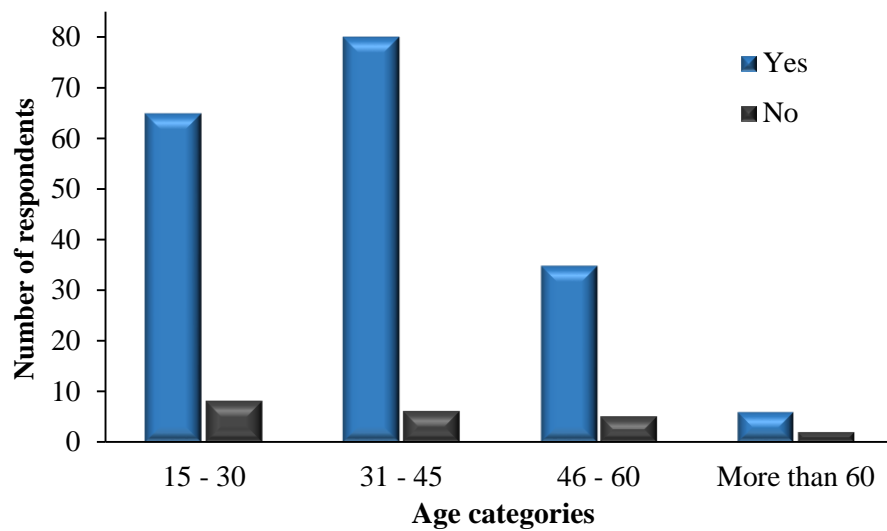
Figure 46: Age distribution (top) and main occupation (bottom) of the respondents.

6.2. Social vulnerability

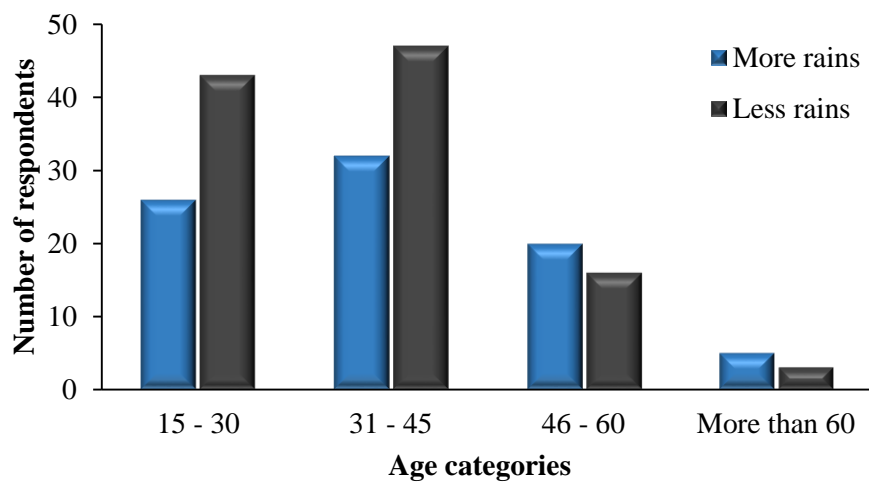
The vulnerability of the rural communities to coastal water degradation was assessed based on the availability and sources of alternative domestic water supply. Groundwater from domestic wells is the main domestic water source for rural communities (Figure 48). Alternative water sources for domestic purposes (Figure 49) include surface water systems (56 %), wells (41 %) and rainwater (3 %). Adaptive capacity to coastal water resource degradation for these coastal rural populations is generally low. Recent national statistics confirms that 74 % of rural population lives below the poverty line of US \$1 dollar per day (**Recensement Général de la Population et de l'Habitat, 2014**). Incapacitated by finances, these rural populations are unable to build modern water infrastructures or pay for high-tech water treatment services. In response to the question about water treatment methods employed before use, only 49 % of respondents admit to treating the water prior to use (Figure 50). Treatment methods include boiling (32 %), filtration (21 %), decantation (8 %) and chlorination (39 %). The rest 51 % uses these water resources for drinking purposes without any prior treatment. This puts them at greater risk of contamination of water-borne diseases. Man-environment relationship is one of hostility in some of the communities. The environment and surface water systems acts as refuse dumping ground (Figure 51). Only a handful of the respondents use the public wastewater discharge systems. In addition, there still exist poor sanitation and sewage systems in most of these communities. Fifty-two percent of the respondents have access to modern toilet facilities. The remaining 48 % practise open defaecation. This practise increases the contributions of nitrates in the coastal water systems. In response to water quality/quantity problems in these rural communities, only 43 % opined that water quality/quantity is a problem. Out of these, 2 % believes that water quality problem is all year round. Fifty-two percent of respondents believe that water quality problems occur only at certain periods of the year, 29 % opined that it is mostly during the dry season, owing to water shortage, while 18 % believes it is mostly pronounced during the wet season. The most important water quality problem highlighted with high probability of occurrence during the dry season is fish mortality/scarcity (Figure 52). The second most important problem is the proliferation of invasive weeds on the lagoon. These heavy floating mats obstruct waterways and render the lagoon non-navigable. An agriculture-related problem with high probability of occurrence during the rainy season is linked to erratic rainfall patterns with consequent delays/uncertainties in planting seasons.

6.3. Resource value

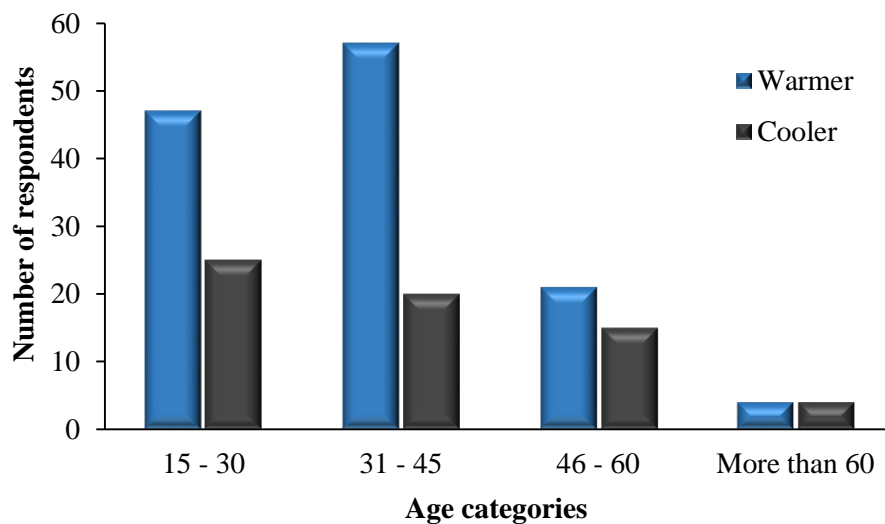
Rural population have adequate knowledge of the importance and ecological benefits of coastal water resources.



Q: Are there changes in local temperature and precipitation patterns?



Q: Are there relatively more or less rain events?



Q: Is surface air temperature relatively warmer or cooler?

Figure 47: Respondents perception of key climate parameters.

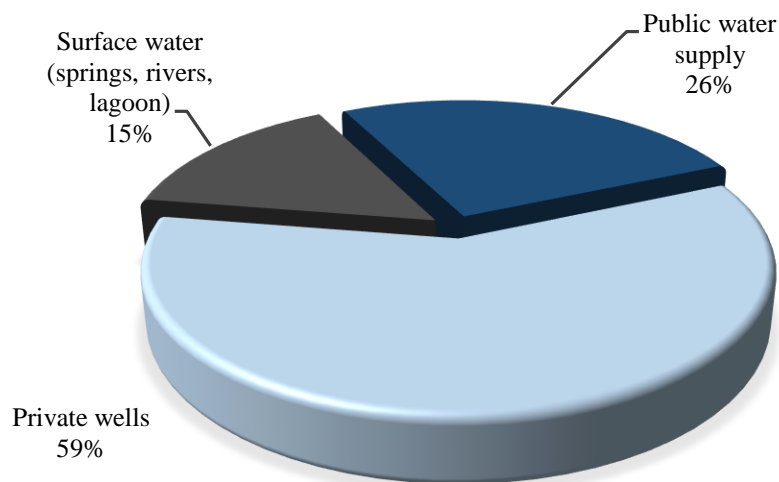


Figure 48: Main sources of domestic water supply.

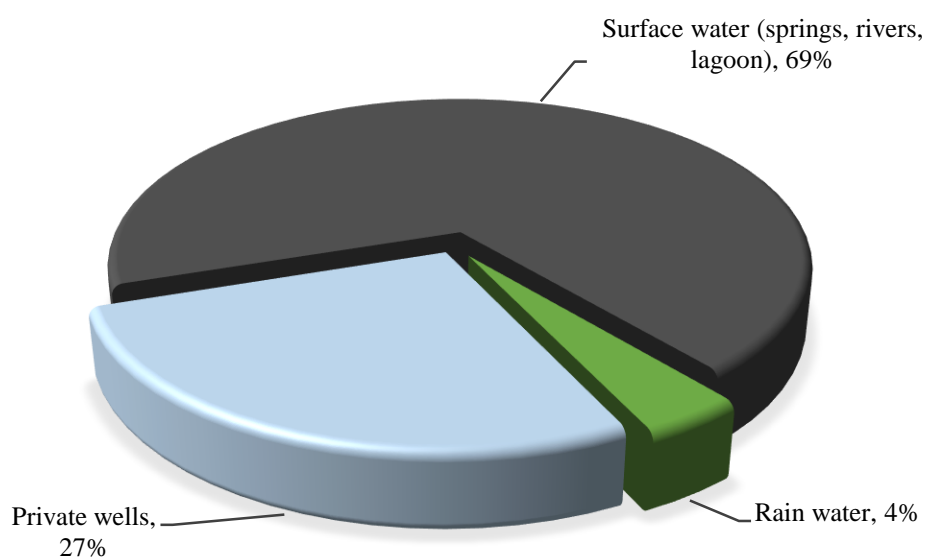


Figure 49: Existing alternative domestic water sources.

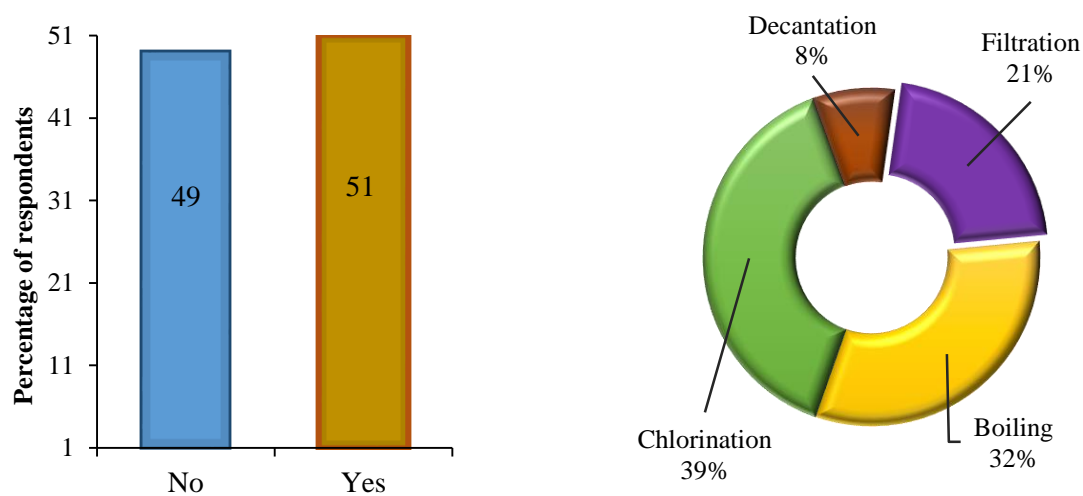


Figure 50: Responses to if water is treated prior to use (left) and treatment methods (right).

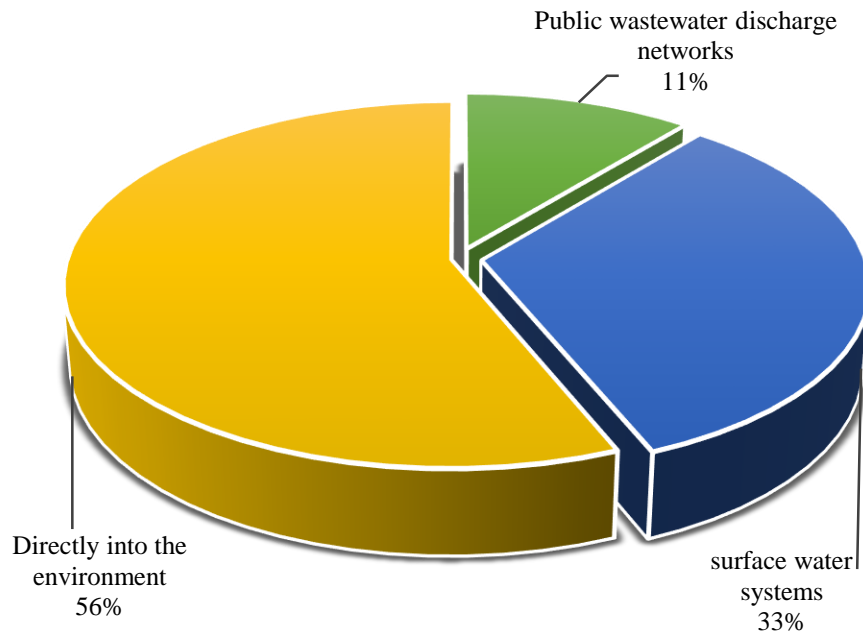


Figure 51: Ways of disposal of domestic wastewater

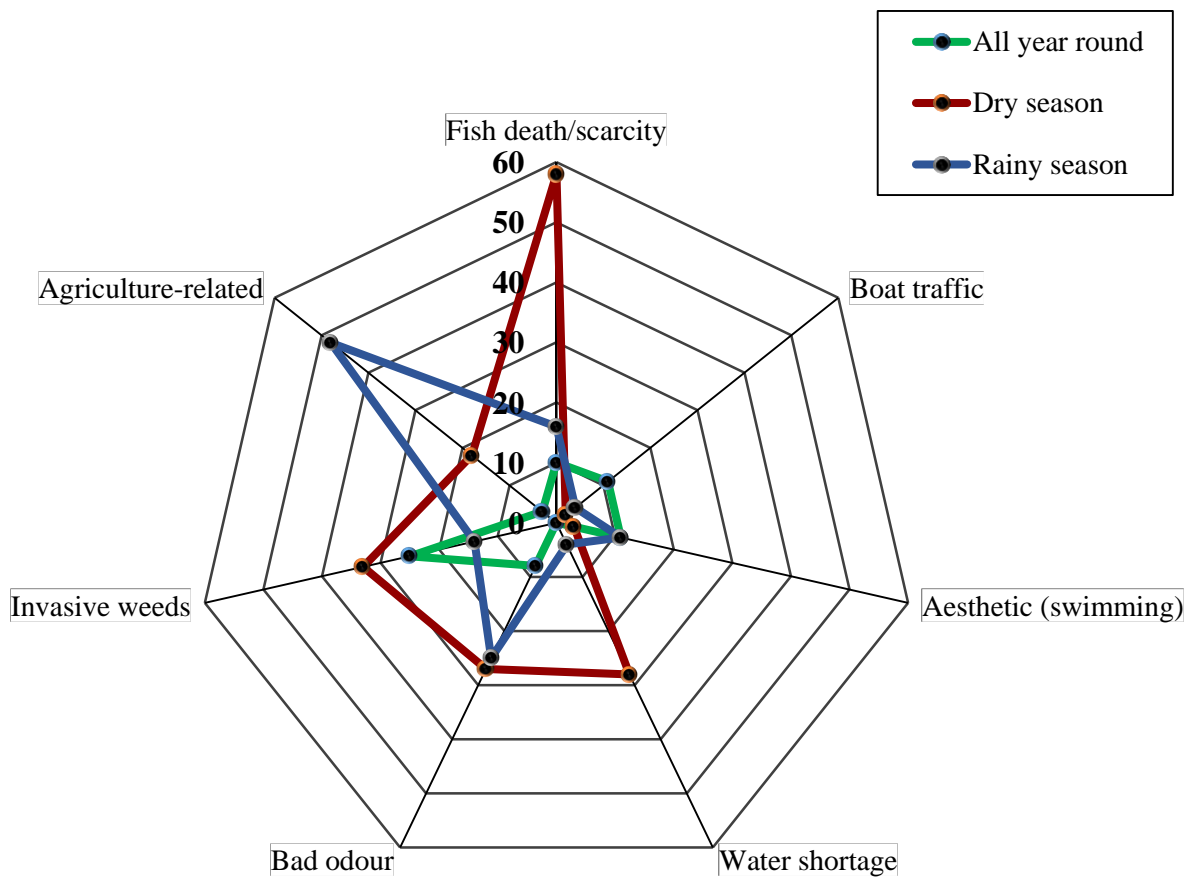


Figure 52: Radar chart on the perception of locals on coastal water degradation and most likely period of occurrence.

There is high direct dependence on these coastal water resources for sustenance (Photo 51). Sixty-three percent of the respondents demonstrate high willingness to make necessary sacrifices and contributions to participate in coastal ecosystem restoration (Figure 53).

At an exchange rate of US \$ 1 to 596.51 XOF FCFA, respondents are more than willing to pay between 1 XOF FCFA to whatever sum is required for the clean-up, restoration and conservation of coastal water resources should the need arise. Therefore, little coercion can help correct indiscriminate use of these natural resources in these riverine communities with high dependence on such resources.

Conservation and sustainable management of resources is an uphill task, as coastal water resources are common pool resources (state property, la Loi N° 98-750 of 23 December 1998). For instance, in the rural communities of Anna (Bingerville), built from resources from fishing activities (as reported by local sources), the aftermath of indiscriminate resource use is transparently evident in its adjacent lagoon waters. Widespread impacts include bad odour, dark-coloured (murky) waters, proliferation of invasive aquatic weeds and severe decline in fish catches. These have hampered the smooth delivery of ecosystem goods and services from the lagoon. According to the environmental committee, local initiatives to constrain contamination of the lagoon waters and conserve aquatic resource have so far met with little success, as these efforts are uncoordinated with no influence over contamination flux from other riverine communities. A joint/collaborative effort from all stakeholders is therefore solicited for conservation goals to be achieved.



Photo 51: Fishing boats lined up in Eloka-To community (Bngerville, Côte d'Ivoire).

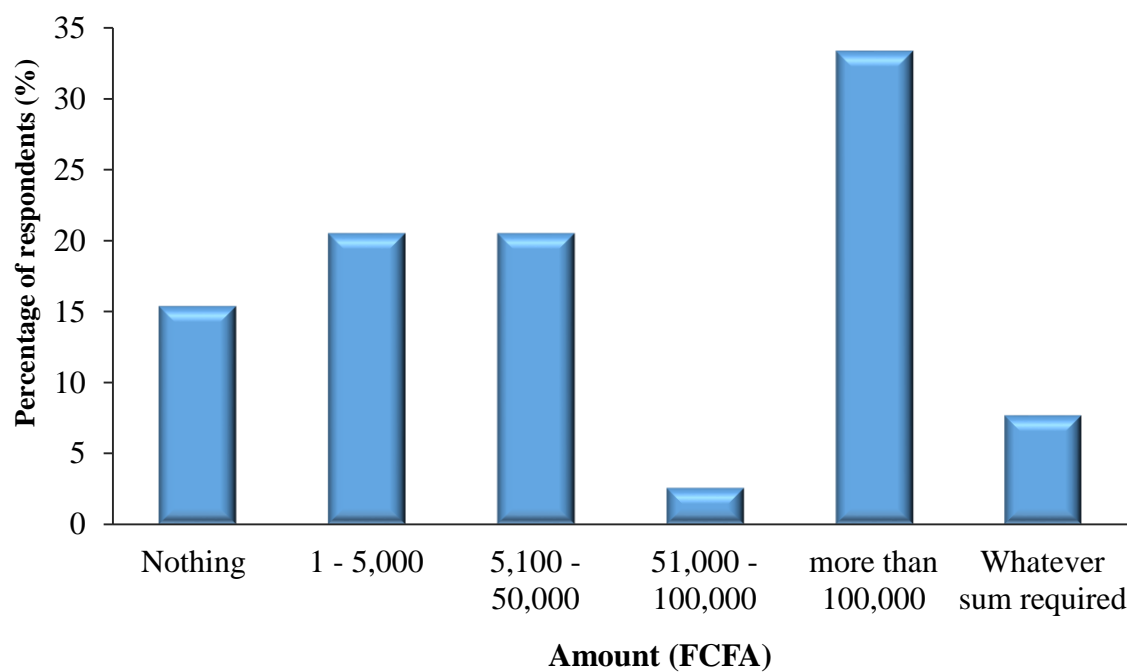


Figure 53: Amounts respondents are willing to pay to safeguard coastal water resources.

CONCLUSION

Although, water is a key natural capital needed to sustain biodiversity and human well-being, aquatic ecosystems are constantly under stress from nature (climate) and human activities. These results demonstrate that spatiotemporal variations in coastal water quality along the east Ivorian coast results from an interplay between nature and humans.

As an international trade route, the canal promotes socio-economic development in Abidjan. This demographic and economic development led to indiscriminate discharge of tons of untreated raw sewages from domestic, industrial, and commercial sources directly into the coastal waters. Another example been hydrocarbon leaks and contamination by ballast waters from incoming vessels to the Abidjan port. Deforestation (forests to other use) is also an offshoot of these socio-economic developmental activities.

Land use patterns, vegetation types, and water availability have an intricate relationship. Over the past 25 years (between 1989/90 and 2014/15), only 18 % of the primary forest is intact along this eastern coast. The main drivers of change are urbanization and agricultural activities. Gross mismanagement of natural capitals (land, water etc.) in the pursuance of short-term gains inflicts long-term damages on the environment. To keep up pace with its growing population and concomitant increase in demand for food and shelter, fertile forestlands are converted to residential and agricultural uses. These changes in land use negatively influence soil water retention capacity, surface run-offs and microclimate. Furthermore, strong dependence on chemicals (herbicides and fertilizers) to compensate for degraded soils and short fallow period (3 years or less) have important consequences on coastal water systems. Agricultural discharges increase nutrient loads (eutrophication) of coastal waters. This in turn can cause degradation in water quality, elicit biodiversity loss and lead to deterioration of socio-economic conditions.

Changing hydrometeorological regimes have direct influence on contaminant exports to coastal waters. These waters are highly prone to saltwater incursion during the dry season (January/February). The converse is true for the rainy season (September/October), when they are susceptible to land-based contamination from discharging rivers with relatively higher risk of degradation. Unabated, pollution poses a main threat to aquatic biodiversity. Urbanized/industrialized areas of the Ébrié lagoon recorded the highest spatiotemporal variations in phytoplankton biomass and were far less diverse. These areas are therefore vulnerability hotspots. Relatively stable phytoplankton communities were recorded at its eastern and western extremities with minimal human influences. Results from exploratory data analyses shows that turbidity and nitrate levels were the main abiotic factors controlling phytoplankton distribution in the uptidal regions of the lagoon, phosphate and turbidity exerts the most control in regions along the lagoon-sea continuum, during the dry season, while total

dissolved solids controls phytoplankton distribution along the Atlantic coast. These are climate-sensitive parameters whose concentrations depends on prevailing hydroclimatic processes. These notwithstanding, other biotic factors that may influence phytoplankton distribution are their reproductive cycles, growth rates, and grazing relationships.

Furthermore, proper management of water resources plays key indirect role in climate mitigation and adaptation. This stems from the fact that the aquatic environment is home to photosynthetic aquatic plants (microscopic and others such as mangroves) that are atmospheric oxygen replenishers with proven ability to store and sequester carbon. Therefore, promoting aquatic ecosystem resilience is critical to the continued delivery of these ecosystem goods and services. For instance, conservation of mangroves would serve dual purposes: a low-cost solution to mitigate climate change and an economically viable adaptation response strategy to climate change. Preliminary polls results show that the riverine communities have high awareness of the benefits derived from the mangrove ecosystems and show strong willingness to conserve them. Therefore, there is need to mainstream indigenous views and concerns into policymaking decisions geared towards conservation, for these efforts to be successful.

In summary, anthropogenic activities as the main drivers of change (degradation) in these coastal waters. Nature's contributions (from precipitation and catchment geology) are superimposed on existing non-climatic stressors. In the agricultural sector, for example, if the uncontrolled use of fertilizers to increase crop yields continue in 'business as usual' fashion, more likelihood of nutrient over-enrichment (eutrophication) should be expected from agricultural run-offs during the wet season.

The feedbacks recorded from the east Ivorian coastal water systems during both studied seasons give a glimpse of these systems' responses to futuristic climate change. This is because successive seasonal changes, aggregate to climate change. The main limitation, however, of this work is the short investigation timeframe (one-year). Improved and long-term monitoring of this environment is highly recommended in order to establish observed trends, as some observations might be singular occurrence, resulting for example from temporal accidental discharges.

Recommended community adaptive response strategies

It is imperative for rural communities to move from a predict-and-control paradigm to one of building resilience (Connor, 2005). The provision and sustainable use of good quality water will satisfy domestic needs, maintain good health status of ecological systems, serve to conserve biological diversity and boost economic growth. Inadequate access to clean water is an important measure of

poverty (**Carter & Bevan, 2008**), and a latent cause of biodiversity erosion (**World Water Assessment Programme, 2009**). Poverty is more than lack of income; it is multifaceted and often associated with lack of clean water, substandard living conditions, and environmental degradation (**Malik, 1998**). Access to water is not just a fundamental human right; it is an intrinsically important indicator of human progress (**United Nations Development Programme, 2006**). It gives substance to other human rights and serves as a springboard for the attainment of wider sustainable development goals. Sustainable Development Goals (SDGs) provides a platform for the improvement of water supplies, which if implemented will help reduce poverty and combat biodiversity erosion. Proper water resources management is precursory to sustainable development. Pollution into these coastal waters must be controlled so as not to outstrip their natural biological self-cleansing capacity. Presently, there exist no insurance(s) for ecological systems/natural capital against natural and/or anthropic disturbances. This coupled with the fact that a system's return to pristine conditions is not always guaranteed after the exceedance of its tolerance limits provides reasons enough to avert at all cause a repetition of the tragedy of the commons (**Hardin, 1968**). One way to correct human-environment hostility and instill behavioural change is through sensitization campaigns. Awareness should be raised as to the symbiotic benefits that can be harnessed by both parties if man treats the environment with less aggression. Environmental education should be incorporated into school curriculum. This would help to galvanize riverine rural communities on the need to protect coastal resources. Furthermore, existing community-based strategies on the use and management of biological resources should be encouraged and promoted. Vernacular laws are already in operation in some riverine communities. For example, in Abéréby, the sustainable management of fish stocks in the coastal lake Lason is tied to the taboo that once commercialized, fish stocks will disappear. In the community of Toukouzou Hozalem, fishing activities are regulated, strictly prohibited on days of religious worship/festivals. In another riverine community of Eloka-To, sustainable management of the mangrove forest is that timber logging are reserved solely for middle-aged men (age 35 and above). They are assigned concessions within mangrove forests and charged with the task of sustainable logging.

Another means to curb coastal water degradation that necessitates government actions is the provision of basic amenities inclusive of adequate sanitation facilities for these rural communities. The high bacterial loads on the lagoon and the microbially unsafe waters of shallow domestic wells attest to prevalent poor hygiene and sanitation habits. One way to stop the indiscriminate discharge of industrial effluents into the coastal waters is by levying of Pigouvian taxes. This makes it cheaper for the polluter(s) to treat pollutants rather than discharge them untreated into the environment (**Hardin,**

1968). Another adaptation strategy would be to encourage livelihood diversification. This will eventually discourage complete direct dependence on natural resources.

Conclusively, nature's most efficient solution to coastal water degradation is through the rehabilitation of degraded mangroves and conservation of existing mangrove forest. Mangroves support both mitigation and adaptation strategies to climate change. As already mentioned in the text, they are renowned for their ability to attenuate coastal waves (coastal protection), stabilize coastlines, act as natural water filters, provide habitat for aquatic stocks and sequester carbon. Their conservation will in the long-term conserve biodiversity conservation and enhance the resilience of riverine communities. Ultimately, man is invited to work with nature in a harmonious and considerate manner to strengthen natural defences and ensure their mutual survival by so doing.

REFERENCES

- Abe, J., N'doufou, G.H.C., Konan, K.E., Yao, K.S. and Bamba, S.B., 2014.** Relations entre les points critiques d'érosion et le transit littoral en Côte d'Ivoire. *Africa Geoscience Review*, 21, pp. 1-2.
- Adger, W.N., Agrawala, S., Mirza, M.M.Q., Conde, C., O'Brien, K., Pulhin, J., Pulwarty, R., Smit, B., Takahashi, K., 2007.** Assessment of adaptation practices, options, constraints and capacity. In: Parry, M.L., Canziani, O.F., Palutikof, J.P., Linden, P.J.V.D., Hanson, C.E. (Eds.), *Climate Change 2007: Impacts, Adaptation and Vulnerability. Contribution of Working Group II to the Fourth Assessment Report of the Intergovernmental Panel on Climate Change*. Cambridge University Press, Cambridge, UK, pp. 717–743.
- Adopo, K.L., Akobe, A.C., Etche, M.A., Monde, S. and Aka, K., 2014.** Situation de l'érosion Côtière au Sud-est de la Côte d'Ivoire, entre Abidjan et Assinie. *Revue Ivoirienne de Science et Technologie*, 24, pp. 223-237.
- Affian, K., Griboulard, R. and Prud'Homme R., 1987.** Contrôle structural de la morphologie de la marge ivoirienne et du Golfe de Guinée septentrional. *Bulletin de l'institute de Géologie du Bassin d'Aquitaine, Université de Bordeaux*, 42, pp. 85-98
- Aggarwal, P.K., Froehlich, K. and Kulkarni, K.M., 2009.** Environmental isotopes in groundwater studies. *Groundwater*, 2, 69.
- Aghui, N. and Biémi, J., 1984.** Géologie et hydrogéologie des nappes de la région d'Abidjan et risques de contamination. *Annales de l'Université Nationale de Côte d'Ivoire série C*, 20, pp. 313-347.
- Akouvi, A., Dray, M., Violette, S., de Marsily, G. and Zuppi, G.M., 2008.** The sedimentary coastal basin of Togo: example of a multilayered aquifer still influenced by a palaeo-seawater intrusion. *Hydrogeology journal*, 16(3), pp. 419-436.
- Allah-Kouadio, R., Cisse, I.B., Gregoire, L., Ouattara, A.D., 2016.** Sustainable development and the emergence of Africa, Grandvaux, pp. 807.
- Allan, J.D., Palmer, M.A. and Poff, N.L., 2005.** Climate change and freshwater ecosystems. In *Climate Change and Biodiversity*. Eds., Lovejoy and L. Hannah. New Haven, C.T.: Yale University Press. pp. 272-290.
- Allersma, E. and Tilmans, W.M., 1993.** Coastal conditions in West Africa-a review. *Ocean & coastal management*, 19(3), pp. 199-240.
- Allison, G.B., Cook, P.G., Barnett, S.R., Walker, G.R., Jolly, I.D. and Hughes, M.W., 1990.** Land clearance and river salinisation in the western Murray Basin, Australia. *Journal of Hydrology*, 119(1-4), pp. 1-20.

- Alongi, D.M., 2002.** Present state and future of the world's mangrove forests. *Environmental conservation*, 29(03), pp. 331-349.
- Alongi, D.M., 2008.** Mangrove forests: Resilience, protection from tsunamis, and responses to global climate change. *Estuarine Coastal and Shelf Science*, 76, pp. 1-13.
- Aman, A. and Fofana, S., 1998.** Spatial dynamics of the coastal upwelling off Côte-d'Ivoire. *Global Versus Local Changes in Upwelling Systems*. ORSTOM, Paris, pp. 139-147.
- Aman, A., Testut, L., Woodworth, P.L., Aarup, A. and Dixon, D.J., 2007.** Seasonal sea level variability in the Gulf of Guinea from altimetry and tide gauge. *Revue Ivoirienne des Sciences et Technologie*, 9, pp. 105-118.
- Anoh, K.P. and Pottier, P., 2008.** Géographie du littoral de Côte d'Ivoire. Elements de réflexion pour une politique de gestion intégrée. CNRS-LETG UMR 6554 et IGT: Nantes-Abidjan, pp. 325 *Les Cahiers d'Outre-Mer*, 251, pp. 485-489.
- Apostolescu, V., 1961.** Contribution à l'étude paléontologique (ostracodes) et stratigraphique des bassins crétacés et tertiaires de l'Afrique occidentale. *Revue Institut français du pétrole*, 16, pp. 779-867.
- Arthur, M.A., Schlanger, S.T. and Jenkyns, H.C., 1987.** The Cenomanian-Turonian Oceanic Anoxic Event, II. Palaeoceanographic controls on organic-matter production and preservation. *Geological Society, London, Special Publications*, 26(1), pp. 401-420.
- Asner, G.P. Scurlock, J.M.O. and Hicke, J.A., 2003.** Global synthesis of leaf area index observations: implications for ecological and remote sensing studies. *Global Ecology and Biogeography*, 12, pp. 191-205.
- Astel, A.M., Giorgini, L., Mistaro, A., Pellegrini, I., Cozzutto, S., and Barbieri, P., 2013.** Urban BTEX spatiotemporal exposure assessment by chemometric expertise. *Water Air and Soil Pollution*, 224, 1-17.
- Avenard, J.M., Eldin, M., Girard, G., Sircoulon, J., Touchebeuf, P., Guillaumet, J.L. and Adjanohoun, E., 1971.** Le milieu naturel de la Côte d'Ivoire. Paris, ORSTOM, 50, pp. 391.
- Back, W., 1960.** Origin of hydrochemical facies of ground water in the Atlantic Coastal Plain. In *Proceedings of 21st International Geological Congress, Copenhagen*, pp. 87-95.
- Bahlburg, H. and Dobrzinski, N., 2011.** A review of the Chemical Index of Alteration (CIA) and its application to the study of Neoproterozoic glacial deposits and climate transitions. *Geological Society, London, Memoirs*, 36(1), pp. 81-92.
- Bakun, A., 1978.** Guinea current upwelling. *Nature*, 271, pp. 147-150.
- Baran, E., 2000.** Biodiversity of estuarine fish faunas in West Africa. *Naga, The ICLARM Quarterly*, 23, pp. 4-9.

- Bauer, S. 2002.** Africa Environment Outlook. Past, Present and Future Perspectives. AMCEN Secretariat, United Nations Environment Programme.
- Berton, Y., 1961.** Les formations sédimentaires du Continental Terminal de Côte d'Ivoire. Rap. B.R.G.M. Abidjan, pp. 44.
- Bessoles, B., 1977.** Géologie de l'Afrique: le craton Ouest Africain (No. 88-89). BRGM.
- Bigot, S., 2004.** Variabilité climatique, interactions et modifications environnementales: l'exemple de la Côte d'Ivoire (Doctoral dissertation), pp. 367.
- Binder, E., 1968.** Répartition des mollusques dans la lagune Ébrié (Côte d'Ivoire). ORSTOM Ser Hydrobiologia, 11, pp. 3–34.
- Binet, D. and Marchal, E., 1993.** The large marine ecosystem of shelf areas in the Gulf of Guinea: long-term variability induced by climatic changes. Large Marine Ecosystems: Stress, Mitigation, and Sustainability, pp. 104-118.
- Bjerknes, J., 1969.** Atmospheric teleconnections from the equatorial pacific 1. Monthly Weather Review, 97(3), pp. 163-172.
- Blarez, E., 1986.** La marge continentale de Côte d'Ivoire-Ghana : structure et évolution d'une marge continentale transformante (Doctoral dissertation).
- Blarez, E. and Mascle, J., 1988.** Shallow structures and evolution of the Ivory Coast and Ghana transform margin. Marine and Petroleum Geology, 5(1), pp. 54-64.
- Bonhomme, M., 1962.** Contribution à l'étude géochronologique de la plate-forme de l'Ouest Africain. Imprimerie Louis-Jean.
- Bouillon. S., Dahdouh-Guebas. F., Rao. A.V.V.S., Koedam. N. and Dehairs. F., 2003.** Sources of organic carbon in mangrove sediments: variability and possible ecological implications Hydrobiologia, 495, pp. 33–39.
- Bowling, I.C. and Baker, P.D., 1996.** Major Cyanobacterial bloom in the Barwon-Darling River, Australia, in 1991, and underlying limnological conditions. Marine and Freshwater Research, 47, pp. 643-657.
- Brittain, S.M., Wang, J., Babcock-Jackson, L., Carmichael, W.W., Rinehart, K.L. and Culver, D.A., 2000.** Isolation and characterization of microcystins, cyclic heptapeptide hepatotoxins from a Lake Erie strain of *Microcystis aeruginosa*. Journal of Great Lakes Research, 26(3), pp. 241-249.
- Brou Yao, T., Servat, E. and Paturel, J.E., 1998.** Contribution à l'analyse des inter-relations entre activités humaines et variabilité climatique: cas du Sud forestier ivoirien. Comptes Rendus de l'Académie des Sciences-Series IIA-Earth and Planetary Science, 327(12), pp. 833-838.

- Brou, Y.T., 2010.** Risques climatiques, pressions foncières et agriculture en Côte d'Ivoire. IAHS-AISH publication, pp. 320-326.
- Brown R.M., McClelland N.I., Deininger R.A. and Tozer R.G., 1970.** A water quality index-do we dare? Water Sewage Works, pp. 339-343.
- Brown, S., Kebede, A.S. and Nicholls, R.J., 2011.** Sea-level rise and impacts in Africa, 2000 to 2100. School of Civil Engineering and the Environment University of Southampton, UK.
- Brownfield, M.E. and Charpentier, R.R., 2006.** Geology and total petroleum systems of the west-central coastal province (7203), West Africa (No. 2207-B), pp. 32.
- Burns, D.A., McDonnell, J.J., Hooper, R.P., Peters, N.E., Freer, J.E., Kendall, C. and Beven, K., 2001.** Quantifying contributions to storm runoff through end-member mixing analysis and hydrologic measurements at the Panola Mountain Research Watershed (Georgia, USA). *Hydrological Processes*, 15(10), pp. 1903-1924.
- Calow, R.C., Robins, N.S., MacDonald, A.M., Macdonald, D.M.J., Gibbs, B.R., Orpen, W.R.G., Mtembezeka, P., Andrews, A.J. and Appiah, S.O., 1997.** Groundwater management in drought-prone areas of Africa. *International Journal of Water Resources Development*, 13(2), pp. 241-262.
- Carpenter, S.R., Fisher, S.G., Grimm, N.B. and Kitchell, J.F. 1992.** Global change and freshwater ecosystems. *Annual Review of Ecology and Systematics*, 23, pp. 119-139.
- Carter, R.C. and Bevan, J.E., 2008.** Groundwater development for poverty alleviation in sub-Saharan Africa. *Applied groundwater studies in Africa*, 13, pp. 25-42.
- Chang, M., 2006.** Forest hydrology: an introduction to water and forests. CRC press, pp. 488.
- Chantraine, J.M. and Dufour, P., 1983.** Etude de faisabilité d'un réseau national d'observations de la qualité des eaux marines et lagunaires en côte d'ivoire. Paris, Ministère de l'Environnement et ORSTOM.
- Charpy, N. and Nahon, D., 1978.** Contribution à l'étude lithostratigraphique du Tertiaire du bassin de la Côte d'Ivoire. Université, Dep. Sciences de la Terre, Abidjan, série Doc., 18, p. 34.
- Chierici, M.A., 1996.** Stratigraphy, palaeoenvironments and geological evolution of the Ivory Coast-Ghana basin. *Géologie de l'Afrique et de l'Atlantique Sud: Actes Colloques Angers*, 1994, 293-303.
- Chorus, I. and Bartram, J., 1999.** Toxic cyanobacteria in water: A guide to their public health consequences, monitoring and management. Spon Press.
- Church, J.A., Clark, P.U., Cazenave, A., Gregory, J.M., Jevrejeva, S.A., Levermann, M.A. Merrifield, G.A. Milne, R.S., Nerem, P., Nunn, D., Payne, A.J., Pfeffer, W.T., Stammer, D. and Unnikrishnan, A.S., 2013.** Sea Level Change. In: *Climate Change 2013: The*

Physical Science Basis. Contribution of Working Group I to the Fifth Assessment Report of the Intergovernmental Panel on Climate Change. Eds., T.F. Stocker, D. Qin, G.K. Plattner, M. Tignor, S.K. Allen, J. Boschung, A. Nauels, Y. Xia, V. Bex and P.M. Midgley]. Cambridge University Press, Cambridge, United Kingdom and New York, NY, USA.

Clark, I.D. and Fritz, P., 1997. Environmental isotopes in hydrogeology. CRC press.

Clifford, A.C., 1986. African oil—Past, present, and future, in Halbouty, M.T., ed., Future petroleum provinces of the world, Proceedings of the Wallace E. Pratt Memorial Conference, Phoenix, December 1984: American Association of Petroleum Geologists Memoir 40, pp. 339–372.

Cocquyt, C., 1998. Diatoms from the northern basin of Lake Tanganyika.

Cohen, J.E., 1995. How many people can the earth support? *The Sciences*, 35(6), pp. 18-23.

Cohn, F., 1853. Ueber lebendige organismen im trinkwasser. *Z. klein. Medizin* 4, pp. 229–237.

Colin, C., 1988. Coastal upwelling events in front of the Ivory Coast during the focal program. *Oceanologica acta*, 11(2), pp. 125-138.

Compère, P., 1975. Algues de la région du lac Tchad. III : Rhodophycees, Euglenophycees, Eryptophycees, Dinophycees, Chrysophycees, Xanthophycees. *Cahiers ORSTOM. Série Hydrobiologie*, 9(3), pp. 167-192.

Connor, R., 2015. The United Nations world water development report 2015: water for a sustainable world (Vol. 1). UNESCO Publishing.

Cook, H.E., Johnson, P.D., Matti, J.C. and Zemmels, I., 1975. IV. Methods of Sample Preparation, and X-ray Diffraction Data Analysis, X-ray Mineralogy Laboratory, Deep Sea Drilling Project, University of California, Riverside. Initial reports of the deep sea drilling project, 25.

Costanza, R., Pérez-Maqueo, O., Martinez, M.L., Sutton, P., Anderson, S.J. and Mulder, K., 2008. The value of coastal wetlands for hurricane protection. *AMBIO: A Journal of the Human Environment*, 37(4), pp. 241-248.

Craig, H., 1961. Isotopic variations in meteoric waters. *Science*, 133(3465), pp. 1702-1703.

Crist, E.P. and Cicone, R.C., 1984. A physically-based transformation of Thematic Mapper data - The TM Tasseled Cap. *Geoscience and Remote Sensing, IEEE Transactions on*, (3), pp. 256-263.

Croneis, C. and Krumbein, W.C., 1936. Down to earth, an introduction to geology (Vol. 2). University of Chicago Press, pp. 484.

Dagnelie P., 1998. Statistiques théoriques et appliquées, 2nd Edition. Bruxelles, Belgique: De Boeck et Larcier, pp. 659.

- Dahanayake, K. and Krumbein, W.E., 1986.** Microbial structures in oolitic iron formations. *Mineralium Deposita*, 21(2), pp. 85-94.
- Dandonneau, Y., 1973.** Etude du phytoplancton sur le plateau continental de Côte d'Ivoire : 3. Facteurs dynamiques et variations spatiotemporelles. *Cahiers ORSTOM. Série Océanographie*, 11(4), pp. 431-454.
- Dansgaard, W., 1964.** Stable isotopes in precipitation. *Tellus*, 16(4), pp. 436-468.
- De-Cáceres, M.D. and Legendre, P., 2009.** Associations between species and groups of sites: indices and statistical inference. *Ecology*, 90(12), pp. 3566-3574.
- Delor, C., Diaby, I., Simeon, Y., Adou, M., Zamble, Z.B., Tastet, J.P., Yao, B., Konan, G., Chiron J.C. and Dommange, A., 1992.** Carte géologique de la Côte d'Ivoire à 1/200 000, Feuille Grand-Bassam. Direction de la Géologie, Abidjan, Côte d'Ivoire.
- DeMaster, D.J., 1981.** The supply and accumulation of silica in the marine environment. *Geochimica et Cosmochimica acta*, 45(10), pp. 1715-1732.
- Desanker, P. and Magadza, C., 2001.** Climate Change 2001 Impacts, Adaptation, and Vulnerability.
- Digbehi, Z.B., Affian, K., Mondé, S., Pothin, K.K. and Aka, K., 2001.** Analyse sédimentologique de quelques facies du Continental terminal de la région de Bingerville, environs d'Abidjan, Côte d'Ivoire. *Bioterre. Revue Internationale des Sciences de la Vie et de la Terre*, 2, pp. 70-84.
- Djagoua, É.V., Affian, K., Larouche, P. and Bachir, M., 2006.** Variabilité saisonnière et interannuelle de la chlorophylle en surface de la mer sur le plateau continental de la Côte d'Ivoire à l'aide des images de SEAWIFS, de 1997 à 2004. *Télédétection*, 6(2), pp. 143-151.
- Djagoua, E.V., Kassi, J.B., Mobio, B., Kouadio, J.M., Dro, C., Affian, K. and Saley, B., 2011.** Ivorian and Ghanaian upwelling comparison: Intensity and impact on phytoplankton biomass. *American Journal of Scientific and Industrial Research*, 2, 740-747.
- Dufour, P., 1982.** Les frontières naturelles et humaines du système lagunaire Ebrié Incidences sur l'hydroclimat. *Hydrobiologia*, 94(2), pp. 105-120.
- Dufour, P. and Berland, B., 1999.** Nutrient control of phytoplanktonic biomass in atoll lagoons and Pacific ocean waters: studies with factorial enrichment bioassays. *Journal of Experimental Marine Biology and Ecology*, 234(2), pp. 147-166.
- Dufour, P., Chantraine, J.M. and Durand, J.R., 1985.** Impact of man on Ebrie lagoon ecosystem (Ivory Coast). In: *Utilisation of coastal ecosystem: planning, pollution and productivity. Proceedings of an international symposium, Rio Grande, RS, Brazil*. L.N. Chao and W.W. Kirby-Smith Eds. University of Rio Grande du Sul, Brazil, pp. 467-484.

- Dufour, P. and Lemasson L., 1985.** Le régime nutritif de la lagune tropicale Ebrié (Côte d'Ivoire). *Océanographie Tropicale*, 20 (1), pp. 41-69.
- Dufour, P., Lemasson, L. and Crémoux, J.L., 1981.** Contrôle nutritif de la biomasse du seston dans une lagune tropicale de Côte d'Ivoire. II. Variations géographiques et saisonnières. *Journal of Experimental Marine Biology and Ecology*, 51(2), pp. 269-284.
- Dufour, P. and Slepoukha, M., 1975.** L'oxygène dissous en lagune Ebrié: influences de l'hydroclimat et des pollutions. *Documents Scientifiques, Centre de Recherches Océanographiques, Abidjan*, 6(2), pp. 75-118.
- Dufrêne, M. and Legendre, P., 1997.** Species assemblages and indicator species: the need for a flexible asymmetrical approach. *Ecological monographs*, 67(3), pp. 345-366.
- Durand, J.R. and Chantraine, J.M., 1982.** L'environnement climatique des lagunes ivoiriennes. *Revue d'hydrobiologie tropicale*, 15(2), pp. 85-113.
- Durand, J.R. and Guiral D., 1994.** Hydroclimat et hydrochimie. In: Durand Jean-René (ed.), Dufour Philippe (ed.), Guiral Daniel (ed.), Zabi S.G.F. (ed.) *Environnement et ressources aquatiques en Côte d'Ivoire : 2. Les milieux lagunaires*. Paris : ORSTOM, pp. 59-90.
- Durand, J.R. and Skubich, M., 1982.** Les lagunes ivoiriennes. *Aquaculture*, 27(3), pp. 211-250.
- Durand, J.R. and Zabi, S.G.F., 1994.** Repères historiques. *Environnement et ressources aquatiques de Côte d'Ivoire*, 2, pp. 24-34.
- Durov, S.A., 1948.** Natural waters and graphic representation of their compositions. *Dokl Akad Nauk SSSR* 59:87–90.
- EEA, JRC and WHO, 2008.** Impacts of Europe's changing climate – 2008 indicator based assessment. European Environment Agency, Copenhagen.
- Ekholm, P., 2008.** N: P Ratio in Estimating Nutrient Limitation in Aquatic Systems. Finnish Environment Institute.
- El Moujabber, M., Samra, B.B., Darwish, T. and Atallah, T., 2006.** Comparison of different indicators for groundwater contamination by seawater intrusion on the Lebanese coast. *Water resources management*, 20(2), 161-180.
- English, S.C., Wilkinson, C.R. and Basker, V.J. 1994.** Survey Manual for Tropical Marine Resources (2nd Edition). Australian Institute of Marine Science, Townsville.
- Falkenmark, M., 1989.** The massive water scarcity now threatening Africa: why isn't it being addressed?. *Ambio* 18(2), 112-118.
- FAO, 2006.** Global Forest Resources Assessment 2005 – progress towards sustainable forest management. FAO Forestry Paper 147. Rome, Italy.

- FAO, 2007.** Mangroves of Africa 1980–2005: country reports. Forest Resources Assessment Working Paper No. 135, Rome, Italy, pp. 10 - 69.
- FAO and UNEP, 1981.** Tropical Forest Resources Assessment Project, Forest Resources of Tropical Africa. Part II: Country Briefs FAO, UNEP, pp. 586.
- Fetter, C.W., 1994.** Applied hydrogeology, 3rd Ed. New York, Macmillan, pp. 691.
- Finch, J.W., 2001.** Estimating change in direct groundwater recharge using a spatially distributed soil water balance model. Quarterly Journal of Engineering Geology and Hydrogeology, 34(1), pp. 71-83.
- Foged, N., 1966.** Freshwater diatoms from Ghana. Collection Biologiske Skrifter Kongelige Danske Videnskabernes Selskab. Bd. 15 n°1, Kommissionaer, Munksgaard, pp. 169.
- Freeze, R.A. and Cherry, J.A., 1979.** Groundwater. Prentice-Hall, Englewood Cliffs, pp. 604.
- Gibbs, R.J., 1992.** A reply to the comment of Eilers et al. Limnology and Oceanography 37, pp. 1338-1339.
- Giri, C., Ochieng, E., Tieszen, L.L., Zhu, Z., Singh, A., Loveland, T., Masek, J. and Duke, N., 2011.** Status and distribution of mangrove forests of the world using earth observation satellite data. Global Ecology and Biogeography, 20, pp. 154-159
- Global Water Intelligence (GWI), 2014.** Côte d'Ivoire reboots its water sector. March 2014 GWI, 15(3), pp. 10.
- Goula, B.T.A., Konan, B., Brou, Y.T., Savane, I., Fadika, V. and Srohourou, B., 2007.** Estimation des pluies exceptionnelles journalières en zone tropicale : Cas de la Côte d'Ivoire par comparaison des lois lognormale et de Gumbel. Hydrological Sciences Journal, 52 (1), pp. 49-67.
- Gray, J.S. and Pearson, T.H., 1982.** Objective selection of sensitive species indicative of pollution-induced change in benthic communities. 1. Comparative methodology. Marine Ecology Progress Series 9, 111-119.
- Gruber, N. and Sarmiento, J.L., 1997.** Global patterns of marine nitrogen fixation and denitrification. Global Biogeochemical Cycles, 11(2), pp. 235-266.
- Guérin-Villeaubreil, G., 1962.** Hydrogéologie en Côte d'Ivoire. Direction de la Géologie et de la Prospection Minière. Mémoire 20, pp. 33.
- Guiral, D., 1992.** L'instabilité physique, facteur d'organisation et de structuration d'un écosystème tropical saumâtre peu profond: la lagune Ebrié. Vie milieu, 42, 73-92.
- Güler, C., Thyne, G.D., McCray, J.E. and Turner, K.A., 2002.** Evaluation of graphical and multivariate statistical methods for classification of water chemistry data. Hydrogeology journal, 10(4), pp. 455-474.

- Hallegatte, S., Green, C., Nicholls, R.J. and Corfee-Morlot, J., 2013.** Future flood losses in major coastal cities. *Nature climate change*, 3(9), pp. 802-806.
- Hansen, J., Nazarenko, L., Ruedy, R., Sato, M., Willis, J., Del Genio, A. and Novakov, T., 2005.** Earth's energy imbalance: Confirmation and implications. *Science*, 308(5727), pp.1431-1435.
- Hardin, G., 1968.** The tragedy of the commons. *Science*, 162(3859), pp. 1243-1248.
- Hardman-Mountford, N.J. and McGlade, J.M., 2003.** Seasonal and interannual variability of oceanographic processes in the Gulf of Guinea: an investigation using AVHRR sea surface temperature data. *International Journal of Remote Sensing*, 24(16), pp. 3247-3268.
- Harrison, R.M., 2007.** Principles of environmental chemistry. Royal society of chemistry, pp. 363.
- Heathwaite, A.L., Bust, T.P., Trudgill, S.T. and Burt, T.P., 1993.** Overview-the nitrate issue. Nitrate: processes, patterns and management, pp. 3-21.
- Heil, C.A., Gilbert, P.M., Al-Sarawl, M.A., Faraj, M., Behbehani, M. and Husain, M., 2001.** First record of a fish-killing *Gymnodinium* sp. bloom in Kuwait Bay, Arabian Sea: chronology and potential causes. *Marine Ecological Progress Series* 214, pp. 1-15.
- Hem, J.D., 1985.** Study and interpretation of the chemical characteristics of natural water (Vol. 2254). Department of the Interior, US Geological Survey, pp. 263.
- Herbland, A. and Le Loeuff, P., 1993.** Les sels nutritifs au large de la Côte d'Ivoire. In *Environnement et ressources Aquatiques de la Côte d'Ivoire. I - Le milieu marine*, Paris ORSTOM. 1, pp. 123-148.
- Hiscock, K.M., 2009.** Hydrogeology: principles and practice. John Wiley & Sons, pp. 408.
- Hooper, R.P., Christophersen, N. and Peters, N.E., 1990.** Modelling streamwater chemistry as a mixture of soilwater end-members - An application to the Panola Mountain catchment, Georgia, USA. *Journal of Hydrology*, 116(1-4), pp. 321-343.
- Huppert, D.D., Moore, A. and Dyson, K., 2009.** Impacts of climate change on the coasts of Washington State. *Washington Climate Change Impacts Assessment: Evaluating Washington's Future in a Changing Climate*, pp. 285-309.
- Hurley, P.M., Leo, G.W., White, R.W. and Fairbairn, H.W., 1971.** Liberian age province (about 2,700 my) and adjacent provinces in Liberia and Sierra Leone. *Geological Society of America Bulletin*, 82(12), pp. 3483-3490.
- Hutchinson, J., Manica, A., Swetnam, R., Balmford, A. and Spalding, M., 2014.** Predicting Global Patterns in Mangrove Forest Biomass. *Conservation Letters*, 7, pp. 233–240.

- Ibe, A.C., and L.F. Awosika., 1991.** Sea level rise impact on African coastal zones. In *A change in the weather: African perspectives on climate change*, ed. S.H. Omide and C. Juma, Nairobi, Kenya: African Centre for Technology, pp. 105-12.
- Iltis, A., 1984.** Biomasses phytoplanctoniques de la lagune Ebrié (Côte d'Ivoire). *Hydrobiologia*, 118(2), pp. 153-175.
- Institute National de la Statistique, INS, 1998.** Recensement General de la Population et de l'habitat, RGPH, Abidjan, Côte d'Ivoire.
- IPCC, 1997.** The Regional Impacts of Climate Change: An Assessment of Vulnerability. Eds., R.T.Watson, M.C.Zinyowera, R.H.Moss. Cambridge University Press, UK, pp. 517
- IPCC, 2007.** Fourth assessment report: Climate change 2007: Climate change impacts, adaptation and vulnerability. Summary for policy makers.
- IPCC, 2014. Jimenez, B.E., Oki, T., Arnell, N.W., Benito, G. Conley, J.G. Döll, P., Jiang, T. and Mwakalila, S.S.** Freshwater resources. In: *Climate Change 2014: Impacts, Adaptation and Vulnerability. Contribution of Working Group II to the Fifth Assessment Report of the Intergovernmental Panel on Climate Change*. Eds., C.B. Field, V.R. Barros, D.J. Dokken, K.J. Mach, M.D. Mastrandrea, T.E. Bilir, M. Chatterjee, K.L. Ebi, Y.O. Estrada, R.C. Genova, B. Girma, E.S. Kissel, A.N. Levy, S. MacCracken, P.R. Mastrandrea, and L.L.White. Cambridge University Press, Cambridge, United Kingdom and New York, NY, USA.
- Jaccard, P., 1912.** The distribution of the flora in the alpine zone. *New phytologist*, 11(2), pp. 37-50.
- Jallow, B.P., Toure, S., Barrow, M.M. and Mathieu, A.A., 1999.** Coastal zone of The Gambia and the Abidjan region in Côte d'Ivoire: sea level rise vulnerability, response strategies, and adaptation options. *Climate Research*, 12(2-3), pp. 129-136.
- Jevrejeva, S., Moore, J.C., Grinsted, A. and Woodworth, P.L., 2008.** Recent global sea level acceleration started over 200 years ago? *Geophysical Research Letters*, 35(8).
- Jones, C.G., Lawton, J.H. and Shachak, M., 1994.** Organisms as ecosystem engineers. In *Ecosystem management*. Springer New York, pp. 130-147.
- Jourda, J.P., 1987.** Contribution à l'étude géologique et hydrogéologique de la région du grand abidjan (Côte d'Ivoire). Thèse de Doctorat de 3ème cycle, Université scientifique, technique et médicale de Grenoble, pp. 319.
- Jourda, J.P. 2002.** Les ressources en eau souterraine de la Côte d'Ivoire et le cas des aquifères transfrontaliers entre la Côte d'Ivoire et le Ghana. *Proceedings of the International Workshop Tripoli, Libya, 2– 4 June 2002*

- Julious, S.A., 2005.** Sample size of 12 per group rule of thumb for a pilot study. *Pharmaceutical Statistics*, 4(4), pp. 287-291.
- Kathiresan, K. and Bingham, B.L., 2001.** Biology of mangroves and mangrove ecosystems, *Advances in Marine Biology*, 40, pp. 81-251.
- Kaiser, H.F., 1958.** The varimax criterion for analytic rotation in factor analysis. *Psychometrika*, 23, pp. 187-200.
- Kaski, S. and Lagus, K. 1996** Comparing self-organizing maps. In: *Proceedings of ICANN96, International Conference on Artificial Neural Networks*. Eds. C. von der Malsburg, W. von Seelen, J. C. Vorbruggen and B. Sendho. *Lecture Notes in Computer Science* vol. 1112, pp. 809-814. Springer, Berlin.
- Kendall, M., 1975.** *Multivariate analysis*. Charles Griffin. London.
- Kendall, C. and Doctor, D.H., 2003.** Stable isotope applications in hydrologic studies. *Treatise on geochemistry*, 5, pp. 319-364.
- Koerselman, W. and Meuleman, A.F., 1996.** The vegetation N: P ratio: a new tool to detect the nature of nutrient limitation. *Journal of Applied Ecology*, pp. 1441-1450.
- Koffi, K.P., 1992.** Quelques aspects de l'érosion actuelle de l'unité littorale de Côte d'Ivoire (Golfe de Guinée). *Centre de Recherches Océanographiques*. B.P. V.18 Abidjan (Côte d'Ivoire), pp. 299-396.
- Kohonen, T. 1995.** *Self-Organizing Maps*, Springer Series in Information Sciences, Vol. 30, Springer, Berlin, Heidelberg, New York, 1995, 1997, 2001, 3rd edition.
- Komárek, J. and Anagnostidis, K., 2005.** Cyanoprokaryota 2. Teil/2nd part : Oscillatoriales. Eds., B. Büdel, L. Krientz, G. Gärtner and M. Schagerl). *Süßwasserflora von Mitteleuropa* 19/2. Elsevier/Spektrum, Heidelberg.
- Komiyama, A., Pongpan, S., Shogo Kato., 2005.** Common allometric equations for estimating the tree weight of mangroves. *Journal of Tropical Ecology*, 21, pp. 471–477.
- Konen, M.E., Jacobs, P.M., Burras, C.L., Talaga, B.J. and Mason, J.A. 2002.** Equations for predicting soil organic carbon using loss-on-ignition for north central US soils. *Soil Science Society of America Journal*, 66(6), pp. 1878-1881.
- Koranteng, K.A., 1998.** The impacts of environmental forcing on the dynamics of demersal fishery resources of Ghana (Doctoral dissertation, University of Warwick).
- Kouakou, K.E., Goula, B.T.A. and Kouassi, M.A., 2012.** Analyze of climate variability and change impacts on hydro-climate parameters: case study of Côte d'Ivoire. *International Journal of Science and Engineering Research*, 3(2), pp. 1-8.

- Kouamelan, A.N., 1996.** Géochronologie et Géochimie des Formations Archéennes et Protérozoïques de la Dorsale de Man en Côte d'Ivoire. Implications pour la Transition Archéen-Protérozoïque (Doctoral dissertation, Université Rennes 1).
- Kouassi, A. M. and Biney, C., 1999.** Overview of the marine environmental problems of the West and Central African region. *Ocean Coastal management*, 42, pp. 71-76.
- Krammer, K. and Lange-Bertalot, H. 1991.** Bacillariophyceae: Centrales. Fragilariaceae. Eunotiaceae. Eds., H. Etti, J. Gerloff, H. Heying and D. Mollenhauer) *Süßwasserflora von Mitteleuropa*, Stuttgart.
- Krebs, C.J., 1994.** Ecology. The Experimental Analysis of Distribution and Abundance. Fourth edn. Benjamin Cummings, New York.
- Kreitler, C.W., 1989.** Hydrogeology of sedimentary basins. *Journal of hydrology*, 106(1), 29-53.
- Kunz, T.J. and Richardson, A.J., 2006.** Impacts of climate change on phytoplankton. Impacts of climate change on Australian marine life: part C, literature review (Eds., A.J. Hobday, T.A. Okey, E.S. Poloczanska, T.J. Kunz and A.J. Richardson), pp. 8-18.
- Laë, R., 1997.** Does overfishing lead to a decrease in catches and yields? An example in two West African coastal lagoons. *Fisheries Management and Ecology*, 3, pp. 101–116.
- Lampinen, J. and Oja, E., 1992.** Clustering properties of hierarchical self-organizing maps. *Journal of Mathematical Imaging and Vision*, 2(2-3), pp. 261-272.
- Leclerc, H.D.A.A., Mossel, D.A.A., Edberg, S.C. and Struijk, C.B., 2001.** Advances in the bacteriology of the coliform group: their suitability as markers of microbial water safety. *Annual Reviews in Microbiology*, 55(1), pp. 201-234.
- Lindeboom, H., 2002.** The coastal zone: an ecosystem under pressure. *Oceans Vol. 2020*, pp. 49-84.
- Lloyd, J.A. and Heathcote, J.A., 1985.** Natural inorganic hydrochemistry in relation to groundwater: An introduction. Oxford Uni. Press, New York, pp. 296.
- Longhurst, A.R., 1962.** A review of the oceanography of the Gulf Guinea. *Bull. Inst. Franc. Afr. Noire (A)* 24 (3), pp. 633-663.
- Lorenzen, C.J., 1967.** Determination of chlorophyll and phaeo-pigments: spectrophotometric equations. *Limnology and oceanography*, 12(2), pp. 343-346.
- Loroux, B.F.E., 1978.** Contribution à l'étude hydrogéologique du bassin sédimentaire côtier de Côte d'Ivoire. Thèse Université de Bordeaux I, France, pp. 93.
- Malik, S., 1998.** Rural poverty and land degradation: a reality check for the CGIAR. Report to the Technical Advisory Committee to the CGIAR. FAO, Rome.
- Manikandan, K., Kannan, P. and Sankar, M., 2012.** Evaluation and Management of Groundwater in Coastal Regions. *Earth Science India*, 5(I), pp. 1-11.

- Markert, B.A., Breure, A.M. and Zechmeister, H.G. Eds., 2003.** Bioindicators & biomonitors: principles, concepts, and applications. (Vol. 6). Gulf Professional Publishing.
- Martin, I. and Tastet, P., 1972.** Le quaternaire du littoral et du plateau continental de Côte d'Ivoire role des mouvements tectoniques et eustatiques. Abidjan, ORSTOM.
- Martínez, M.L., Intralawan, A., Vázquez, G., Pérez-Maqueo, O., Sutton, P. and Landgrave, R., 2007.** The coasts of our world: Ecological, economic and social importance. *Ecological Economics*, 63(2), pp. 254-272.
- Mazón, J. and Pino, D., 2013.** The role of sea-land air thermal difference, shape of the coastline and sea surface temperature in the nocturnal offshore convection. *Tellus A*, 65.
- Mazor, I., 1991.** Applied chemical and isotopic groundwater hydrology.
- McGuire, K. and McDonnell, J., 2007.** "Stable isotope tracers in watershed hydrology." *Stable Isotopes in Ecology and Environmental Science*, pp. 335-374.
- Mensah, M.A. and Koranteng, K.A., 1988.** A Review of the Oceanography and Fisheries resources in the coastal waters of Ghana, 1981-1986. Report-Marine Fishery Research (Ghana).
- Meyer, J.L., Sale, M.J., Mulholland, P.J. and Poff, L.N. 1999** "Impacts of Climate Change on Aquatic Ecosystem Functioning and Health. *Journal of the American Water Resources Association*, 35(6), pp. 1373-1386.
- Miikkulainen, R. 1990** Script recognition with hierarchical feature maps. *Connection Science*.
- Millennium Ecosystem Assessment, 2005.** Ecosystems and human well-being: wetlands and water synthesis. World Resources Institute, Washington, DC.
- Mitchell, P., 2006.** Guidelines for quality assurance and quality control in surface water quality programs in Alberta. Alberta Environment.
- Morlière, A., 1970.** Les saisons marines devant Abidjan. *Documents Scientifiques, Centre de Recherches Océanographiques, Abidjan*, 1(2), pp. 1-15.
- Morlière, A. and Rebert, J.P., 1972.** Etude hydrologique du plateau continental ivoirien. *Documents Scientifiques, Centre de Recherches Océanographiques, Abidjan*, 3(2), pp. 1-30.
- Moss, B., 1967.** A Spectrophotometric Method for the Estimation of Percentage Degradation of Chlorophylls to Pheo-Pigments in Extracts of Algae. *Limnology and oceanography*, 12(2), pp. 335-340.
- Moss, B., 2010.** Ecology of freshwaters: a view for the twenty-first century, 4th edn. John Wiley and Sons. pp. 268-287.
- Mtoni, Y.E., Mjemah, I., Msindai, K., Van Camp, M. and Walraevens, K., 2012.** Saltwater intrusion in the Quaternary aquifer of the Dar es Salaam region, Tanzania. *Geologica Belgica*, 15(1-2), pp. 16-25.

- Müller, G., 1979.** Schwermetalle in den Sedimenten des Rheins-Veränderungen seit 1971. Umschau, 79(24), pp. 778-783.
- Munsell Color, 2011.** Geological Rock-Color Chart, Grand Rapids, MI.
- Muzuka, A.N.N. and Shunula, J.P., 2006.** Stable isotope compositions of organic carbon and nitrogen of two mangrove stands along the Tanzanian coastal zone. Estuarine Coastal and Shelf Science, pp.447–458.
- Nairn, A. and Stehli, F. Eds., 1973.** The ocean basins and margins vol. 1: the southern Atlantic. Plenum press New York.
- Neal, C., Neal, M., Reynolds, B., Maberly, S.C., May, L., Ferrier, R.C. and Parker, J.E., 2005.** Silicon concentrations in UK surface waters. Journal of Hydrology, 304(1), pp. 75-93.
- Negri, A.J., Adler, R.F., Nelkin, E.J. and Huffman, G.J., 1994.** Regional rainfall climatologies derived from Special Sensor Microwave Imager (SSM/I) data. Bulletin of the American Meteorological Society, 75(7), pp. 1165-1182.
- Nicole, M., 1994.** A preliminary inventory of coastal wetlands of Côte d'Ivoire (Vol. 12). IUCN, pp. 80.
- Nixon, S.W., Ammerman, J.W., Atkinson, L.P., Berounsky, V.M., Billen, G., Boicourt, W.C., Boynton, W.R., Church, T.M., Ditoro, D.M., Elmgren, R. and Garber, J.H., 1996.** The fate of nitrogen and phosphorus at the land-sea margin of the North Atlantic Ocean. Biogeochemistry, 35(1), pp. 141-180.
- Nkwoji, J.A., Onyema, I.C. and Igbo, J.K., 2010.** Wet season spatial occurrence of phytoplankton and zooplankton in Lagos Lagoon, Nigeria. Science World Journal, 5, pp. 7-14.
- Oberholster, P.J., Myburgh, J.G., Govender, D., Bengis, R. and Botha, A.M., 2009.** Identification of toxigenic Microcystis strains after incidents of wild animal mortalities in the Kruger National Park, South Africa. Ecotoxicology and Environmental Safety, 72, pp. 1177-1182.
- Oga Yei, M.S., Sacchi, E. and Zuppi, G.M., 2007.** Origin and effects of nitrogen pollution in groundwater traced by $\delta^{15}\text{N}\text{--NO}_3$ and $\delta^{18}\text{O}\text{--NO}_3$: The case of Abidjan (Ivory Coast). Advances in Isotope Hydrology and its Role in Sustainable Water Resources Management (IHS—2007), pp.139.
- Oteri, A.U. and Atolagbe, F.P., 2003.** Saltwater Intrusion into Coastal Aquifers in Nigeria. In The Second International Conference on Saltwater Intrusion and Coastal Aquifers—Monitoring, Modeling, and Management. Mérida, Yucatán, México. Environments and the 1st Arab Water Forum, pp. 1-15.
- Ouattara, A. 2000.** Premières données systématiques et écologiques du phytoplancton du lac d'Ayamé (Côte d'Ivoire). Thèse de l'Université Catholique de Leuven, Belgique, pp. 200.

- Oude Essink, G.H.P., 1996.** Impact of sea level rise on groundwater flow regimes: A sensitivity analysis for the Netherlands. TU Delft, Delft University of Technology.
- Paasche, E., 1980.** Silicon. The physiological ecology of phytoplankton, 7, pp. 259-284.
- Pàges, J., Lemasson, L. and Dufour, P.H., 1979.** Eléments nutritifs et production primaire dans les lagunes du Côte d'Ivoire : cycle annuel. Archives Scientifiques, Centre de Recherches Océanographiques, Abidjan, 5(1), pp. 1-64.
- Park, Y.S., Céréghino, R., Compin, A. and Lek, S., 2003.** Applications of artificial neural networks for patterning and predicting aquatic insect species richness in running waters. Ecological modelling, 160(3), pp. 265-280.
- Parry, M.L., Canziani, O.F., Palutikof, J.P. van der Linden, P.J. and Hanson, C.E. Eds., 2007.** Climate Change 2007: Impacts, Adaptation and Vulnerability. Contribution of Working Group II to the Fourth Assessment Report of the Intergovernmental Panel on Climate Change, Cambridge University Press, Cambridge, UK, pp. 982.
- Persson, T., Rudebeck, A., Jussy, J.H., Colin-Belgrand, M., Priemé, A., Dambrine, E., Karlsson, P.S. and Sjöberg, R.M., 2000.** Soil nitrogen turnover—mineralisation, nitrification and denitrification in European forest soils. In Carbon and nitrogen cycling in European forest ecosystems. Springer Berlin Heidelberg, pp. 297-311.
- Petroci and Beicip, 1990.** Côte d'Ivoire petroleum evaluation. Ministère des Mines, Abidjan (Côte d'Ivoire), pp. 99.
- Phillips, D.L., Newsome, S.D. and Gregg, J.W., 2005.** Combining sources in stable isotope mixing models: alternative methods. Oecologia, 144(4), pp. 520-527.
- Piper, A. M., 1944.** A graphic procedure in geochemical interpretation of water analyses. Trans Am Geophys Union, 25, pp. 914-923.
- Pözlbauer G., 2004.** Survey and comparison of quality measures for selforganizing maps. In J'an Parali'c, Georg P'özlbauer, and Andreas Rauber, editors, Proceedings of the Fifth Workshop on Data Analysis (WDA'04), Sliezsky dom, Vysoké Tatry, Slovakia, June 24-27 2004. Elfa Academic Press, pp. 67-82.
- Poorter, L., Bongers, F., Koume, F.N. and Hawthorne, W.D. (Eds.), 2004.** Biodiversity of West African forests: an ecological atlas of woody plant species. CABI.
- Prosser, K.N., Valenti, T.W., Hayden, N.J., Neisch, M.T., Hewitt, N.C., Umphres, G.D., Gable, G.M., Grover, J.P., Roelke, D.L. and Brooks, B.W., 2012.** Low pH preempts bloom development of a toxic haptophyte. Harmful Algae, 20, pp. 156-164.
- Prüss, A., 1998.** Review of epidemiological studies on health effects from exposure to recreational water. International journal of epidemiology, 27(1), pp. 1-9.

- Rabalais, N.N., Turner, R.E., Díaz, R.J. and Justić, D. 2009.** Global change and eutrophication of coastal waters. *ICES Journal of Marine Science: Journal du Conseil*, 66(7), pp. 1528-1537.
- Raffaelli, D., Raven, J. and Poole, L., 1998.** Ecological impact of green macroalgal blooms. *Oceanography and Marine Biology Ann. Rev.* 36, pp. 97–125.
- Rasmusson, E.M. and Wallace, J.M., 1983.** Meteorological aspects of the El Nino/southern oscillation. *Science*, 222(4629), pp. 1195-1202.
- Ray, G.C. and Hayden, B.P., 1992.** Coastal zone ecotones. In *Landscape boundaries*, Springer, New York, pp. 403-420.
- Reid, H. and Huq, S., 2005.** Climate change-biodiversity and livelihood impacts. *Tropical forests and adaptation to climate change*, pp. 57.
- Richter, B.C., Kreitler, C.W. and Bledsoe, B.E., 1991.** Identification of sources of ground-water salinization using geochemical techniques. US Environmental Protection Agency, Office of Research and Development, Robert S. Kerr Environmental Research Laboratory.
- Rodelli, M.R., Gearing, J.N., Gearing, P.J., Marshall, N. and Sasekumar, A., 1984.** Stable isotope ratio as a tracer of mangrove carbon in Malaysian ecosystems. *Oecologia*, 61, pp. 326-333.
- Rougerie, G., 1960.** Le façonnement actuel des modelés en Côte d'Ivoire forestière. *Mém. IFAN*, 58, pp. 542.
- Rozanski, K., Araguás-Araguás, L., and Gonfiantini, R., 1993.** Isotopic patterns in modern global precipitation. *Climate change in continental isotopic records*, pp. 1-36.
- Russi, D., Ten Brink P., Farmer A., Badura T., Coates D., Förster J., Kumar R. and Davidson N., 2012.** The Economics of Ecosystems and Biodiversity for Water and Wetlands. Final Consultation Draft.
- Saenger, P. and Bellan, M. F. (1995).** The mangrove vegetation of the Atlantic Coast of Africa: a review, Université de Toulouse, Toulouse, France.
- Salard-Cheboldaeff, M., 1990.** Intertropical African Palynostratigraphy from Cretaceous to Late Quaternary Times. *Journal of African Earth Science*. Vol. 11 (1-2), pp. 1-24.
- Saley, M.B., Tanoh, R., Kouame, K.F., Oga, M.S., Kouadio, B.H., Djagoua, E.V., Oulare, S., Youan, T., Affian, K., Jourda, J.P. Savane, I. and Biemi, J., 2009.** Variabilité spatio-temporelle de la pluviométrie et son impact sur les ressources en eaux souterraines : cas du district d'Abidjan (sud de la Côte d'Ivoire). In 14e colloque International en évaluation environnementale, Niamey, pp. 26-29.
- Sanderson, M., Santini, M., Valentini, R. and Pope, E., 2012.** Relationships between forests and weather.

- Sankaré, Y. and Etien, N., 1991.** Analyse des effets de l'ouverture du chenal de Grand Bassam (estuaire du fleuve Comoé, Lagune Ebrié) sur la macrofaune benthique lagunaire. *Journal Ivoirien d'Océanologie et de Limnologie*, 1(2), pp. 81-90.
- Scanlon, B.R., Reedy, R.C., Stonestrom, D.A., Prudic, D.E. and Dennehy, K.F., 2005.** Impact of land use and land cover change on groundwater recharge and quality in the southwestern US. *Global Change Biology*, 11(10), pp. 1577-1593.
- Scheren, P.A.G.M., Kroeze, C., Janssen, F.J.J.G., Hordijk, L. and Ptasiński, K.J., 2004.** Integrated water pollution assessment of the Ebrié lagoon, Ivory Coast, West Africa. *Journal of Marine Systems*, 44(1), pp. 1-17.
- Schlüter, T., 2008.** Geological atlas of Africa, Berlin: Springer, pp. 301.
- Schmitt, A., 1998.** Trophiebewertung planktondominierter Fließgewässer-Konzept und erste Erfahrungen. *Münchener Beiträge zur Abwasser Fischerei und Flussbiologie*, pp. 394-411.
- Schön, S. 1988.** Cell counting. In: *Experimental Phycology: A Laboratory Manual*. Eds., C.S. Lobban, D.J. Chapman and B.P. Kremer). Cambridge University Press, NY.
- Schwartz, M.L. 2005.** *Encyclopaedia of coastal science*. Springer, pp. 1211.
- Sclater, J.G., Bowin, C., Hey, R., Hoskins, H., Peirce, J., Phillips, J. and Tapscott, C., 1976.** The Bouvet triple junction. *Journal of Geophysical Research*, 81(11), pp. 1857-1869.
- Servat, E., Paturel, J.E., Kouame, B., Travaglio, M., Ouedraogo, M.A.H.A.M.A.N., Boyer, J.F. and Marieu, B., 1998.** Identification, caractérisation et conséquences d'une variabilité hydrologique en Afrique de l'Ouest et Centrale. *IAHS Publication*, pp. 323-338.
- Seu-Anoi, N.M., Kone, Y.J.M., Kouadio, K.N., Ouattara, A. and Gourene, G., 2013.** Phytoplankton distribution and its relationship to environmental factors in the Ébrié lagoon, Ivory Coast, West Africa. *Vie et milieu*, 63(3-4), pp. 181-191.
- Shannon, C.E. and Weaver, W., 1949.** *The mathematical theory of communication*. Urbana, IL.
- Simeon, Y, Delor, C., Diaby, I., Gadou, G., Kohou, P., Tastet, J.P., Yao, B., Konan, G. and Dommanget, A., 1992.** Carte géologique de la Côte d'Ivoire à 1/200 000 ; Feuille Abidjan. Direction de la Géologie, Abidjan, Côte d'Ivoire.
- Simon, B., 2007.** La marée – la marée océanique et côtière. Edition Institut Océanographique, pp. 434.
- Simon, P. and Amakou, B., 1984.** La discordance oligocène et les dépôts postérieurs à la discordance dans le bassin sédimentaire ivoirien. *Bulletin de la Société Géologique de France*, (6), pp. 1117-1125.
- Smith-III, T.J., 1992.** Forest structure. *Tropical mangrove ecosystems*, Robertson, A.I, Alongi, D.M. Ed. American Geophysical Union, Washington, DC.

- Spalding, M., Kainuma, M., and Collins, L., 2010.** World Atlas of Mangroves, Earthscan, London, Washington DC, pp. 319.
- Spengler, A. and Delteil J.B., 1964.** Le bassin secondaire-tertiaire de Côte d'Ivoire. In : Reyre, D. (ed.). Bassins sédimentaires du littoral africain, Association Service Géologique Africain, Paris, pp. 99-113,
- Sprague, R.A., Melvin, J.A., Conradi, F.G., Pearce, T.J., Dix, M.A., Hill, S.D. and Canham, H., 2009.** Integration of core-based chemostratigraphy and petrography of the Devonian Jauf Sandstones, Uthmaniya area, Ghawar field, eastern Saudi Arabia. Search and Discovery Article, 20065, pp. 34.
- Suthers, I., and Rissik, D. Eds., 2009.** Plankton: A guide to their ecology and monitoring for water quality. CSIRO Publishing, pp. 256.
- Tagini, B., 1971.** Esquisse structurale de la Côte d'Ivoire. Essai de géotectonique régionale. - SODEMI éd., Abidjan, pp. 302.
- Tastet, J.P., 1971.** Le contexte géologique du site d'Abidjan. Annales Universitaire d'Abidjan, série G.
- Tastet, J.P. and Guiral, D., 1994.** Géologie et sédimentologie. In : Durand Jean-René (ed.), Dufour P. (ed.), Guiral D. (ed.), Zabi S.G.F. (ed.). Environnement et ressources aquatiques en Côte d'Ivoire : 2. Les milieux lagunaires. Paris, ORSTOM, 2, pp. 35-58.
- Thornthwaite, C.W., 1948.** An approach toward a rational classification of climate. Geographical Review 38, pp. 55–94.
- Tolman, C.F. and Poland, J.F., 1940.** Ground-water, salt-water infiltration, and ground-surface recession in Santa Clara Valley, Santa Clara County, California. Eos, Transactions American Geophysical Union, 21(1), pp. 23-35.
- Tomlinson, P.B., 1986.** The botany of mangroves. Cambridge, London, New York, New Rochelle.
- Touré, B., Kouamé, K.F., Souleye, W., Collet, C., Affian, K., Ozer, A., Rudant, J.P. and Biémi, J., 2012.** L'influence des actions anthropiques dans l'évolution historique d'un littoral sableux à forte dérive sédimentaire : la baie de Port-Bouët (Abidjan, Côte d'Ivoire). Géomorphologie, (3), pp. 369-382.
- Townsend, D.W., Mayer, L.M., Dortch, Q. and Spinrad, R.W., 1992.** Vertical structure and biological activity in the bottom nepheloid layer of the Gulf of Maine. Continental Shelf Research, 12(2), pp. 367-387.
- Tsyban, A., Everett, J.T. and Titus, J.G., 1990.** World oceans and coastal zones. Climate Change: The IPCC Impacts Assessment. Contribution of Working Group II to the First Assessment Report of the Intergovernmental Panel on Climate Change, pp. 1-28.

- United Nations, 1988.** Groundwater in North and West Africa: Côte d'Ivoire. In: Groundwater in North and West Africa. Natural Resources/Water Series No.18, ST/TCD/5. ISBN 92-1-104203-8, New York.
- UNEP, 2010.** 'Africa water Atlas'. Division of Early Warning and Assessments (DEWA). Nairobi, Kenya.
- United Nations Human Settlements Programme, 2014.** The State of African Cities.
- Valiela, I., Foreman, K., LaMontagne, M., Hersh, D., Costa, J., Peckol, P., DeMeo-Andreson, B., D'Avanzo, C., Babione, M., Sham, C.H. and Brawley, J., 1992.** Couplings of watersheds and coastal waters: sources and consequences of nutrient enrichment in Waquoit Bay, Massachusetts. *Estuaries*, 15(4), pp. 443-457.
- Van Dijk, G.M., Van Liere, L., Amiraal, W., Bannink, B.A. and Cappon, J.J., 1994.** Present state of the water quality of European rivers and implications for management, *Sci. Total Envir.*, 145, pp. 187–195.
- Varlet, F., 1958.** Le régime de l'Atlantique près d'Abidjan. *Études Éburn.* (IFAN), 7, pp. 97-222.
- Velasco, V., Tubau, I., Vázquez-Suñe, E., Gogu, R., Gaitanaru, D., Alcaraz, M., Serrano-Juan, A., Fernández-García, D., Garrido, T., Fraile, J., Sanchez-Vila, X., 2014.** GIS-based hydrogeochemical analysis tools (QUIMET). *Computers & Geosciences*. CAGEO-D-13-00373R2.
- Vengosh, A., Spivack, A.J., Artzi, Y. and Ayalon, A., 1999.** Geochemical and boron, strontium, and oxygen isotopic constraints on the origin of the salinity in groundwater. *Water Resources Research*, 35(6), pp. 1877-1894.
- Verstraeten, I.M., Fetterman, G.S., Meyer, M.T., Bullen, T. and Sebree, S.K., 2005.** Use of tracers and isotopes to evaluate vulnerability of water in domestic wells to septic waste. *Groundwater Monitoring & Remediation*, 25(2), pp. 107-117.
- Vesanto, J., Himberg, J., Alhoniemi, E. and Parhankangas, J., 1999.** Self-organizing map in Matlab: the SOM Toolbox. In *Proceedings of the Matlab DSP conference*, Vol. 99, pp. 16-17.
- Vicente-Serrano, S.M., Beguería, S. and López-Moreno, J.I., 2010.** A multiscalar drought index sensitive to global warming: the standardized precipitation evapotranspiration index. *Journal of Climate*, 23(7), pp. 1696-1718.
- Visser, P.M., 1990.** De primaire productie van het Markermeer. Microbiology Laboratory, University of Amsterdam.
- Vollenweider, R.A., 1969.** A manual on methods for measuring primary production in Aquatic environments. Oxford/Edinburgh, Blackwell scientific publications, 1969, -S 213.

- Voronoi, G., 1907.** "Nouvelles applications des paramètres continus à la théorie des formes quadratiques." *J. reine angew. Math*, 133, pp. 97-178.
- Weast, R.C., 1981.** CRC Handbook of Chemistry and Physics 61st edition. Chemical Rubber Co., 1981: F-202.
- Wedepohl, K.H., 1995.** The composition of the continental crust. *Geochimica et cosmochimica Acta*, 59(7), pp. 1217-1232.
- Wetzel, R.G., 2001.** Limnology. Lakes and River Ecosystems. Third Edition, Academic Press, San Diego, California, U.S.A.
- Wognin, V., Coulibaly, A., Akobe, A., Monde, S. and Aka, K., 2013.** Morphologie du littoral et cinématique du trait de côte de Vridi à Grand-Bassam (Côte d'Ivoire). *Journal of Environmental Hydrology*, 21, pp. 1-10.
- World Health Organization, 1996.** Guidelines for Drinking-water Quality Volume 2: Health Criteria and Other Supporting Information, Second edition, pp. 973.
- World Health Organization, 2003.** Assessing Microbial Safety of Drinking Water Improving Approaches and Methods: Improving Approaches and Methods. OECD Publishing.
- Wright, J.B., Hastings, D.A., Jones, W.B. and Williams, H.R., 1985.** Geology and mineral resources of West Africa. Allen and Unwin, London, UK, pp. 187.
- Wulff, F. and Rahm, L., 1988.** Long-term, seasonal and spatial variations of nitrogen, phosphorus and silicate in the Baltic: an overview. *Marine environmental research*, 26(1), pp.19-37.
- Wyman, R.L., 1991.** Global climate change and life on earth. Chapman and Hall Ltd.
- Yidana, S.M., Banoeng-Yakubo, B. and Akabzaa, T.M., 2010.** Analysis of groundwater quality using multivariate and spatial analyses in the Keta basin, Ghana. *Journal of African Earth Sciences*, 58(2), pp. 220-234.
- Zhou, M., Brandt, P., Pelster, D., Rufino, M.C., Robinson, T. and Butterbach-Bahl, K., 2014.** Regional nitrogen budget of the Lake Victoria Basin, East Africa: syntheses, uncertainties and perspectives. *Environmental Research Letters*, 9(10), p.105009.

Webography

- Abeygunawardena, P., Vyas, Y., Knill, P., Foy, T., Harrold, M., Steele, P., Tanner, T., Hirsch, D., Oosterman, M., Rooimans, J., Debois, M., Lamin, M., Liptow, H., Mausolf, E., Verheyen, R., Agrawala, S., Caspary, G., Paris, R., Kashyap, A., Sharma, A., Mathur, A., Sharma, M. and Sperling, F., 2009.** Poverty and climate change: reducing the vulnerability of the poor through adaptation. Washington, DC: World Bank. Available from <http://documents.worldbank.org/curated/en/534871468155709473/Poverty-and-climate-change-reducing-the-vulnerability-of-the-poor-through-adaptation> (accessed 20.10.2016).
- African Centre of Meteorological Applications for Development (ACMADa), 2014.** Dekad 21st to 31 January 2014. Ten-day climate watch bulletin No. 3. Available from <http://www.Acmad.org>. (accessed 31 12 15).
- African Centre of Meteorological Applications for Development (ACMADb), 2014.** Dekad 21st to 31 October 2014. Ten-day climate watch bulletin No. 30. Available from <http://www.Acmad.org>. (accessed 31 12 15).
- Aman, A., 2007.** National report on sea level observing activities, Côte d'Ivoire. Available from http://www.gloss-sealevel.org/publications/documents/cotedivoire_gex2007.pdf.
- BIO Intelligence Service, 2014.** Soil and water in a changing environment, Final Report prepared for European Commission (DG ENV), with support from HydroLogic (accessed 20.10.2016).
- Brownlow, A.H., 1979.** Geochemistry. Engelwood Cliffs, NJ. Available at <http://home.wlu.edu/~kuehns/geo311/f09/weathering6.pdf> (accessed 19.1.2016).
- CBD/Ramsar, 2006.** Guidelines for the rapid ecological assessment of biodiversity in inland water, coastal and marine areas. Secretariat of the Convention on Biological Diversity, Montreal, Canada, CBD Technical Series no. 22 and the Secretariat of the Ramsar Convention, Gland, Switzerland, Ramsar Technical Report no. 1. Available from http://www.ramsar.org/sites/default/files/documents/library/lib_rtr01.pdf (accessed 7.5.2013).
- Convention on Biodiversity, 2009.** Fourth National Report on Côte d'Ivoire (2005 – 2009). Available at <http://www.cbd.int/doc/world/ci/ci-nr-04-fr.pdf>.
- Diaz, R., Selman, M. and Chique, C., 2011.** Global Eutrophic and Hypoxic Coastal Systems. World Resources Institute. Eutrophication and hypoxia: Nutrient pollution in Coastal Waters map. Available at http://www.docs.wri.org/wri_eutrophic_hypoxic_data-sets_2011-03.xls.

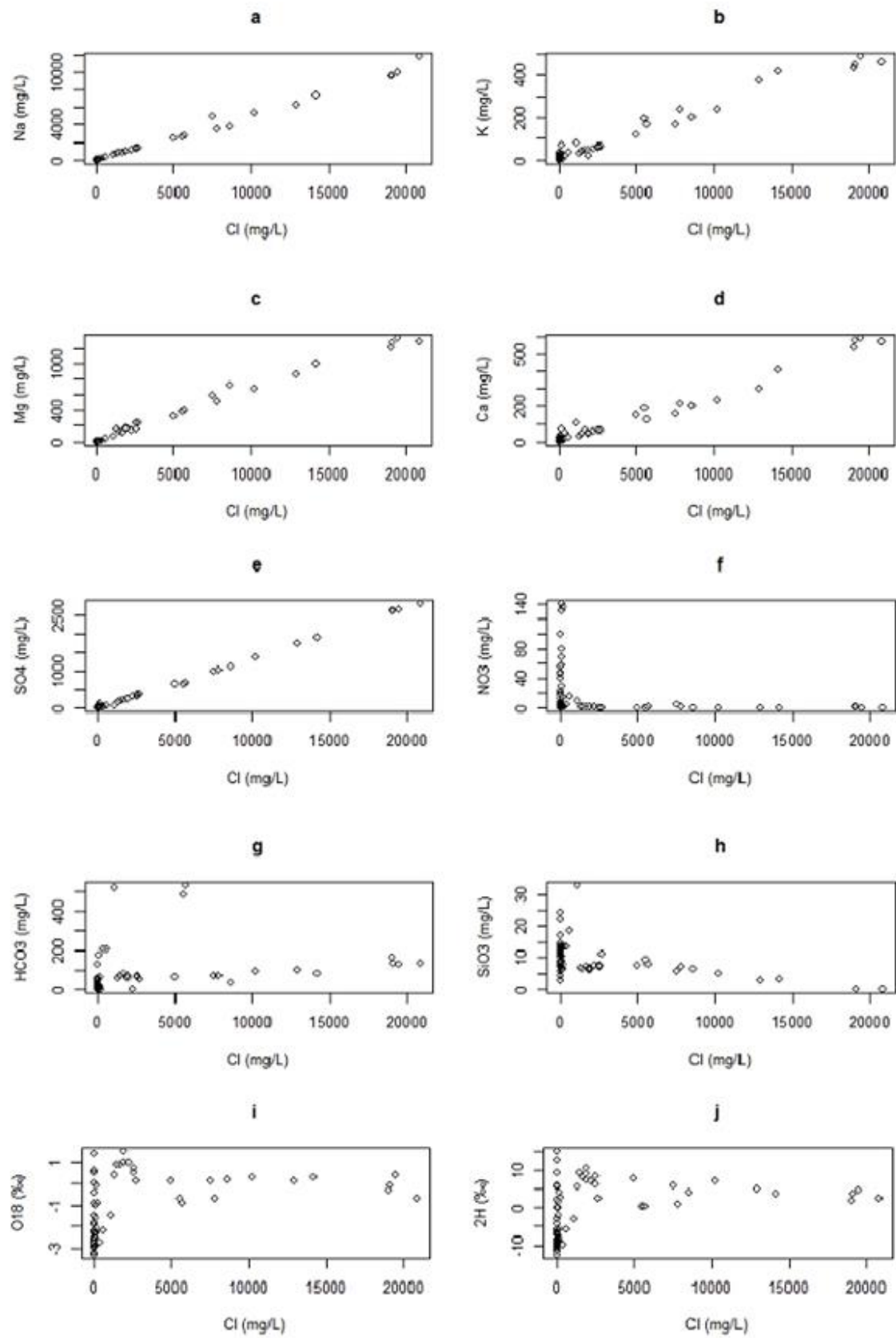
- Environmental Protection Agency, 2011.** Aquatic ecosystems, water quality, and global change: challenges of conducting multi-stressor global change vulnerability assessments. National Centre for Environmental Assessment, Washington, DC; EPA/600/R-11/011F. Available from the National Technical Information Service, Springfield, VA, and online at <http://www.epa.gov/ncea> (Accessed 25.1.13).
- FAO, 2015.** AQUASTAT Main Database, Food and Agriculture Organization of the United Nations (FAO). (accessed on 28.10.2016).
- Fonds Monétaire International, FMI, 2009.** Côte d'Ivoire: Stratégie de Réduction de la Pauvreté/Rapport d'Étape au titre de l'année 2009-Rapport du FMI No. 09/156, Washington, pp. 199. Available from <https://www.imf.org/external/french/pubs/ft/scr/2009/cr09156f.pdf> (accessed 7.1.2013).
- Guha-Sapir, D., Hoyois, Ph., Below, R., 2015.** Annual Disaster Statistical Review 2014: The Numbers and Trends. Brussels: CRED; Available online at http://www.cred.be/sites/default/files/ADSR_2014.pdf (accessed 11.3.16).
- Hammer, Ø., Harper, D.A.T. and Ryan, P.D. 2001.** PAST: Paleontological statistics software package for education and data analysis. *Palaeontologia Electronica* 4(1), pp. 9 Available at <http://www.uq.edu.au/dinosaurs/documents/past.pdf> (accessed 13.4.2014).
- Hauhouot, C., 2002.** « Les problèmes de l'aménagement de l'estuaire du fleuve Comoe à Grand-Bassam », *Les Cahiers d'Outre-Mer* [En ligne], 219 | Juillet-Septembre 2002. mis en ligne le 13 février 2008. Available from <http://com.revues.org/1012> (accessed 27.10.16).
- Institute of Research for Development, 1996.** UNEP, International Soil Reference and Information Centre (ISRIC), *World Atlas of Desertification*, 1997. Available from http://www.grida.no/graphicslib/detail/deforestation-in-west-africa-case-cote-divoire_8cb5 (accessed 3.3.16).
- Kathiresan, K.** “3.3. Methods of studying Mangrove.” Available online at <http://dev.ourworld.unu.edu> (accessed 5.1.13).
- Kelly D. 2005.** Seawater intrusion topic paper (final), Island County: WRIA 6 Watershed, pp. 27. Available at <https://fortress.wa.gov/ecy/publications/publications/1203271.pdf> (accessed 11.02.2016).
- Lagabrielle, E., Metzger, P., Martignac, C., Lortic, B., Durieux L., 2005.** Guide critique d'utilisation des informations produites dans le cadre du projet TEMOS à La Réunion. Available at https://agritrop.cirad.fr/531308/1/document_531308.pdf (accessed 16.11.15).

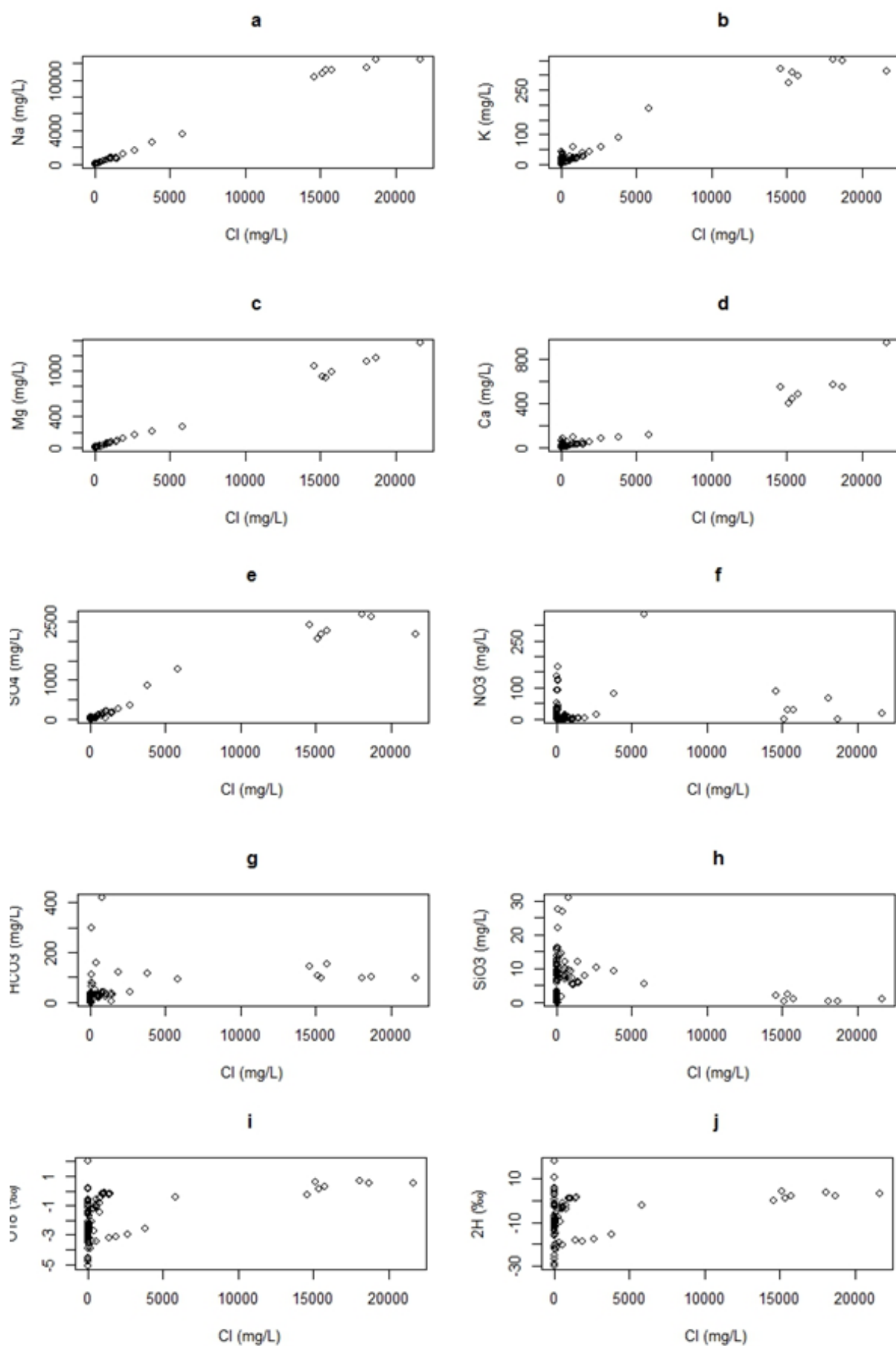
- Lagabrielle, E., Metzger, P., Martignac, C., Lortic, B., Durieux L., 2007.** Les dynamiques d'occupation du sol à La Réunion (1989-2002). Available at <http://mappemonde.mgm.fr/num14/articles/art07205.pdf> (accessed 9.11.15)
- Murphy, S., 2007.** General Information on Dissolved Oxygen. In City of Boulder: USGS Water Quality Monitoring. Available at <http://bcn.boulder.co.us/basin/data/BACT/info/DO.html>
- National Drought Mitigation Center, 2007.** Drought indices. <http://drought.unl.edu/DroughtBasics/TypesofDrought>. Accessed on the 9th October, 2015.
- National Oceanic and Atmospheric Administration, 1998.** "Oxygen Depletion in Coastal Waters" by Nancy N. Rabalais. NOAA's State of the Coast Report. Silver Spring, MD: NOAA. http://state_of_coast.noaa.gov/bulletins/html/hyp_09/hyp.html.
- National Oceanic and Atmospheric Administration, 2014.** (on-line). Can humans drink seawater? Available from <http://oceanservice.noaa.gov/facts/drinksw.html>.
- National Oceanic and Atmospheric Administration, 2016.** Annual CO₂ growth rates. Available from <https://www.co2.earth/co2-acceleration> (accessed 13.1.16).
- Nicholls, R.J., Wong, P.P., Burkett, V.R., Codignotto, J., Hay, J., McLean, R., Ragoonaden, S. and Woodroffe, C.D., 2007.** Coastal systems and low-lying areas. . Climate Change 2007: Impacts, Adaptation and Vulnerability. Contribution of Working Group II to the Fourth Assessment Report of the Intergovernmental Panel on Climate Change, M.L. Parry, O.F. Canziani, J.P. Palutikof, P.J. van der Linden and C.E. Hanson, Eds., Cambridge University Press, Cambridge, UK, pp. 315-356. Available from <http://ro.uow.edu.au/cgi/viewcontent.cgi?article=1192&context=scipapers>.
- N'kaka, N., 2013.** Dabou : Mort mystérieuse de plusieurs poissons : des familles touchées, les chiens soccombent, Abidjan touchée. Soir info. www.linfodrome.com/societe-culture/9427-dabou-mort-mysterieuse-de-plusieurs-poissons (accessed 17.6.13).
- Petschick, R., 2000.** MacDiff version 4.2.5. manual Available at http://www.geologie.unifrunkfurt.de/Staff/Homepages/Petschick/PDFs/MacDiff_Manual_E.pdf (verified 16.4.07).
- R Core Team, 2012.** R: A language and environment for statistical computing. R Foundation for Statistical Computing, Vienna, Austria.
- Roose, E. and Chéroux, M., 1966.** Les sols du bassin sédimentaire de Côte d'Ivoire. ORTSOM.
- Struder, E., 2006.** Marée noire en Côte d'Ivoire : le pétrole maudit. Available from <https://tazpacific.wordpress.com/2006/09/11/maree-noire-en-cote-divoire/>
- Stuckelberger, A., 2008.** Water, Public Health and the Right to Development: The Imperatives of the United Nations MDG. Journal of Humanitarian Medicine, 8(1), pp. 2-7. Available at http://www.iahm.org/journal/vol_8/num_1/text/vol8n1p2.htm

- Twigg, J., 2004.** Good practice review. Disaster risk reduction. Mitigation and preparedness in development and emergency programming. Available online at http://www.ifrc.org/PageFiles/95743/B.a.05.%20Disaster%20risk%20reduction_%20Good%20Practice%20Review_HP.N.pdf.
- United Nations Development Programme, 2006.** Human Development Report 2006: Beyond scarcity : power, poverty and the global water crisis. New York, Basingstoke: Published for the United Nations Development Programme by Palgrave Macmillan. Available at <http://hdr.undp.org/sites/default/files/reports/267/hdr06-complete.pdf>.
- United Nations Environment Programme, UNEP, 2002.** Global Environment Outlook 3: Past, Present and Future Perspectives. Available at <http://www.grida.no/publications/other/geo3/?src=/geo/geo3/english/pdf.htm>.
- United Nations Framework Convention on Climate Change, 2007.** Climate Change: Impacts, Vulnerabilities, and Adaptation in Developing Countries. Bonn, Germany, pp. 68. Available from <https://unfccc.int/resource/docs/publications/impacts.pdf> (accessed 17.10.16).
- UNICEF Humanitarian Action report, 2007.** Côte d'Ivoire, pp. 212-216. Available from http://www.unicef.org/har07/files/HAR_FULLREPORT2006.pdf.
- Wilhite, D.A. and Glantz, M.H., 1985.** Understanding: the drought phenomenon: the role of definitions. *Water international*, 10(3), pp. 111-120. Available at <http://digitalcommons.unl.edu/cgi/viewcontent.cgi?article=1019&context=droughtfacpub> (accessed 18.1.13).
- World Meteorological Organization, 2012.** Standardized Precipitation Index User Guide (M. Svoboda, M. Hayes and D. Wood). Geneva. Available online at http://www.wamis.org/agm/pubs/SPI/WMO_1090_EN.pdf (accessed 18.1.13).
- World Water Assessment Programme, 2009.** The United Nations World Water Development Report 3: Water in a Changing World, Paris: UNESCO Publishing, and London: Earthscan. Available from http://webworld.unesco.org/water/wwap/wwdr/wwdr3/pdf/WWDR3_Water_in_a_Changing_World.pdf (accessed 12.15).
- Wozacek, S., 2001.** Die klastischen Sedimente von Süd-Elfenbeinküste: Provenanz, Umlagerungsprozesse und Entstehung des Goldvorkommens' Belle Ville'. Available online at http://elib.uni-stuttgart.de/opus/volltexte/2001/953/pdf/Kap05_08.pdf (accessed 13.3.16).

APPENDICES

Appendix I: Scatterplots of different ions versus chloride concentration for the dry (top) and rainy seasons (bottom), respectively.





Appendix II: Social survey questionnaires

REPUBLIQUE DE COTE D'IVOIRE
Union-Discipline-Travail

Ministère de l'Enseignement supérieur
et de la Recherche Scientifique



UNIVERSITÉ FELIX HOUPHOUËT-
BOIGNY
UFR BIOSCIENCES

WASCAL



Centre for Development Research
University of Bonn

ENQUÊTE SOCIALE

Catégorie d'âge :15 - 30 ☐ 31 – 45 ☐ 46 – 60 ☐ > 60 ☐

Sexe : Masculin ☐ Féminin ☐

Profession : Etudiant ☐ Commerçant ☐ Paysan ☐ Pêcheur ☐ Autres ☐

Nombre des membres du ménage (ou nombre d'habitants de la maison) : 2 - 4 ☐ 5 – 7 ☐ >8 ☐

A/

Avez-vous remarqué des changements dans la quantité de pluies (précipitations) et des températures au cours de ces dernières années ? Oui ☐ Non ☐

Si Oui, laquelle ? Moins de pluie ☐ plus de pluie ☐

Avez-vous remarqué des changements de températures au cours ces dernières années ?

Si oui, lesquelles ? Plus en plus chaud ☐ plus en plus frais ☐

B/

Quelle est la principale source d'eau potable de votre ménage ? Alimentation en eau de la ville ☐ puits privé ☐ eau de surface (rivière / lagune / source) ☐

Avez-vous d'autres sources d'eau pour d'autres usages domestiques ? Oui ☐ Non ☐

Si oui, lesquels _____

Si la source d'eau est l'eau de puits ou les eaux de surface :

Combien de temps vous mettez pour aller chercher de l'eau à la source ?

Sur place ☐ 15 -30 minutes ☐ 30 - 45 minutes ☐ > 45 minutes ☐

Quelle est la quantité d'eau qui vous pouvez puiser a ce temps ? _____

Avez-vous traité ces eaux d'une quelconque manière avant de la boire ? Oui ☐ Non ☐

Si oui, comment ? _____

Pensez-vous que la qualité de l'eau et sa quantité sont un problème dans cette région ? Oui ☐ Non ☐

Si oui, est-ce un problème durant toute l'année ou seulement à certaine période de l'année ?

Toute l'année ☐ Saison sèche ☐ saison des pluies ☐

Quel genre de problème de qualité/ quantité d'eau ?	Toute l'année	Saison sèche	Saison des pluies	Commentaires
La mort/manqué de poisson et crabes				
Trop de bateaux				
Natation				
Pas d'eau pour les usages domestiques				
Odeur de l'eau				
Mauvaises herbes en les eaux surface				
Culture/ production agricole				

Parmi les problèmes évoqués, lequel est le plus important ? _____

C/

Comment vous débarrassez-vous des eaux usées ? Système de traitement des eaux usées de la ville ☐
directement à l'eau de surface ☐ dans l'environnement ☐

Quel type de toilette utilisez-vous ? Moderne ☐ traditionnel ☐

D/

Les plantes aquatiques/végétation riveraine sont-elles utiles pour vous ? Oui ☐ Non ☐

Si oui, de quelle manière _____ quelle sont les parties plus importantes ? _____

Si non, pensez-vous qu'elles devraient être toutes coupées ? Oui ☐ Non ☐

E/ Chaque solution a un coût

Accepteriez-vous de payer (monétaire) ou faire des sacrifices (arrêter la pêche pour une période de temps, ne pas couper les arbres, arrêter les feux de brousse, l'utilisation contrôlée des engrais) pour résoudre ces problèmes de qualité/quantité de l'eau et environnement dans votre région ? Oui ☐ Non ☐

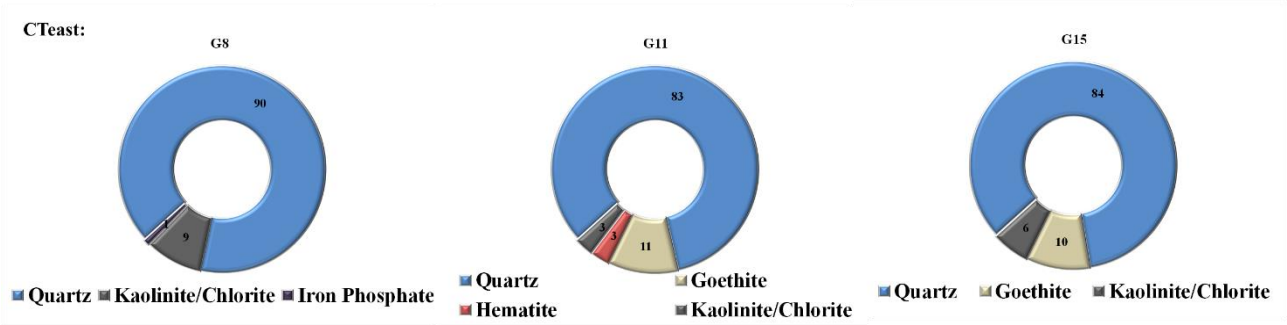
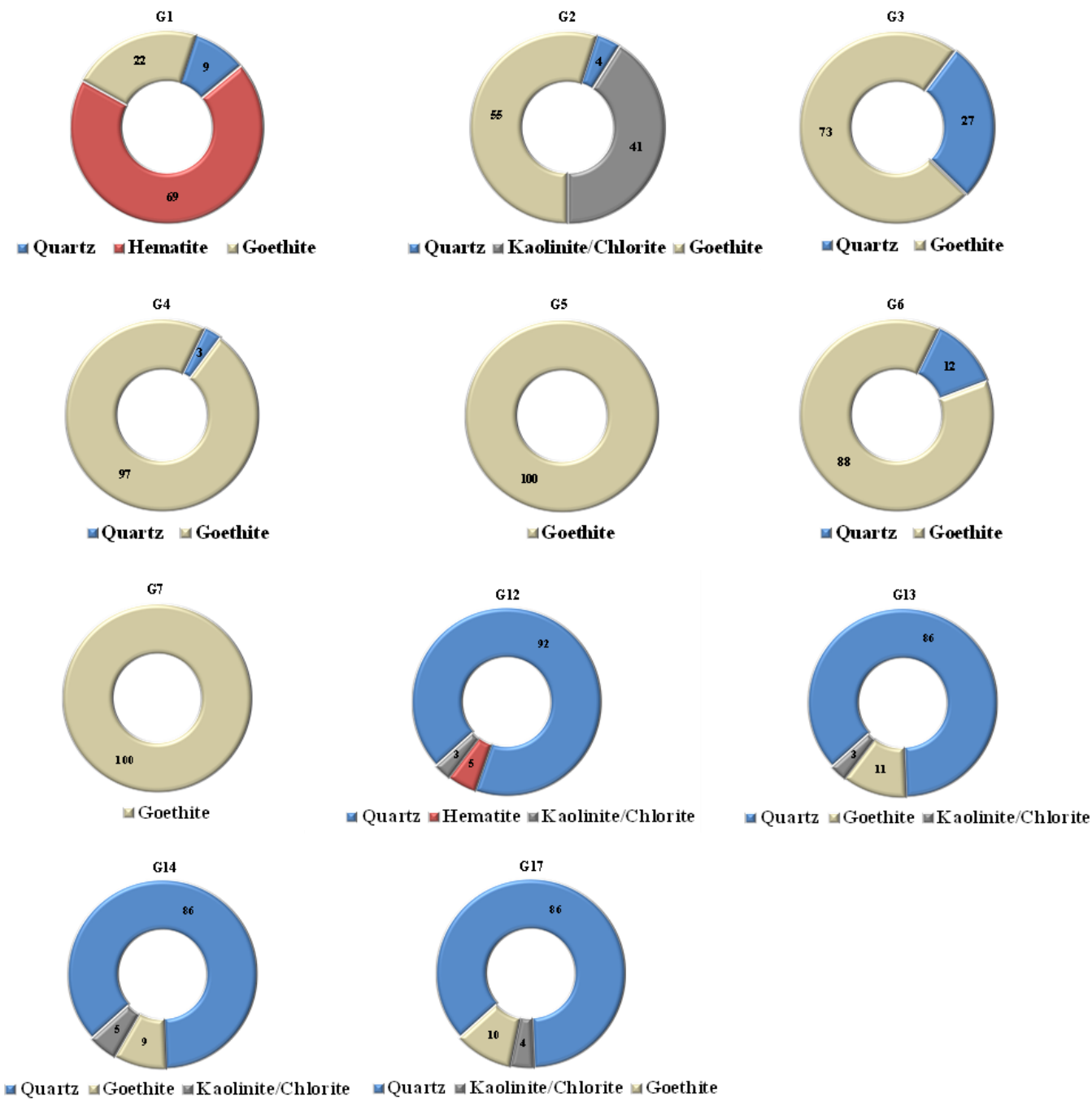
Pensez-vous que ces sacrifices sont nécessaires ? Oui ☐ Non ☐

Combien êtes-vous prêt à payer mensuellement (FCFA) pour résoudre les problèmes ? _____ ou
préfériez-vous plutôt recevoir de l'argent du gouvernement ? Oui ☐ Non ☐

Si oui, combien êtes-vous prêt à recevoir mensuellement (FCFA) du gouvernement ? _____

Appendix III: Mineralogical composition of outcrops corrected for Cook indices (Cook *et al.*, 1975).

CTwest:





Appendix IV: Résumé de Thèse

L'eau est l'une des ressources fondamentales de la vie offerte naturellement à l'humanité par les systèmes écologiques. Une eau de bonne qualité n'est pas importante seulement qu'en tant que source d'eau pour les usages domestiques, mais elle l'est aussi pour le fonctionnement adéquat, la conservation de la biodiversité. Elle est un facteur clé du développement économique (**World Water Assessment Programme, 2009**). L'accès insuffisant à l'eau potable pour les usages ménagers est une mesure importante de la pauvreté (**Carter & Bevan, 2008**) qui est la cause majeure de l'érosion de la biodiversité (**World Water Assessment Programme, 2009**).

Comme souligné par le Rapport sur le Développement Humain (**PNUD, 2006**), l'accès à l'eau n'est pas seulement un droit fondamental de l'homme, il constitue un indicateur intrinsèque essentiel du progrès humain. Il constitue un pilier aux autres droits de l'homme et sert de tremplin pour la réalisation de plus grands objectifs de développement durable. Il est évident que le développement futur du continent Africain dépend fortement de l'accès à l'eau (**Desanker & Magadza, 2001**).

En Côte d'Ivoire, 40 % de la population attirés par l'eau, habite la très dynamique zone côtière qui couvre 1% de la surface nationale (322.463 km²). Ce qui exerce une énorme pression sur les ressources côtières d'eau, une situation qui pourra être aggravée par les changements climatiques. Le Groupe d'experts Intergouvernemental sur l'Évolution du Climat (GIEC) prédit des impacts drastiques sur les systèmes hydrauliques qui se manifesteront sous forme d'inondation, de sécheresse ou d'intrusion de la mer selon des situations géographiques. Dans les côtes ivoiriennes, l'assèchement des puits et la diminution de la quantité des pluies et des flux des cours d'eau sont des signes évidents des effets du climat sur la disponibilité en eau. Ceci fait du suivi et de la conservation des ressources en eau une priorité dans cette région. Cependant, les décisions d'aménagement ne seront efficaces qu'avec une connaissance parfaite de l'état actuel des ressources en eau et des effets saisonniers sur leur disponibilité.

Cette étude examine la géomorphologie et les impacts de la saisonnalité sur les ressources en eau dans une bande de 15 km du littoral oriental de la Côte d'Ivoire en utilisant la télédétection/les techniques de SIG, la géologie, la géochimie, la microbiologie et la sociologie. Des échantillons d'eau de pluie (n= 30), d'eau souterraine (puits et forages, n= 81) et d'eau de surface (lagune Ebrié et littoral Atlantique, n= 69) ont été prélevés en saison sèche (Janvier/Février) et hivernale (Septembre/Octobre) de l'année 2014 pour des analyses géochimique (ions majeur – Na⁺, Ca²⁺, K⁺, Mg²⁺, Cl⁻, HCO₃⁻, SO₄²⁻, NO₃⁻), isotopique (oxygène-18 et deutérium) et biologique (Phytoplancton et coliformes fécaux).

Du point de vue géomorphologique, la pente de la zone d'étude se situe approximativement entre zéro (0) et 70 degrés vers la mer. Les unités d'occupation du sol sont les terres agricoles (50%), les plans d'eau (32%), les établissements humains (13%) et les forêts (5%). De 1989/90 à 2014/15, c'est-à-dire en 25 ans seulement, l'urbanisation a déjà dévasté 31,83% de forêts et 37,42% de terres agricoles.

Sur le plan hydrologique, l'auteur signale que les indices standardisés de précipitation et d'évapotranspiration (ISPE), déterminés sur la base des données météorologiques multi-décennales (1971-2014), ont révélé qu'au cours des années 1987, 1998/99 et 2013/14 la sécheresse est restée modérée. Du point de vue hydrogéologique, les milieux aquifères, composés en grande partie de silice (98%), favorisent une acidification accrue des eaux souterraines (pH de 3,9 à 7,4) en rapport avec d'intense capacité de dissolution de la silice. Dans cette région, les changements de régimes hydrologiques exercent une forte influence sur la chimie des eaux côtières et le transport des contaminants. En outre, les résultats géochimiques et isotopiques stables (oxygène-18 et deutérium) révèlent que, dans cette région, l'influence marine est dominante pendant la saison sèche alors que les processus continentaux (fluviaux et pluviométriques) dominent pendant la saison des pluies. Dans le diagramme de Piper, la majorité des échantillons d'eau souterraine (87 % et 80 % respectivement pour la saison sèche et hivernale) appartient au faciès chloruré sodique (Na-Cl) en rapport avec la présence d'intrusion d'eaux salines dans les eaux douces. Les concentrations maximales en chlorure dans les eaux souterraines sont de 1088 mgL^{-1} et de $785,2 \text{ mgL}^{-1}$ respectivement pendant la saison des pluies et la saison sèche. Quant aux nitrates, leurs teneurs varient entre 0,3 - $139,5 \text{ mgL}^{-1}$ et 0 - $165,9 \text{ mgL}^{-1}$ dans les eaux souterraines ; et entre 0,01 - 3,6 et 0,01 - $332,3 \text{ mgL}^{-1}$, dans les eaux de surface, respectivement pendant les saisons sèche et pluvieuse. Ainsi, les saisons peuvent avoir des impacts disproportionnés sur ces ressources côtières d'eau. Cette étude indique que pour ces eaux côtières, la dégradation est plus accentuée durant l'hivernale. En concluant, les activités anthropiques sont à la base du changement dans cet environnement. La contribution naturelle est infime.

Concernant la microbiologie, la distribution du phytoplancton est fonction du flux saisonnier des nutriments dans les eaux de surface du littoral. La biomasse maximale de phytoplancton était de $11,3 \cdot 10^6$ et de $15,4 \cdot 10^6 \text{ cellules mL}^{-1}$, respectivement pour la saison sèche et la saison des pluies avec une croissance floristique variant entre 16,4 et 80,8 %. Les variations temporelles, les plus élevées en biomasse, ont été relevées dans les alentours de la lagune Ebrié soumise à une forte influence marine. Les diatomées étaient le taxon dominant, alors que les cyanobactéries étaient les plus abondantes. La diversité relativement faible du phytoplancton (indice de Shannon inférieur à 1) et la dominance mono-spécifique localisée sont des signes de perturbations des conditions aquatiques. Les résultats

de l'analyse des données exploratoires confirment que le silicate et la salinité sont les facteurs environnementaux majeurs influençant les modèles de distribution du phytoplancton. L'afflux de ces éléments dans les eaux côtières est contrôlé de façon saisonnière. Lorsque les processus marins dominent pendant la période d'étiage, la salinité augmente avec une décroissance concomitante de l'abondance de phytoplancton, tandis que pendant la période de crue, où les cours continentaux dominent, il y a un fort afflux de silicate dû aux intempéries dans les eaux côtières avec pour corolaire, l'augmentation de l'abondance de phytoplancton. Certaines localités ne respectent cependant pas cette tendance. Par exemple, les zones de la station I (est) de la lagune, excessivement riches en éléments nutritifs recueillis à partir de ruissellements provenant des activités agricoles durant la saison de crue, ont enregistré soit une stagnation ou une régression drastique de l'abondance de phytoplancton.

Enfin, s'agissant des enquêtes sociologiques avec les communautés riveraines, les populations de cette zone ne pourront rien faire d'autre que de subir les effets de la dégradation des eaux sur cette partie du littoral ivoirien. Car, ces eaux constituent la source principale d'approvisionnement en eau potable des ménages (pour 53 %) et une source secondaire pour 97 % de la population. En plus, environ 30 % de la population dépendent directement de ces ressources en eau du littoral pour leur subsistance.

Cette étude a cependant relevé que les solutions naturelles les plus efficaces pour conserver et promouvoir la biodiversité dans ces environnements côtiers est la forêt de mangrove. Elle est reconnue pour sa capacité à atténuer les vagues côtières, à agir comme des filtres à eau naturelles, à procurer un habitat pour les espèces aquatiques et à séquestrer le carbone. Les racines de mangrove contenant en moyenne 46 % de carbone sont capables de fixer annuellement jusqu'à 176 Mg C ha^{-1} . Par conséquent, leur conservation assurera la préservation de la biodiversité et représente une importante stratégie pour l'atténuation et l'adaptation. Enfin, l'homme est invité à œuvrer de façon harmonieuse et réfléchie avec la nature en vue de renforcer les protections naturelles et assurer ainsi leur survie mutuelle.

En somme, les données recueillies sur les eaux côtières pendant les différentes saisons donnent une idée de la réaction de ces systèmes aux changements climatiques futurs. Cela est dû au fait que les changements successifs de saison induisent les changements climatiques. Cependant la principale limite est que ces résultats sont basés sur des recherches conduites sur une seule année. Perfectionné un suivi environnemental à long terme et des efforts d'échantillonnage plus représentatifs sont recommandés en vue d'établir des évolutions observées et de confirmer des tendances générales.

PUBLICATIONS

Based on the results, different manuscripts are under/have been prepared. These are:

Osemwegie, I. Niamien-Ebrottie, J., Kone, J.F., Biemi, J. and Reichert, B., 2016. Characterization of Phytoplankton Assemblages in a Tropical Coastal Environment using Kohonen Self-Organizing Map. *African Journal of Ecology*. Version of record online: 30 Dec. 2016. <http://dx.doi.org/10.1111/aje.12379>.

Osemwegie, I., N'da H.D., Stumpp, C., Reichert, B. and Biemi, J., 2016. Mangrove Forest Characterization in southeast Côte d'Ivoire. *Open Journal of Ecology*, 6, 138-150.

Multiproxy Assessment of Water Flow Pathways in Coastal Water Systems, SE Côte d'Ivoire (under review).

Other manuscripts are still been conceptualized.